FEDERAL UNIVERSITY OF ITAJUBA
GRADUATE PROGRAM IN
ELECTRICAL ENGINEERING

Tiago Elias Castelo de Oliveira

The Concept of Dynamic Hosting Capacity of Distributed Renewable Generation Considering Voltage Regulation and Harmonic Distortion

28th of September 2018, Itajuba – Brazil.

GRADUATE PROGRAM IN
ELECTRICAL ENGINEERING

Tiago Elias Castelo de Oliveira

The Concept of Dynamic Hosting Capacity of Distributed Renewable Generation Considering Voltage Regulation and Harmonic Distortion

Ph.D. thesis submitted to the Graduate Program in Electrical Engineering as a part of the requirements to obtain the title of **Ph.D. in Electrical Engineering**

Concentration Area: Electric Power Systems
Supervisor: Prof. Ph.D. Paulo Fernando Ribeiro
Co-supervisor: Prof. Ph.D. Benedito Donizeti Bonatto
International Supervisor: Prof. Dr. Pedro M. S. Carvalho – Instituto Superior Tecnico, Lisboa – Portugal

28th of September 2018, Itajuba – Brazil

To my parents, Benedito and Valerie.

"Most people say that it is the intellect which makes a great scientist.
They are wrong; it is character"
Albert Einstein.

ACKNOWLEDGMENTS

I would first like to thank my Ph.D. thesis advisors Professor Paulo F. Ribeiro and Professor Benedito D. Bonatto of the *aPTIs* SG^2 at Federal University of Itajuba as well as Pedro M. S. de Carvalho of IST at Lisbon University. The door of Professor Paulo Ribeiro and Professor Pedro Carvalho's office was always open, whenever I found myself struggling or had a question about my research. They consistently allowed this research to be my own study but steered me in the right direction whenever they thought I needed it.

I would also like to thank the experts who were involved in the validation survey for this research project: Professor Antonio Carlos Zambroni de Souza, Professor Vladimir Cuk and Professor Math Bollen. Without their passionate participation and input, the validation survey could not have been successfully conducted.

I would also like to acknowledge *ERASMUS MUNDUS – SMART*^{2} as the second co-operator of this thesis, and I am gratefully indebted to them for the very valuable opportunity of doing my international exchange in Lisbon.

Moreover, I'm grateful to Vladimir Ćuk, who invited me to go and visit TU/e (Technological University of Eindhoven), where I could learn and appreciate the work which has been developed at the PQ lab. I'd also like to thank Vladimir for giving me the necessary data to use in this study. Furthermore, I would like to thank CHESF for the measurement harmonic data regarding the FIFA World Cup 2018, which was useful and very important to this study. Also, to Professor Paulo Ribeiro and Mr. Lucio, who provided the measurement data from the PQ meters regarding the World Cup PQ campaign. Finally, I would like to thank Mr. de Apráiz, Mr. Barros, and Mr. Diego, for the report from Spain with a brief analysis regarding the Spanish matches.

I must also express my very profound gratitude to my parents, Valerie and Benedito, and to my friends from Europe, Brazil and aPTIs SG^2 group for providing me with unfailing support and continuous encouragement throughout my years of study and through the process of researching and writing this thesis. Last, but not least. , I would like to say thank you, from the bottom of my heart, to Luisa Condessa, who has been teaching me English, and helping me. Even in rough times she was there showing me that I was capable of reaching my goals and get over my difficulties. Without her, it wouldn't have been possible to achieve what I've achieved at this point in my academic life.

This accomplishment would not have been possible without all of you. Thank you.

The author, Tiago Elias Castelo de Oliveira

SUMMARY

LIST OF FIGURES

LIST OF TABLES

LIST OS ABBREVIATION

ANEEL	Electrical Energy National Agency
aPTIs-SG2	Advanced Power Technologies and Innovation in Systems and Smart Grid Group
BD	Background Distortion
CHESF	San Francisco Hydroelectric Company
CNPq	National Council of Scientific and Technological Development
DER	Distributed Energy Resources
DG	Distributed Generation
DHC	Dynamic Hosting Capacity
EES	Energy Storage System
h	Harmonic Order
HC	Hosting Capacity
IEC	International Electrotechnical Commission
IEEE	Institute of Electrical and Electronics Engineers
IHD	Individual Harmonic Distortion
IST	Technical Superior Institute
ONS	National Electrical System Operation
PCC	Common Coupling Point
PRODIST	Proceedings for Electrical Energy Distribution in the National Electrical System
PQ	Power Quality
PV	Photovoltaic Panel
p.u.	Per Unit
QMAP	Excellence Center in Power Quality, Measurement, Automation and Protection
RMS	Root Mean Square
SMPS	Switched Mode Power Supply
THD	Total Harmonic Distortion
TU/e	Technological University of Eindhoven
UNIFEI	Federal University of Itajuba

ABSTRACT

This thesis introduces a brief analysis on hosting capacity and related concepts as applied to distribution network systems. Furthermore, it addresses the applicability of hosting capacity study methodologies to harmonic voltage distortion caused by photovoltaic panels (PV) connected at a low-voltage (LV) side of a university campus grid. The analysis of the penetration of new distributed generation technologies, such as PV panels, in the distribution grid of the campus was carried out via measurement processes, and later by computer simulations analysing a new concept of the hosting capacity approach in relation to voltage harmonics distortion. The voltage rise due to harmonic injection is analysed and discussed with the aim of validating the discussed model and also putting forward recommendations for connecting PV generation across other network systems. Furthermore, it presents a new approach for hosting capacity in relation to harmonic voltage distortion with variance in time, be it daily, weekly, monthly or even yearly. This concept is addressed as Dynamic Hosting Capacity (DHC). General aspects of DHC are demonstrated, as well as its applications using energy storage systems as a mitigation tool to control the voltage profile for the system and increasing the hosting capacity profile.

Keywords: distributed generation, distributed energy resources, power quality, hosting capacity, voltage rise, harmonic distortion, dynamic hosting capacity, energy storage systems.

1. INTRODUCTION

1.1 Motivation

Nowadays, traditional centralized electricity generation is not the only source of production delivered to distribution network systems. At present, the term Distributed Generation (DG) has come to be used to refer to new production paradigms, which involve the smart grid concept and its derivatives. In addition to the concept, DG also refers to production methods in which only a fraction of generated electric power is delivered by consumers that own small generation units. These are usually designated as Distributed Energy Resources (DER). DG can also be referred to as decentralized generation or dispersed generation (CARVALHO et al., 2008). The benefits from DGs range from economic, technical and environmental to others. Over time, the concept of DG has evolved, and in the literature (TAN et al., 2013) it is possible to find several widely used definitions such as any source of electric power of limited capacity, directly connected to the distribution network wherein it is consumed by end users.

Up to this point, DG or more generally DER integration is expected to increase at a fast pace. The photovoltaic systems (PV) are believed to be the most important type of DERs around the world due to their reliability as well as the mainstream technology. In a global scenario, the PV electricity reached around 227 GW at the end of 2015 (WORLD ENERGY RESOURCES, 2016). As mentioned before, PV has been the mainstream solar power technology. The global installed solar power capacity between 2005 and 2015 is shown in Figure 1.1.

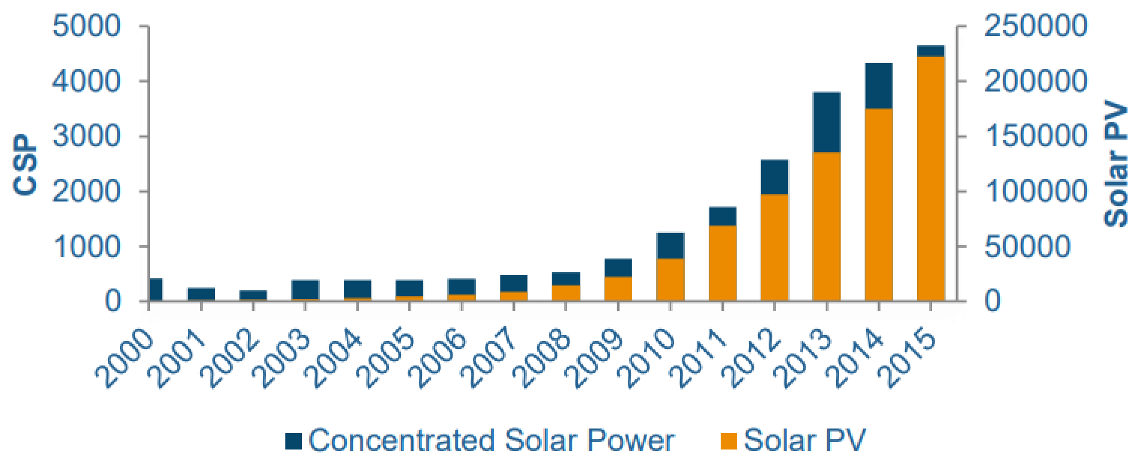

Figure 1.1 – Global installed solar power capacity, 2000 – 2015 (MW) (“WORLD EBERGY RESOURCES, 2016).

Worldwide, based on (WORLD ENERGY RESOURCES, 2016), China is a leader in relation to PV installations cumulating 23% of the world PV matrix, followed by the USA (14%), Japan (14%), Germany (13%) and Italy (6%). The rest of the world has 30%. The cumulative global PV installations are shown in Figure 1.2.

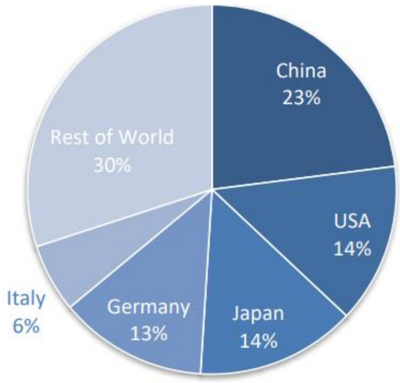

Figure 1.2 – Cumulative Global PV installations 2016 (“World Energy Resources Solar | 2016”, 2016).

The large-scale integration of PV, as well as any kind of DERs, has important impacts on network security, reliability and quality of service. One of the major service impacts of PV integration is voltage magnitude rise (BOLLEN et al, 2008; CARVALHO et al, 2008). This is especially relevant in the case of unitary power factor control of the power electronic converters, which are in the interface of PV systems. The integration of PVs may cause other disturbance in normal operating conditions. In fact, a large PV penetration can result in several voltage quality issues.

Note that voltage rise impacts can be amplified by voltage waveform harmonics, which may be significant in PV and other electronically connected generation technologies that inject harmonic currents. Depending on the PV connection point and network characteristics of the electrical network system, voltage distortion caused by harmonic current injection may, or may not, reduce the system hosting capacity beyond the limits imposed by the maximum rise of the fundamental voltage component (BOLLEN, 2008, 2017; OLIVEIRA et al., [s.d.]).

Generally, the impact of DG/DERs can be quantified using a set of power indicators. The nature of the impact depends on the characteristics of the network system itself (OLIVEIRA, 2015; RYLANDER; SMITH; SUNDERMAN, 2015; BOLLEN, 2017). For PV systems, a feeder’s PV hosting capacity may be defined as the largest PV generation system which can be integrated without violating the limits of these feeders to which it is connected. The maximum amount of generation can be classified as: the worst hosting capacity, hosting capacity and the best hosting capacity. They are connected directly to the worst, existing and best background levels, respectively. Figure 1.3 illustrates this concept.

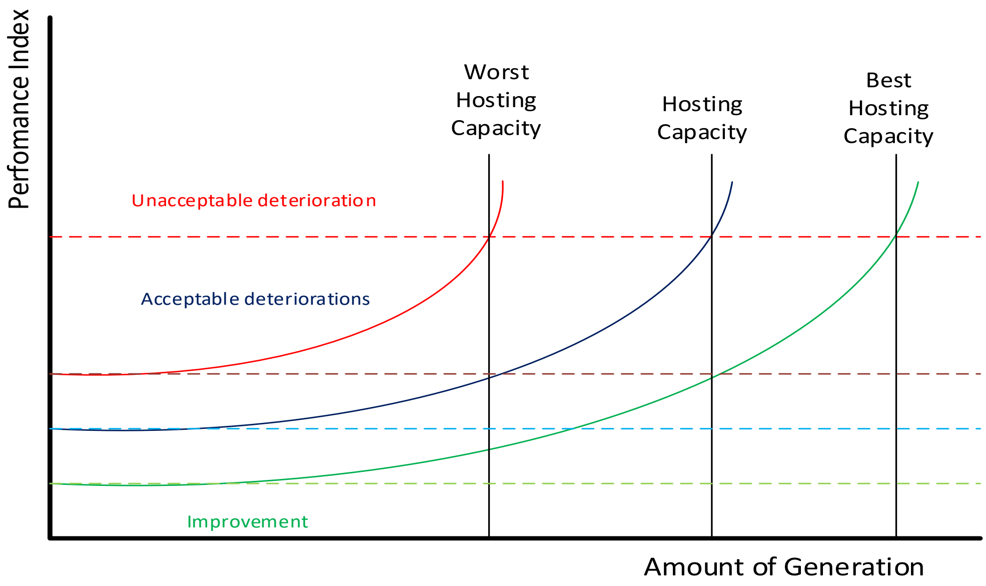

Figure 1.3 – Hosting capacity general approach – worst, usual and best cases.

It is important to emphasize that, according to local standards (IEEE 1159, 2009; PRODIST, 2015; BOLLEN; RÖNNBERG, 2017), a voltage rise violation is considered as a primary feeder violation when the recorded voltage data registers voltages greater than 1.05 per unit (p.u.).

According to (BOLLEN; RÖNNBERG, 2017), many studies have been done on the impact of local generation on the grid, where overcurrent and overvoltage, for example, are the capacity limitations most commonly studied to date. In other words, a large scale of active power electronics, either in production or consumption, can result in further phenomena, the interharmonics or supraharmonics cited above. Another aspect has also been considered in current studies: the amount of capacitance connected to the grid that is expected to increase at all voltage levels in the grid, which takes further analysis in order to preclude the impacts on the power quality of the distribution grid. As we can see, (BOLLEN; RÖNNBERG, 2017) shows us an overview of the power quality issues which is related to major challenges in this field.

The present research will address the overvoltage rise, due to characteristic harmonics and non-characteristic harmonics (harmonics and interharmonics up to 2 kHz). For these occurrences, the impact on voltage quality must be studied as well as the impact of emission by other equipment connected to the grid. Moreover, this part of the planning should cover a combination of measurements, simulation studies and relevant information about the grid. Furthermore, capacity limitation, which is derived from the hosting capacity, is a function of the consequent impact on power quality, such as the voltage rise and background harmonic voltage, among others (DUBEY, 2017; DUDIAK, 2014; ETHERDEN, 2011; RYLANDER et al., 2013). This aspect is detailed in the following section and provides the validity and scope of the present work. This new approach has many applications in the field of local hosting capacity, for example, a new approach to find a time variant hosting capacity in order to bring more dynamism to its global results as an improved concept. Thus, a practical application will be shown throughout the document.

1.2 Research Objectives

A large scale of power electronics at the interface of DERs, as well as electronic equipment of consumers, have been considered in the electrical systems (SÁIZ-MARÍN et al., 2014), which can result in further phenomena regarding harmonic injections into the system. Another aspect addressed in current studies is the amount of capacitance and the number of inverters connected to the grid, both of which are expected to increase at all voltage levels in the grid. Firstly, this thesis has the purpose to demonstrate that the harmonic injections into the system could impact the voltage rise profile at the PCC. Secondly, our research will address the behaviour of devices whose harmonic injection changes over a specific period of time changed their harmonic emissions. Seemingly, those phenomena are variant in time, which means its power quality indexes are changeable throughout a period of time. Consequently, the maximum amount of generation possible to connect to the grid will be variant following the tendency of dynamic providing. Moreover, this approach seeks to address a way to calculate a global hosting capacity value within a dynamic profile determined for a PV installation.

Furthermore, this thesis identifies and improves the control of a solution for the voltage rise problem in electrical grids using a storage system. The storage system is examined with the intention of finding the best contribution to decrease the voltage rises, thus improving the local and the dynamism of the hosting capacity. We believe that we have designed an innovative solution for distribution systems in relation to voltage rise indexes due to PVs, or even DERs, connected at the electrical grid.

In order to address this research question, the following sub-questions are formulated, and they are addressed in the subsequent chapters of this thesis.

The first sub-question is formulated while interpreting the primary issues and motivators of the creation of a global hosting capacity methodology. The hosting capacity approach is capable of answering which limits must be respected in the systems. However, there are limitations when these phenomena are analysed separately and, as a result, different hosting capacity values will be found, and this could create doubts in relation to which value should be considered for planning. In order to determine the proper hosting capacity value, new challenges proposed by a hypothesis into the distribution grid due to the connection of PVs are analysed and detailed. The new opportunities established by these approaches should then be studied and classified. Therefore, the first sub-question is formulated as follows:

(i) *What are the advantages and implications of creating a global hosting capacity analysis with respect to different power quality phenomena?*

It is worthy to highlight that some implications using just one power quality index significantly underestimate other consequences due to the negligence of other phenomena and their effects. One of these significant impacts is related to the maximum amount of generated power that can be planned for the system, the hosting capacity value. A global hosting capacity can be defined as the hosting capacity approach, which presents an integration of other phenomena that are related to a determined level of power quality issues. The advantage of an integrated platform that considers two or more power quality issues is related to the more realistic values of hosting capacity, whose importance is connected to the planning and improvement of electrical networks.

(ii) *How could a dynamic hosting capacity be used in order to allow for better planning and improving into the distribution systems?*

It may be assumed that the dynamism of a hosting capacity profile will achieve two significant values, maximum and minimum in order to produce an analytical effect to the grid. To the best of our knowledge, the minimum value will be the deterministic value to describe the effectiveness of the grid, where the region under the minimum value can be considered unacceptable for working conditions, which means that the harmonic background at the PCC, as well as the voltage values, are almost crossing their respective limits, imposed by standards and regulations. On the other hand, the maximum value determines that the region has the best power qualities indexes, but to achieve these values it is necessary to carry out power conditioning improvements, which can be led by previous studies in the grid. Conversely, the maximum value determines the region where the best power quality indexes can be found. This range of values suggests that there is an acceptable region where the DERs system will be working at their limits considering power quality issues.

(iii) *How is the hosting capacity approach impacted, in terms of background distortion, especially in unusual occasions, such as global events?*

Background distortion will directly impact the value of the hosting capacity in relation to electrical grids. As far as we know, the bigger the background distortion is, the lower the hosting capacity value will be. However, careful attention must be exercised in worldwide events, such as the FIFA world cup, where there is satisfactory agreement between the number of TV sets connected during the matches and the impact on the harmonic distortion. These results thus need to be interpreted with care and attention.

(iv) Special Issue: How can the voltage rise problem be mitigated by incorporating a storage system at the PCC regarding the reversed power flow?

Storage systems are attracting considerable interest as a way of avoiding the voltage rises in regard to the bidirectional power flow, as well as improving the hosting capacity of the system. As far as we know, it is possible to understand that there will not be voltage rise at the PCC because, with the exceeded energy being storage, the bidirectional power flow would no longer takes place. Thus, storage systems are a possible improvement into the distribution system.

(v) How could the network planning and improvement procedures be optimised by applying an integrated hosting capacity methodology, and what would its impact be on voltage profile disturbances mitigation?

This issue will be answered in the conclusion section of this study.

1.3 State of the Art

The term hosting capacity is recognized as being the most important demonstrating parameter in evaluating the penetration of DER into the electrical system regarding power quality indexes, such as, voltage rises, harmonic distortion, overcurrent, among others. Hosting capacity studies are generating considerable discussions in terms of the maximum amount of power generation allowed for electrical systems, either distribution or transmission, without causing any disturbances. The hosting capacity method is considered a useful feature for quantifying those values in order to bring more reliability and security to the systems.

The hosting capacity concept made its first appearance in an EU research project, EU-DEEP, (European Distributed Energy Partnership) (BOLLEN, 2017; ETHERDEN, 2011; J. DEUSE, D. BENINTENDI, 2005). The term was firstly proposed by André Even in March 2004 (ETHERDEN; BOLLEN, 2011). Afterwards, other authors have developed further discussions about hosting capacity over some similar projects (BOLLEN; RÖNNBERG, 2017; J. DEUSE, D. BENINTENDI, 2005). What is known about hosting capacity is largely based on overvoltage issues, which directly impact its value.

In the literature, there are some examples of the hosting capacity definition in different fields, even before 2004 when the term in electrical systems came up. The concept has been used in areas such as internet servers, watermarking of images, settlement of refugees, as mentioned in (BOLLEN, 2017). As an illustration, the term hosting capacity has been already used in computer science, where it defines the capacity of a web server to host many access calls (ETHERDEN, 2011). In his doctoral thesis of 2012, Nicholas Etherden cited that, up until the beginning of 2013, over 150 scientific journal and conference papers had been published mentioning the hosting capacity term. Moreover, the author analysed that the number of publications has increased after 2010. Since then, the hosting capacity concept has been used as a term and as a methodology by network operators, by researchers as well as energy regulators (BOLLEN, 2017; ETHERDEN, 2012). Additionally, the hosting capacity concept has been used to evaluate the benefits of voltage regulation of the electrical system in order to improve it.

Several studies, for example (ALTIN, 2014; CAPITANESCU et al., 2014; DUBEY, 2017; RYLANDER et al., 2015; SANTOS et al., 2014), have been carried out on the hosting capacity concept in many different paths. Those studies calculated the hosting capacity for distribution networks in regard to voltage rises, as an example, as well as for new “prosumers” (producers and consumers at the same time). Different methods have been applied to determine the hosting capacity value of existing distribution networks to accept DER. Most recent evidence suggests a statistical approaches, aimed at defining the optimal generation location and sizing (ABDEL-SALAM et al., 2013; BACCINO et al., 2012; CAPITANESCU et al., 2014; MENNITI et al., 2012; RYCKAERT et al., 2003). The hosting capacity has been estimated as a common part of large network operators, which allows for the integration of more renewable electricity production into the electrical networks under analysis (BOLLEN, 2017). It is important to highlight that what makes the hosting capacity method unique is the use of power quality indexes in order to calculate a global value of hosting capacity, providing the system with a bigger range of reliability. More recent shreds of evidence (BOLLEN, 2017; ETHERDEN, 2012) suggest that other performances indexes, such as stability and protection and its limits, can be defined as a variable to the hosting capacity method. Other authors have analysed different impacts and methods to define the hosting capacity concept, as will be shown below.

In (DUBEY; SANTOSO, 2017), studies have shown that a high photovoltaic (PV) penetration can cause voltage rises as well as reverse power flow concerns in the distribution network. It shows the hosting capacity for PV systems depends on various key factors, such as the voltage class of the feeder, PV location, short circuit capacity, voltage regulations, among others. The main focus of the author was to calculate the sensitivity of the hosting capacity to various factors affecting it.

In (SÁIZ-MARÍN et al., 2014), the authors investigated the local hosting capacity for a wind-harvesting network, which may be limited because of steady-state bus voltage limits. Also, the paper addresses how the wind farm voltage control provision takes place and how to increase the local hosting capacity.

Another important issue is addressed in (BACCINO et al., 2012). The paper describes a methodology, based on an extension of the hosting capacity concept, aimed at assessing the effects of plug-in electric vehicles (PEVs), which have been charging on low voltage distribution networks (LV). Moreover, an index called time-dependent hosting capacity was proposed, thus making it possible to include in its formulation the charging duration of PEVs as well as the grid’s constraints.

More recent evidence (BOLLEN, 2017; ETHERDEN, 2012) addressed the hosting capacity as a tool for distribution-system planning under uncertainties. The tool was illustrated by estimating the willingness of two low-voltage networks for increasing amounts of customers with PV panels or with EV chargers. Moreover, general aspects of the hosting capacity calculations have also been discussed, such as performance indices, limits and calculation methods. Those aspects are discussed in relation to other phenomena as well (overcurrent, voltage unbalance, harmonic, among others).

A mathematical model will be introduced in this thesis, addressing an applicability of new local PV hosting capacity methodologies in relation to voltage rise due to harmonic distortion caused by PV connected at a LV. The researcher analyses the penetration of those PVs in a university campus, which was carried out via measurement processes and later, by computer simulations, thus evaluating this new concept.

Further work needs to be carried out to establish whether the hosting capacity concepts could be extended in dynamic analysis, for example, which is particularly relevant when the power quality indexes have a time dependency in its uncertainties.

Additional work on time dependency would help to more accurately estimate the hosting capacity for real situations.

The hosting capacity approach has raised many questions in need of further investigation in order to bring deeper conclusions. This is a vital issue for future researchers. As shown before, future work should concentrate on enhancing the quality of the hosting capacity results in one unique platform since, as demonstrated, there are many ways to calculate the hosting capacity value for different phenomena and type of DERs. These findings suggest the following directions for future research: linked power quality issues for the distribution system, hybrid systems and its impacts, physical issues of DERs, among others. The prospect of being able to accurately calculate the hosting capacity, serves as a continuous stimulus for future work.

1.4 Thesis Outline

The research questions posed in Section 1.2 are addressed in 6 chapters of this thesis. The first chapters of the thesis will provide an overview of the fundamental concepts in order to best understand the new approach proposed by the author. The three sub-questions will be mainly addressed in the numerical analysis group (Chapter 6) and Implementation (Chapter 7). The chapters are organized as follows.

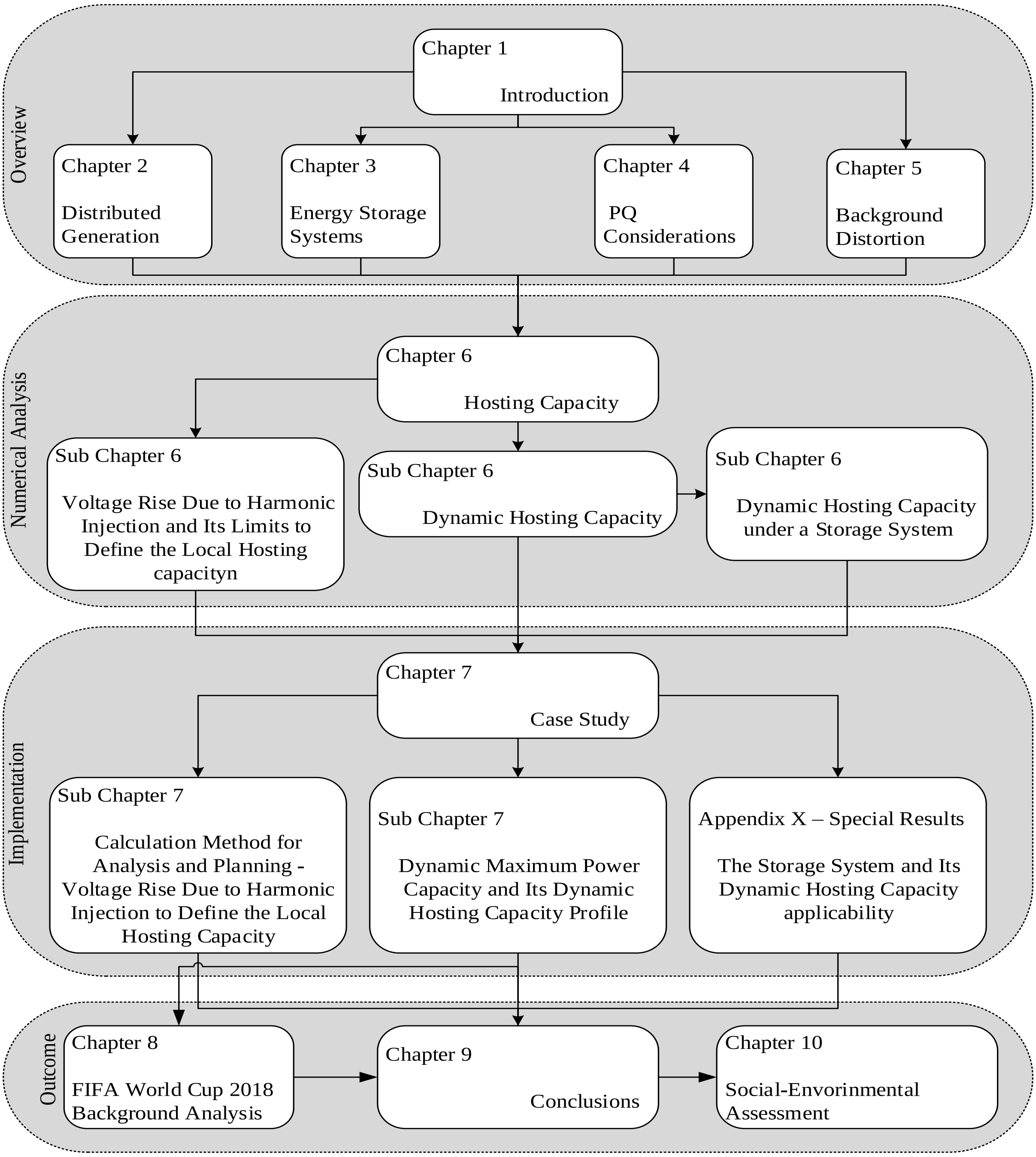

Figure 1.4 – Schematic of the thesis structure.

Chapter 2: **Distributed Generation**. This chapter provides the background information of the Distributed Generation (DG) concept and how it has come to be used to refer to new production paradigms. Thus, the Distributed Energy Resources (DER) are defined as well referring to a fraction of generated electric power delivered by consumers that own small generation units. In this chapter, the large-scale integration of DG/DERs has important impacts on the network, where the security, reliability and quality of service are shown. A discussion of power quality issues is in the scope of this chapter.

Chapter 3: **Power Quality Considerations.** This chapter is organized in two main sections, the local and international standards in relation to the power quality phenomena. Problems regarding voltage rise and harmonic distortion are discussed in adjacent sections, as are their numerical limits and calculation procedures.

Chapter 4: **Energy Storage Systems.** Energy storage technologies are becoming more and more important regarding the mitigation of challenges due to interconnection of DG/DERs into the distribution grid. In this chapter, a brief overview of energy storage systems is given. As the purpose of this chapter is to present an overall benefit from storage systems applied into distribution systems, it is important to notice that a specific technology will not be chosen, just a general one.

Chapter 5: **The Background Distortion.** In this chapter, the purpose is to provide a brief discussion of the definition and modelling of *Background Harmonic Distortion (BHD)* regarding electrical systems due to additional connections, such as consumers, distributed degeneration, nonlinear loads, among others.

Chapter 6: **Hosting Capacity Concept.** In this chapter, the concept of PV local hosting capacity will be discussed and applied through the evaluation of allowed voltage rises due to the harmonic distortion, as will its application be considering the dynamism of the local PV hosting capacity. Thus, storage systems will be presented as a powerful tool to improve the distribution systems under analysis.

Chapter 7: **Case Study.** This chapter validates the proposed method in three main parts. The first part addresses an application of calculation of the local PV hosting capacity value considering voltage rises due to the harmonic distortion caused by the electronic power of the inverters and the harmonic background of the network. Moreover, in this chapter, a benefit of this method is addressed as dynamic hosting capacity, using the data collected from the system analytically, and by observing a set of results. The last part also addresses an extension of the results from the previous section, in order to demonstrate the efficiency of energy storage systems to solve voltage rise problems due to reverse power flows. This solution will be proposed as an integration into the existing operational system.

Chapter 8: **Case Study – The Impact of FIFA World Cup 2018 on Background Distortion**: This chapter discusses the impact of Brazil's national team's matches on the electrical grid. Firstly, a general analysis regarding the load profile is presented. Secondly, the harmonic distortion profile is provided by measurements in the transmission system. Then, local measurements are made in order to analyse the power quality indexes as well as their dynamic hosting capacity profile and their impact on the system.

Chapter 9: **Conclusions:** This chapter covers the overall conclusions, recommendations and contributions from the current research for future and possible researches.

Chapter 10: **Social and Envorinmental Assessments:** This chapter covers an overview of the impact of the hosting capacity approach considering the improvement of social and environmental issues. The hosting capacity approach can be examined as a tool aimed at maximizing socio-environmental well-being.

2. DISTRIBUTED GENERATION

2.1 Initial Considerations

This chapter gives a brief overview of Distributed Generation (DG) and Distributed Energy Resources (DERs), including its general concepts, basic aspects and impact into the grid. This chapter begins by examining the general concept and basic aspects of DG, as well as its current technologies. The next section looks at the questions of DERs and its characterisation into the distribution systems. Impact issues regarding the connection of DG and DERs are discussed in later sections of this chapter.

2.2 Distributed Generation Concept – DG

Distributed Generation (DG) is widely considered to be the most important concept in the sustainability worldwide scenario. DG is defined as the generation directly installed in the distribution network, very near to the demand (ENERGY; CHALLENGE, 2017). In other words, the integration of renewable energy sources into distribution systems is called DG (SHAYANI, 2010).

It is known that the presence of small generators close to the loads may result in a range of benefits to the power system, as well as to the concessionaires. These benefits are listed below according to (CEMIG, 2018).

i. Postponement of investments regarding the expansion of distribution and transmission systems;
ii. Lower environmental impacts and its benefits;
iii. Improvement of the voltage level into the systems, over the heavy load period;
iv. Energy efficiency due to the reduction of losses and electricity transmission;
v. Diversification of the energy matrix;
vi. The encouraging for creating new business models, which will be applicable to the energy sector.

In this context, the Distributed Energy Resources (DERs) can be defined as well.

2.3 Distributed Energy Resource Concept – DER

In addition to the concept of DG, another concept can also be associated to production methods in which only a fraction of generated electric power is delivered by consumers that own small generation units (ANDRÉN et al., 2014). These are usually designated as Distributed Energy Resources (DERs). Other definitions of DERs present it as small, geographically and dispersed generation resources located in the distribution systems (ANDRÉN et al., 2014). Additionally, still according to (ANDRÉN et al., 2014; RIBEIRO et al., 2001), DERs could partially or completely offset consumer electrical demand. DERs typically use renewable energy technologies, such as small hydro, biogas, solar power, biogas and wind power. Additionally, DERs can be designated as energy storage devices, which are often called Distributed Energy Storage Systems (DESS). Moreover, DERs are designated as a tool for energy efficiency and demand response resources.

Within the next few years, DERs are likely to become an important component in the global energy system, mainly in the context of the energy evolution (ANDRÉN et al., 2014; MEHRIZI-SANI, 2013). Some researchers have addressed the question of efficiency improvement and falling technology costs, which are designed to accelerate this tendency. This fact is going to happen within DG, specially DERs. Issues of regulatory frameworks have been trying to catch-up with a range of technologies, as well as changing energy users demand in many countries around the world.

According to (MEHRIZI-SANI, 2013), DERs will rapidly become an issue, with countries that do not take the necessary steps to integrate it facing sensitive energy risks, infrastructure executions and investments challenges. A major issue of DERs is related to the environmental aspects. Furthermore, DERs could offer major benefits to reduce carbon emissions and address localized pollution, as some consumers are using them to achieve their own environmental goals. It is important to highlight that DERs will improve the environmental sustainability of the grids.

2.3.1 Enabling more DERs in the Grid

Countries, which have been having rapidly increasing volumes of DERs, are deploying an extensive variety of tools and strategies to integrate these sources and technologies without compromising reliability, security and affordability, according to (SLAUGHTER; MOTYKA; MCCUE, 2016).

A challenge in the field of DERs is to find the most indispensable solution, where DERs can be integrated, and that enable their use in order to bring safety and improvement to the grids. The community has raised some issues about this topic. In the light of recent events in integration and enabling of DERs, there is considerable concern about these matters. Ten solutions are listed below according to (SLAUGHTER; MOTYKA; MCCUE, 2016):

i. Redesigning markets;
ii. Improving forecasting;
iii. Accessing dispatchable centralized generation resources;
iv. Tapping into dispatchable DERs;
v. Deploying energy storage;
vi. Expanding transmission;
vii. Increasing regional coordination;
viii. Planning/optimizing location of DERs;
ix. Testing new technologies and Modernizing the grid.

2.4 The Classification of DG and DERs.

Alternative renewable sources of generation may take the form of wind power, fuel generators, photovoltaic cells, micro turbines, among others. The use of these sources is being promoted due to their development, as they can present the most efficiency and lowest cost of installation and solution. Table 2.1 classifies them according to their size, which means, their most common installed capacity.

Table 2.1– Classification of DG and DERs in the distribution systems (AEMC, 2018).

Classification	Technical Definition	Typical Installation
Micro	Less than 2 kW and connected to low voltage network	Rooftop solar PV
Mini	Greater than 2 kW and up to 10 kW single phase or 30 kW three phase	Fuel cells, combined heat and power systems
Small	Greater than 10 kW single phase or 30 kW three phase but no more than 1MW	Biomass, small hydro
Medium	Greater than 1MW but no more than 5MW	Biomass, hydro, local wind generating units
Large	Greater than 5MW	Co-generation, hydro, solar thermal. Many wind farms are connected in distribution systems

2.5 The Impact of DG/DER into the Distribution Systems

In the history of DG and DERs integration, the focus has always been to find a safe, reliable and cost-effective interconnection into the distribution grids, since the main purpose has always been to follow the energy policies objectives and customer preferences (REW, 2018).

Renewable sources cause impacts when connected to the conventional distribution grid due to the change of topology, because the distribution systems are passive and planned for the presence of a source generator or utility and for unidirectional power flow. These systems will be classified as active systems if they present a bidirectional power flow cooperating as energy consumer and power generator. As the distribution systems were not designed to receive this bidirectionality of the energy flow, these could present problems due to the growth of the DG and DERs into the system (TREVISAN, 2011). Previous work (TREVISAN, 2011; GONÇALVES et al., 2010) has focused on other main impacts, such as: voltage regulation problems, frequency variation, changing of short-circuit -level, non-intentional islanding, power quality disturbance in general, economic problems due to the level of penetration of these DG and DERs sources, among others.

The insertion of a few sources of GD and DERs into the distribution system has practically no impact, unless the distribution system presents a systemic weakness. However, the world's tendency is that there will be a considerable growth of DGs and DERs in the next few years, making the disturbances very significant, with remarkable effects on the grid.

In relation to the power quality disturbances due to the insertion of DG and DERs, we can list impacts such as voltage rises, short interruptions, long-term interruptions, harmonic distortions, voltage fluctuations, voltage imbalances, among others (OLIVEIRA et al., 2015). In the next subtopics voltage rises and the harmonic distortion due to DG and DERs will be defined and described as the base objective of this thesis.

2.5.1 The Voltage Rise due to DG/DERs – Power Quality Disturbance

The presence of DG and DERs in the distribution system can compromise the efficiency of the system regarding voltage variations. The voltage variations can compromise the power quality indexes provided to the consumer, as well as lead to a reduction in the lifetime of voltage regulating equipment.

A serious monitoring of the voltage profile in the busbars is necessary in order to analyse if its limits are being exceeded. When the power flow is reversed, the voltage rise may increase too much depending on the amount of generation exported to the load connected at the PCC. As an example, if the relationship between the PV and the installed load is high, the voltage rise will be a major problem, which means, the higher the generation is and the less the consumption of load is, the higher the voltage rise will be.

2.5.2 The Harmonic Injection due to DG/DERs – Power Quality Disturbance

In the current DG and DERs scenario, due to the large presence of power electronics devices in the distribution systems, voltage distortions have been observed in the feeders (HARRISON; DJOKIC, 2012). Some DG and DERs technology, such as PV systems, are connected to the distribution network through inverters, which use power electronic interfaces. The insertion of this type of generation source can inject harmonic components into the system (OLIVEIRA et al., 2015). Several international standards establish the amount of harmonics that can be injected into the power grid due to the DG and DERs electronic interface. These standards will be discussed and detailed further.

2.6 Final Considerations

The concept of DG and DERs within the distribution systems have been presented as well as their technologies, which have been lately applied to the renewable energy field, considering their benefits and challenges over the years. The main impacts caused by this type of generation were conceptualized. The power quality consideration can be found in the following chapters in order to amplify what has been discussed before.

3. ENERGY STORAGE SYSTEMS

3.1 Initial Considerations

Power systems, such as transmission and distribution, are experiencing massive changes due to the new grids technologies, which have been impacting directly their operational systems and quality of service. Lately, a considerable growth of electronic loads has taken place, which has resulted in serious issues in the power quality field. Moreover, with the continued electric load growth, the generation and transmission systems have not been able to expand properly in order to meet these demands (RIBEIRO et al., 2001). Additionally, power sources into the distribution system have been included as well, such as the DG and DERs, which are the new reality in the distribution grid. To go over the main points, all those scenarios result in technical, environmental, operational and governmental regulation issues.

In this context, energy storage technologies applied into the systems can provide impactable benefits in order to improve issues of supply and power quality in the distribution systems, for example. In this scenario, energy storage systems have become an important tool leading to an improvement of the grid, supplying the load demand, when it becomes bigger than the local generation, as well as solving power quality disturbances (RIBEIRO et al., 2001; ABDULGALIL et al., 2018). Regarding the power quality, the energy storage system can provide instantaneous voltage support in order to maintain the voltage profile. This can be achieved by injection or absorption of active or reactive power (SPERTINO et al., 2012; DRINČIĆ, 2018). To reach this goal, a mathematical hypothesis should be proposed regarding local hosting capacity, which is going to be discussed in further chapters. The present chapter aims to call into question the technologies of energy storage systems and their applicability into the power quality field.

3.2 Energy Storage Systems Technologies

The term “energy storage system” has come to be used to refer to any kind of electricity storage, but AC energy can be stored if the electricity is converted in electromagnetic, electrochemical, kinetic or potential energy (RIBEIRO et al., 2001). According to (RIBEIRO et al., 2001; ABDULGALIL et al., 2018; DRINČIĆ, 2018), three important factors must be considered in the energy storage system. Firstly, the amount of energy that can be stored. Secondly, the rate of energy which can be transferred into or out of the device. Last, but not least, the technology of the device, which will impact directly its application.

The power energy ranges regarding near-to-midterm technologies have been used by (RIBEIRO et al., 2001) to refer to the four possible energy storage technologies. It is important to highlight their benefits, such as transmission enhancement, power oscillation damping, dynamic voltage stability, tie-line control, short-term spinning reserve, load levelling, under-frequency load shedding reduction, circuit break reclosing, subsynchronous resonance damping, and power quality improvement (RIBEIRO et al., 2001; DRINČIĆ, 2018). The type of technologies is shown in Figure 3.1.

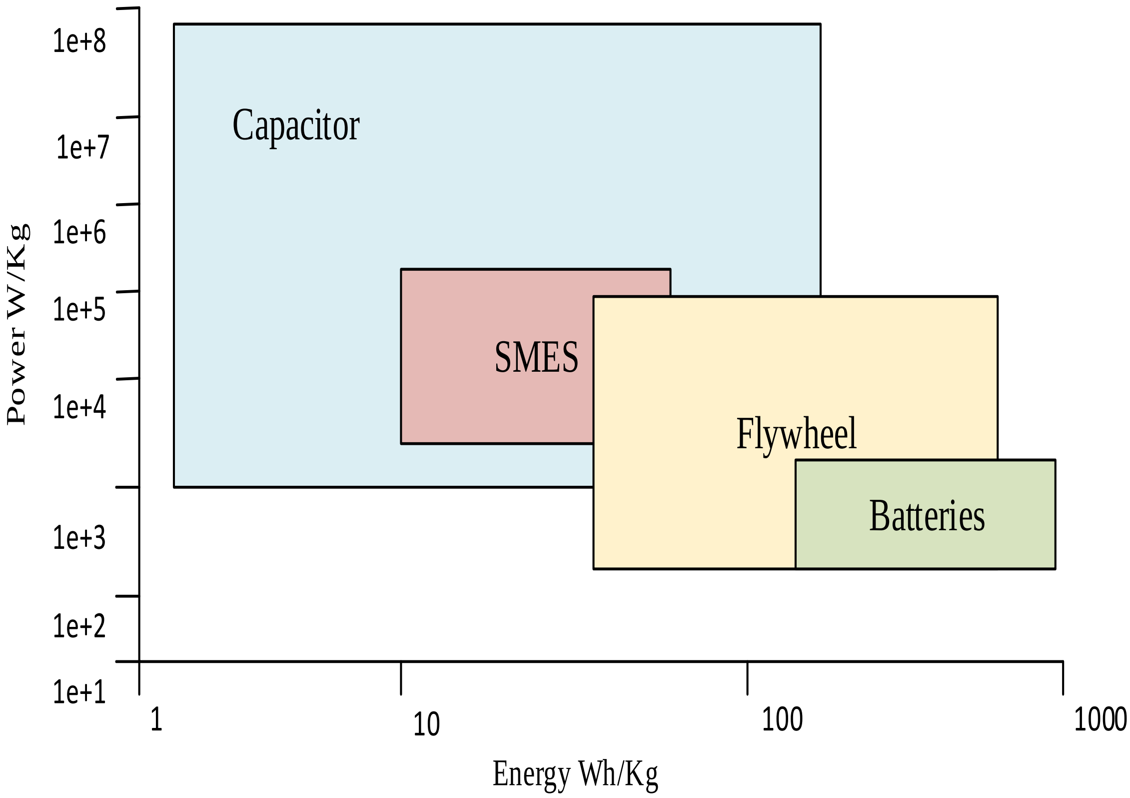

Figure 3.1 – Specific power and specific power rangers technology (RIBEIRO et al., 2001).

3.3 Energy Storage Systems Technologies

It has been suggested (RIBEIRO et al., 2001) that a range of technologies seems to be an innovative approach into the energy storage systems, which is shown in Table 3.1.

Table 3.1 – Energy Storage Systems Technologies.

Technology	Advantages	Disadvantages	Applications
Superconducting Magnetic Energy Storage (SMES)	SMES systems have attracted the attention of both electric utilities and military – (a charge-discharge efficiency over 95%);	SMES is still costly when compared to the other technologies, but several factors have been taking in account to decrease its cost – coil configuration, energy capability, structure and operating temperature.	Load levelling, dynamic stability, transient stability, voltage stability, frequency regulation, transmission capability enhancement, power quality improvement.
Battery Energy Storage Systems (BESS)	One of the most cost-effective energy storage technology; They are "charged" due to internal chemical reaction; mature technology; High energy density. High energy capability, round trip efficiency, cycling capability, life span and initial cost.	Due to the chemistry, BESS cannot operate at high level power for long periods, heating results from rapid and deep discharges, which impacts its lifetime (limited cycle of life) and environmental concerns.	Offers a wide range of power system applications such as area regulation, area protection, spinning reserve, and power factor correction.
Advanced Capacitors	Ultracapacitors: high peak-power, low energy situations. Also, capable of floating at full charge for ten years; can provide extended power availability during voltage sags and momentary interruptions; can be stored completely discharged, installed easily, are compact in size, and can operate effectively in diverse (hot, cold, and moist) environments; available commercially at lower power levels.	DC storage has a limited use as large-scale energy storage devices for power systems;	Ultra-capacitors and hyper capacitors have been used in power quality applications. Ultra-capacitors: DC bus of motor drives; interfaced to the DC bus of a distribution static compensator
Flywheel Energy Storage (FES)	Compact lightweight energy storage devices; New technologies - high charge/discharge efficiency	Rotational losses due to drag from air and bearing losses result in significant self-discharge, which poses problems for long-term energy storage	Several power system applications, including power quality applications; peak shaving; stability enhancement.
Other technologies	pumped hydroelectric systems, compressed air energy storage (CAES), and flow batteries (a variation on the fuel cell now in the demonstration stage).		

3.1 Final Considerations

A discussion of energy storage systems and their technologies has been presented. Further questions regarding energy storage systems can be found in the references cited throughout chapter 3. Our conclusions are drawn in the application section using the previous knowledge in respect to the application of energy storage systems in distribution networks.

4. POWER QUALITY CONSIDERATIONS

4.1 Initial Considerations

According to (COMMITTEE, 2006). the term power quality (PQ) has come to be used to refer to “the concept of powering and grounding electronic equipment in a manner that is suitable to the operation of that equipment and compatible with the premises wiring system and other connected equipment.” In the literature, power quality tends to be used to refer to designate the best path in the electrical system regarding voltage systems in order to turn out its sinusoidal form at nominal voltage level (OLIVEIRA et al., 2014). The subject, which we shall call “*power quality issues*” is any kind of disturbance from the sinusoidal form that leads to a non-nominal level, which can be defined as power disturbance as well. These subjects can be defined as: overvoltage, undervoltage, swell, interruption, harmonics, among others. Two main types of these aspects will be dealt with in more details. These aspects are: voltage rise or overvoltage and harmonic voltage distortion.

In this chapter, the meaning of the national and international standard of the cited aspects will be discussed further.

4.2 Power Quality National Standards – PRODIST

The first considerations of PQ in Brazil were conceived in 1995, when the Brazilian Electric System went through an innovative restructuring process related to its new regulation. In the history of regulation of electricity in Brazil, the *Electrical Energy National Agency* (ANEEL) was created in 1996. Afterwards, ANEEL has created the *National Operator of the Electric System* (ONS), whose duty is to establish and control procedures regarding generation and transmission systems. Since 2008, ANEEL has been launching regulation procedures in relation to distributions grids called *Procedures for Distribution of Electric Energy in the National Electrical System* – PRODIST (PRODIST Modulo 8, 2015; PRODIST Módulo 3, 2012; COLNAGO et al., 2012). Additionally, ONS has also created what they refer to as “grid procedures for transmission and generation grids”.

It is important to notice that all this restructuring of the Brazilian electrical system had the aim to introduce a competition in generation, “deverticalization” of utilities and establish an open access to the generation, transmission and distribution systems (COLNAGO et al., 2012). Figure 4.1 presents an overview of the Brazilian electrical system regulatory and operation agencies.

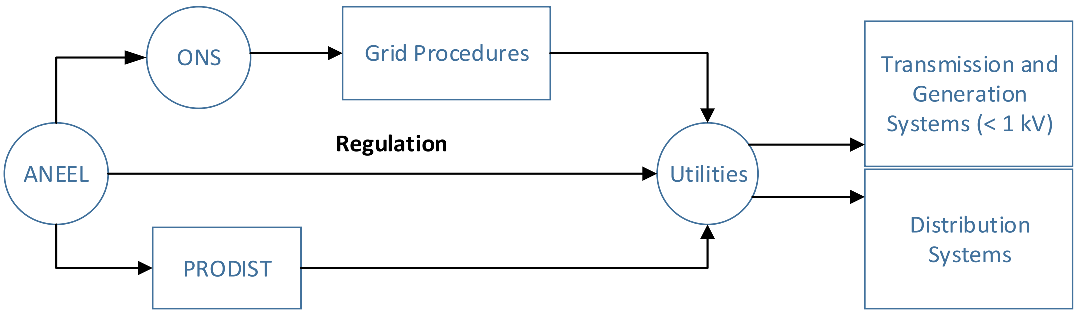

Figure 4.1 – Relation among agents, system and its national standards, based on (COLNAGO et al., 2012).

It has now been suggested by PRODIST an entire chapter dedicated to PQ issues (PRODIST Modulo 8, 2015), which is called the PQ standards – Module 8. This chapter presents all the PQ indexes and their limits, calculi methods, protocols to be followed in order to analyse and bring improvements to the distribution networks (PRODIST Modulo 8, 2015). Thus, the PQ standard is separated in two groups: Quality of Service and Quality of Product. The Quality of Service is concerned with the reliability of the system regarding sustained interruptions, while the Quality of Product is concerned with the steady state and transient phenomena. The subject of study in this thesis relates to the Quality of Product, classified in: Steady State Voltage, Harmonic Voltage, Voltage Unbalance, Voltage Fluctuation, Voltage Sag and Swell, Frequency Variation and Power Factor.

Although there are several PQ indexes which could be further analysed, the following subsections will concern to the Steady State Voltage in relation to voltage rise and the harmonic voltage. These two factors are the base of the methodology that is going to be proposed in the following chapters, and for this reason both base phenomena must be well understood.

4.2.1 Steady State Voltage – Voltage Acceptable Levels

In the section Steady State Voltage – section 2 of (PRODIST Modulo 8, 2015), this study presents the appropriate, precarious and critical limits for the steady state voltage level, as well as the individual and collective voltage indicators. Thus, the measurement and recording data are defined in order to register when the voltage measurement exceeds its indicator's limits. The steady state measurement is performed in intervals of 10 minutes at the PCC and its period is one week, which is equal to 1008 intervals.

Furthermore, the term "*electrical voltage compliance*" is defined, which refers to the comparison of the voltage value obtained by deterministic measurement, at the PCC, to the voltage levels specified such as: adequate, precarious and critical.

Regarding the contracted voltages at the distribution level, the voltage is contracted at the point of connection (PCC), where, for the nominal operating voltage higher than 1 kV, it must be between 95% and 105% of the nominal operating voltage of the system. Thus, the measurement period can be classified in a set of voltage levels. Figure 4.2 shows the voltage values normalized by Module 8 of PRODIST.

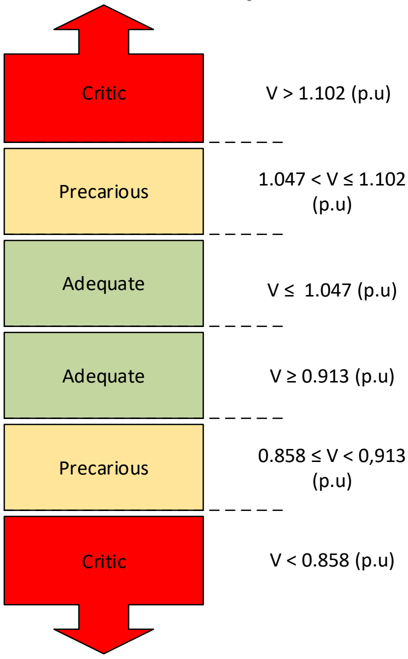

Figure 4.2 – Voltage values in relation to measurement analysis based on (PRODIST Modulo 8, 2015; COLNAGO et al., 2012).

4.2.1 Voltage Unbalance

Voltage unbalance is a phenomenon characterized by any difference in the amplitudes between the three phases of voltage in the three-phase system considering the electrical phase difference of 120º between the phases related to the same system (PRODIST Modulo 8, 2015). Thus, one way to calculate the unbalance voltage is given by (4.2.1).

$$FD(\%) = \frac{V_-}{V_+} x100 \tag{4.2.1}$$

Where, V_- is the magnitude of the negative sequence of voltage and V_+ is the magnitude of the positive sequence of voltage.

Voltage unbalance has been raising interest due to single-phase production units, mainly PV, which will increase the unbalance voltage in the low-voltage networks (CIGRE, 2018). The majority of them will be connected to the low-voltage feeder, which can have side effects at the PCC, one of the main concerns regarding unbalance voltage into distribution systems.

Experiments on voltage unbalance were carried out by (SCHWANZ et al., 2017) regarding the high-penetration of single-phase photovoltaic inverters, using a stochastic model to estimate the increase in voltage unbalance with random distribution of the inverters over the three-phase system. In their analysis of voltage unbalance due to single-phase inverters, they show the rise in unbalance voltage for customers connected to the rural network in Northern Sweden, for example. Figure 4.3 shows voltage unbalance for a given number of customers with PV.

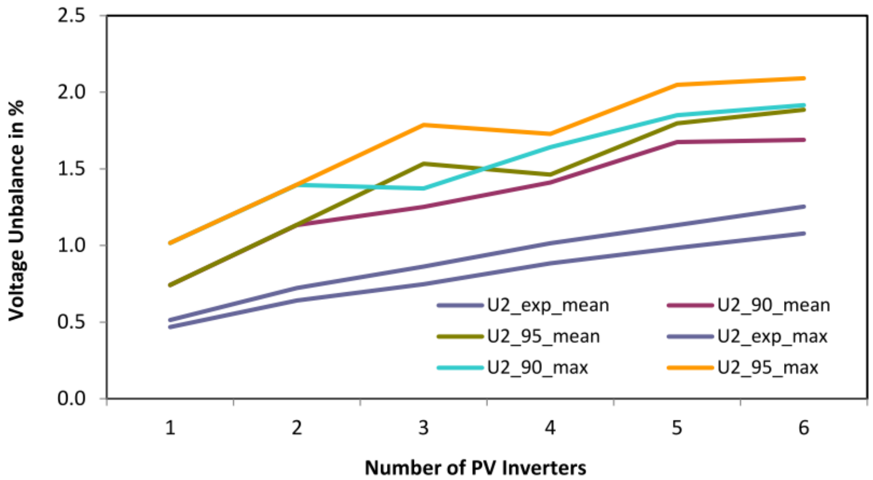

Figure 4.3 – Voltage unbalance versus the number of PV inverters (SCHWANZ et al., 2017).

It is possible to notice that there is an increase in voltage unbalance due to the high-penetration of PV inverters. Furthermore, large single-phase loads, such as vehicle charges and heat pumps will rise the unbalance voltage in the systems (CIGRE, 2018). It is important to highlight that there is less similarity when compared to solar production, but it must be considered as well.

4.2.2 Harmonic Voltage Distortion

In (PRODIST Modulo 8, 2015), the harmonic distortion is defined as the phenomena associated to deformations in the voltage and current waveforms in relation to the sinusoidal signal of the fundamental frequency. In this scenario, the background harmonic distortion can be defined as the aggregated level of harmonic distortion present in the supply voltage of a PCC, previous to the connection of a new linear or non-linear load or generator. This distortion may vary along the day in shape, in magnitude and phases of individual components, as well as it may consequently add or reduce the resulting distortion after the connection of a new non-linear load or generator. This distortion is due to the flow of non-sinusoidal currents into the system. In section 4 of PRODIST – Module 8, the terms used to calculate the harmonic distortion are defined, namely: total harmonic voltage distortion ($DTT\%$), total harmonic voltage distortion for non-multiple pairs ($DTT_p\%$), total harmonic voltage distortion for odd components non-multiple of 3 ($DTT_i\%$), and total harmonic voltage distortion for the multiple components of 3 ($DTT_3\%$).

The mathematical expressions to calculate the $THD\%$ and $IHD_h\%$ are shown in (4.2.2)and (4.2.3):

$$DTT_{P,I,3}(\%) = \frac{V_h}{V_1} x100 \tag{4.2.2}$$

$$DTT(\%) = \frac{\sqrt{\sum_{h=2}^{hmax} V_h^2}}{V_1} x100 \tag{4.2.3}$$

Where,
$h = 2 \dots 50$;
V_1 Harmonic voltage of fundamental frequency;
V_h Harmonic voltage amplitude of order h.

The limits of harmonic distortion are well defined by Module 8, where the standard suggests reference values for when the electrical grid is being planned. In Table 4.1, the planning and analysis values for voltage level ≤ 1 kV are shown and defined regarding the national standards.

Table 4.1- Limits of the harmonic distortion (PRODIST Modulo 8, 2015);

Indicator	Vn ≤ 1 kV
DTT95%	10 %
DTT(P)95%	2.5 %
DTT(I)95%	7.5 %
DTT(3)95%	6.5 %

These values will be considered in distribution systems regarding DG/DERs insertion. They will also be used as comparing parameters to analyse the network efficiency and its impact due to the harmonic background. The PRODIST may have a limitation with respect to the harmonic individual distortion. This limitation is evidence of major acceptable harmonic individual values which may or may not bring considerable impacts and variance when compared to international standards. For this reason, this study will be based on international standards and the presentation of the local standard will be used as a comparative parameter.

4.3 Power Quality International Standards – IEEE considerations

This section presents an overview of international limits for electrical systems from IEEE standards. There are two main IEEE standards regarding harmonic distortion. These standards are: The IEEE 519, which sets limits for harmonic voltage and current at the PCC. According to (KEY; HALL, 1992), this standard is used to prevent harmonic currents traveling back to the power system which may or may not affect other consumers. On the other hand, the IEEE 1547 intends to test the harmonic interconnection in order to analyse its access under a controlled set of external and internal conditions of the DER unit, which will meet the harmonic limits specified by this standard (IEEE, 2003). In order to understand the harmonic emission and its consequences into the electrical systems, these two standards will be briefly discussed below.

4.3.1 IEEE Std 519-2014 – Recommended Practice and Requirements for Harmonic Control in Electric Power Systems

In order to calculate the individual harmonic distortion (IHD) and the total harmonic distortion (THD), it is used the same formulation given in (4.2.2) and (4.2.3), respectively.

According to (KEY; HALL, 1992), at the PCC, the IEEE 519 recommends that the harmonics in the system is considered a cooperative responsibility which involves both end-users and system operators or owners. The standard recommends voltage and current limits. Therefore, the recommended values are based on the fact that some level of the harmonic distortion will be acceptable, which means both owners and users could work willingly to keep the harmonic voltage level within acceptable limits (PRODIST Modulo 8, 2015; KEY; HALL, 1992). However, the limitation of harmonic current injections could be determined by users, thus the voltage distortion can be kept at acceptable levels.

The IEEE 519 also recommends that the limits must be applied at the PCC and it shouldn't be applied to neither individual piece of equipment not at points within the user's facility [6]. At the PCC, users and operators should follow all values in percentage of rated power frequency voltage. The voltage distortion limits are shown in Table 4.2. As mentioned before, the values shown below refer to the level ≤ 1 kV.

Table 4.2 – Voltage distortion limits to V ≤ 1 kV (IEEE 519, 2014).

Voltage at PCC	Individual Harmonic Distortion (%)	Total Harmonic Distortion (%)
V ≤ 1kV	5.0	8.0

The results set up is based on the IEEE 519 standard proposed by (IEEE 519, 2014). It was chosen this particular apparatus on account of the fact that the values shown before will effectively answer the questions, which are going to be proposed later in this study. However, it was opted for these values because they represent an average value for those distortions' limits.

4.3.2 IEEE Std 1547-2003 – IEEE Standard for Interconnecting Distributed Resources with Electric Power Systems

The IEEE 1547 is the first standard which discussed interconnection standards of DERs into electric power systems. Conventionally, the utility grid wasn't designed to accommodate active generation as well as a storage system at the distribution level (IEEE 1547, 2003). The problem is ruled by major issues and obstacles when the DER is being used and integrated in the distribution grid. Moreover, the IEEE 1547 will focus on the technical specifications for the interconnection of DERs, where it will provide better requirements due to the performance, operation, testing and maintenance of the interconnection of DERs (IEEE 1547, 2003). It is important to notice that the IEEE 1547 includes DER synchronous machines, induction machines and power inverters/converters. The standard also defines that the criteria should apply to a capacity equal to 10 MVA or less at the PCC.

According to (IEEE 1547, 2003), for example, "*the DERs should be operated with a predominant voltage source with a short circuit capacity no less than 20 times the DER rated output current at fundamental frequency.*" Furthermore, the frequency output and voltage of the source should correspond to the rated voltage and frequency of the DER. Thus, the IEEE 1547 standard was prepared according to the motivation shown before. In (IEEE 1547, 2003), further evidence and instructions can be found.

At this point, the IEEE 1547 determines that the harmonic voltage, while powering a resistive load at 100% of the machine, should not exceed the limits shown in Table 4.3 – Maximum harmonic voltage distortion in percent of rated voltage (IEEE 1547, 2003). (IEEE 1547, 2003).

Table 4.3 – Maximum harmonic voltage distortion in percent of rated voltage (IEEE 1547, 2003).

Individual Harmonic Order	h<11	11≤h<17	17≤h<23	23≤h<35	35≤h	THD
(%)	4.0	2.0	1.5	0.6	0.3	5.0

4.4 New Types of Power Quality Disturbances

Within the next few years, new types of technologies are set to become an important component of new types of PQ disturbances. Those new technologies related to smart grids will shortly become an issue regarding new types of emissions from a new type of equipment connected to the grids (CIGRE, 2018). The main problem of these new types of PQ disturbances is no longer related to regular harmonic emissions, such as 3rd, 5th or 7th order. The new demand in the area of PQ disturbances is to define the types of abnormal emissions. Thus, these abnormal emissions can be classified into three main groups: interharmonics, subharmonics and supraharmonics based on recommendations from (CIGRE, 2018).

4.4.1 Interharmonics

According to (CIGRE, 2018) "*Interharmonics are spectral components at frequencies that are not integer multiple of the system fundamental frequency. Subharmonics are interharmonics with frequencies lower than the fundamental frequency.*" The levels of interharmonics into distribution and transmissions systems are expected to increase. This will take place as a result of the integration of new types of sources, such as DG devices (wind turbines and PV inverters, for example), industrial equipment with high efficiency, commercial loads and residential equipment (refrigerators, washing machines, among others) (CIGRE, 2018).

4.4.2 Subharmonics

Subharmonics are described as being the result of the emission of interharmonics with frequencies lower than 50 or 60 Hz, for example, from wind turbines (CIGRE, 2018).

4.4.3 Supraharmonics

The term suprharmonics has been used by (CIGRE, 2018) to refer to all frequency components in the range between 2 kHz and 150 kHz. For example, FACTS active converters and VSC-HVDC will emit supraharmonics at the switching frequency (emissions at a frequency of 12.4 kHz) (CIGRE, 2018). Moreover, still according to (CIGRE, 2018), grid-size battery storage connected through active converters is expected to inject supraharmonics.

4.5 Final Considerations

We have presented both local and international standards regarding PQ issues such as overvoltage and harmonic distortion. The evidence from this chapter points towards the idea that all standards have the same principle, particularly when the discussed topic is harmonic distortion. The results of this investigation support the idea that we are free to follow the which fits better regarding the cases; it depends on the needs of the system and the system's particularities. Taken together, these findings suggest a role for PQ issues.

In this research, it is followed specific standard considerations, which will be defined. The voltage values suggested by PRODIST – Module 8 will be used in order to analyse the voltage rises issues for the system. In relation to harmonic distortions, the IEEE 519 will be considered as a base standard. In this case, the IEEE 519 has shown more conservative harmonic limits. These topics are reserved for future discussion in the next chapter.

5. THE BACKGROUND DISTORTION

5.1 Initial Considerations

The purpose of this chapter is to present a brief discussion on the definition of *Background Harmonic Distortion* regarding electrical systems due to additional connections, such as consumers, distributed degeneration, nonlinear loads, among others.

Truthfully, high levels of Background Harmonic Distortion can result in equipment malfunction, decrease the likelihood of meeting international standards, for example IEEE 519 or IEEE 1547 (IEEE 519, 1992; WALLACE; BENDRE; WOOD, 2013) as well as the impact of the maximum amount of generation that can be connected at the PCC defined as the hosting capacity value.

5.2 State of the Art of Background Distortion

One of the key questions in the summarisation of background distortion is related with the type of sources that can be aggregated, which will either cause positive or negative impacts. Their impact aggregation will depend on the nature of these loads and sources. There is a considerable number of studies on the background distortion field. What is known about the background distortion is largely based on worldwide campaign measurement. Several authors have attempted to define the background distortion based on harmonic injection in the majority of the cases, but at the time this study is being written, there are still concepts under analysis regarding these fields. In this section, this study describes some of the main analysis conducted on background distortion aiming at clarifying concepts that will later on be presented in this thesis. In general terms, harmonic distortion, either current or voltage, can be defined as a way to describe the principle of background distortion.

In (ĆUK; COBBEN, KLING; RIBEIRO, 2013), the authors analysed the summation of harmonic currents, based on field measurements. Their justifications are based on harmonic sources, which can produce different harmonic currents. Those harmonic distortions depend on the load level. Thus, due to this fact, the harmonic voltage changing at the PCC will cause different current distortions. The authors highlighted that this process is time-varying, which makes it difficult to determine the exact magnitude and phase of harmonic currents at any given moment. Moreover, they propose a measurement campaign at different industrial systems using a 15channelmeasurement system, with three channels of voltage and 12 channels of current. They describe that the total current for one phase of the system at the LV busbar was measured taking into account the currents of all devices or group of devices connected at the same time. In Figure 5.1, the topology used by the authors can be consulted.

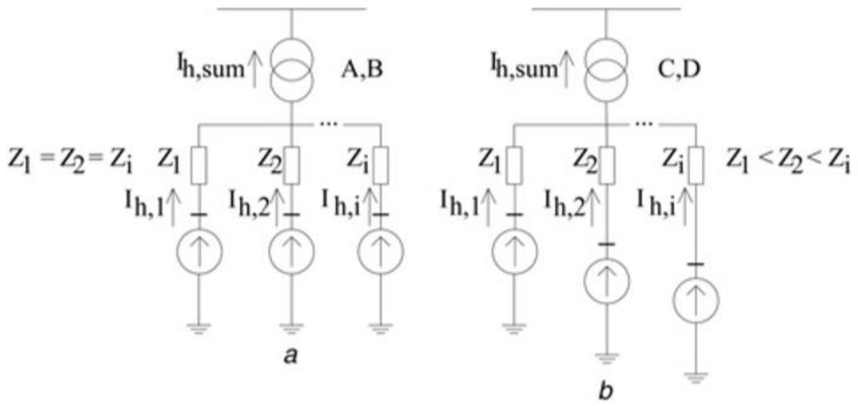

Figure 5.1 – Topology of measured sites according to (CUK; COBBEN, KLING; RIBEIRO, 2013).

It is important to highlight that the authors have conducted two different types of measurements considering the length of the cables. Thus, at locations A and B, where the loads are connected 20 meters closer to the busbar and the cables have the same length, the topology is the same. On the other hand, at locations C and D, the load distances are different. Further results and analysis can be verified in (ĆUK; COBBEN; KLING; RIBEIRO, 2013). They concluded that their analysis and technique can be useful for predicting harmonic current summation when compared to probabilistic studies, for example.

Ryckaert and co-workers (RYCKAERT; GHIJSELEN; MELKEBEEK, 2003) have investigated the influence of the background distortion on the load behaviour of the shunt harmonic impedance considered. Their justification was based on the fact that shunt harmonic impedances, or SHI, have proved very effective in relation to the reduction when compared to the harmonic propagation. Thus, in their paper, they show that SHI can reduce the line current as well as the THD caused by polluting loads, when they are modelled as simple current sources. Moreover, the paper presents an efficient model regarding the maiming power system and the polluting loads. In section 5.4, their model will be used as a starting point to describe the electrical model of linear and non-linear loads to conduct background distortion studies.

Experiments on modelling of harmonic injectors were carried out on harmonic modelling sources in 2012 by a group of researchers (ĆUK; COBEEN; KLING; RIBEIRO, 2012). They suggested that calculating harmonic voltages and currents into electrical grids needs more efficient and precise models of linear loads. Also, the authors suggested that the use of equivalent models without taking into account the impact of all impedances can lead to disassociate harmonic voltage and currents, which can directly impact the background distortion value. In their paper, they proposed a harmonic impedance technique estimation in LV networks. Thus, their analysis can be a guideline for LV networks regarding harmonic analysis. It is well-known that the appropriate choice of load models and network representations can be vital to determine the harmonic voltage and its background impact on the grids.

It is important to highlight that not only harmonic current source models and linear and non-linear models are important in terms of background distortion. The limits imposed by international standards are vital during the process of background distortion. Thus, the authors (ĆUK; COBBEN; RIBEIRO, 2014) presented a paper with a review of international limits for public networks. Furthermore, they pointed out shortcomings of these international standards, as well as propositions and improvements for these standards. In their review of international harmonic limits, (ĆUK; COBBEN; RIBEIRO, 2014) question the need for a revision of the voltage limits origins from measurement fields and current limits from emission measurements. Moreover, they concluded that the relation between the voltage and current limits regarding the IEEE 519 and IEC 61000-2-12 and 3-6 do not apply to all harmonic orders. An important point that the authors raised is that the standards are not evolving. They justified this with the fact that, currently, there are no problems in relation to harmonic voltage in the grids. They draw our attention to adopt less strict requirements in relation to the IEC and IEEE standards for LV systems. For example, in relation to a voltage THD limit, a percentage of 8% would work with no concerns and for IHD at least 3% for low-order odd orders. Although the authors have proposed some improvements to international standards, the short-term effects of harmonic voltage and currents could be carefully further analysed in other researches.

Finally, a recent review of the literature on this topic (PAPIC et al., 2018) found that it is essential to determine the contribution of facilities to the background harmonic distortion measured at the PCC. Then, the authors propose consistent test systems that can be used to validate a proposed method, as well as to compare different approaches that have been analysed throughout the years. They consider examples on how to use the grid to assess the contribution of harmonics. They also highlight that harmonic distortion at the PCC is caused by both sides of the system, the consumer side and the supply system side, both based on a mathematical model that will be discussed further ahead in this chapter. Thus, the developed benchmark system is realistic because it represents a typical medium and low voltage network supplying industrial loads. Moreover, the harmonic sources are modelled in a time domain, instead being modelled as statical current and voltage sources. These models represent with security the reality of the background distortion sources into the grids.

It is important to highlight that there is a considerable amount of literature on the background distortion. What is known about the background distortion is largely based on papers from the 30’s, when the harmonic contribution first became a concern, up until now. What was listed in this section is one of the recent and important researches in this field. This chapter also contributes with a summarisation of the background distortion review, a basis to understand the next topics regarding hosting capacity and its importance in this study field.

5.3 Aggregated Sources

There is a multiplicity of sources which can cause background harmonic distortion in the grids. Furthermore, those sources will influence the previous PCC in reference to the Total Harmonic Distortion (THD) levels defined by international standards, such as IEEE 519 (IEEE 519, 2014).

Voltage harmonic distortion is affected by harmonic currents flowing through power system impedances, such as long-distance cable parasitic inductance, distribution transformer's series impedance (WALLACE; BENDRE; WOOD, 2013) and electrical energy converters. In relation to facilities and substations, personal computers and television in household installations or commercial buildings are the largest sources of harmonic currents (WALLACE; BENDRE; WOOD, 2013; EIRGRID, 2015).

Some researchers have addressed the issue of the behaviour of the load in respect to the harmonic distortion. The behaviour of loads in respect to voltage distortion is addressed in (GHIJSELEN; RYCKAERT; MELKEBEEK, 2002), where the polluting loads can be defined and modelled as a set of current sources in parallel, defined for each harmonic order. Concerning nonlinear loads connected to the Low-Voltage busbar (LV), it is important to highlight that the harmonic levels have decreased over the years. This fact is shown in (RUBENS et al., 2006; LEITÃO et al., 2007) where the power supply of the modern television receivers have presented a much smaller harmonic injection content. In addition, the higher number of television receivers produced a higher level of harmonic cancellation. Even though these levels are lower, they must be accounted for into the system.

As long as the nonlinear loads are connected into the system, their connection will cause voltage harmonic distortions, and thus, the Background Harmonic Distortion must be considered regarding the planning and improvement of electrical networks. Based on this fact, it is important to consider the combined effect between the additional harmonic contribution generated by nonlinear equipment installed in facilities into the system and the households with typical nonlinear loads, as well as their interaction in order to define the final Background Harmonic Distortion level (EIRGRID, 2015).

5.3.1 Power Electronics in the Grid

A recent review of literature on this topic (CIGRE, 2018) found that HVDC was considered as a source of harmonics in transmission level. More recent evidence reveals that the shift from line-commutated HVDC (passive converters) to self-commutated HVDC (active converters) will address the impact of emission of low harmonic orders, such as 5^{th} and 7^{th}, 11^{th} and 13^{th}, 17^{th} and 19^{th}, which will become less significant than expected. On the other hand, higher frequencies and possibly interharmonics will have their emissions increased by these devices, as they are known as sources of harmonics. In this case, appropriate filters should be connected when required (CIGRE, 2018). Nevertheless, into transmission and distribution systems, FACTS has been used for power flow control, voltage regulation and for correction of stability issues. Thus, the implementation of these devices into the systems will be related to their harmonic injection and their effect over the systems. Moreover, the harmonic distortion caused by FACTS will be affected by an interaction between them and the network components, as well as its topology. Operation conditions changes may be included as a concern (GARCÍA; SEGUNDO; MADRIGAL, 2014).

5.3.2 Equipment connected to the Grid

New types of equipment that have been connected into the distribution grids may inject typical harmonic frequencies (3^{rd}, 5^{th}, 7^{th}, 9^{th} etc.). A recent review of the literature on this topic (CIGRE, 2018; CHIDURALA et al, 2015; RÖNNBERG et al, 2013; YANG; BOLLEN; LARSSON, 2015; YANG et al, 2015) suggests that their injection is low when compared to power electronics connected to the grid. Nevertheless, it has lately been proposed the most important issues related to the connection of DG sources into the grid is related to their diversity as much as generators and loads (CIGRE, 2018). An increasing number of studies have found that the background emissions present in PV inverters, wind turbines, water heaters, televisions and electric ovens do not work at the same time, which will impact their harmonic emissions regarding the PCC, where all these devices are connected (CHIDURALA et al, 2015; RÖNNBERG et al, 2013; YANG; BOLLEN; LARSSON, 2015; YANG et al, 2015). Based on this fact, those devices are important to consider regarding the background distortion that can be found into the grids. The next subsection will carefully analyse the harmonic emissions from some common devices connected into distribution grids.

5.3.2.1 Compact Fluorescent (CFL's) and Light Emitting Diodes (LED's) Lamps

It is well-known that CFL's and LED's would result in large increases of harmonic and current distortion in the grid (RÖNNBERG; BOLLEN; WAHLBERG, 2010). A number of studies have found that the increase in distortions level, even in the worst case, is minor than expected. Moreover, these distortions can result in cases where the aggregation effects due to these lamps may lead to a decrease in harmonic levels (BLANCO et al, 2013; GRADY et al, 1995; RÖNNBERG; BOLLEN; WAHLBERG, 2010). In Figure 5.2, the results of an investigation can be observed, where incandescent lamps were replaced by a combination of LED's and CFL's lamps (RÖNNBERG; BOLLEN; WAHLBERG, 2010).

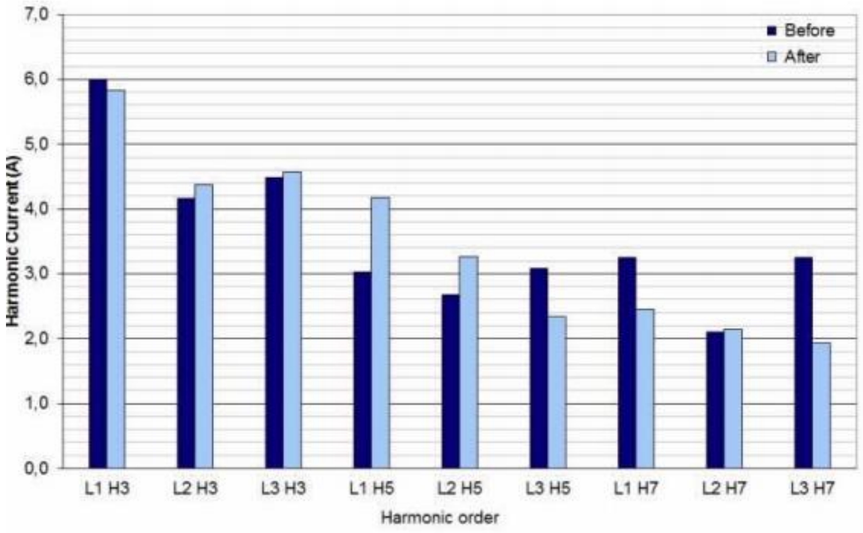

Figure 5.2 – Harmonic current emission before and after replacement of incandescent lamps by CFL's and LED's according to (CIGRE, 2018).

According to (CIGRE, 2018), the results of harmonic distortion are related with the cancellation between the non-incandescent lamps and other pieces of equipment that inject harmonics into the grid. It is important to highlight that the result of an interaction between the lamps and the equipment will directly impact the background harmonic emission.

5.3.2.2 Computers and Residential Loads

Some preliminary work on the influence of the computers was carried out in 2009. Measurements were registered during the LAN parties, where many computers were being used to play computer games (LARSSON, 2009). The conclusions of this study were summarised in three main points: there was no change in current amplitude and no change in power consumption, but the most remarkable result was the large reduction in harmonic distortion. Figure 5.3 shows the change in harmonic current throughout the years.

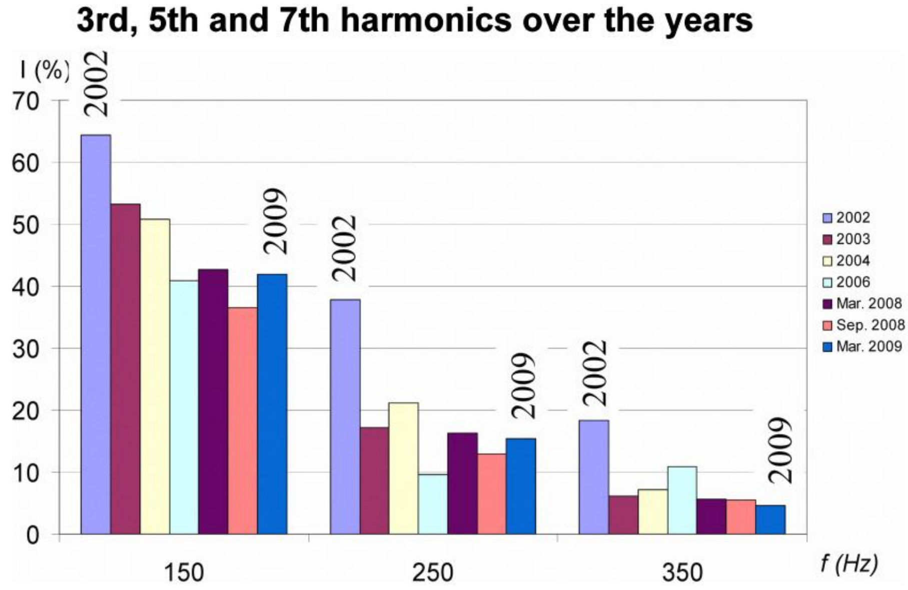

Figure 5.3 – Change in harmonic currents throughout the years (LARSSON, 2009).

Residential users may include computers, laptops, CFL's lamps, routers, battery chargers and monitors, among others. These devices are highly time-variant due to continuous changes in their load conditions, as well as system parameters, for example, voltage distortion (LARSSON, 2009). Thus, it is possible to state that not only will the magnitude of the current harmonic emission regarding those devices change, other changes are possible, namely on their phase angle. Moreover, these changes will modify their aggregation with other pieces of equipment in the grid causing disturbances on the voltage distortion (CIGRE, 2018). It is important to note that these impacts can be either positive or negative. An example of a positive impact is cited in (CIGRE, 2018). In terms of this positive impact, even a rising magnitude of harmonic current can cause a constructive impact on the voltage harmonic, but this will only occur as long as the phase shift leads to a voltage reduction over the Thevenin impedance at the PCC, reducing the background harmonic voltage and improving the conditions of the system.

To illustrate, Figure 5.4 shows an example of 5^{th} harmonic current emitted by typical residential devices.

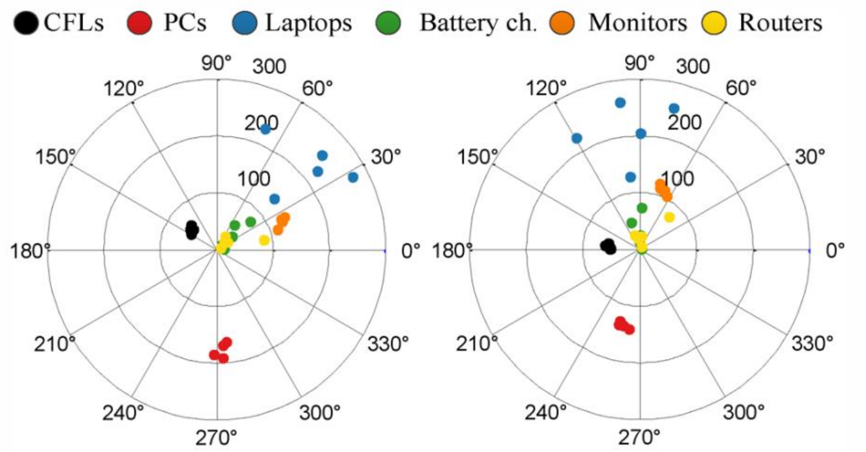

Figure 5.4 – 5th harmonic current of different devices, according to (LARSSON, 2009).

5.3.2.3 Electric Vehicles

Electric vehicles (EV's) are increasingly becoming a vital factor in harmonic injection due to the power electronic used in their charger. According to (MÖLLER et al., 2015), these rectifiers are equipped with power factor correction. Those devices will cause a switching frequency, commonly in the range of 10 kHz. Those circuits will generate a low harmonic order causing distortion in the grid to which they are connected. Thus, these devices are expected to cause unbalance in the grid, as well as background harmonic distortion. It is well-known that harmonic currents can be either nearly constant or distorted, which depends on the voltage distortion (MÖLLER et al., 2015). In order to illustrate their emissions, Figure 5.5 and Figure 5.6 show a measured individual emission regarding 3rd and 5th harmonic based on results from (MÖLLER et al., 2015).

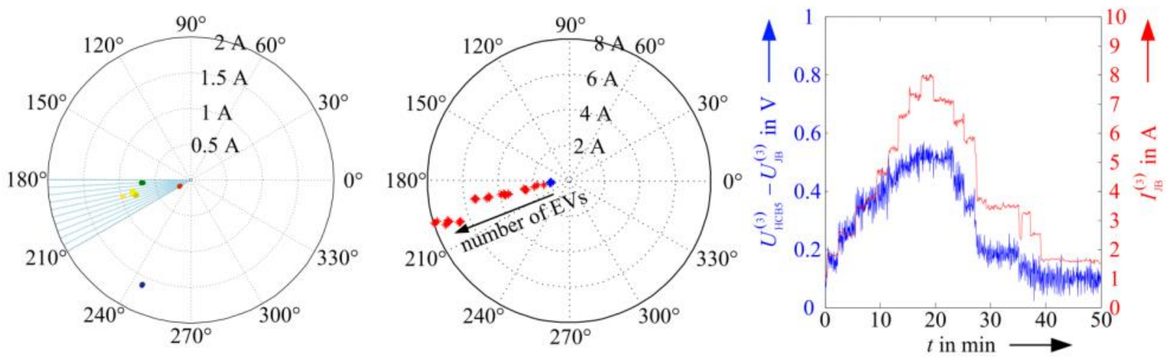

Figure 5.5 – 3rd harmonic current of EVs and their impact on the 3rd harmonic voltage, according to (MÖLLER et al., 2015).

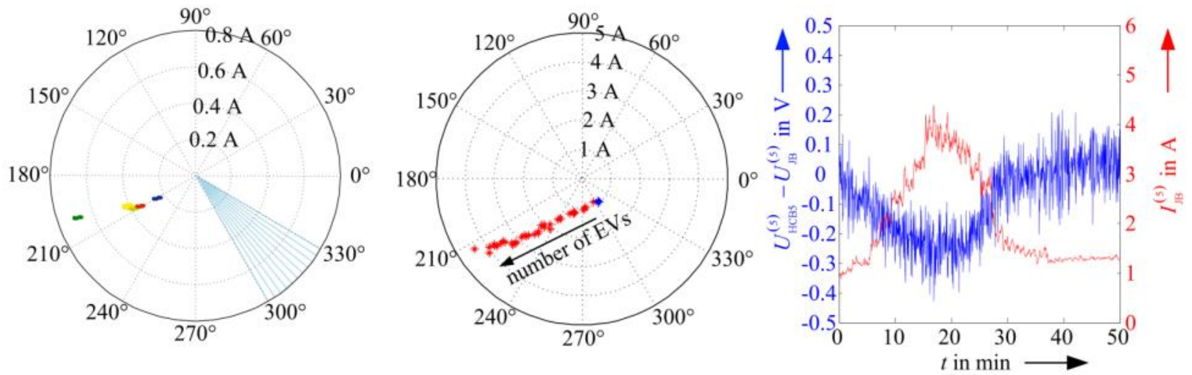

Figure 5.6 – 5th harmonic current of EVs and their impact on the 5th harmonic voltage, according to (MÖLLER et al., 2015).

In a previous analysis (CIGRE, 2018), a voltage harmonic reduction occurred at the end of the feeder, which reaches a minimum value when all EV's are connected. Also, according to (CIGRE, 2018), this occurs when the background distortion is not already taken over by the harmonic emissions from the charges.

5.3.2.4 PV Inverters

A similar behaviour from PV inverters can be correlated to EV's. It has been shown in (CIGRE, 2018) that a significant phase angle shift and an increasing of the harmonic current should be considered and analysed when connected to a distribution grid. In Figure 5.7 an example is shown when an LV grid has more than 50% of PV and its impact.

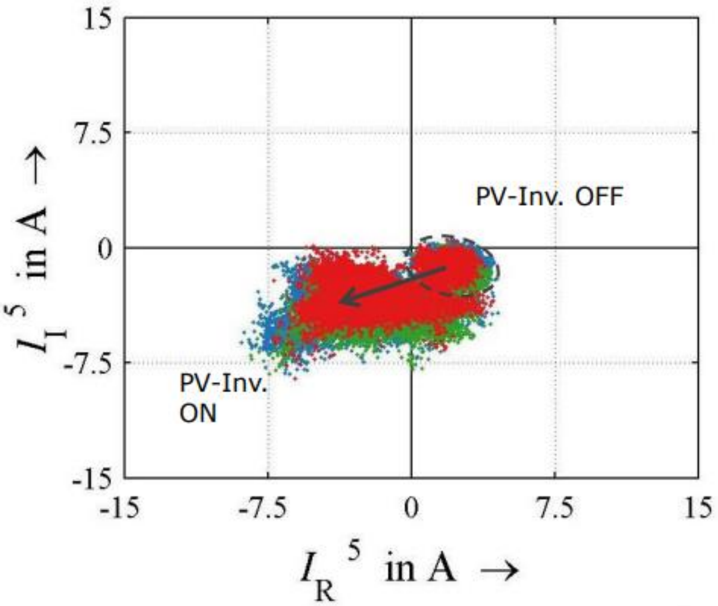

Figure 5.7 – 5th harmonic changes due to large introduction of PV into a distribution grid, according to (CIGRE, 2018).

5.3.2.5 Conclusion of Aggregate Loads and Sources

Electronic equipment and devices are the primary cause of harmonic distortion into the grid. The previous discussion shows that a large integration of either large equipment, such as EV's or PV sources or even a large number of small devices, such as those connected in the residential circuits, could result in harmonic distortion rise. It is important to highlight that these devices and equipment can cause either positive or negative impacts, and the latter depend on the number of devices connected, the grid topology, among others. One exception that can be exemplified is worldwide events, such as the FIFA world cup. During the world cup, the number of TVs and computers connected into the distribution grid can modify significantly the background distortion causing reliability issues or even impacting the hosting capacity value, previously measured to the system.

This thesis will show and discuss this particular topic throughout the case study.

5.4 The Definition of Background Distortion

Background Harmonic Distortion can be defined as the aggregated level of harmonic distortion present in the supply voltage at a PCC excluding the connection of a new linear or non-linear load or generator to the PCC. This distortion may vary throughout the day in shape and/or in magnitude and phase of individual components. Thus, it may consequently increase or reduce the resulting distortion after the connection of a new non-linear load or generator at the PCC.

5.4.1 Modelling and Methods of Background Distortion Source

As mentioned before, in order to define the contribution level of nonlinear loads, it is assumed that the polluting loads can be modelled as an equivalent Norton, which means it can be modelled as a simple current source according to (GHIJSELEN; RYCKAERT; MELKEBEEK, 2002). Thus, according to (CIGRE, 2018), the maiming power system can be as assumed to be linear under the analysis. Moreover, the terms "primary emission" and "secondary emission" are introduced to explain the source of emission. In this case, the primary emission is the emission originating form devices connected at the PCC, whereas the secondary emission is the emission originating outside of the device where a non-fundamental component in the background voltage distortion will result in a distorted current. For example, the distortion from fluorescent lamps with a high frequency defined as primary emission. On the other hand, the current distortion due to inverters at terminals of a wind turbine at the PCC is classified as secondary emission (CIGRE, 2018).

In order to represent the voltage distortion caused by the background harmonic distortion, the equivalent Norton of the load at the PCC can be transformed into an equivalent Thevenin as well, where a power system voltage for the harmonic order h is represented by a voltage source $E_m(h)$, an internal impedance defined as $Z_m(h)$ and the equivalent current defined as $I_m(h)$, according to (RYCKAERT; GHIJSELEN; MELKEBEEK, 2003). The voltage at the PCC point is given by $V_m(h)$. Moreover, the harmonic impedance of the linear loads connected at the PCC is represented by $Z_p(h)$. Thus, the current source of the polluting loads connected at the PCC is characterized by $I_p(h)$. Finally, the pursued shunt harmonic impedance is represented as $Z_s(h)$. The model described is shown in Figure 5.8.

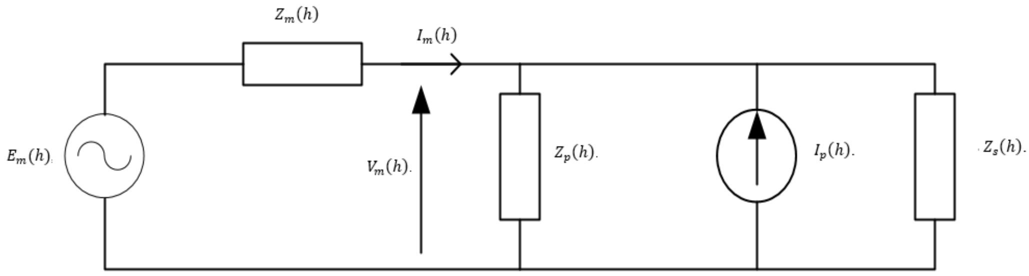

Figure 5.8 – Power system representing the background distortion model (GHIJSELEN; RYCKAERT; MELKEBEEK, 2002).

The method given in (PAPIC et al., 2018) is accurate considering an equivalent of the circuit regarding two harmonic equivalent sources: the utility voltage $E_m(h)$, and costumer voltage $E_c(h)$, as well as the utility impedance $Z_m(h)$ and customer impedance $Z_c(h)$, defined at a harmonic order h. In this case, the Norton equivalent can be turned into the Thevenin equivalent on the costumer side. Thus, the system can be given by Figure 5.9.

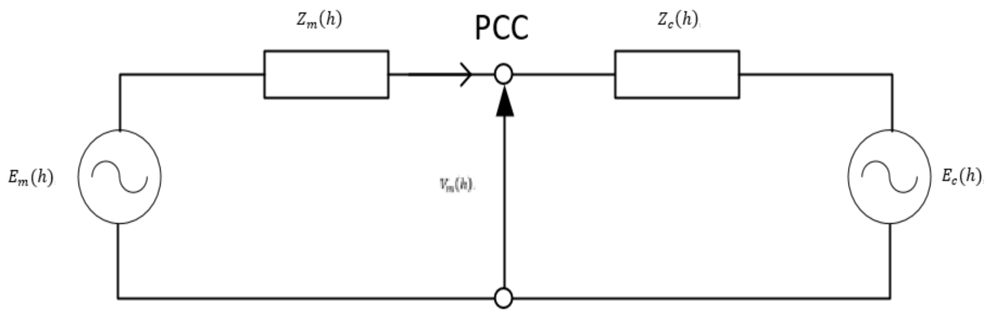

Figure 5.9 – Power system representing the background distortion model as a two Thevenin Equivalent (PAPIC et al., 2018).

These contributions can be calculated as the following equations (5.2.1) and (5.2.2).

$$E_m(h) = \frac{Z_m(h)}{Z_m(h) + Z_c(h)}\, E_c(h) \tag{5.2.1}$$

$$E_c(h) = \frac{Z_c(h)}{Z_m(h) + Z_c(h)}\, E_m(h) \tag{5.2.2}$$

It is important to highlight that for these models, both sides must be analysed as harmonic contribution, which means that the contribution of utility and the contribution from the prosumer will be implemented by using a superposition method in order to determine the background distortion at the PCC (PAPIC et al., 2018).

In order to understand the equivalent voltage at the PCC, the IEC voltage phasor method cited in (PAPIC et al., 2018) allows us to find the total voltage harmonic distortion at the PCC considering the background voltage and the customer installation. In this case, the voltage harmonic distortion before connecting any nonlinear load by costumer's side is defined as $\bar{V}_{background}$. Moreover, the voltage phasor $\bar{V}_{emission}$ is the voltage vector that estimates the voltage drop at the costumer's side. Thus, the voltage vector at the PCC $\bar{V}_{PCC}$, which consists of the voltage background and customer harmonic voltage emission, is shown in Figure 5.10.

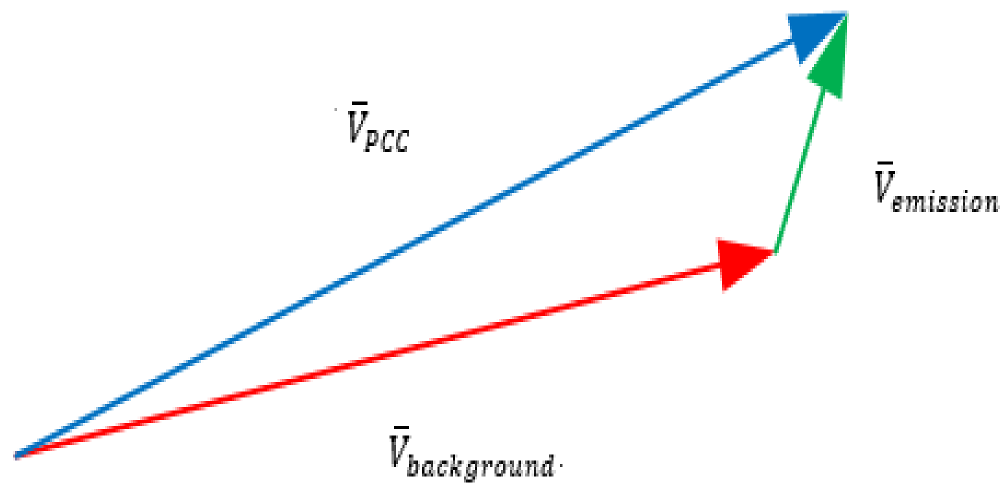

Figure 5.10 – Voltage Phasor Diagram based on IEC (PAPIC et al., 2018).

5.5 Impacts of the Background Distortion

The presence of harmonics voltage distortion into electrical networks can lead to several impacts, such as, increase losses, heating of components, loss of equipment life, power factor and others (BROWNE; PERERA; RIBEIRO, 2007). As it has been defined before, nonlinear loads are the main cause for pollution of the waveform in the electrical system and must be considered.

Moreover, televisions can cause considerable disturbance that depends on the time of the year around the world, as an example, during the World Cup (BROWNE; PERERA; RIBEIRO, 2007; LEITÃO et al., 2007; RIBEIRO et al., 2011; RUBENS et al., 2006). During this time of the year, television viewers will switch on their equipment at the same time considering different time zones. The impact of television viewing and other electronic loads on the utility grid harmonic distortion may be of great relevance as discussed in (TESTA; LANGELLA, 2007). It is commonly considered that in industrial countries, the 5^{th} harmonic will be significant and coincidently characterized by the peak of television viewing. Given these points, television receivers have power supplies which create current harmonics into the system (BROWNE; PERERA; RIBEIRO, 2007; TESTA; LANGELLA, 2007). Thus, based on these phenomena, it is safe to assume that the hosting capacity for the system will be decreased as a function of the increase of harmonic background level (OLIVEIRA et al., 2018). Furthermore, an important relation between the harmonic background level, voltage rise, and the hosting capacity value can be defined according to (OLIVEIRA et al., 2018), where, the bigger the background is, the bigger the voltage rise will be, and as a consequence, the lower the hosting capacity acceptable region will be.

5.5.1 Impact of the Background Distortion During the FIFA World Cup 2018

Although many papers have discussed all the effects of background voltage distortion through different devices and throughout the years, few studies have addressed the problem of background distortion during the FIFA world cup, where a large number of TVs are connected into the distribution grids, causing significant disturbances during the matches. Previous work has only focused on the impact during the FIFA world cup in many countries, especially in Brazil (ENGINEERING, 2015; LEITÃO et al., 2007; RIBEIRO et al., 2011; RUBENS et al., 2006).

As mentioned before, harmonic distortions on the electrical grid can become much more serious on specific occasions, when massive events are occurring, such as the FIFA world cup or other worldwide televised event. Moreover, the impact of this harmonic distortion will depend on the topology of the grid, electrical parameters and even cultural subjects. In Figure 5.11, an example of a measurement during the FIFA World Cup 2010 regarding Brazil matches can be examined (RIBEIRO et al., 2011).

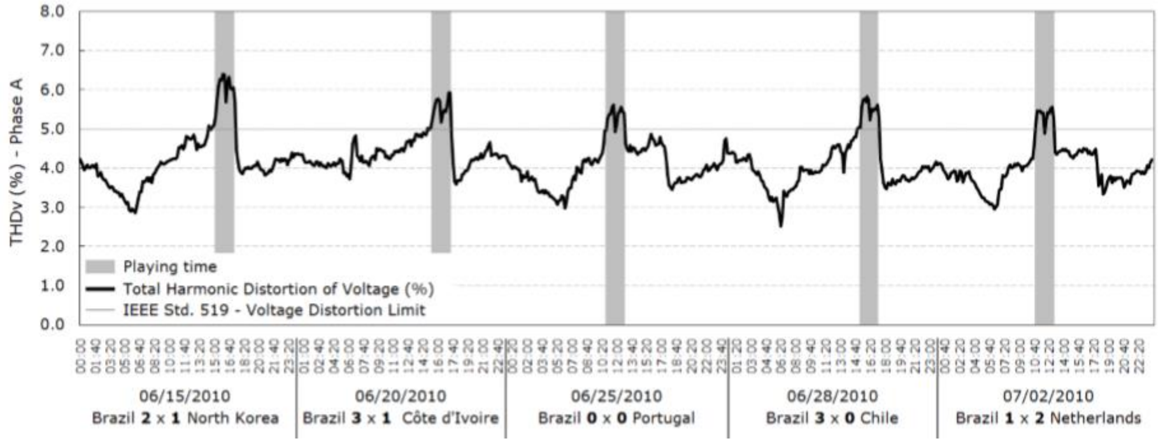

Figure 5.11 – THD profile at different days of Brazil matches (RIBEIRO et al., 2011).

It is easy to notice that during the matches the harmonic distortion increased substantially, which will directly impact the background distortion of the system. Thus, the distortion reduction at half-time is related to a temporary load demand causing a damping and lower impedance at all frequencies (RIBEIRO et al., 2011).

Still in accordance to (RIBEIRO et al., 2011), in Figure 5.12 the 5th harmonic voltage at 230 kV in the Northeast of Brazil during the Brazil versus Portugal match was measured. According to (RIBEIRO et al., 2011), typical 5th harmonic voltage on a typical day is under 0.5%.

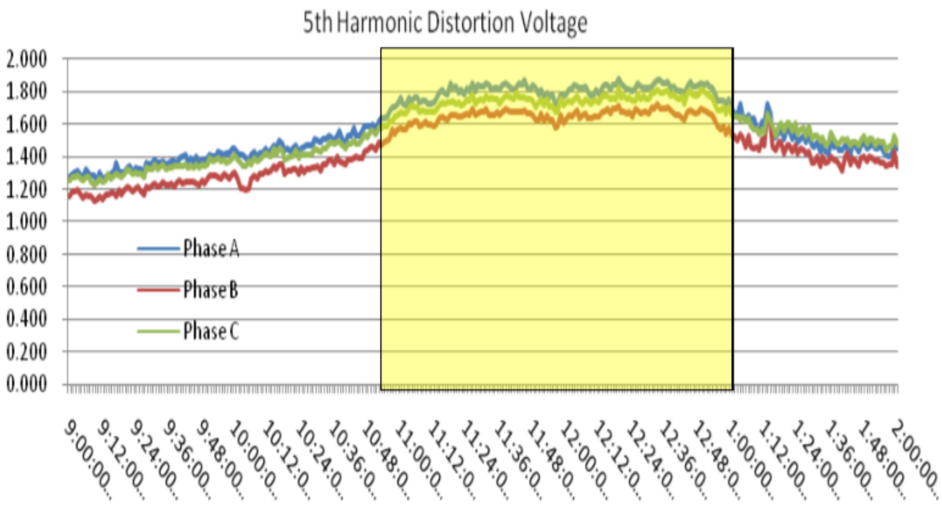

Figure 5.12 –THD of voltage at 230 kV during a Brazilian match on the World Cup 2010 (RIBEIRO et al., 2011).

Accordingly, the paper concludes that the impact of TV viewing must be considered on normal days, as well as during highly popular events, as a way to analyse the impact of the background distortion in the system. It is clear from these results that a significant increase of harmonic pollution can take place, especially in the 5th harmonic order. Those results show that the harmonic background can be rigorous due to linear and non-linear loads connected at the same time. Moreover, it can be concluded that the number of devices connected will produce impacts on the final background distortion value, even if it has been shown in the previous section that, separately, they will not lead to considerable consequences.

5.6 Final Considerations

In this chapter, the definition and requirements for the nonlinear contributions and its background distortion are determined. It is well known that harmonic distortion at the PCC is caused by the harmonic sources on both sides of the system: the shape of the utility system, as well as the customer facilities.

The summary of the background distortion has been done in order to define the correct model, which will be defined by the results of this thesis. It is important to highlight that the background distortion model has an important contribution to the hosting capacity value regarding distribution systems.

6. THE HOSTING CAPACITY CONCEPT

6.1 Initial Considerations

The impact of DG/DERs can be quantified using a set of indicators that accentuate its performance. In some cases, the system's performance will improve after the DG/DERs connection, or there will be negative impacts on the system. Nevertheless, it is important to realize that those performance indexes should not be exceeded (MENNITI et al., 2012) . The performance index is defined as the hosting capacity that a system has in hosting DG/DERs, respecting the limits of the proposed indicators (ETHERDEN; BOLLEN, 2011).

In the next sections, the concept of PV local hosting capacity will be applied through the evaluation of allowed voltage rises due to the harmonic distortion, as well as through its application to the concept of Dynamic Hosting Capacity. Thus, an application of the storage systems will be demonstrated as a powerful tool to improve the distribution systems under analysis.

6.2 The Definition of Hosting Capacity Concept

Both the concept and application of hosting capacity have been studied by researchers in order to elaborate a new significant strategy to plan and improve network systems, especially for new generation sources. For distributed energy resources, the hosting capacity approach has been introduced as a communication tool between stakeholders concerning the connection of DG to the electric grid (BOLLEN; RÖNNBERG, 2017). In this context, hosting capacity is understood as the maximum generation that can be integrated into the distribution grid without causing excessive disturbances in the power quality, where the term excessive means beyond the limits imposed by the standards maximum voltage rise, harmonics, flicker, etc.

The maximum PV generation that can be integrated into the system is called PV hosting capacity (CAPITANESCU et al., 2014; DE OLIVEIRA et al., 2016; DUBEY; SANTOSO, 2017; RYLANDER et al., 2015; SÁIZ-MARÍN et al., 2014). In this section, PV hosting capacity is defined with respect to voltage rise caused by harmonic voltage disturbances at the point of common coupling (PCC). Figure 6.1 illustrates the evolution of a generic performance index for the hosting capacity as a function of the insertion level of a DG (DE OLIVEIRA et al., 2016; ETHERDEN; BOLLEN, 2011; SANTOS et al., 2015). It is worth noting that there is a restricting range of the hosting capacity defined between two limit curves: the worst-case scenario, for the lower limit curve, and the best-case scenario, for the upper limit curve. The difference between the curves is based on the difference between possible background voltage distortions at the PCC. This approach for the limits of hosting capacity is shown in Figure 6.1. Voltage distortions at the PCC can be caused by electronic devices, generators, transformers, non-linear loads and others.

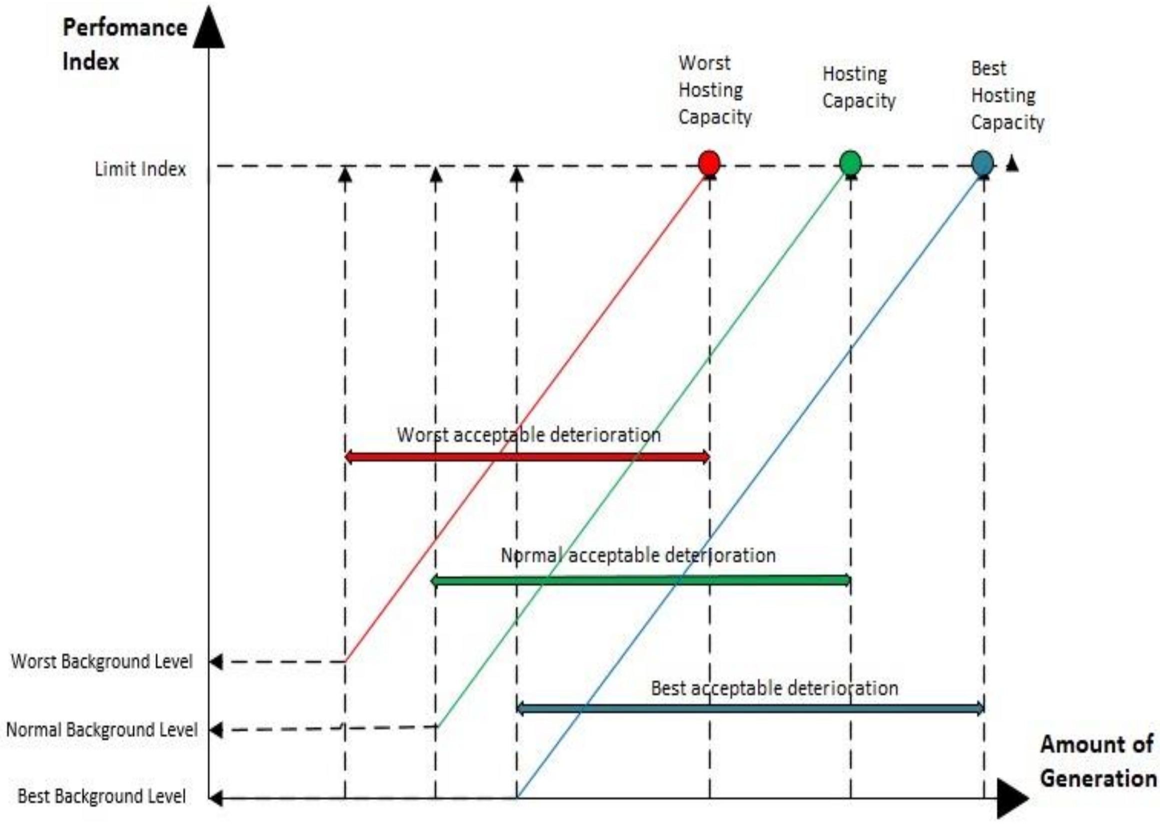

Figure 6.1- Range curves of a generic performance index versus the amount of distributed generation.

According to the literature (BOLLEN; RÖNNBERG, 2017), it is important to take into account uncertainties when conducting a hosting capacity analysis, as they will modify the deterioration region when hosting capacity is analysed. Possible examples of such uncertainties include customers' type of installations, three-phase or single-phase, customer connection phase if single-phase, PV panel orientation, the type of the inverter, implemented reactive power control if any, and others. As shown in Figure 6.1, the curve range will represent the acceptable deterioration region between the best hosting capacity range (the line designating the best hosting capacity and the best background level) and the worst capacity range (the line designating the worst hosting capacity and the worst background level), which defines the region where it is possible to keep the system operating, without uncertainties, while respecting its limits index defined by local standards.

6.2.1 Voltage Rise Due to Harmonic Injection and Its Limits to Define the Local Hosting Capacity

Power electronic devices are expected to inject harmonic currents. The larger the devices are, in general the greater the impacts will be (BOLLEN; RÖNNBERG, 2017).

As long as the electronic devices are connected to the network and are injecting harmonic currents, voltage distortion will occur and, consequently, voltage rise will occur as a result of root mean square (RMS) magnitude dependence on voltage waveform.

According to international and national standards, the limits for voltage harmonic distortion and voltage rise have been defined (e.g., PRODIST Módulo 8, 2015, C4-115 CIGRE, 2014; IEEE 1159, 2009). In the following, it is used both the voltage harmonic distortion limit and the voltage rise limit to define PV hosting capacity.

Assuming that a PV installation can be modelled as a current source and that the PV is connected at the LV side of a secondary substation at a PCC for which the Thévenin's impedance is essentially resistive (i.e., $X \ll R$), the system's hosting capacity P_g^{max} is usually approximated by (6.2.1), given a known voltage magnitude at the PCC, V_o (BOLLEN; HASSAN, 2011; CARVALHO; CORREIA; FERREIRA, 2008), δV^{max} as the overvoltage relative margin and R_f as the Thévenin's resistance at the PCC:

$$P_g^{max} = \frac{(V_o)^2}{R_f} \delta V^{max} \qquad (6.2.1)$$

where,

$$\delta V^{max} = (V^{max} - V_o)/V_o \, . \qquad (6.2.2)$$

Equation (6.2.1) neglects harmonic injection by the PV source and voltage distortion at the PCC. To consider harmonic injection by the source and distortion at the PCC, (6.2.1) needs to be rewritten based on typical parameters of a LV feeder model (CARVALHO; CORREIA; FERREIRA, 2008). Details of the feeder model used, and corresponding voltage rise formulae are provided in the following.

Take the model depicted in Figure 6.2 for which the Thévenin equivalent impedance at the PCC is given by $R_f + jX_f$. The complex power injected by a PV system and the complex power absorbed by the local load are defined as $S_g = P_g + jQ_g$ and $S_L = P_L + jQ_L$, respectively. The net injected active power and reactive power at the PCC are defined as $P = P_g - P_L$ and $Q = Q_g - Q_L$, respectively.

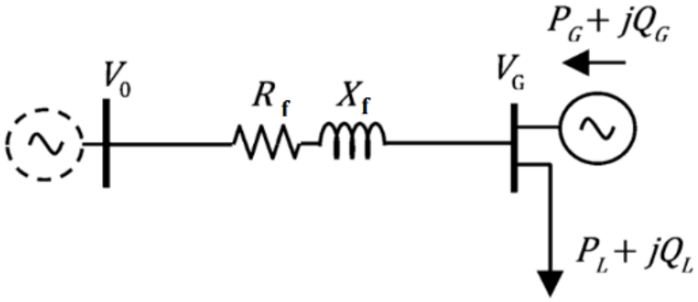

Figure 6.2 – Feeder model with PV (CARVALHO; CORREIA; FERREIRA, 2008).

According to the literature (CARVALHO; CORREIA; FERREIRA, 2008; DUBEY; SANTOSO, 2017), the voltage difference between the PCC and the voltage source can be expressed, for the fundamental frequency, by (6.2.3).

$$\dot{V}_G - \dot{V}_o = (R_f + jX_f)\left[\frac{P + jQ}{\dot{V}_G e^{j\theta}}\right]^* \tag{6.2.3}$$

where the voltage at the PCC is denoted by $\dot{V}_G . e^{j\theta}$ and the voltage at the source is $V_0 . e^{j0}$.

Applying the conjugated properties, (6.2.3) can be expanded into (6.2.4),

$$V_g - V_o = \frac{P(R_f cos\theta - X_f sin\theta) + Q(X_f cos\theta + R_f sin\theta)}{V_g} \tag{6.2.4}$$

Assuming that $cos\theta \approx 1$ and $sin\theta \approx 0$ (DUBEY; SANTOSO, 2017), (6.2.4) can be approximated by (6.2.5) for the fundamental frequency $h = 1$.

$$\Delta V^1 = V_g - V_o \approx \frac{PR_f + QX_f}{V_g} \tag{6.2.5}$$

Equation (6.2.5) can be generalized for other harmonic orders $h \neq 1$ as in the following.

$$\Delta V^h \approx \frac{P^h R_f + Q^h h X_f}{V_g^h} \tag{6.2.6}$$

The maximum voltage rise at the PCC is experienced when load (L) is at its minimum and generation (G) at its maximum. Thus, one can use (6.2.6) to compute an upper bound for voltage rise assuming that the power factor (PF) of net load can be controlled by the PV system at the PCC ($tan(\varphi) = Q^1/P^1$).

$$\Delta V^1.V_g^1 \approx P^1R_f + Q^1X_f \tag{6.2.7}$$

$$\Delta V^1.V_g^1 \approx P^1(R_f + tan(\varphi)X_f) \tag{6.2.8}$$

Neglecting the PV source harmonic content and the voltage distortion at PCC, the maximum power injected by PV can now be given by (6.2.9) assuming that the maximum of ΔV^1 is $V_g^{max,\ 1} - V_0^1$, where $V_g^{max,\ 1}$ is the voltage limit for the fundamental frequency.

$$P_g^{max,1} = \frac{V_g^{max,\ 1}(V_g^{max,\ 1} - V_0^1)}{R(1 + tan(\varphi)\frac{X_f}{R_f})} + P_L^{min} \tag{6.2.9}$$

Assuming that loads have negligible harmonic content, then (6.2.9) can be written for other harmonic orders as in the following.

$$P_g^{max,\ h} = \frac{V_g^{max,\ h}(V_g^{max\ ,\ h} - V_o^h)}{R(1 + tan(\varphi)\frac{hX_f}{R_f})} \tag{6.2.10}$$

Where, V_o^h is the harmonic voltage at the PCC.

As long as the conditions under which the model of PV is considered a current source, it is possible to explain the sum of the power to represent the hosting capacity of DERs. Also, it is equally important to emphasize that the sum of these injected currents will impact the RMS voltage at the PCC. Since the RMS voltage is the square root of the sum of squares of each harmonic voltage, it can be expressed by (6.2.11):

$$V_{RMS} \approx \sqrt{\sum_{h=1}^{51} V_h^2} \tag{6.2.11}$$

In this case, the power generated in relation to the RMS voltage can be rewritten as (6.2.12), using (6.2.11):

$$P_g = \frac{{V_{RMS}}^2}{R_f} = \frac{\left(\sqrt{\sum V_h^2}\right)^2}{R_f} = \frac{\sum V_h^2}{R_f} \tag{6.2.12}$$

Then the hosting capacity at the PCC can be defined as the sum of the maximum power possible, based on (6.2.12), to be injected for each frequency:

$$P_g^{max} = \sum_{h=1}^{h} P_{PV}^{max,\ h} = \frac{1}{R}\sum_{h=1}^{51} \frac{V_g^{max,\ h}(V_g^{max,\ h} - V_o^h)}{(1 + tan(\varphi)\frac{hX_f}{R_f})} \tag{6.2.13}$$

Where,

$V_g^{max,h}$ is the allowed voltage magnitude for harmonic order *h*;

V_o^h is the actual voltage magnitude of harmonic order *h* at the PCC;

φ is the $arcos(PF)$, where the PF is the power factor at the PCC.

If we use (6.2.13) and notice that, for $V \leq 1\ kV$, standards impose that individual voltage distortion be below 5% for $h \geq 2$ and below 105% for the fundamental frequency, $h = 1$, then, the hosting capacity is given by (6.2.14)

$$P_g^{max} = \frac{1.05(1.05 - V_o^1)}{R_f(1 + tan(\varphi)\frac{X_f}{R_f})} + \sum_{h=2}^{h} \frac{0.05(0.05 - V_o^h)}{R_f(1 + tan(\varphi)\frac{hX_f}{R_f})} \tag{6.2.14}$$

6.2.2 Sensitivity Analysis of Hosting Capacity

Several factors may affect hosting capacity, namely, harmonic voltage, power factor, minimum load of the distribution feeder, and voltage regulation equipment, among others (DUBEY; SANTOSO, 2017). We will elaborate on some of these factors in the following subsections.

A) Harmonic Voltage

The calculation of the hosting capacity using (6.2.14) considers the voltage harmonics, from the fundamental order up to the 50^{th} harmonic order, as well as performance index limits, which depend on local standards (BOLLEN; RÖNNBERG, 2017; PRODIST Módulo 8, 2015, C4-115 CIGRE, 2014; IEEE 1159, 2009). Moreover, the injection of harmonic current into the system depends on the equipment connected at the PCC and the PV system inverters. The latter can be controlled by a prosumer as the equipment is manufactured according to standards. The former cannot be controlled. The background voltage at the PCC cannot be controlled as it is virtually impossible to know what is causing the harmonic voltage distortion. Therefore, two extreme scenarios will be imposed to analyse how the harmonic injection can impact the hosting capacity.

As an example, let us consider a scenario where the voltage for the fundamental order is set at 1.00 p.u. and the other harmonic voltages for h ≥ 2, up to 15, are set at

0.03 p.u. It is important to realize that, for this scenario, a high distortion is considered as it is dependent on the background and all the electronic devices connected at the PCC. The other scenarios consider a non-high voltage distortion for h ≥ 2 up to 15 and the voltage distortion will set in at 0.01 p.u. In fact, a decrease in harmonic voltage would increase the hosting capacity as shown in the equation below:

$$\frac{P_g^{\max\prime}}{P_g^{max}} = \frac{1.05(1.05-1)+\sum(0.05-0.01)0.05}{1.05(1.05-1)+\sum(0.05-0.03)0.05} = \frac{0.1525}{0.0775} = 1.12$$

As can be observed, the decrease in harmonic voltage increases the hosting capacity by almost 12%. Therefore, the improvement of the voltage distortion signals depends on the harmonic filters connected to the system. On the other hand, referring to voltage regulation equipment, and keeping the harmonic background constant, (DUBEY; SANTOSO, 2017) argues that a reduction of V_o^1 to 0.98 p.u., for example, would result in 1.5 times higher hosting capacity with respect to (6.2.14).

B) Set Reactive Power on the Inverters

According to the literature (DUBEY; SANTOSO, 2017), the power factor at the PCC can increase the hosting capacity as well. Let us set the base value for the PF at 0.8 inductive. In order to demonstrate the sensibility due to the PF change, we compute a new value for the hosting capacity for a new PF value now set at 0.8 capacitive, which corresponds to the inverter injecting reactive power instead of absorbing it. The ratio between hosting capacities is then given by the following expression:

$$\frac{P_g^{\max\prime}}{P_g^{max}} = \frac{(1+\tan(cos^{-1}(0.8))\,{}^{X}/_{R}}{(1+\tan(cos^{-1}(-0.8))\,{}^{X}/_{R}} = 7$$

If we assume that the relation X/R at the PCC is unitary, leads to a new hosting capacity that is about 7 times higher than the base case. In (DUBEY; SANTOSO, 2017, results with smaller PF variations led to ratios of 2.35.

6.3 The Concept of Dynamic Hosting Capacity for DERs

Recent research has tended to focus on hosting capacity calculation at specifics instants of time (FAN et al., 2016; RENO et al, 2014). These references show the hosting capacity related to voltage regulation and reverse power flow. However, it is necessary to consider also the impact of harmonics on the voltage regulation caused by renewables. This poses a problem as hosting capacity conditions vary in time. The main limitation of looking statically at hosting capacity lies in its reliability, particularly when the system is under constant harmonic injection due to all the electronic devices connected to the electrical system, thus making it a dynamic harmonic injection issue. One question that needs to be raised is how a dynamic harmonic injection could affect the global hosting capacity value due to its impact on the voltage profile.

A related hypothesis maintains that a dynamic harmonic injection, originating from external conditions, such as the background harmonic injection, as well as distortion from the inverters (for PVs, for example), leads to a dynamic hosting capacity profile which follows the tendency of their harmonic injection. This suggests that it presents a constructive curve in time, showing that should be considered when planning and improvement issues will be considered to electrical distribution systems.

The fundamental characteristic of Dynamic Hosting Capacity (DHC) allows to increase and improve the usual hosting capacity by applying a time variance, which can describe its behaviour against external and internal variations of the system, such as load conditions, background harmonic distortion, irradiation index, among others. In accordance to the section 6.2, the hosting capacity at the PCC can be defined as the sum of maximum power possible, based on (6.2.14), to be injected for each frequency. Furthermore, time variation is set as a vital factor in (6.3.1) within this analysis.

$$P_g^{max}(t) = \sum_{h=1}^{h} P_{PV}^{max,\ h}(t) = \frac{1}{R_f}\sum_{h=1}^{h} \frac{V_g^{max,\ h}(V_g^{max,\ h} - V_o^h(t))}{(1 + tan(\varphi)\frac{hX_f}{R_f})} \quad (6.3.1)$$

It is important to underline that the maximum and minimum amount of power depends on the harmonic voltage values which are defined for each instant of time. A generic graph of DHC is shown in Figure 6.3.

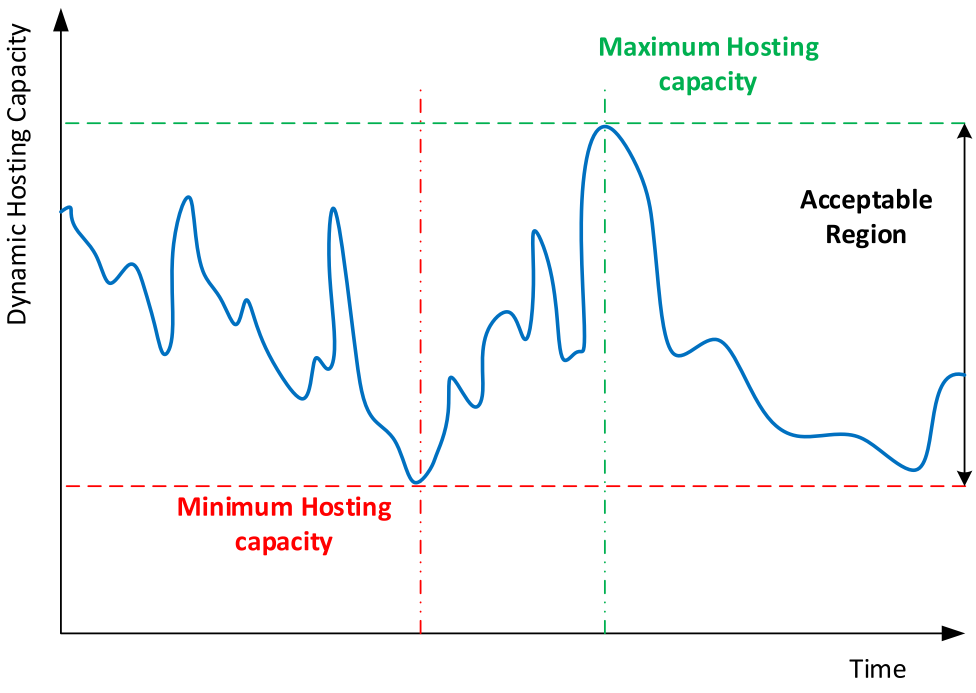

Figure 6.3– Dynamic hosting capacity (DHC) approach.

The maximum and minimum hosting capacities values do have analytical consequences to the grid. The minimum value will be the deterministic value used to describe the effectiveness of the grid since the region under the minimum value can be considered unacceptable for working conditions. That is, the harmonic background at the PCC, as well as the voltage values are almost crossing their respective limits imposed by standards. On the other hand, the maximum value determines that the region has the best power qualities indexes. But to achieve these values it is necessary to carry out conditioning improvements, which can be led by previous studies in the grid. This range of values suggests that there is an acceptable region defined between the minimum and maximum hosting capacity value. Thus, the region can be also defined as the region where the DERs system will no longer work properly considering power quality issues. As a conclusion based on the previous fact, the large the accept region is, the better the system performance will be.

This implies that the DHC analysis is important to create better conditions on the grid considering DERs. These findings add t a growing body of literature on the hosting capacity concept and its derivations.

6.4 Final Considerations

In this chapter, we presented a new concept for calculating the local hosting capacity as a contribution to the context of planning and improving DERs installations into distribution systems. The definition of DHC has been discussed, as well as its application to energy storage systems.

In the next chapter, these proposed concepts of hosting capacity will be applied through the evaluation of voltage rises, due to harmonic distortion levels, through the determination of the DHC profile and its improvement concerning energy storage systems, which will be presented further in APPENDIX X as a scientific proposed methodology.

7. CASE STUDY

7.1 Initial Considerations

This chapter presents the measurement results of a real system and its applicability using the hypothesis proposed in Chapter 6. The actual systems in question deal with the installation of the PV at the QMAP building and previous simulations regarding the expansion of this generation system, and also in relation to new PVs into the campus. These new PVs will be connected to the feeder from the supply point in the main substation at UNIFEI, which supplies the QMAP distribution transformer and other buildings in the campus. The data used are part of the measurement results at QMAP.

This chapter is organized into three mains sections. The first section gives an overview of the hosting capacity approach related to the voltage rise and harmonic injection proposed in Chapter 4 as a new hypothesis. Thus, the new methodology aims to find the hosting capacity value through the integration of two important phenomena in the power quality field. In this context, the measurement results in the QMAP building were used, totalling one week of measuring following the PRODIST measurement protocol – MODULE 8 (2015) with the PV connected and working. Problems and applicability regarding the use of PV local hosting capacity in relation to voltage rise due to harmonic voltage are discussed in later sections.

The second section examines the applicability of Dynamic Hosting Capacity (DHC) using the results shown in the previous section. It is important to highlight that the concept of DHC applied is based on the equation used in section one, which means, the base of this section needs to be correctly understood in order to extend its procedure of calculation. Thus, the DHC profile and its importance will be shown in two different analysis, daily and weekly, where it is possible do calculate the hosting capacity maximums and minimums of the system in order to get a better planning and improvement.

Finally, the objective of this study is to apply and analyse the hypothesis of PV local hosting capacity, as well as dynamic hosting capacity and its applicability in order to present a new tool for planning and improving electrical networks with DERs.

7.2 Equipment of Measurement and Analysis

The equipment package used to collect the data was DRANETZ, which has been shown and better detailed in (OLIVEIRA et al., 2015). This equipment is characterized by its high resolution and the ability to monitor network events of power quality, power flow and transient events in electrical systems.

The models used are the Power Guide 4400 family and Power Explore Px5 that meet the standards IEC 61000-4-15 and IEC 61000-4-30 class A, also the EN50160 with multiple configurations in alternating current, direct current and communication via RS 232, Ethernet and USB. Figure 7.1 and Figure 7.2 are photos of both meters.

Figure 7.1–DRANETZ *Power Guide 4400.*

Figure 7.2–DRANETZ *Power Explore Px5.*

The software application used for the data captured by DRANETZ was the DRAW-VIEW 6, a Windows-based software that allows you to easily and quickly view and analyse all the monitored data with easy access and customizable options that meet the needs of all projects. The software allows to easily export its data to Microsoft EXCEL.

7.2.1 Measurement Points through PQ Analysers.

Figure 7.5 presents the single-line diagram showing the locations where the PQ analysers were connected in the QMAP substation. It is important to highlight that the QMAP building has a 150-kVA distribution transformer with an input voltage level of 13.8 kV and output voltage of 220 V, dry characteristic and a percentage impedance of about 4.16%, supplying two distribution frames of loads. This information will be detailed in the next section.

The PQ analysers were installed in two locations in the building's substation. The justification of the locations is given by the possibility of an amplified analysis of the power delivered by the PV and the analysis of the bidirectionality of the power flow on the LV side of the distribution transformer. Thus, it is possible to investigate the phenomena of harmonic voltage distortion and RMS variation of voltage on the 220V bus-bar.

The points of measurement are, according toc:

1) Output of the PV, after the autotransformer that is connected to the 220 V bus-bar of the building;
2) In the LV of the distribution transformer;

The measurement locations are shown in the single-line of Figure 7.5 of the section 6.3. Besides, Figure 7.3 and Figure 7.4 show the connection of the PQ analysers.

Figure 7.3– PQ Analyser installed in the output of the PV (OLIVEIRA et al., 2015).

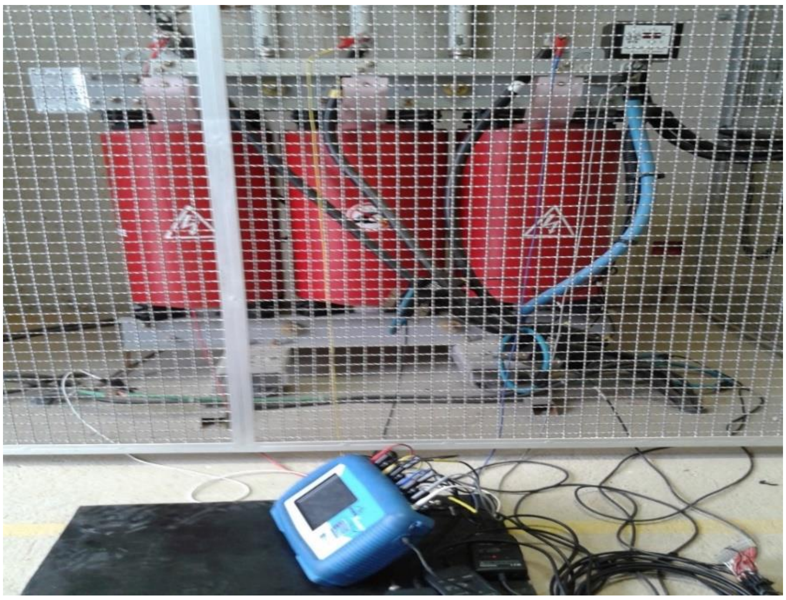

Figure 7.4– PQ Analyser installed at the output of the distribution transformer in the building (OLIVEIRA et al., 2015).

7.3 Experimental Data and a Brief Analysis

The distribution system for this analyse is a 220 V feeder with one bus, one 150 kVA transformer connected to 13.8 kV–220 V, one PV system with 15 kW_p (solar panels + inverter + autotransformer), described in the section 5.2.1. It's important to notice that peak generation for the minimum load is a number close to 15 kW_p even though the maximum load of this system is a number between 4 – 8 kW, where the reminiscent generation is distributed at 13.8 kV as a bidirectional power flow at the university system for the other buildings connected to this same feeder. The electric schematic of the described circuit is shown in Figure 7.5, as cited before. In Table 7.1, the values of parameters are shown as well.

Table 7.1 – Parameters of the QMAP System (OLIVEIRA et al., 2015).

Parameter	**Default Value**
Autotransformer	45 kVA, 380/230–220/127 V, $Z =$ 1.2%
Transformer	150 kVA 13.8 kV–220/127 V, $Z = 4\%$
PV cable	18 m x 3F, 6 mm^2 Cu
PV system + Inverters	15 kWp + 2 Inverters (7.5 kW_p)
CEMIG 13.8 kV	S_{cc}= 1000 MVA

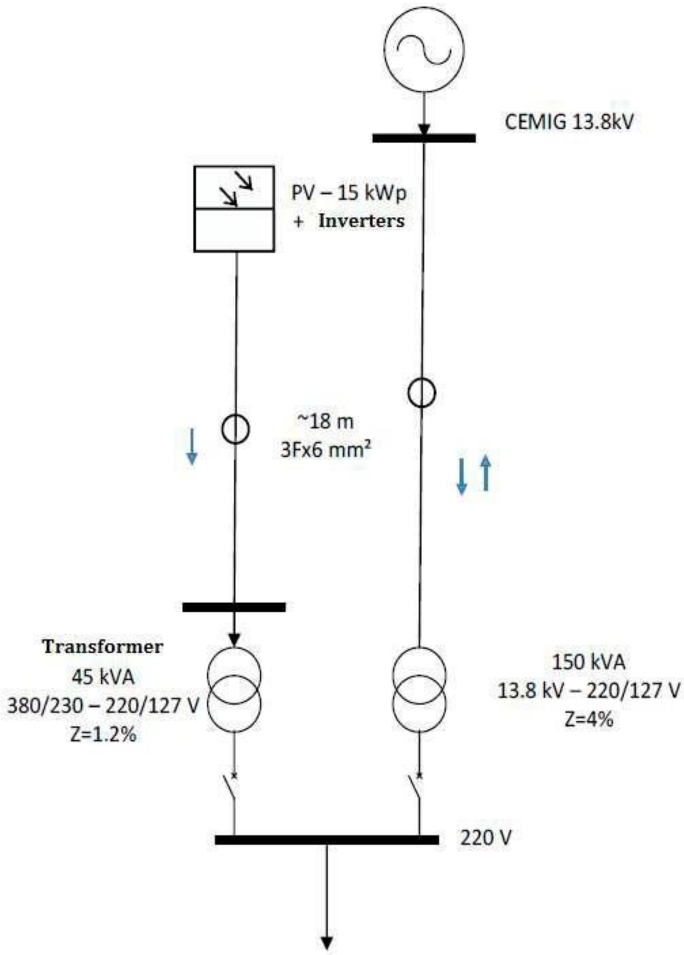

Figure 7.5 – One-line diagram for the PV System of the QMAP sited in UNIFEI's (Federal University of Itajuba) campus.

In order to illustrate the calculation of hosting capacity by the maximum capacity equation, the voltage rise, and harmonic source will be validated by the PQ analysers described in section 7.2.1 to get the equivalent data of the voltage profile, harmonic injection, frequency and others. As described and justified before, both pieces of equipment were installed on the 220 V sides of both the transformer and the autotransformer. As a result, it is possible to measure the bidirectional power flow as well as the voltage profile, simultaneously.

The RMS magnitude of the nodal voltage and of current injection at the 220 V bus were recorded over the course of one week, with 10-min resolution (OLIVEIRA et al, 2015) resulting in 1008 valid data records used for analysis. Harmonic power and other power quality indices were also measured. Measurements were undertaken according to Brazilian standards for power quality regulation (PRODIST Módulo 8, 2015; PRODIST Módulo 1, 2012). Based on these obtained data, the results from Equations (6.2.1) and (6.2.14) are compared against each other as well as against actual measurement data.

Figure 7.6 shows a sample of the data obtained in different time periods (different dot symbols and colours for different days) projected into two dimensions: (i) active power injected by the 15 kW_p PV systems, at the abscissa axis, and (ii) RMS voltage rise margin at the PCC, at the ordinate axis. The chosen time-range is between 07:00 a.m. to 06:00 p.m.

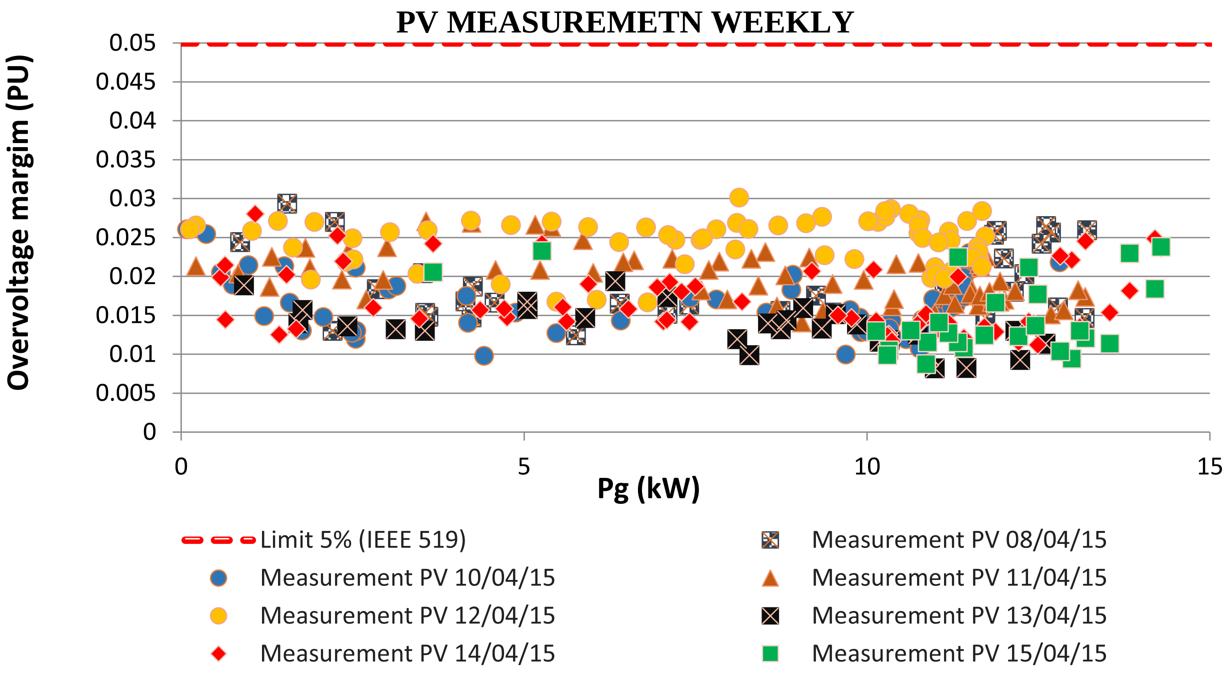

Figure 7.6- Hosting capacity experimental data.

Figure 7.7 filters the data of Figure 7.6 for just one day, where the amount of energy produced was at its maximum and PF was within a narrow range: we eliminated data records within that day for which the PF was outside the range [0.77; 0.96]. The projection of the filtered data onto δV^{max} and P_g^{max} is then compared with the estimation given by Equations (6.2.1) and (6.2.14), respectively, using the same overvoltage margin. For the results of Equation (6.2.14), it was used a constant power factor of 0.80 inductive, which represents the average PF in the period. Results show that the derived model expressed by (6.2.14) represents the experimental data were obtained quite well, as the data points match the linear equation estimated by (6.2.14).

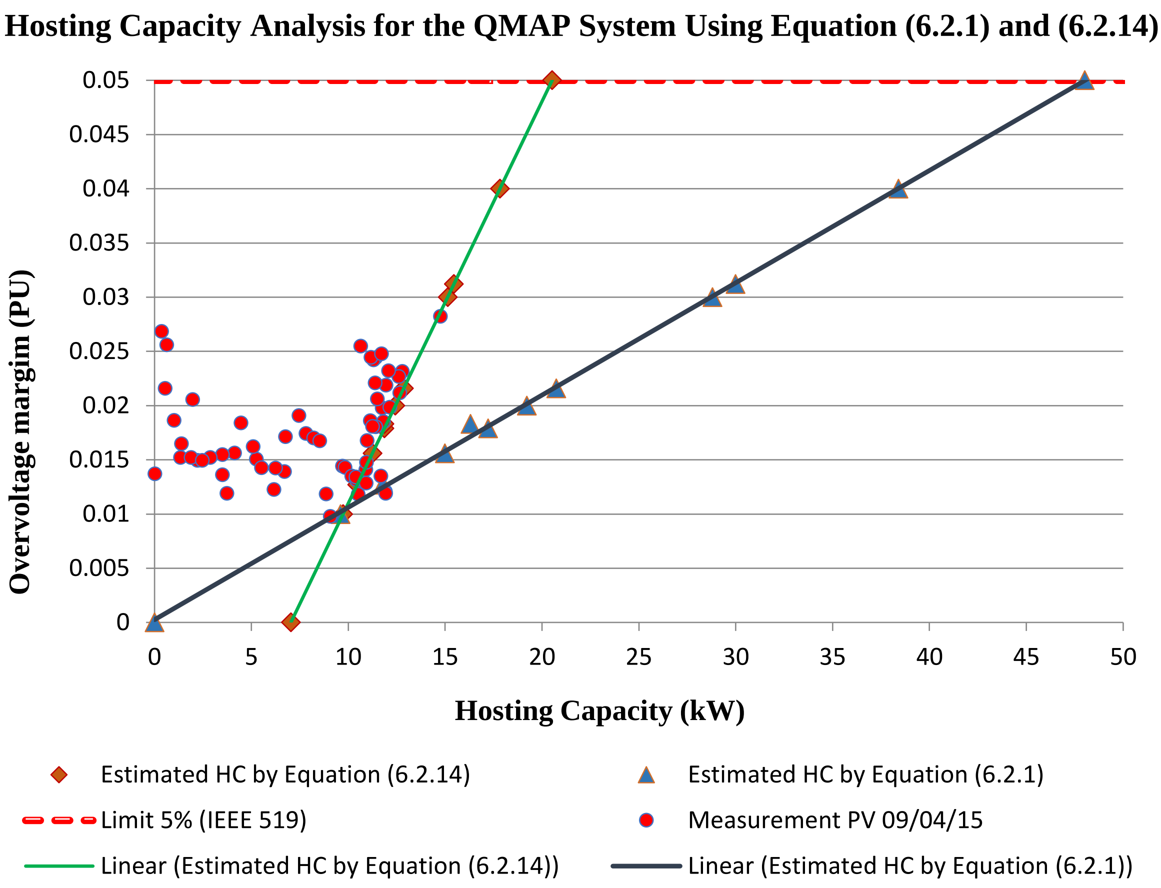

Figure 7.7 – Hosting capacity validation against (6.2.1) and (6.2.14).

Moreover, and perhaps more importantly, results also show that Equation (6.2.1) significantly overestimates the PV system's hosting capacity by neglecting harmonic current injection effects and the power factor at the PCC, which accounts for a significant amount of the difference for the estimated PV production. Note that (6.2.1) estimates a 48 kW_p hosting capacity for a 5% allowed voltage rise, while (6.2.14), more realistically, limits such capacity to half of that value, i.e., 22 kW_p.

7.3.1 Calculation Method for Analysis and Planning – Voltage Rise Due to Harmonic Injection to Define the Local Hosting Capacity

In order to illustrate the use of the hosting capacity approach related to the voltage rise and harmonic injection demonstrated in (6.2.14), a thorough analysis is shown in this section to exemplify the different impacts and behaviours of the approach discussed earlier. For this application of the hosting capacity approach, it was chosen to define four different scenarios with the following characteristics:

I. A worst-case scenario is defined in two strands as part of an extreme situation. First, it was considered that all harmonic voltages are 5% for $h \geq 2$, which leads to $\delta V_h = 0$ in equation (6.2.14). This situation corresponds to the system being at the maximum harmonic limit. Second, it was considered the case where the power factor is at the minimum possible, which in this case is zero. This scenario defines an unacceptable region where the system is where the PV unit cannot be integrated into the distribution system.

II. A best-case scenario is also defined in two strands, in a similar way to that used for the worst-case scenario. First, it was considered all harmonic voltages as negligible for $h \geq 1$, which leads to $\delta V_h = 5\%$. This situation corresponds to the system having a voltage waveform that is 100% sinusoidal. Secondly, it was considered the case where the power factor is at the maximum, which in this case is above 90%.

III. A third scenario is defined as the real case wherein the power factor range was [0.77; 0.82].

IV. Finally, the fourth scenario is used to illustrate the behaviour of the hosting capacity approach when only the fundamental frequency is considered in (6.2.14) and compared with case (III), which considers all harmonic orders.

When the hosting capacity is analysed, it is necessary to define a system's performance index. In this case, the voltage rise limit considered is the performance index for the Brazilian standard, where the limit used is 5% at the bus voltage under analysis. For the present analysis, the four scenarios were defined previously, as was the limit performance index for the hosting capacity. This analysis is shown in Figure 7.8. As a result, it is possible to illustrate the hosting capacity approach taken and its acceptable deterioration region.

In Figure 7.8, it is possible to observe a sample of the data obtained for the specific time periods as denoted in the Figure 7.7 the "+" symbols. The data has a direct relation with the power factor at the PCC, which is variable due to the load variation in that period, the solar incidence, etc. The data obtained falls within the power factor's range of [0; 0.9], which results from the characteristics discussed in (I) to (IV).

For the extreme case, it can be noted that there is a hatched region where the system can work as long as the limit performance index is respected. In this case, the system can be set up within a hosting capacity range between 0 and 25 kW_p considering an acceptable deterioration region. However, it is important to underline that the background level at the PCC can be the cause of an important relation between the amount of energy that can be produced and the limit for practical purposes. The curve for a realistic situation, with a power factor set at 0.8, which was described in (III), considering the existing harmonic background at the PCC, leads to a hosting capacity of about 21 kW_p. On the other hand, from the moment the background distortion at the PCC is neglected, and just the fundamental frequency is considered, the hosting capacity for the same situation decreases abruptly to 14 kW_p, which is below the maximum generation capability of the system. For this reason, it is possible to say that, in this case, the higher the harmonic background is, the lower the hosting capacity will be. Finally, it is important to highlight that, as PF = 0 has been chosen for the worst-case scenario, the unacceptable deterioration area is no existent for logical reasons due to the PV system and its operating characteristics.

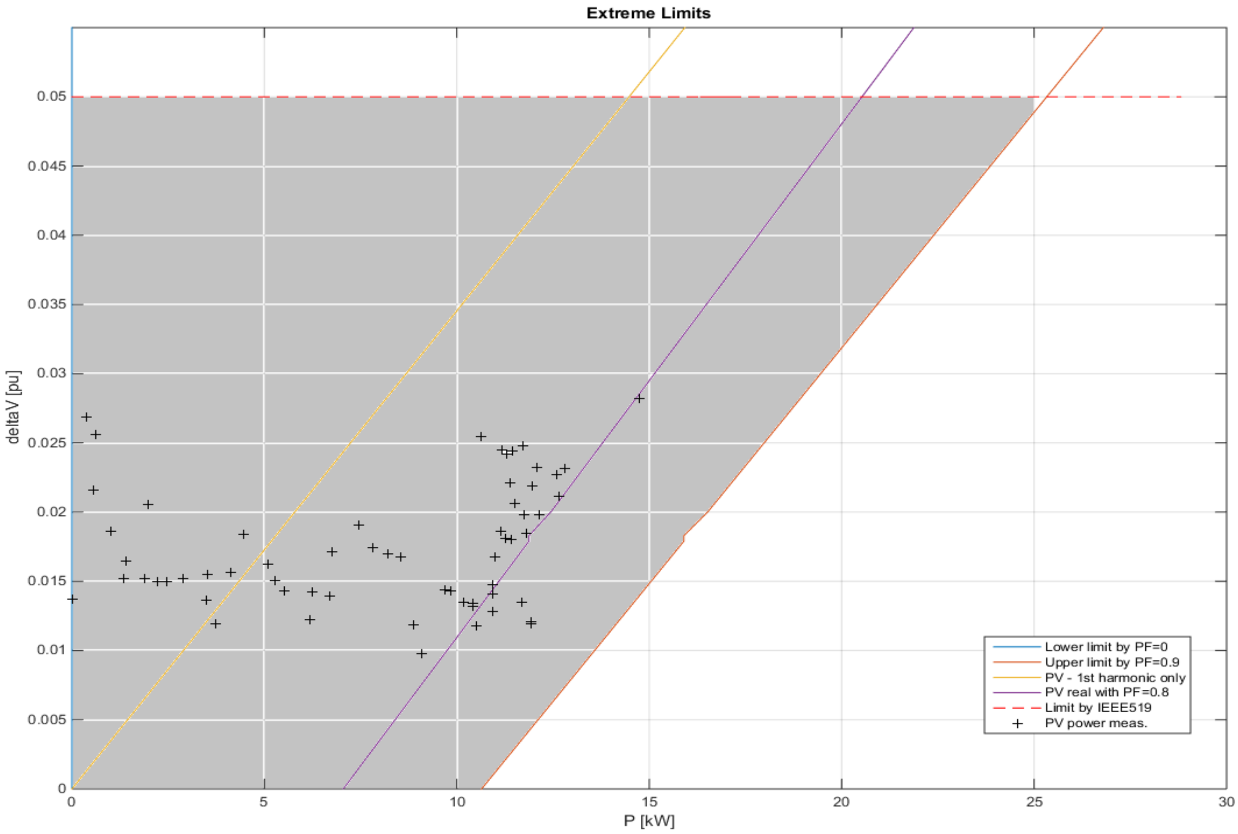

Figure 7.8 – Hosting capacity approach for the four scenarios.

To illustrate the use of the hosting capacity approach discussed before, the following example can define the behaviour of the system considering a specific power factor for the lower and upper limits, which will impact the acceptable and unacceptable deterioration regions for the system under analysis. Figure 7.9 shows the hosting capacity variation for three different power factors: 0.1, 0.6 and 0.9. It is possible to observe that the lower the power factor is, the lower the acceptable deterioration region will be. Moreover, it is important to realize that, even for the best-case scenario, which will set the upper limit, the impact is not as large as the impact in the worst-case scenario, where the amount of energy set is impacted directly by the background at the PCC.

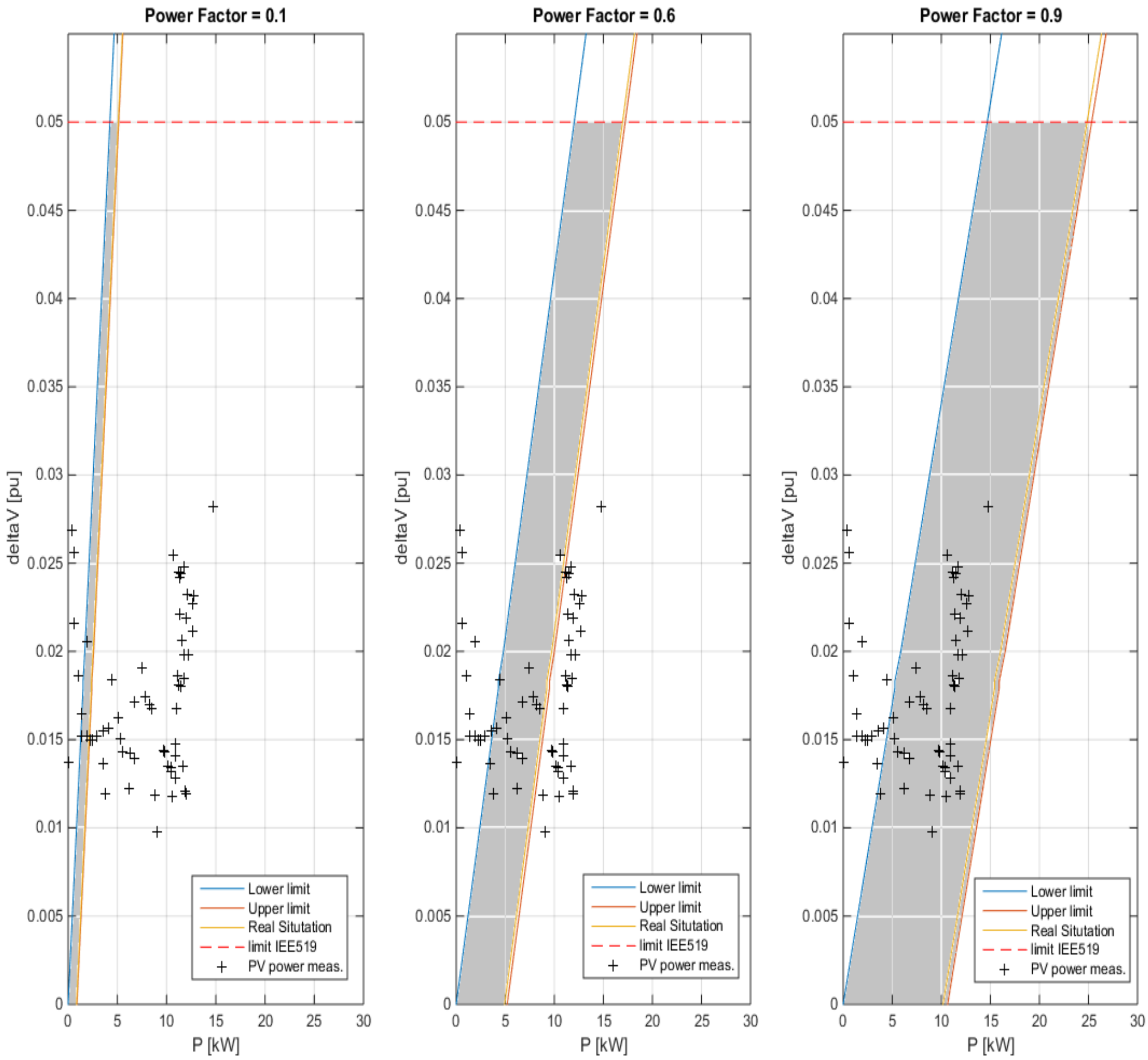

Figure 7.9 – Variation of the hosting capacity region for different power factor.

7.3.2 Simulation of Sensitivity Analysis of the Local Hosting Capacity Definition

It is well-known that several factors may or may not affect the value of the hosting capacity into the distribution systems. Based on what has been discussed in section 6.2.2, we will go through a simulation in order to better define those factors that affect the value of the hosting capacity based on (6.2.14). These tests will highlight the impact of electrical parameters into the value of the hosting capacity considering a radial system with single-phase DGs. Thus, the considered system is based on the household installations at the Technological University of Eindhoven (TU/e) (PQ LAB at TUe, 2015). The system is shown in Figure 7.10.

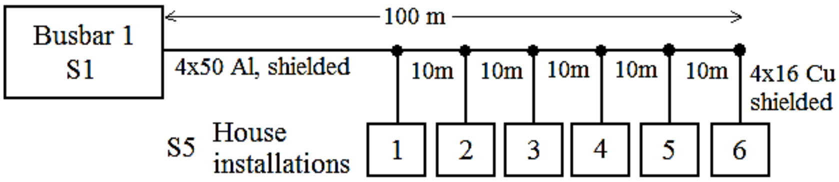

Figure 7.10 – Conceptual diagram of the connection of the household installations (PQ LAB at TUe, 2015).

Regarding Figure 7.10, it has been defined 6 PCC to connect the DG sources, as well as the loads. Also, it can be observed that the length of smaller cables should be approximately 10 – 30 meters long, type 4x16 mm^2 Cu shielded. The feeder is 100 meters long, type 4x50 mm^2 Al shielded. These values will be considered to determine the $R_{th} + jX_{th}$ for each PCC in the system. In the following items, the characteristics of the system will be further explained.

The next items will describe the technique to obtain the fundamental parameters to calculate the local hosting capacity for the system, as well as the main characteristics and variables of the system.

7.3.2.1 The Harmonic Power Flow used as a Simulation Tool

In order to assess the parameters to find the local hosting capacity based on (6.2.14) a Harmonic Power Flow (HPF) has been developed via Matlab®. A conventional power flow technique is a tool which determines electrical parameters such as voltage, current, active and reactive power, power factor at different points of the system, among others. In this case, only fundamental frequency is considered regarding voltage and currents' quantities into the electrical grid. Thus, by definition, a HPF is a tool which is used to predict the level and propagation of harmonic voltage and the current created by one or more harmonic devices connected into the electrical grid. At this point, single-phase DG has been considered as a case study in order to compose the developed HPF. This model was chosen because it is one of the most realistic ways to represent a distribution system considering DG.

The design of the HPF was based on a simple power flow solution which has been adapted to harmonic devices connected into the system. It was decided that the best method for this investigation was to analyse the impact of single-phase generation, as well as single phase load. Through the use of the HPF, we are able to calculate the harmonic voltage vector from the fundamental order until the 15^{th} harmonic order. In this case, the following algorithm can be found in **APPENDIX A.**

7.3.2.2 Definition of the System's Parameters

The radial system was prepared in accordance with Figure 7.10. All six busbars of the system were carefully checked to connect one single-phase DG and one-single phase load. The allocation procedure was obtained via the HPF Matlab® program and the connected points were randomly generated into the algorithm. The DG and load allocation of the system is shown in Table 7.6 in black shading. It is important to notice that most of the DG sources and loads allocated are connected in the phase C (green phase) of the system.

Table 7.2 – Allocation of the loads and the DG sources into the system.

Node						
6	5	4	3	2	1	Phase
						A
						B
						C

Once the GD sources and the loads allocation have been defined, the equivalent impedance of the system is calculated based on data shown in Figure 7.10. In this case, the equivalent impedance per kilometre in p.u. is $Z_l = 0.641 + j0.15\ (pu/km)$. It is important to highlight that the base values considered are: 400 V and 100 kW. Thus, the length of the busbar was defined based on Figure 7.10. The respective lengths, in meters, from the main busbar to the nodes are shown in Table 7.3. In this case, the main busbar is defined as node 0.

Table 7.3 – Lengths of the system.

From 0 to 1	From 1 to 2	From 2 to 3	From 3 to 4	From 4 to 5	From 5 to 6
50 meters	10 meters	10 meters	10 meters	10 meters	10 meters

This study used traditional techniques based on recommendations of a residential harmonic distortion spectrum and harmonic current injection of inverters. Firstly, the residential harmonic distortion was prepared in accordance with the traditional background distortion injected by linear and non-linear loads (OLIVEIRA et al., 2015). This model was chosen because it is one of the most practical ways to demonstrate the behaviour of residential loads considering their background distortion. In addition, the base value of the load was chosen as $2\ kW, cos\varphi = 0.8\ (inductive)$.

Secondly, the inverters of the DG unities were selected in order to define their current harmonic injection into the system based on a traditional spectrum which can be found in (OLIVEIRA et al., 2015). Through the use of the current harmonic spectrum by the DG, together with the background distortion created by linear and nonlinear loads, we were able to find the total harmonic voltage distortion for each PCC in the system.

The outlined spectrum regarding the background voltage distortion created by the loads is shown in Table 7.4

Table 7.4 –Background voltage distortion spectrum – Residential load (OLIVEIRA et al., 2015).

Order	V (%)
1	100
3	3 – 1
5	5 – 3
7	5 – 3
>7	1 – 0.5

The outlined spectrum regarding the harmonic current injection created by the inverters of the DG is shown in Table 7.5.

Table 7.5 –Typical current spectrum created by inverters (OLIVEIRA et al., 2015).

Order	I (%)
1	100
3	2 – 1
5	5 – 4
7	2 – 3
>7	1 – 0.5

7.3.2.3 Definition of the Sensitivity Analysis and Results

The aim of the HPF is to find the harmonic voltage vector considering the nonlinear and linear loads, as well as the DG sources connected at the PCC. As a result, it is possible to calculate the hosting capacity value for each phase and for each PCC. This simulation opted for a small sample of harmonic orders, in this case until the 15^{th} harmonic order, due to the relevant impact of the first orders such as the 3^{rd}, the 5^{th} and the 7^{th} harmonic orders.

It was decided that the best procedure for this investigation was to conduct a sensitivity study of the local hosting capacity when electrical parameters have been gradually changed in order to analyse their impact on the local hosting capacity final value, as a sensitivity analysis. In this case, the design of the local hosting capacity evaluation was based on two factors:

- A harmonic distortion ranging from 0.5% to 5% (Limit imposed by international standards);
- A power factor at the PCC ranging from 0.5 to 1.

The local hosting capacity was gradually found when those parameters were modified. It is important to notice that when the power factor was improved, the harmonic distortion kept constant and when the harmonic injection was altered, the power factor also kept constant.

A. General Results

In the first step of the process, the total local hosting capacity profile for the system has been drawn considering a constant power factor and random harmonic injection. The total local hosting capacity profile is shown in Figure 7.11.

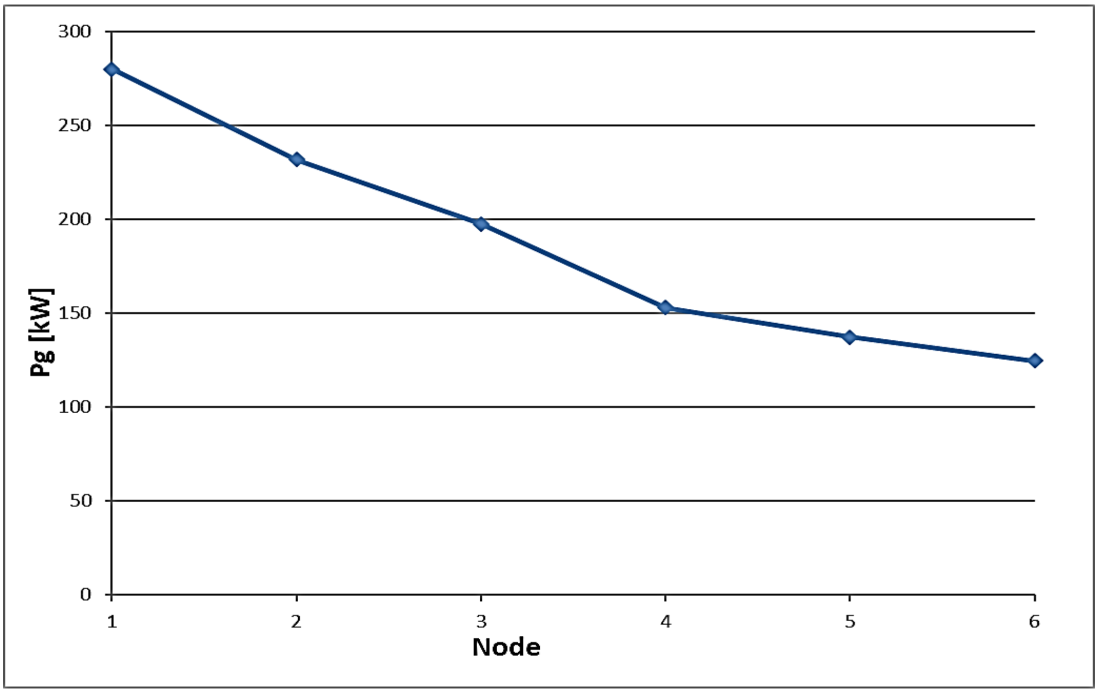

Figure 7.11 – Total local hosting capacity profile for the system

Interestingly, the total hosting capacity decreased gradually from 280 kW, in node 1, to 124 kW, in node 6. Generally speaking, we can conclude that the further the node is, the lower the hosting capacity will be. This result is significant only due to the voltage drop in the feeder from node 1 to node 6. The first set of analysis confirmed the impact of the distance on the local hosting capacity value. As soon as the total local hosting capacity has been defined, it was possible then analyse the local hosting capacity per phase, in order to illustrate the impact of the allocation of the loads and the DG sources.

The association between the allocated phase and the hosting capacity value is worth mentioning because those variables are related between themselves. The total phase hosting capacity profile is shown in Figure 7.12.

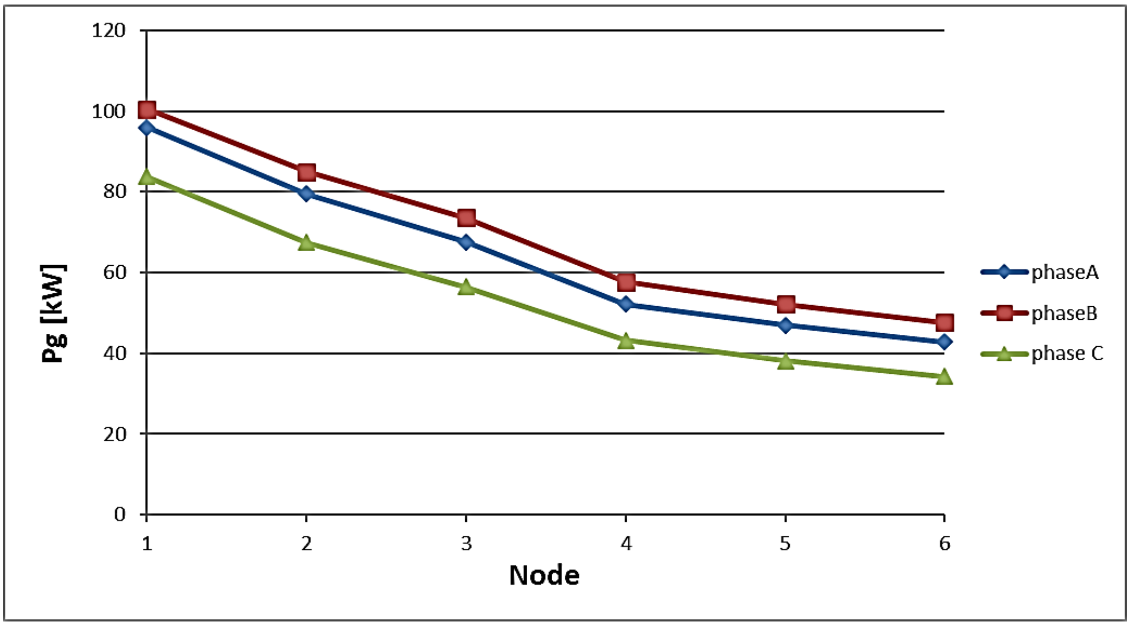

Figure 7.12 – Phase local hosting capacity profile for the system.

The most remarkable result to emerge from the data is that phase C has the lowest hosting capacity profile when compared to the hosting capacity profile of phases A and B. Remarkably, this association is related to the fact that most of the loads and DG sources are allocated in phase C. As far as we know, this causes remarkable values of voltage rise on phase C considering the significant quantity of reverse power flow. Significantly, phases A and B have almost the same profile due to the fact that just one load and one DG have been allocated to those phases, therefore the voltage rise will be essentially the same. It believes that the results emphasise the validity of our model considering single-phase generation. These results have further strengthened our confidence in that the impact of the voltage rise due to harmonic distortion is worth mentioning in order to define the hosting capacity profile.

B. *Sensitivity Analysis of the Power Factor*

These next tests revealed that the power factor value at the PCC has a significant impact on the local hosting capacity. Let's take a look at Figure 7.13 where it has been computed the power factor for the system at 0.5, 0.8, 0.9 and 1.

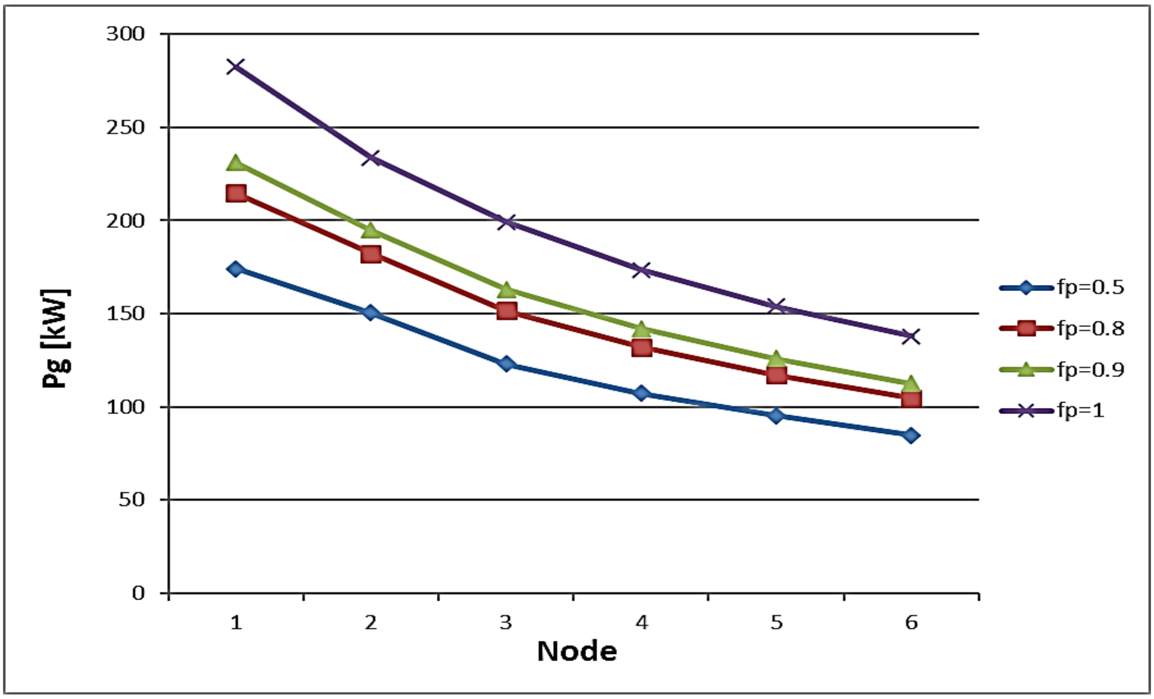

Figure 7.13– Total Local hosting capacity profile considering PF = 0.5, 0.8, 0.9 and 1.

The power factor at the PCC can increase the local hosting capacity. There is significant positive association between the power factor and the local hosting capacity for each node in the system. In order to illustrate the sensitivity analysis, let's take a look at node 6 of the system. As expected, the total hosting capacity value, regarding a power factor equal to 0.5, reached a value of 84 kW. On the other hand, when the power factor was set to 1.0 (resistive) the total hosting capacity value found was 134 kW. This analysis captures the response of the improvement regarding the total hosting capacity for the system in an average value of 59.5 %, as shown in Figure 7.14. There is satisfactory agreement on the fact that a small change in the power factor can improve the total local hosting capacity.

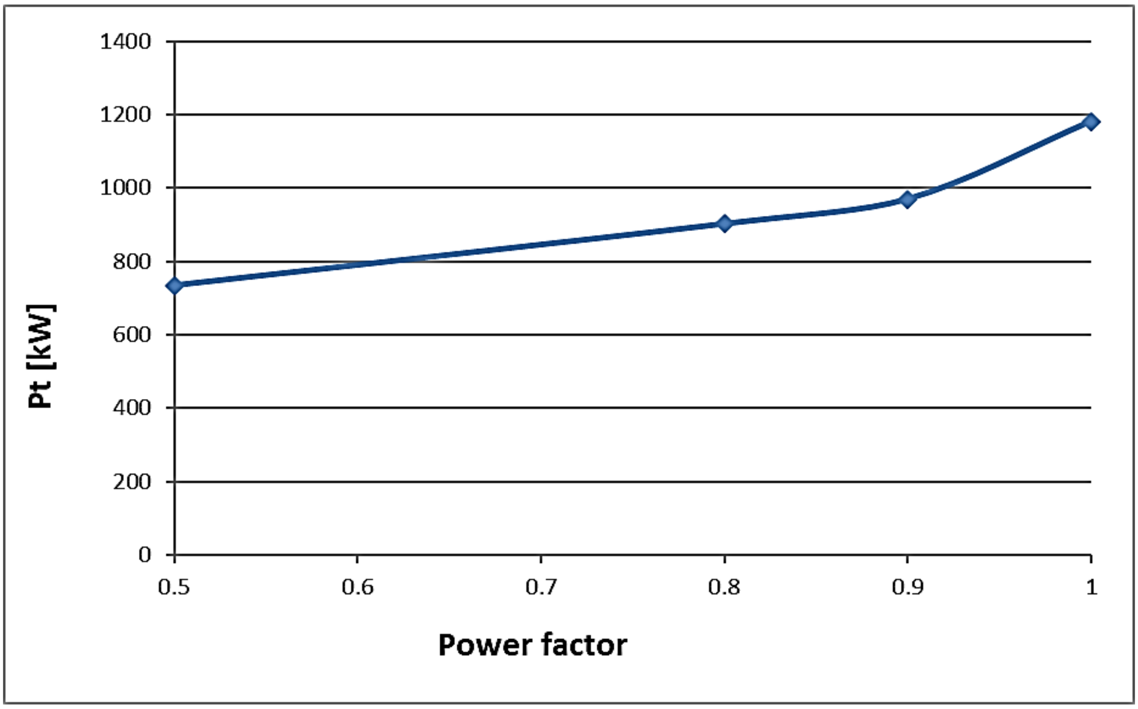

Figure 7.14–Sensitivity profile for the PF change.

C. *Sensitivity Analysis of Harmonic Distortion*

As mentioned before, the injection of harmonic current into the system depends on the equipment connected at the PCC and the DG sources system inverters. The latter can be controlled by the producer when the equipment is manufactured according to international standards, but the background voltage at the PCC cannot be controlled. Therefore, sensitivity analysis scenarios will be imposed to investigate how the harmonic injection can impact the total local hosting capacity for the system.

As a forecast, these experiments demonstrate that the voltage distortion can decrease the value of the total local hosting capacity for the system. In this case, let us consider a scenario where the voltage for the fundamental order is set at 1.01 p.u. and the other harmonic voltages for $h \geq 2$, up to 15, are set at 0.05, 0.01, 0.03, 0.04 and 0.05 p.u. The total local hosting capacity profile for these distortions is shown in Figure 7.15.

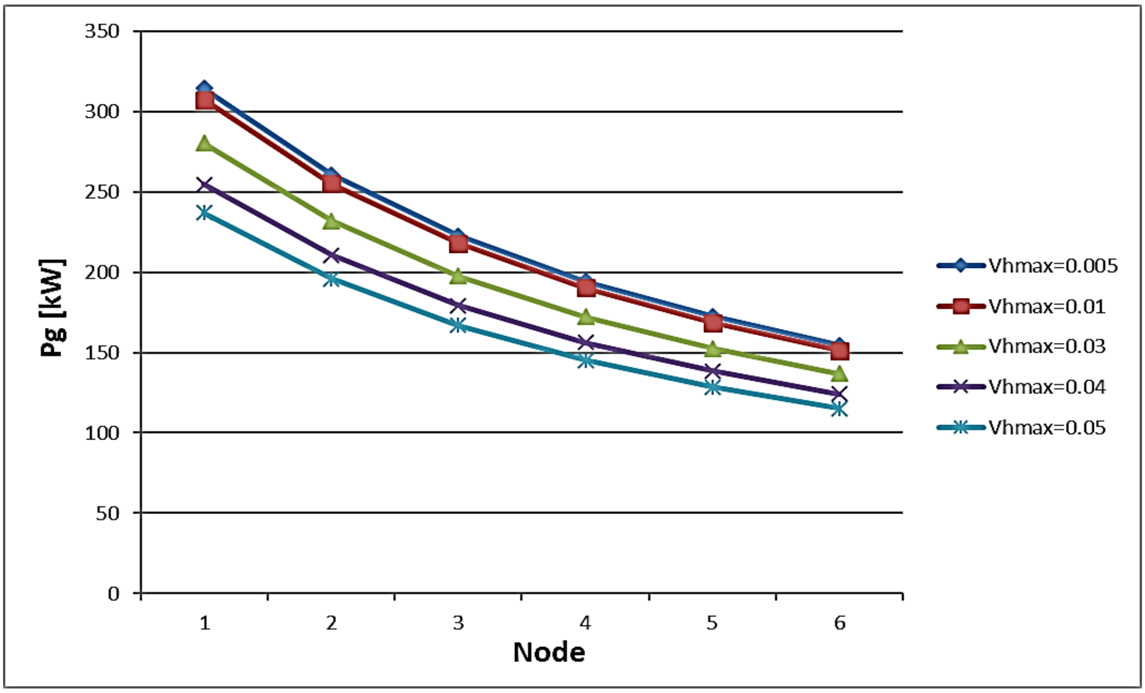

Figure 7.15– Total Local hosting capacity profile considering voltage distortion equal to 00.05, 0.01, 0.03, 0.04 and 0.05 p.u.

It is important to realise that a decrease in harmonic voltage would increase the total local hosting capacity as shown in the results of Figure 7.15. As hypothesized, the experiment demonstrates that the higher the voltage distortion is, the lower the hosting capacity will be. Regarding node 6, those findings would seem to demonstrate that the local hosting capacity value for 0.05 p.u of voltage distortion is 115 kW and for 0.005 p.u of voltage distortion, the hosting capacity value reached 151 kW, which means that the local hosting capacity reached almost 31% of improvement when the voltage distortion decreased 10 times. An implication of this fact is the possibility of an average of 32% of improvement when the voltage distortion decreases. The conclusion is shown in Figure 7.16.

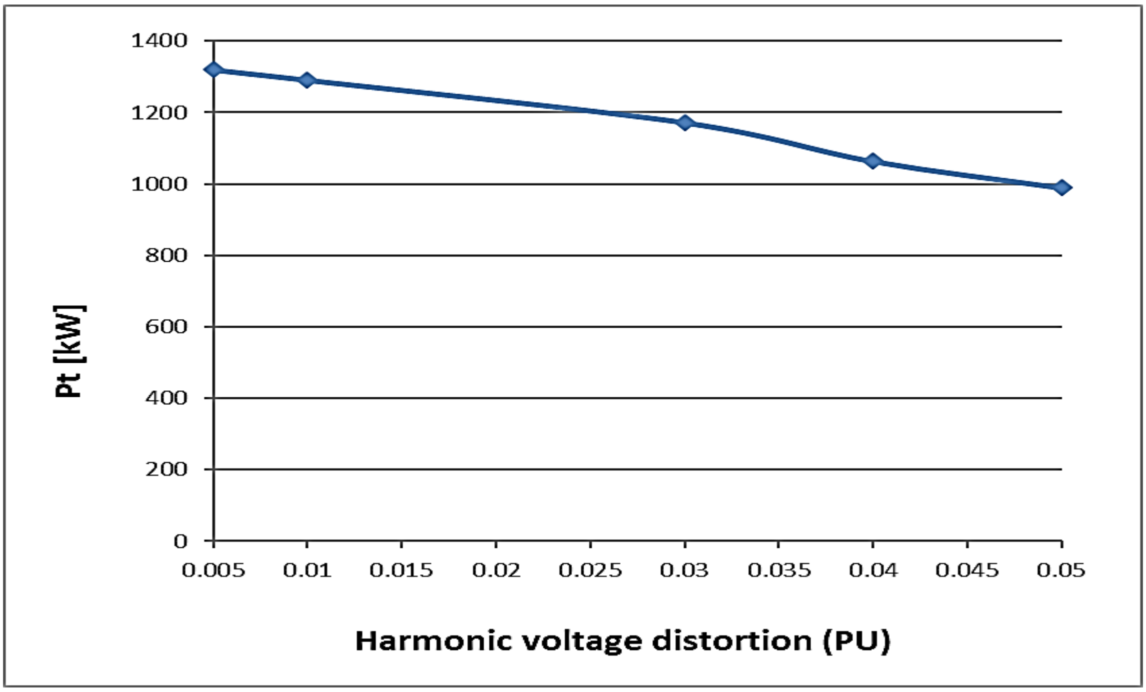

Figure 7.16–Sensitivity profile for the harmonic voltage distortion change.

7.3.2.4 General Conclusions

The evidence from this section points toward the idea that a sensitivity analysis can provide a better understanding of the proposed local hosting capacity methodology regarding voltage rise due to harmonic distortion. The results of a sensitivity analysis indicate the idea that the power factor variation and the improvement of the harmonic distortion can cause impact on the local hosting capacity value. We have found a cutting-edge solution for the changing of electrical parameters in order to improve the local hosting capacity value. Moreover, we have provided further evidence that the bigger the local hosting capacity is, the higher the local hosting capacity will be. Furthermore, the lower the harmonic distortion is, the higher the local hosting capacity will be.

Moreover, details of the harmonic power flow results and the hosting capacity calculation regarding this section can be consulted in **APPENDIX B**.

7.4 The Dynamic Hosting Capacity Application

In order to illustrate the calculation of DHC by the maximum capacity equation given in (6.3.1), the voltage rise, and harmonic source will be validated by specific measuring equipment to get the equivalent data of the voltage profile, harmonic injection, THD profile, frequency, and others.

This seems to be a useful approach to get a weekly power quality measurement. Thus, the DHC capacity can be calculated in order to define a hosting capacity profile considering the maximum amount of energy calculated by (6.3.1).

It is believed that this method could probably be usefully employed in determining the range of values where the hosting capacity is valid to keep the efficiency of the grid. This would appear to indicate that the maximum and minimum values of the hosting capacity must be respected. For example, there is a slight probability that the minimum value would be lower than the already installed power, which means the system was underestimated by planners and its harmonic background has not been properly considered. Thus, the minimum value will be set up considering the installed power. On the other hand, the maximum value would lend itself well for use by future improvements of the grid.

7.4.1 Dynamic Maximum Power Capacity Daily and Its Dynamic Hosting Capacity Profile

The first set of analysis examined the impact of the DHC on the measured system. The association between the measurements' power generation data and maximum power generation was tested and plotted for all the days in the measured week. Interestingly, for all values of power generation measured, a maximum amount of power generation was calculated using (6.3.14) creating a linear dependency between them. Those results are shown in Figure 7.17 through Figure 7.23, where a significant association between the maximum amount of power generation points is found through linear regression using the $y = ax + b$ formulation.

If a linear extrapolation is created using these points, it is possible to determine the hosting capacity when the calculated line crosses the overvoltage limit index at 5%. For example, for the 9th of April 2015, the linear regression found regarding the maximum amount of power calculated is equal to $y = 0.0035\,x - 0.0333$, where the variable y represents the overvoltage margin of the system, and x represents the calculated power for any overvoltage margin considered. In this case, the overvoltage margin of 5% will be replaced in y in order to find its respective x value. Thus, the final solutions contained represent the average hosting capacity in relation to the chosen day. In Figure 7.17, it is possible to see that the hosting capacity calculated is 24 kW for the 9th of April 2015.

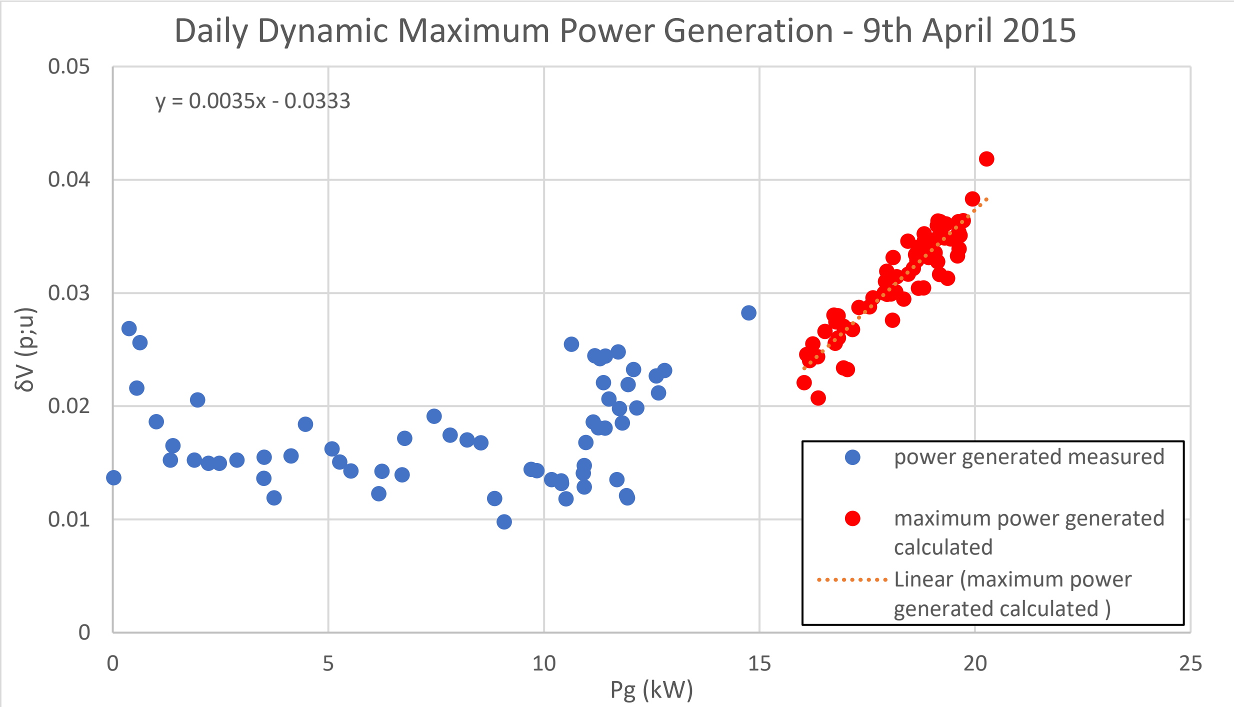

Figure 7.17 – The linear dependency in relation to the maximum amount of energy calculated by (6.3.1) –April 9th, 2015.

These tests were reproduced to other days. The results are shown in the following graphs. As mentioned before, a linear extrapolation is created using those points to determine the hosting capacity when the line crosses the overvoltage limit index at 5% for all days. Based on this fact, it is evident in Figure 7.18 that the hosting capacity calculated is 23.5 kW for the 10th of April 2015.

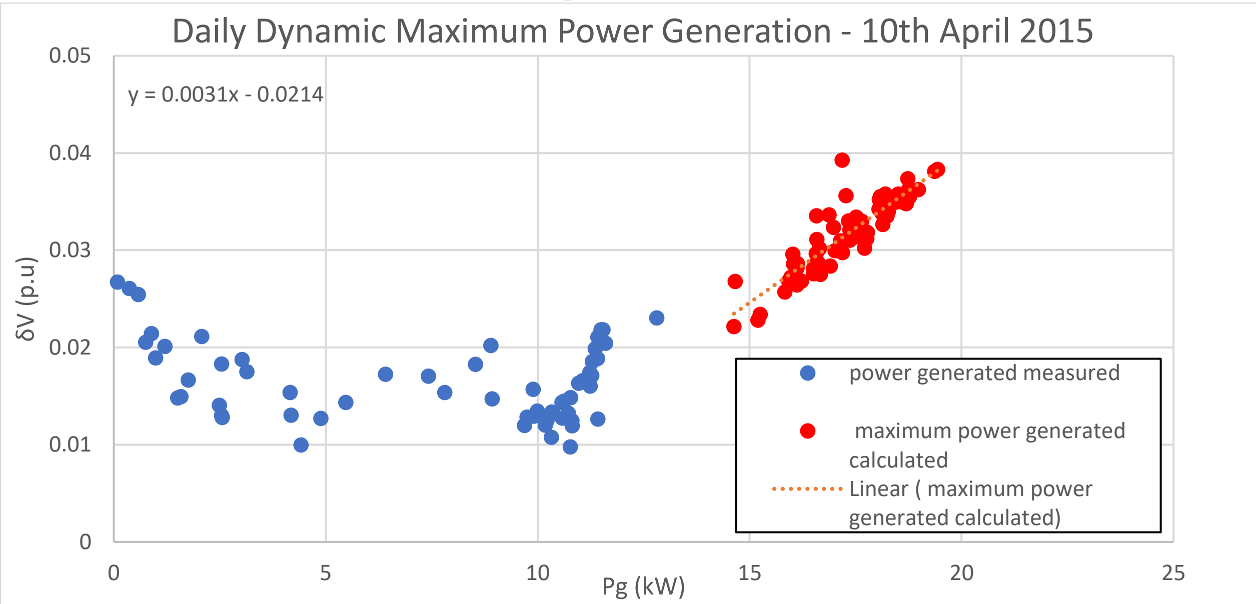

Figure 7.18 – The linear dependency in relation to the maximum amount of energy calculated by (6.3.1) –April 10th, 2015.

Regarding the 11th of April 2015, it is possible to see in Figure 7.19 that the hosting capacity calculated using its linear regression is 23.4 kW.

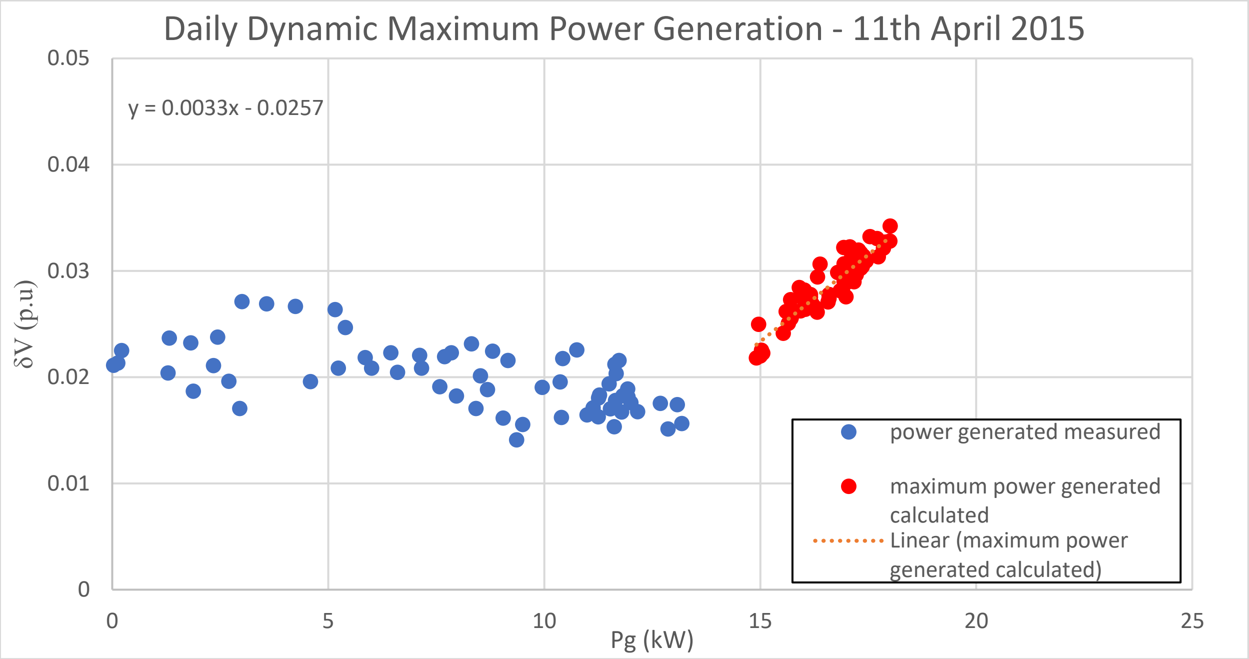

Figure 7.19 – The linear dependency in relation to the maximum amount of energy calculated by (6.3.1) –April 11th, 2015.

After having calculated the linear regression for the 12th of April day, we found it to be 20 kW as we can see in Figure 7.20, which is less than the average value found before.

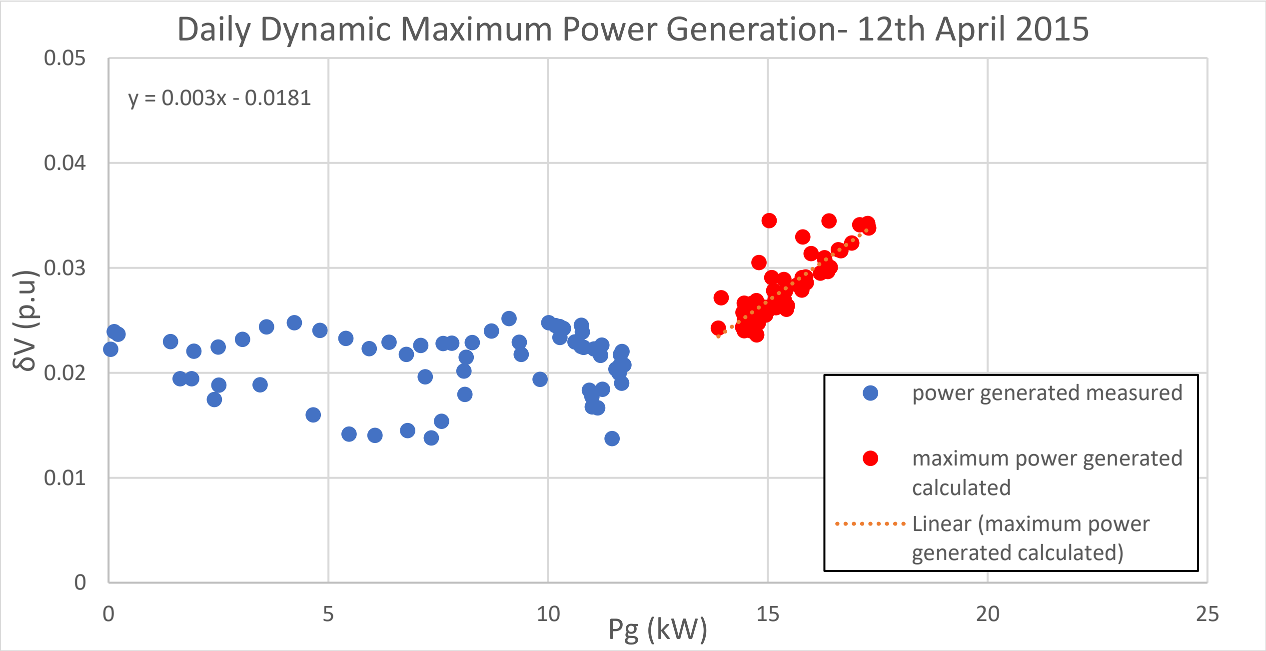

Figure 7.20 – The linear dependency in relation to the maximum amount of energy calculated by (6.3.1) –April 12th, 2015.

For the 13th of April 2015, Figure 7.21 shows that the hosting capacity calculated is 23.3 kW.

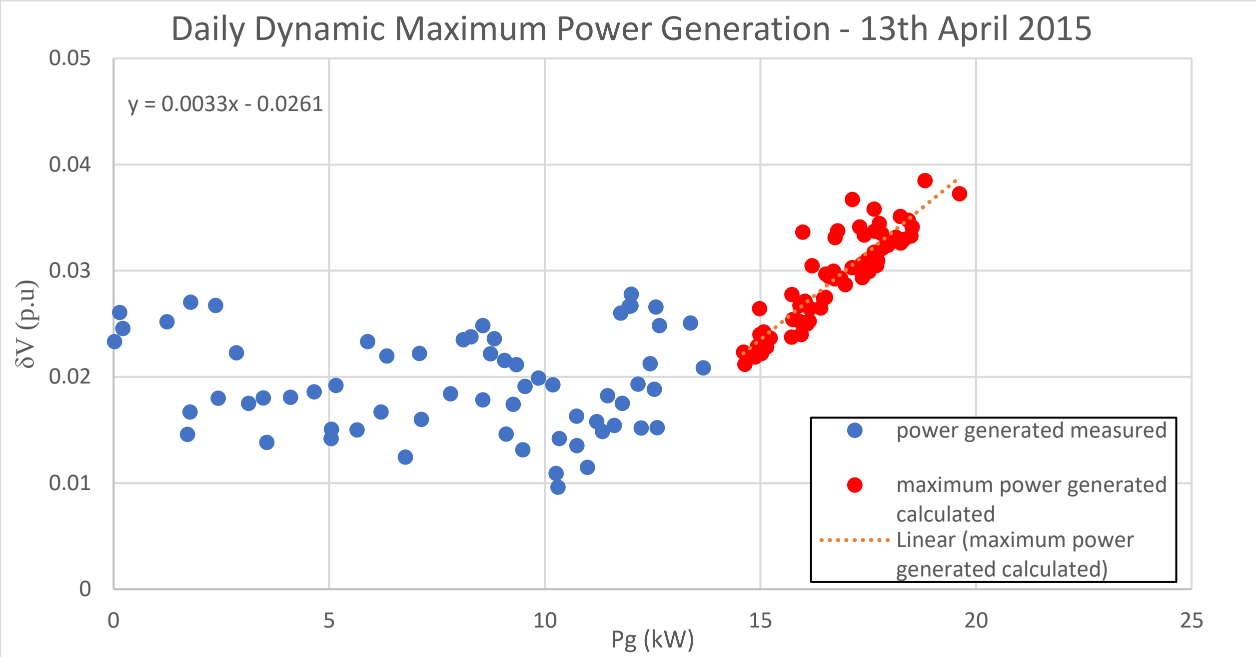

Figure 7.21 – The linear dependency in relation to the maximum amount of energy calculated by (6.3.1) –April 13th, 2015.

Figure 7.22 gives us the hosting capacity calculated for the 14th of April 2015, which is 23.6 kW.

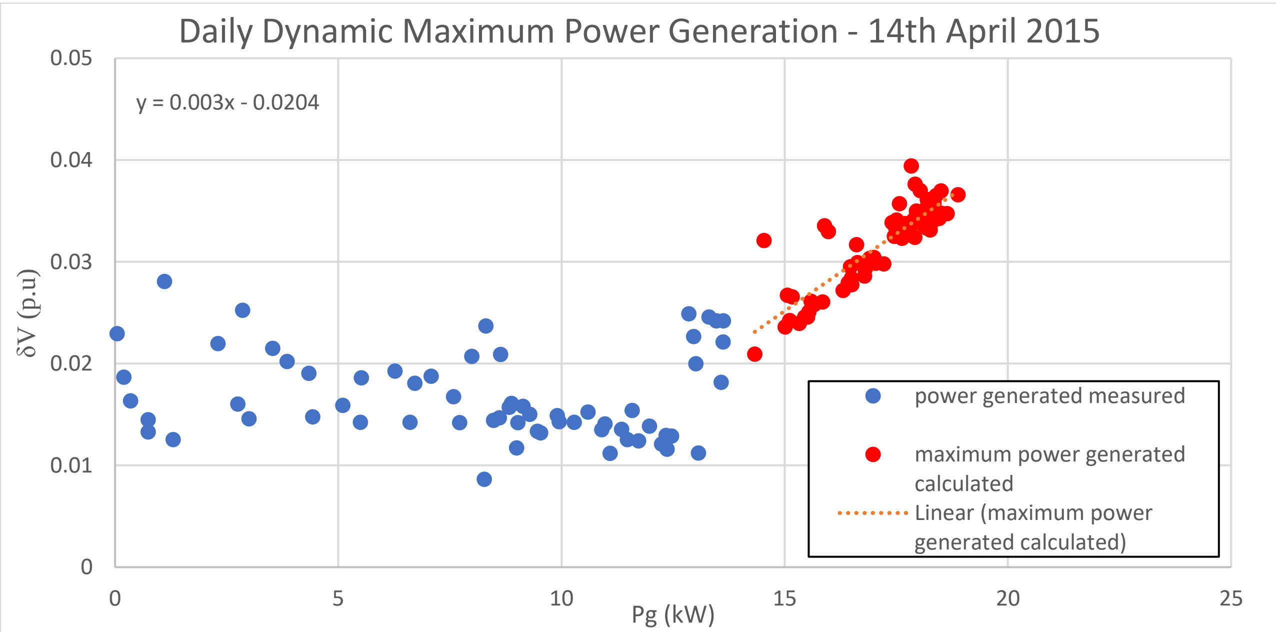

Figure 7.22 – The linear dependency in relation to the maximum amount of energy calculated by (6.3.1) –April 14th, 2015.

Finally, regarding the 15th of April 2015, it is possible to see in Figure 7.23 that the hosting capacity calculated using linear regression is 23.6 kW as well.

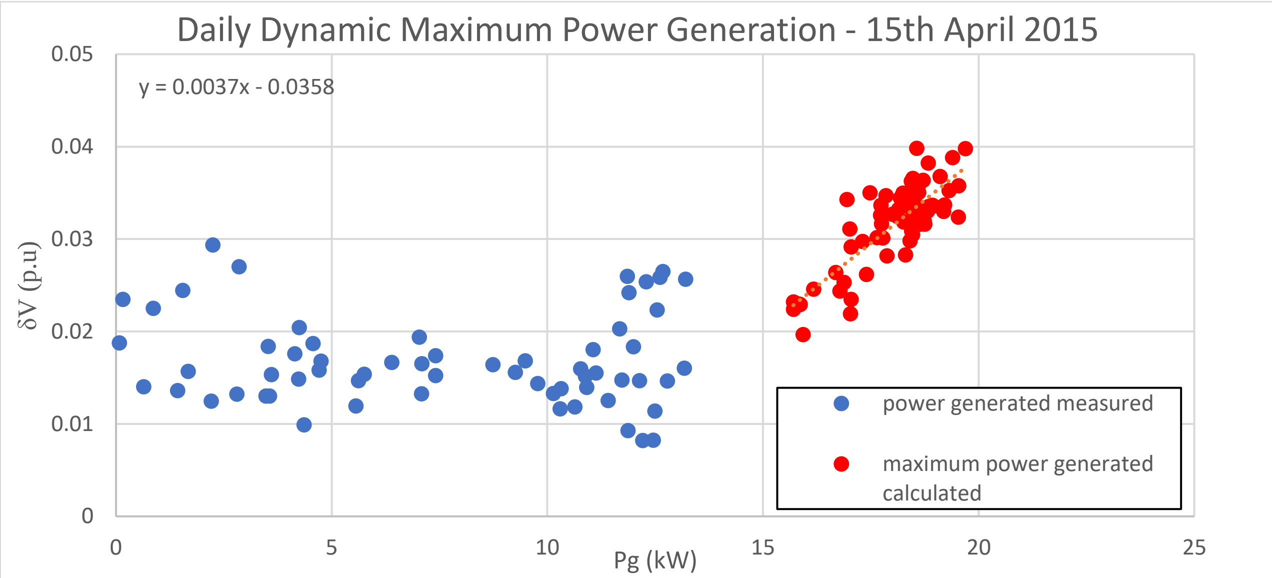

Figure 7.23 – The linear dependency in relation to the maximum amount of energy calculated by (6.3.1) –April 15th, 2015.

These tests highlighted that there is a possible DHC profile for the measured week in order to draw a better view of the behaviour of the system. Moreover, the results on local hosting capacity for all the days presented before can be summarised in Table 7.6.

Table 7.6 – Hosting Capacity values for the measured week.

	9th April	10th April	11th April	12th April	13th April	14th April	15th April
HC	24 kW	23.5 kW	23.4 kW	20 kW	23.3 kW	23.6 kW	23.6 KW

This method represents a useful and initial alternative to drawing the DHC profile considering the day mentioned before, where for each instant of measurement, a maximum power generation, using (6.2.14), has been calculated. Therefore, as stated earlier, a linear association is calculated for all these instants of time using the overvoltage margin as well as the measured power from the PV. These factors will be responsible for this result. Let's take a look at Figure 7.24 where an exemplification of the calculation of the daily DHC is given.

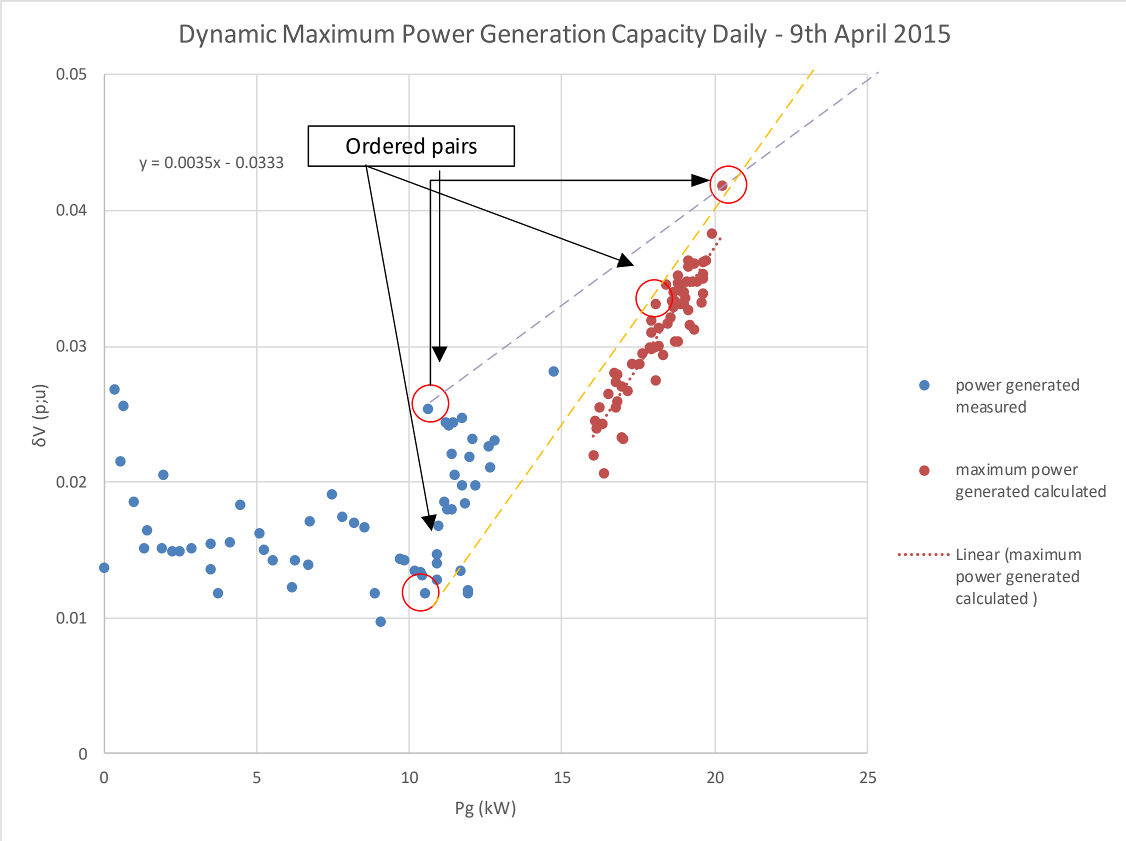

Figure 7.24 – Exemplification of calculation of dynamic daily hosting capacity in relation to April 9th, 2015.

As in the local hosting capacity method shown in section 6, when these lines cross the limit index at 5%, a group of lines will be drawn as a result of the hosting capacity value. These lines are created due to the existence of the ordered pairs: the measured pair $(\delta V; P_g)$ and the calculated pair $(\delta V_{max}; P_g^{max})$ by (6.2.14). It is important to notice that all ordered pairs are related by an instant in time. In Figure 7.24, as an example, we have defined two ordered pairs in order to illustrate the method. For each ordered pair, as mentioned before, we will extend those lines until they reach the limit index set as 5% of the overvoltage margin. In the example, the purple line created by the first ordered pair will reach a hosting capacity value of 5% of the maximum overvoltage margin of 25 kW. On the other hand, the yellow line created by the second ordered pair will reach 23 kW of hosting capacity for a certain instant in time. Based on this methodology, we will repeat the procedure for all ordered pairs created by equation (6.3.1). Thus, the daily DHC profile for April 9th is shown in Figure 7.25.

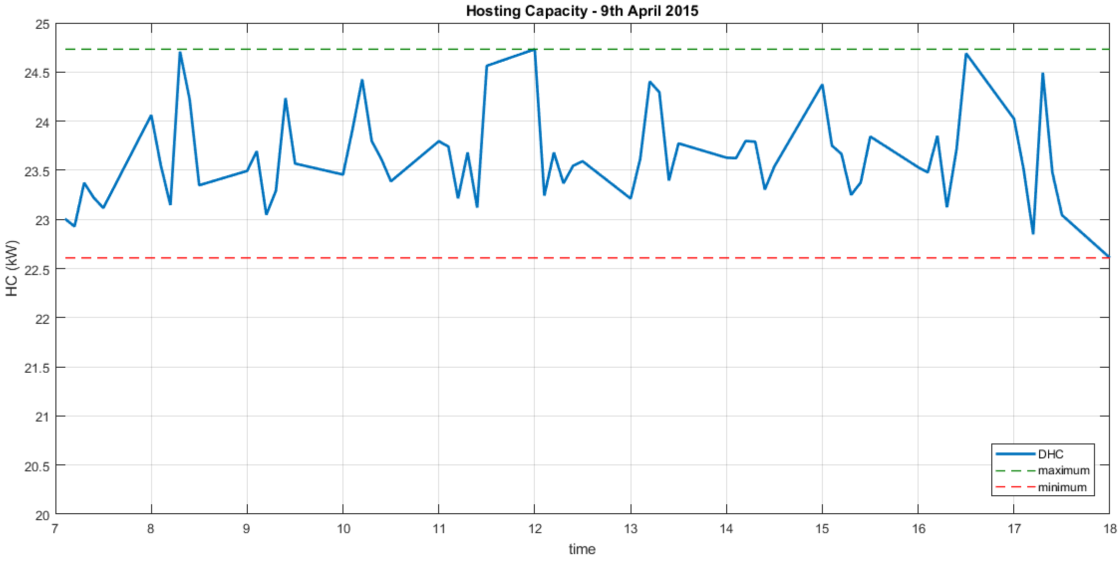

Figure 7.25 – The dynamic daily hosting capacity in relation to April 9th, 2015.

The average score for the 9th of April was 24 kW, as calculated through the daily DHC profile. Surprisingly, some values of hosting capacity are slightly higher and lower than the average. These phenomena might have occurred because some external and internal factors had contributed to these differences. In this case, the maximum daily hosting capacity is 24.8 kW, whereas the minimum value is 22.6 kW. In relation to one of the highest value, it is possible to offer an explanation. This result is only significant at a moment when there is almost no solar production because it is early in the morning or there are clouds covering the panels. The voltage rise will be low due to the lack of solar production, coupled with the fact that the building is empty. For example, one of the highest DHC found was at 12 p.m., which is defined as lunch time and all the building's equipment are turned off, while of the presence of some clouds in the sky might have decreased the solar production as well. On the other hand, the smaller values observed in the daily DHC could be explained as a result of a huge solar production and no load being fed at that moment. Moreover, the minimum value reached was at 06:00 p.m., which might have happened because most of the electronic equipment of the building was turned on and injecting high levels of distortion at the PCC. Unfortunately, it cannot be ruled out that the factors cited before may have influenced the extreme local hosting capacity values. Further analysis must be conducted. As a conclusion, due to the special characteristic of the building connected to the system, the lower the solar production is, the lower the voltage rise will be. Finally, it can be offered an explanation regarding the region between the maximum value and the minimum value. As mentioned in section 6.3, the smaller the acceptable region is, the worse the conditions of the grid will be. In this case, the performance regarding the 9th of April could be related to the fact that the day has presented one of the biggest solar production as shown in Figure C.1. Thus, if the load of the building is lower than expected and the PV production is almost reaching its peak, the range of harmonic distortion, as well as the voltage rise, would impact its DHC profile.

Thus, those results will be reproduced for the other days, as mentioned before, following the instructions previously described in Figure 7.24.

The second daily profile refers to the 10^{th} of April and is shown in Figure 7.26.

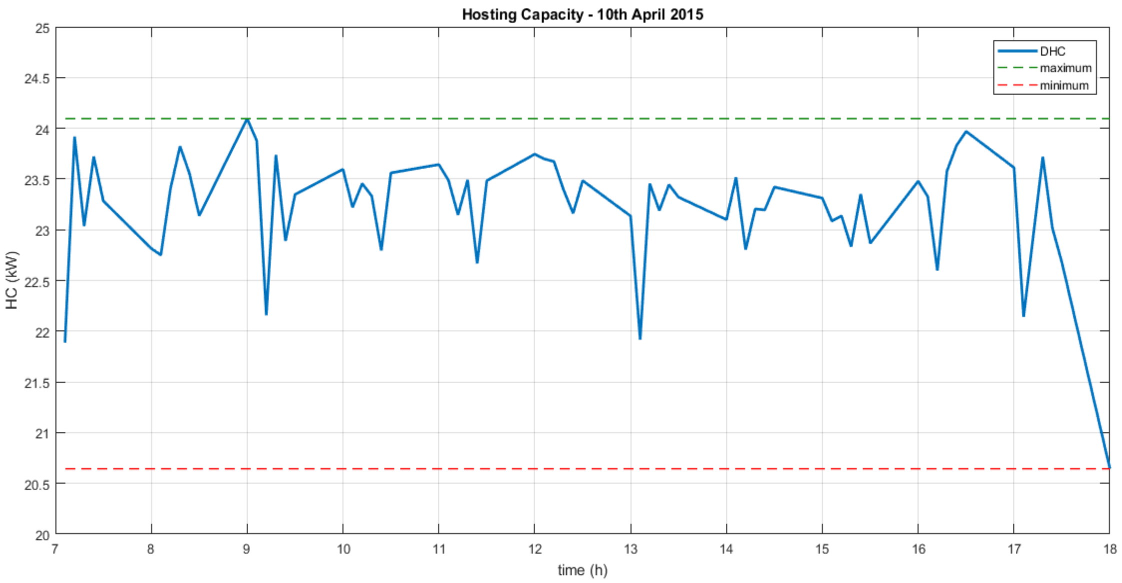

Figure 7.26 – The dynamic daily hosting capacity in relation to April 10^{th}, 2015.

.

The average score for the 10^{th} of April was 23.21 kW, as calculated through the daily DHC profile. Surprisingly, the region between the maximum value and the minimum value is bigger than the previous day, 9^{th} of April, which can explain a better improvement to the system because, as mentioned in Chapter 6, the larger the acceptable region is, the better the receptivity of the grid will be. This might have occurred since the system was in better voltage and distortion conditions than before. These phenomena might have taken place due to some external and internal factors contributing to these differences. Also, the higher value of the hosting capacity was registered almost at the same time as on the 9^{th} of April. In this case, the maximum daily hosting capacity is 24.1 kW, whereas the minimum value is 20.6 kW. In relation to the higher value, it is possible to offer the same explanation given before. This result is only significant at a moment when there is almost no solar production because it is early in the morning or there are clouds covering the panels. The voltage rise will be low due to the lack of solar production, coupled with the fact that the building is empty. On the other hand, the smaller values observed in the daily DHC could be explained as a result of a huge solar production and no load being fed at that moment. Moreover, the minimum value reached was registered at 06:00 p.m. as well. As mentioned before, it might have related to the fact that most of the electronic equipment of the building was turned on and injecting high levels of distortion at the PCC. It is important to notice that the acceptable region is larger than the previous day, which can offer a better grid performance. Moreover, it is related to the fact of the PV production regarding the 10th of April 2015 was lower than the day before.

The third daily profile pertains to the 11th of April and is shown in Figure 7.27.

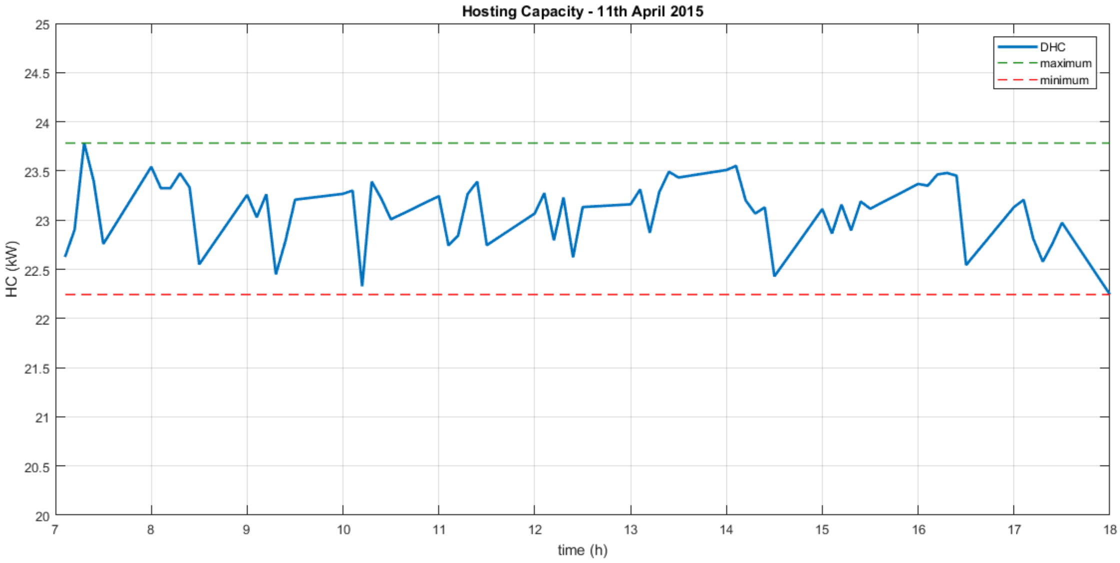

Figure 7.27 – The dynamic daily hosting capacity in relation to April 11th, 2015.

The average score for the 11th of April was 23.01 kW as calculated through the daily DHC profile. Surprisingly, the region between the maximum value and the minimum value is similar to the 9th of April. This might be explained by the system's comparable voltage and distortion conditions. In this case, the maximum daily hosting capacity is 23.78 kW, whereas the minimum value is 22.24 kW. In relation to the higher value, it is possible to offer an explanation. This result is only significant at a moment when there is almost no solar production because it is early in the morning or there are clouds covering the panels. The voltage rise will be low due to the lack of solar production, coupled with the fact that the building is empty. For example, the highest DHC found was at 07:00 a.m., which is defined as the beginning of the morning and all the building's equipment is turned off, while there is also no solar production yet. On the other hand, the smaller values observed in the daily DHC could be explained by it being a result of a huge solar production and no load being fed at that moment. Moreover, the minimum value reached was registered at 06.00 p.m. as well. As mentioned before, it might have related to the fact that most of the electronic equipment of the building was turned on and injecting high levels of distortion at the PCC. It is important to notice that the acceptable region is slighter than the previous day, which can offer a not remarkable grid performance. Moreover, it is related to the fact of the PV production and load conditions regarding the 11th of April 2015 was higher if compared to the day before, as shown in Figure C.1.

The fourth daily profile pertains to the 12th of April and is shown in Figure 7.28.

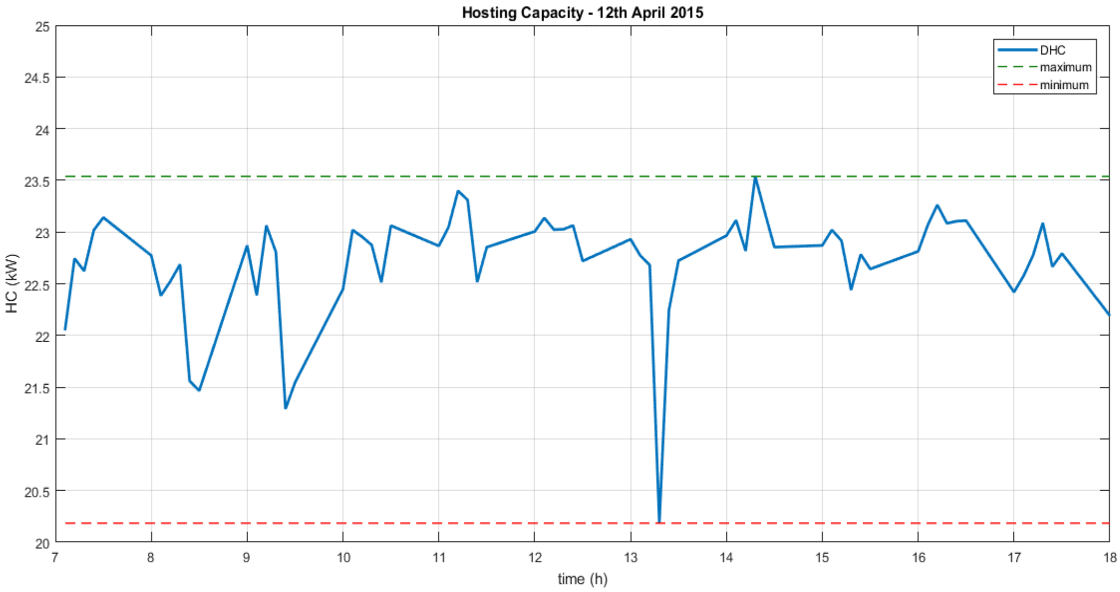

Figure 7.28 – The dynamic daily hosting capacity in relation to April 12th, 2015.

The average score for the 12th of April was 22.71 kW as calculated through the daily DHC profile. Surprisingly, the region between the maximum value and the minimum value is similar to the 10th of April. This might be explained by the system's comparable voltage and distortion conditions. In this case, the maximum daily hosting capacity is 23.58 kW, whereas the minimum value is 20.15 kW. In relation to the higher value, it is possible to offer an explanation. This result is only significant at a moment when there is almost no solar production because there are clouds covering the panels. The voltage rise will be low due to the lack of solar production, coupled with the fact that the building isn't empty. For example, the highest DHC found was at 02:00 p.m., which is defined as the middle of the afternoon and all the building's equipment is turned on, while there is also no solar production yet. On the other hand, the smaller values observed in the daily DHC could be explained by it being a result of a huge solar production and no load being fed at that moment. Moreover, the minimum value reached was registered at 01:00 p.m. as well. As mentioned before, it might have related to the fact that most of the electronic equipment of the building was turned on and injecting high levels of distortion at the PCC. As mentioned in section 6.3, the larger the acceptable region is, the better the conditions of the grid will be. In this case, the performance regarding the 12th of April could be related to the fact that the day has presented the lowest solar production as shown in Figure C.1. Moreover, it can be related to the fact that the load of the building could be higher, and the PV production had the smallest average production, which will impact on the range of harmonic distortion, as well as the voltage rise. Thus, the acceptable region was larger than the other days of measurement.

The fifth daily profile pertains to the 13th of April and is shown in Figure 7.29.

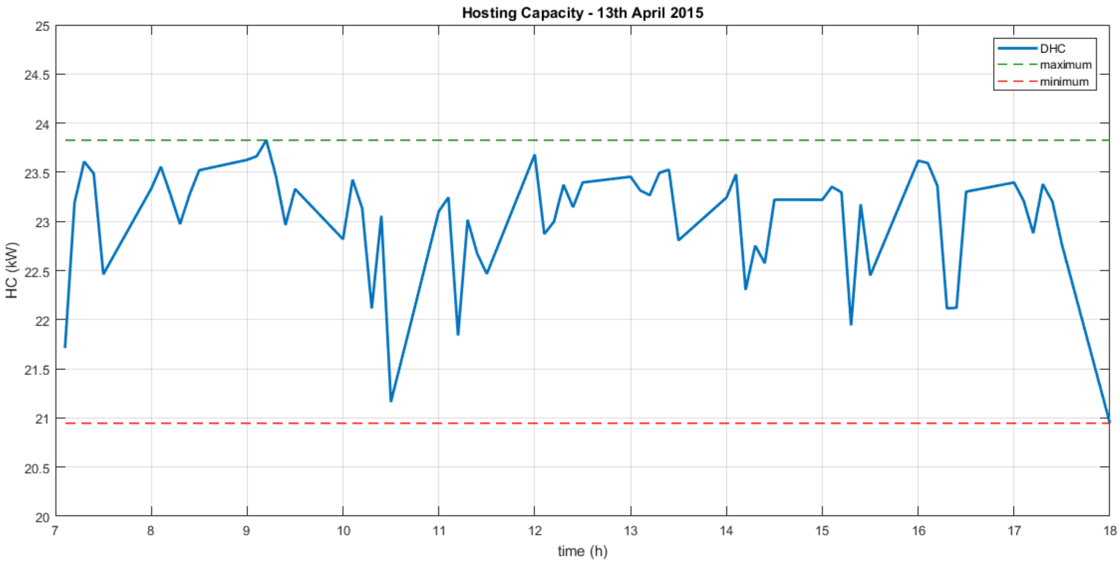

Figure 7.29 – The dynamic daily hosting capacity in relation to April 13th, 2015.

The average score for the 13th of April was 23.02 kW, as calculated through the daily DHC profile. Surprisingly, the region between the maximum value and the minimum value is similar to the previous day, 10th of April. This might have occurred since the system was in better voltage and distortion conditions than before. These phenomena might have taken place due to some external and internal factors contributing to these differences. Also, the higher value of the hosting capacity was registered at 09:00 a.m. In this case, the maximum daily hosting capacity is 23.82 kW, whereas the minimum value is 20.94 kW. In relation to the higher value, it is possible to offer the same explanation given before. This result is only significant at a moment when there is almost no solar production because it is early in the morning or there are clouds covering the panels. The voltage rise will be low due to the lack of solar production, coupled with the fact that the building is empty. On the other hand, the smaller values observed in the daily DHC could be explained as a result of a huge solar production and no load being fed at that moment. Moreover, the minimum value reached was registered at 10:00 a.m. as well. As mentioned before, it might have related to the fact that most of the electronic equipment of the building was turned on and injecting high levels of distortion at the PCC. It is important to notice that the acceptable region is slightly larger if compared to other days of measurement, which can offer a better grid performance. Moreover, it is related to the fact of the PV production and load conditions regarding the 13th of April 2015 as shown in Figure C.1.

The sixth daily profile pertains to the 14th of April and is shown in Figure 7.30.

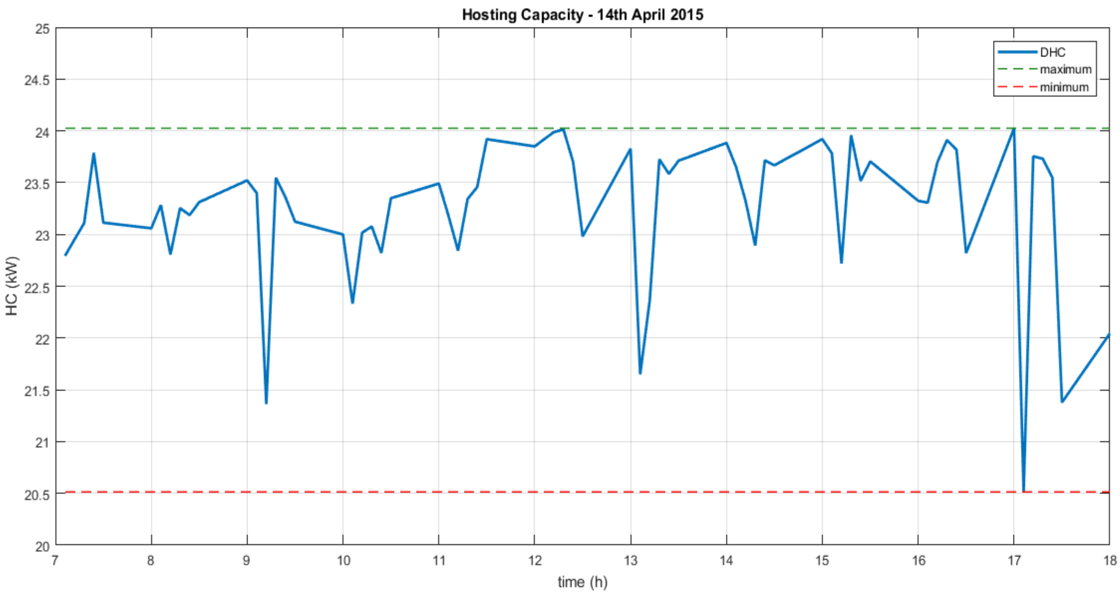

Figure 7.30 – The dynamic daily hosting capacity in relation to April 14th, 2015.

The average score for the 14th of April was 23.25 kW, as calculated through the daily DHC profile. Surprisingly, the region between the maximum value and the minimum value is similar to the previous day, 13th of April. This might have occurred since the system was in better voltage and distortion conditions than before. These phenomena might have taken place due to some external and internal factors contributing to these differences. Also, the higher value of the hosting capacity was registered in three different periods at 12:00 a.m., 02:00 p.m. and 03:00 p.m., which are worthy to mention. In this case, the maximum daily hosting capacity is 24 kW, whereas the minimum value is 20.54 kW. In relation to the higher value, it is possible to offer the same explanation given before. This result is only significant at a moment when there is almost no solar production because there are clouds covering the panels. The voltage rise will be low due to the lack of solar production, coupled with the fact that the building is empty. On the other hand, the smaller values observed in the daily DHC could be explained as a result of a huge solar production and no load being fed at that moment. Moreover, the minimum value reached was registered at 10:00 a.m. as well. As mentioned before, it might have related to the fact that most of the electronic equipment of the building was turned on and injecting high levels of distortion at the PCC. It is important to notice that the acceptable region is larger if compared to other days of measurement, which can offer a better grid performance. Moreover, it is related to the fact of the PV production and load conditions regarding the 14th of April 2015.

Finally, the last daily profile pertains to the 15th of April and is shown in Figure 7.31.

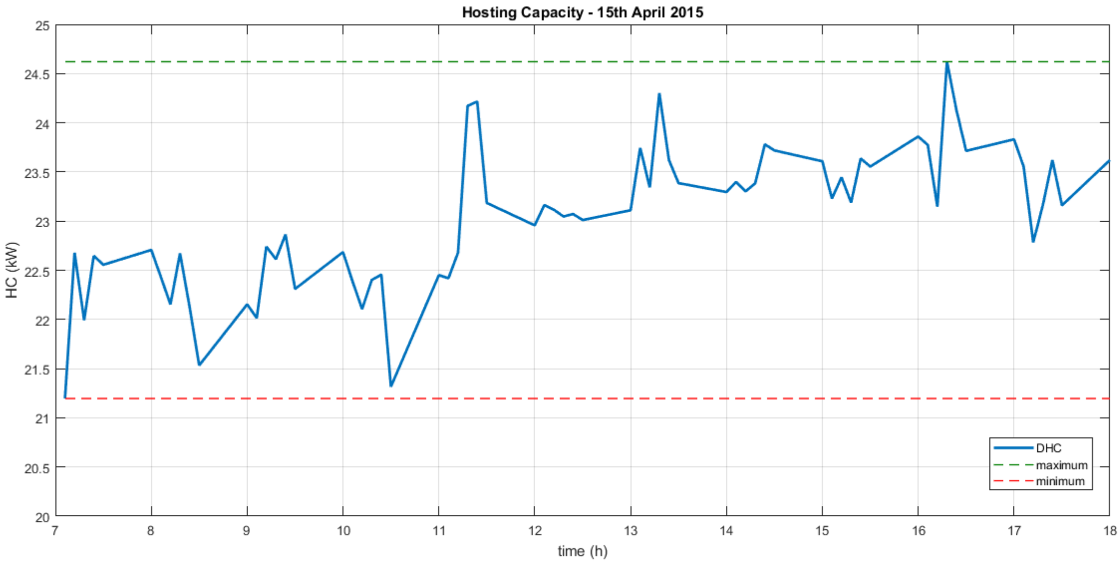

Figure 7.31 – The dynamic daily hosting capacity in relation to April 15th, 2015.

The average score for the 15th of April was 23.02 kW, as calculated through the daily DHC profile. Surprisingly, the region between the maximum value and the minimum value is similar to the previous day, 14th of April. This might have occurred since the system was in better voltage and distortion conditions than before. These phenomena might have taken place due to some external and internal factors contributing to these differences. Also, the higher value of the hosting capacity was registered at 12:00 a.m. In this case, the maximum daily hosting capacity is 24.64 kW, whereas the minimum value is 21.19 kW. In relation to the higher value, it is possible to offer the same explanation given before. This result is only significant at a moment when there is almost no solar production because it is early in the morning and there are clouds covering the panels. The voltage rise will be low due to the lack of solar production, coupled with the fact that the building is empty. On the other hand, the smaller values observed in the daily DHC could be explained as a result of a huge solar production and no load being fed at that moment. Moreover, the minimum value reached was registered at 10:30 a.m. as well.

As mentioned before, it might have been related with the fact that most of the electronic equipment of the building was turned on and injecting high levels of distortion at the PCC. It is important to note that the acceptable region is larger if compared to some days of measurement, which can offer a better grid performance. Moreover, it is related with the PV production and load conditions for the 15th of April 2015.

These tests highlighted that there is a relation between the PV production and the area, which can be calculated in relation to the maximum and minimum daily hosting capacity. Strong related evidence was found, making it possible to sustain that the higher the PV production is, the worse the performance of the grid will be or the smaller the daily hosting capacity area will be. Therefore, the daily hosting capacity area can be defined as energy-hosting capacity (EHC) and this relation can be calculated as given in (7.4.1).

$$EHC_{daily} = (HC_{max} - HC_{min}).(12\ hour)\ [kWh] \tag{7.4.1}$$

The average score for the daily EHC was calculated using (7.4.1) based on the maximum and minimum values discussed in Figure 7.25 through Figure 7.31. Moreover, the values of PV production were taken from Figure C.1. The data and results are shown in Table 7.7.

Table 7.7 – Daily EHC and PV maximum production.

Day	Daily EHC (kWh)	Max PV production (kW)
09/04/2015	50.95374	14.7561
10/04/2015	82.81773	12.8069
11/04/2015	36.94982	13.1786
12/04/2015	80.47586	11.7228
13/04/2015	69.1255	13.6711
14/04/2015	84.26921	13.6245
15/05/2015	82.18106	14.2848

Based on the values from Table 7.7, the daily EHC profile and the maximum PV generation can be drawn, which is shown in Figure 7.32.

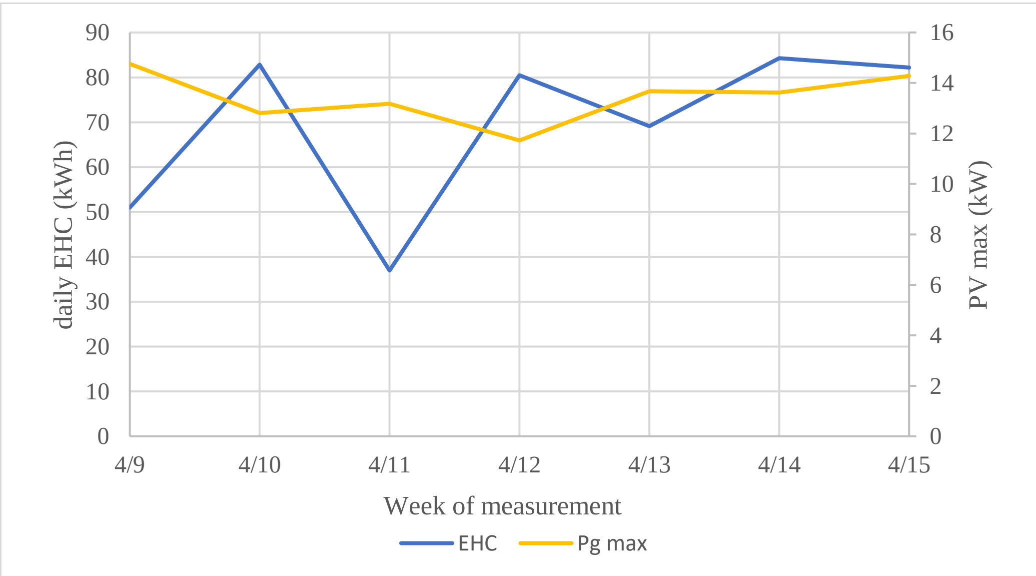

Figure 7.32 – Daily EHC profile versus maximum PV generation.

These results are only significant for the performance of the grid based on the PV production. Interestingly, this association is related to the maximum PV production, as well as the load conditions at the PCC. It is important to highlight that our results could not be tested on loading conditions, because there was no exclusive measurement of the load level. Thus, the single most marked observation to emerge from the data comparison was the larger the PV production is, the smaller the energy-hosting capacity (daily hosting capacity area) will be, which can be mitigated by power quality improvement processes. These mitigation processes can be found in the next sections.

7.4.2 Dynamic Weekly hosting capacity

As mentioned before, it is important to underline that these results weren't exclusively for one day of measurement. They were extrapolated to other days during the week of measurement as shown in Figure 7.25 and Figure 7.26. The most remarkable result which emerges from the set of data is that the weekly DHC profile is drawn for the system using the values of Table 7.6. Interestingly, the results are related to the maximum and minimum points in the final curve, as shown in Figure 7.33, where the maximum hosting capacity found remained at 23.8±0.5 kW and the minimum hosting capacity was 19±0.5 kW, describing a 5 kW gap between these two values. The DHC profile, as well as the lower and upper limits for the maximum amount of power generated, are shown in Figure 7.33.

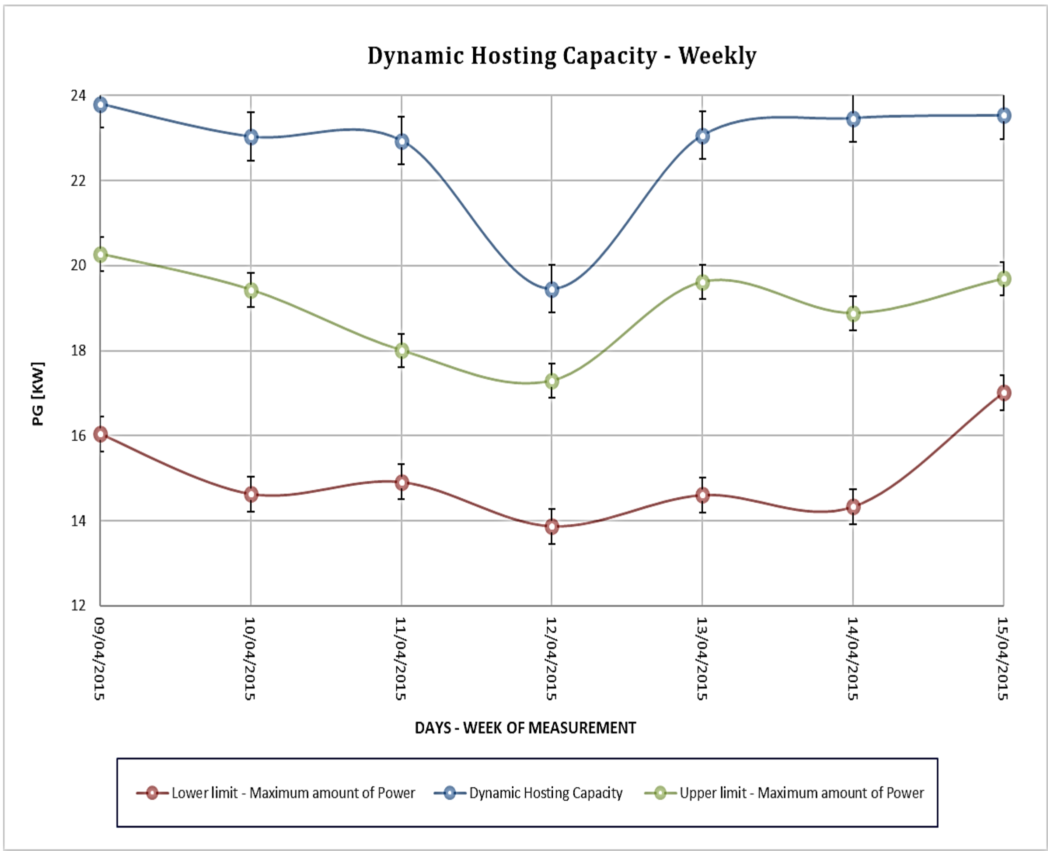

Figure 7.33 – The Dynamic Hosting Capacity Profile Weekly.

It is fundamental to note that the DHC profile has a strong association to external and internal phenomena into the system, which will be shown in the next figures. This analysis will show what has been discussed in Chapter 6 in relation to the impact of the harmonic distortion into the voltage rise due to DERs, where the Total Harmonic Distortion (THD) was used to confirm the association with the voltage rise.

Firstly, in Figure 7.34 – a, the THD profile of the system is shown. Also, it is possible to estimate that the highest value of the measured THD regarding the week of measurement is related to the high incidence of the 5th harmonic Figure C.2**.** which is a consequence of the inverters connected to the system. Nevertheless, this value has been found to be typical of PV systems. It is worth observing in Figure 9 that the day 12th of April had the highest THD distortion regarding the measured week. The most striking result to emerge from the data, shown in Figure 7.34 – b, is that the highest voltage value was on the 12th of April as well. Thus, the association between the THD and the voltage rise is worth mentioning. Consequently, the equation (6.2.14) captures the exact response of the voltage rises due to the harmonic distortion. Therefore, here is a satisfactory agreement between the THD and the voltage profile as well as the hosting capacity value. These results are only significant at a DHC profile level.

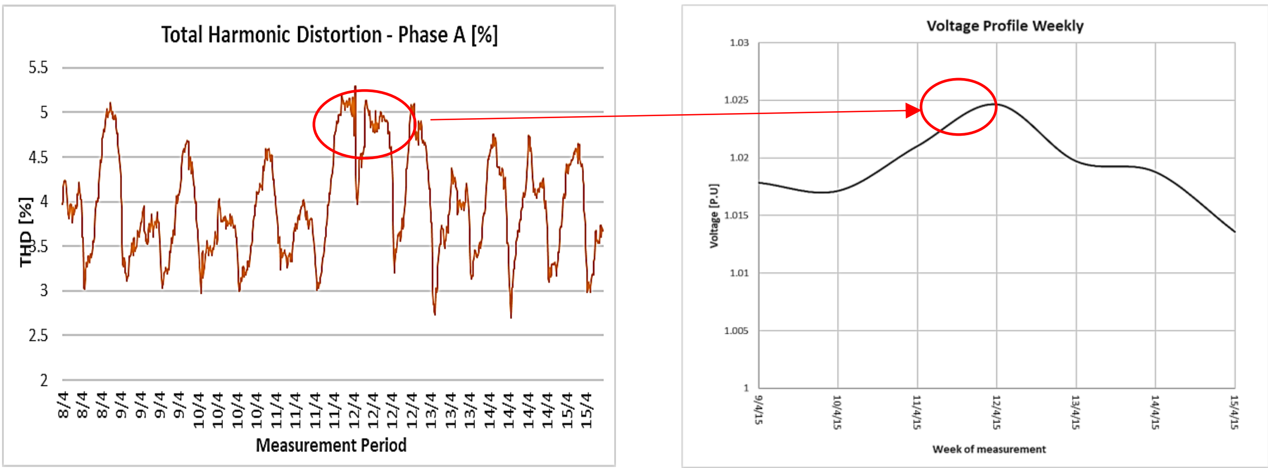

(a) (b)

Figure 7.34 – (a) The Total Harmonic Distortion for the System and (b) voltage rise profile for the system.

These results further the knowledge of the DHC and its consequences into the system. The minimum value of the local hosting capacity is directly connected to the THD, which impacts the voltage rise as shown in Figure 7.34 – b. As a conclusion, the higher the THD is, the higher the voltage rise is and the more limited the local hosting capacity will be. On the other hand, the lower the THD is, the lower the voltage rise is and the less limited the local hosting capacity will be, giving a bigger range to increase the local power generation.

From this perspective, the results emphasize the validity of the proposed model to calculate a DHC due to harmonic voltage distortion and its consequences on the voltage rise. These tests revealed that the DHC must be considered and calculated for the systems in order to minimise issues of planning and improvement and to give a new perspective regarding this prevailing analysis tool. Thus, the experiments are in line with the previous results shown in Chapter 6 and its consequences cited in the last paragraph. Regarding this association, the results were plotted in Figure 7.35, where the relation between the voltage rise and the hosting capacity value is shown.

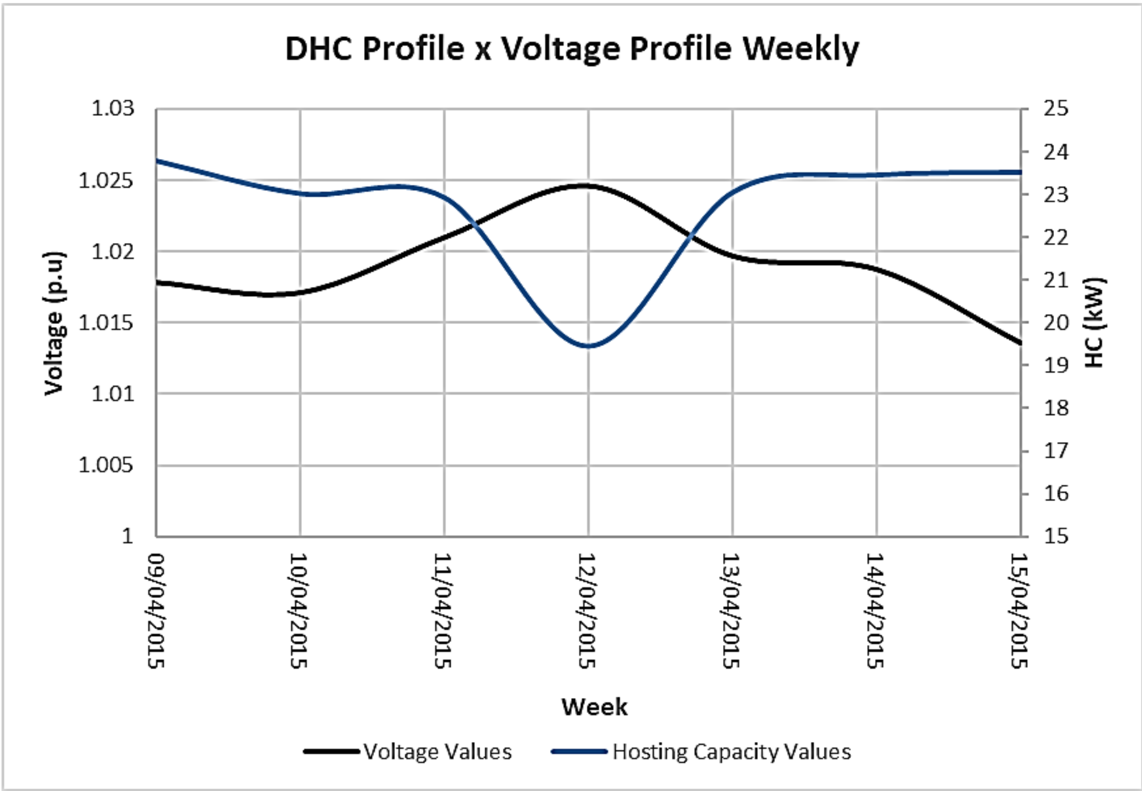

Figure 7.35 – The comparison between the DHC profile versus the voltage profile.

7.5 Final Considerations

In this chapter it was presented an application of the local dynamic hosting capacity approach, which has been applied and introduced as an important planning tool to analyse and predict the impact related to power quality phenomena following the insertion of PVs systems, or even any kind of DERs, in distribution network systems.

The methodology was divided in three important blocks. The first block of analysis was necessary to show the hosting capacity approach in order to build a network model for this analysis: a performance index, which will be determined by the need of the system under analysis; a corresponding limit according to local standards, which must be respected to make the system acceptable; and a method to calculate the value of the performance index as a function of the amount of new production and consumption. The present analysis related two performance indexes on a grid, in order to extend an analysis on both voltages rise and harmonic voltage distortion, as a consequence of the insertion of the PV system into the grid. Furthermore, this study developed and applied a new and more detailed equation to establish the hosting capacity approach, considering several mandatory variables, namely, the harmonic background at the PCC, the power factor for the installation, their impact on the voltage rise and, on the voltage, harmonic distortion, following the PV's connection to the grid.

Secondly, it was calculated a dynamic hosting capacity based on the local proposed hosting capacity approach. This study also highlights the importance of determining upper and lower limits, which lead to an acceptable deterioration region for the local hosting capacity both daily and weekly. There is a cutting-edge solution for an applied expansion when the performance of the system is evaluated. Taken together, these findings suggest a role for a practical application to the dynamic hosting capacity concept regarding the improvement and expansion of the grid using energy storage systems (**APPENDIX X**). The dynamic hosting capacity guarantees that the performance of the grid will be improved when an energy storage system is applied, and it can be generalized using the overvoltage margin caused by the PVs.

In summary, the measurements for the system were an important tool to determine the main characteristics of the grid under analysis, in order to demonstrate the efficiency of the proposed methodology. The findings of this research have important planning and operational implications in relation to electrical networks and the insertion of DERs.

8. SPECIAL CASE STUDY – HARMONIC DISTORTION AND THE HOSTING CAPACITY DURING FIFA WORLD CUP 2018

8.1 Initial Considerations

The purpose of this section is to provide an analysis regarding harmonic voltage distortion measured during a day of FIFA World Cup 2018 matches. In the period of the Brazilian match, a huge number of non-linear loads, such as television and computers, are introduced into the electrical systems. The first set of analysis relates to the load behaviour considering the Brazilian electrical system. Thus, the harmonic voltage distortion is provided by the CHESF, a federal power utility of the Northeast of Brazil. Afterwards, a local PQ measurement was given at the QMAP building in the Federal University of Itajuba in order to support the finding of a dynamic hosting capacity profile during a Brazilian match. The aim of our chapter is to analyse and describe the impact of the background harmonic distortion on the hosting capacity value for the system. Finally, an international scenario (Spain) is considered in order to compare the difference between the background distortion from two absolutely different countries, both culturally and electrically speaking.

8.2 FIFA World 2018 Cup and Its Impact on the Background Distortion Profile

The world cup is, unquestionably, one of the most important events worldwide. It is a moment where the population of the majority of the countries that are participating in this event, will be connected at the same time to the same electrical system in order to follow the matches and celebrate them regardless of the result. Moreover, television became the easiest way to watch those games, even with the advent of the internet. According to (RUBENS et al., 2006) the modern televisions set are equipped with SMPS (Switched Mode Power Supply). Due to the capacitive features of these power supplies into TV, they are a potential source of harmonic voltage distortion, as well as of non-linear loads that have become more and more commonly connected to our grids.

It is important to highlight that there are billions of TVs and computers worldwide, which can be considered the biggest source to inject harmonic frequencies into the distribution systems based on the number of such pieces of equipment spread around the world. In order to understand the behaviour of a typical TV device, a waveform of current supply is shown in Figure 8.1. In addition, the harmonic spectrum is shown in Figure 8.2.

Figure 8.1 – Current waveform of a typical TV set according to (RUBENS et al., 2006).

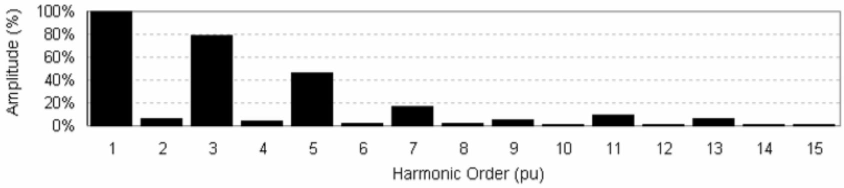

Figure 8.2 – Spectrum of a typical TV set according to (RUBENS et al., 2006).

Researchers and experts have always seen the World Cup as a particular harmonic distortion phenomenon into distributions systems, where millions of TV and computers sets are connected at the same time to the same distribution grid. Thus, as those devices are operating simultaneously, they will maximize the current injection into the grid. Based on this fact, the games of the World Cup have become an important issue in power quality analysis.

This item is a general report of power quality phenomena, as well as of their impact on the dynamic hosting capacity for the system through measurements during the three World Cup matches that the Brazilian national team participated in: on the 17th, 22nd and 27th of June 2018. Furthermore, these measurements will be compared to the ones registered on days where the Brazilian national team didn't play, in order to show their impact on the electrical system. Moreover, this item seeks to address how to analyse those phenomena regarding power quality indexes. The following topics will present electrical measurement results into three big campaigns: the load shape/demand of the Brazilian electrical system regarding the ONS (National Operator of the Electrical Power System) FIFA World Cup 2018 reports, harmonic measurements of CHESF (San Francisco Hydroelectric Company) at 69 kV busbar of the Northeast of Brazil and, finally, the power quality measurements at QMAP (Excellence Center in Power Quality, Measurement, Automation and Protection) at 220 V busbar with 27 kW of PV source. Within the framework of these ideas, we will focus on the calculation of the dynamic hosting capacity based on the QMAP measurements in order to analyze the impact of the FIFA World Cup 2018 on the power quality profiles. It is important to notice that we will relate the local measurements through the national results of the World Cup phenomena.

8.2.1 National Electrical Metering Campaign based on ONS Reports

First of all, the behaviour of the load during the Brazilian team's matches will be analysed. The National Operator of the Electric System (ONS) has prepared a special campaign for the National Interconnected System (SIN) during the FIFA World Cup 2018. This campaign was in accordance with resolution Nº01/2005 regarding the Monitoring Committee of the Electrical Sector (ONS, 2014). According to ONS, the campaign started two hours before the matches in Brazil and ended two hours after the match. Moreover, this type of campaign is necessary due to the specificities of the behaviour of the load during the matches of the World Cup. These characteristics can be classified as reduction and growth of the demand in the period before the games of the Brazilian team, during the intervals, and, mainly, immediately after the end of these matches. These tests are important to highlight their association with the power quality phenomena which are going to be discussed in the next sub sections.

8.2.1.1 Brazil x Serbia – 27th June 2018 – Load and Demand Analysis

Let's take a look at the first match against Serbia on the 27th of June 2018 at 03:00 p.m. The consumption of energy into the SIN has presented the behaviour shown in Figure 8.3. In addition, the load curves for this day of the match, which fell on a Wednesday, and for another Wednesday, on which no relevant event took place, have been plotted in the same figure.

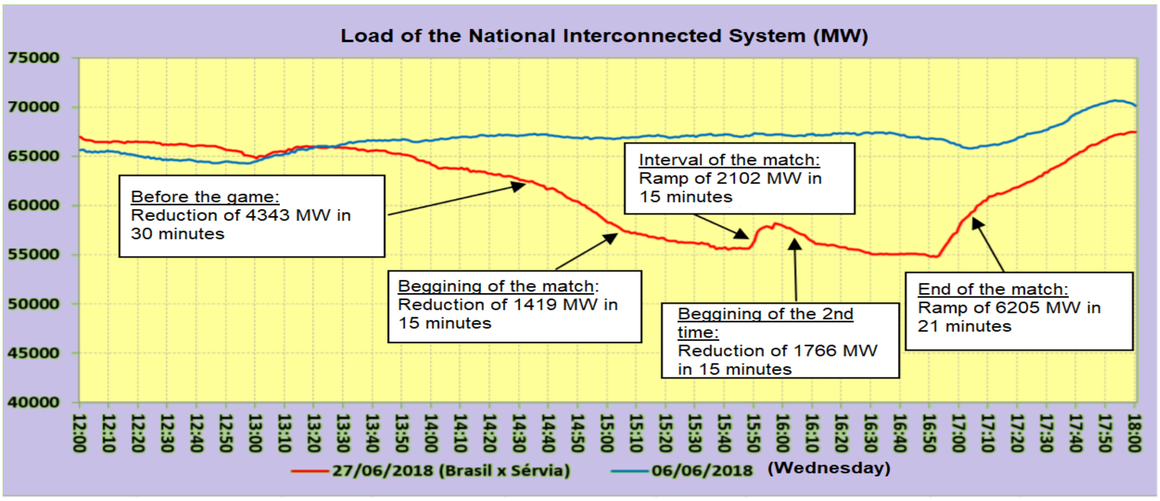

Figure 8.3 – Demand curve: 27th June 2018 x 06th June 2018 (ONS, 2018).

It is important to notice that during the first hours of the day of the match, the load was 1,300 MW over the normally observed load on a normal Wednesday. Thus, before the beginning of the game, at around 01:30 p.m., it was possible to observe a load reduction ramp of 7,746 MW in 1h40 minutes. When the match started, an 1,886 MW load reduction ramp was registered in 15 minutes. Thus, during the first half of the match, the average load difference for this period was 8,855 MW, comparing to a normal Wednesday. Furthermore, during the interval, a load growth ramp was observed. The load growth was approximately 2,102MW in 15 minutes. On the other hand, at the beginning of the second half, a load reduction ramp reached 1,766 MW in 15 minutes. By the same token, the average load difference observed during this period was 11,203 MW comparing to a normal Wednesday. Finally, after the end of the game, a load growth ramp was observed, and it reached 6,205 MW in 21 minutes. In general, analysing this figure, a considerable load reduction is observed during the match broadcast when compared to a common day.

The daily demand curve was calculated and is presented in Figure 8.4.

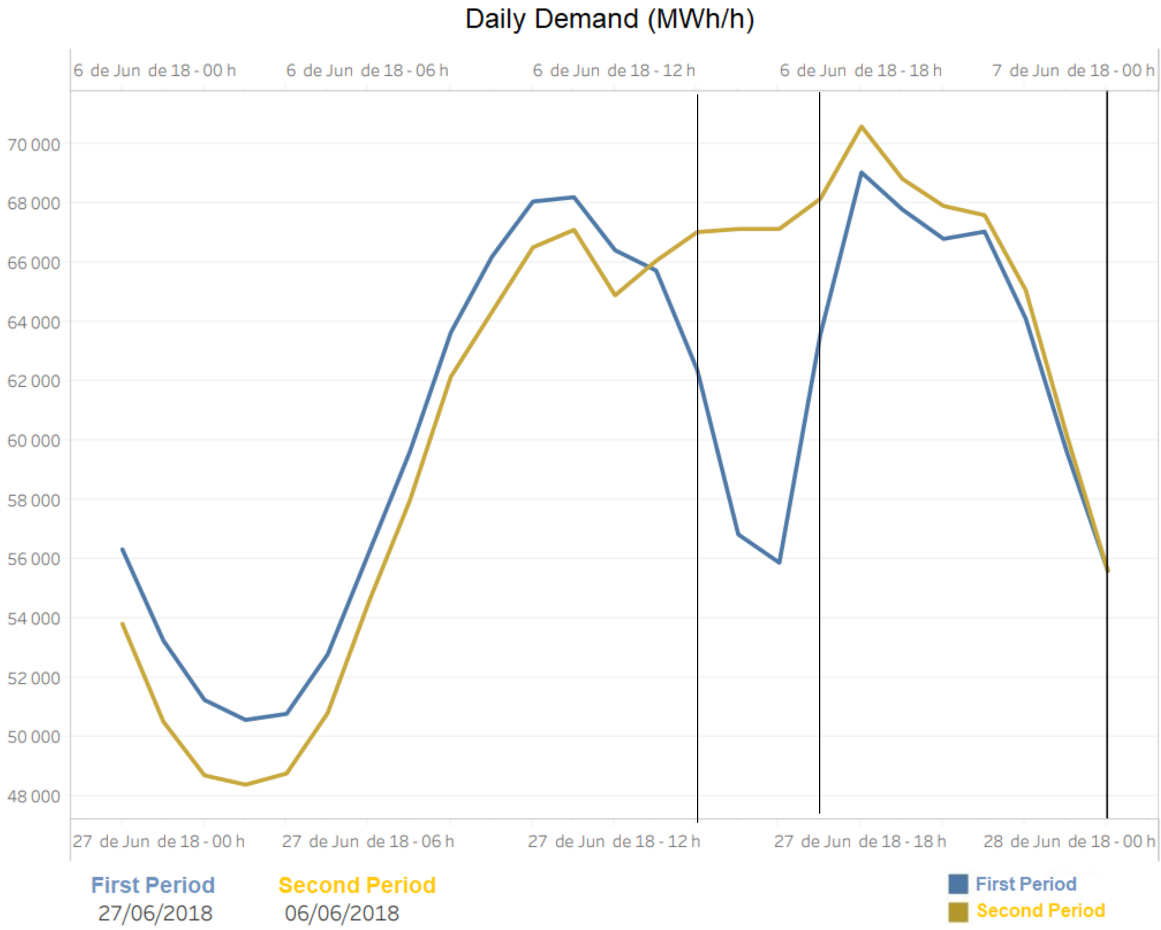

Figure 8.4 – Demand curve: 27th June 2018 x 06th June 2018 (ONS, 2018).

It is important to highlight that the demand at 02:00 p.m. for both periods was 62,383 MWh. From this point, which was close to the beginning of the match (03:00 p.m.), the demand decreased in a demand reduction ramp reaching 56,835 MWh in one hour. Moreover, between the beginning of the match until the interval, the demand increased just 0.954 MWh. Thus, after the beginning of the second half of the match, the demand growth ramp increased having reached 55,881 MWh at the end of the match. It is worth noting that the behaviour of the demand curve for both days were similar.

8.2.2 National Electrical Metering Campaign based on CHESF Reports

CHESF has a transmission system formed by AC transmission lines with more than 20 thousand kilometres of lines operating at the voltages of 500, 230, 138 and 69 kV. Its transmission system interconnects the hydroelectric plants to the main load centres of the states of the Northeast as well as merges the systems in the North, Southeast and Centre-West of Brazil regions.

Recently, CHESF has adopted special measures in its electrical system, performing inspections and anticipating preventive facility and transmission lines maintenance to increase the reliability of the electric energy service, mainly in the metropolitan regions of the Northeaster capitals, during the FIFA World Cup 2018. In this case, the values were measured with digital power meters. The measurement received was as follows:

(i) Total voltage harmonic distortion regarding phases A, B and C;
(ii) The 3rd, 5th, 7th, 11th and 13th harmonics of the voltage regarding phases A, B and C.

In this case, the period interval was measured in a 30-second interval in different points of the system. For our analysis, the busbar of 69 kV (SE Maceio, Alagoas state – Subsystem EAST) was taken in order to provide an analysis about harmonic distortion in the period of a Brazilian game as well during a common day. The limits of the individual harmonic order and the total voltage harmonic distortion based on (PRODIST Module 8) are shown in Table 7.8 for two different voltage levels.

Table 8.1 – Total Harmonic Distortion and Individual Harmonic Distortion based on (PRODIST Module 8).

Indicator	**Vn ≤ 1 kV**	**69 kV ≤ Vn ≤ 230 kV**
DTT95%	10 %	5 %
DTT(P)95%	2.5 %	1 %
DTT(I)95%	7.5 %	4 %
DTT(3)95%	6.5 %	3 %

Where,

DTT95% is DTT% (Total Voltage Harmonic Distortion) indicator value that was exceeded in only 5% of valid readings;

DTT(P)95% is DTT(P)% (Total voltage harmonic distortion for non-multiple even components of 3) indicator value that was exceeded in only 5% of valid readings;

DTT(I)95% is DTT(I)% (Total voltage harmonic distortion for non-multiple odd components of 3) indicator value that was exceeded in only 5% of valid readings; DTT(3)95% is DTT(3)% (Total voltage harmonic distortion for multiple components of 3) indicator value that was exceeded in only 5% of valid readings.

Based on what has been presented before, the following topic will discuss the results of the cited metering campaign of PQ related to harmonics during the game Brazil x Servia on the 27th of June 2018, as well as on a given common day, when there is no game happening (20th of June 2016). Both measurements took place at the substation of Maceio (SE Maceio) in the Northeast.

8.2.2.1 Brazil x Serbia – 27th June 2018 – Harmonic Profile Analysis

Figure 8.5 shows the voltage THD during the Brazil X Serbia match as well as the variation in relation to a common working day.

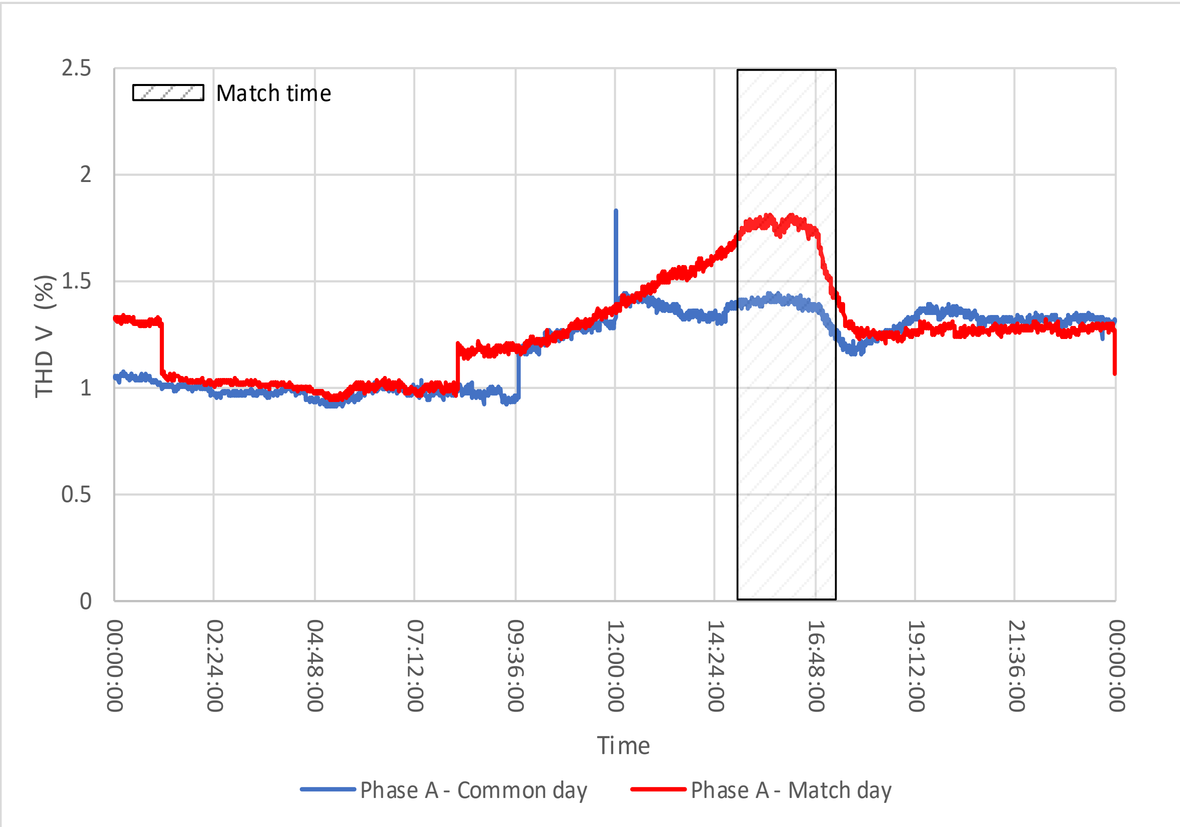

Figure 8.5 – Total Voltage Harmonic Distortion: 27th June 2018 x 20th June 2018.

It is important to notice in Figure 8.5 that the distortion decreased during half-time, which seems to be caused by a temporary increase regarding the load demanded as shown in Figure 8.3, which causes a damping and lower system impedance on the harmonic frequencies under analysis. Also, according to Figure 8.5, the THD of voltage increased substantially during the game, although the maximum value registered is in total conformity with the limits adopted by Table 7.8. In this case, the maximum THD distortion reached during the match was 1.8 %.

Figure 8.6 illustrates the IHD (3rd, 5th, 7th, 11th and 13th) regarding phase A, also during the match day and on a common day. It can be examined that the 5th harmonic voltage component, at 300 Hz, prevails above all the reminiscent others. These measurement analysis shows that the 5th harmonic level increased during the period of the matches that Brazil played, at a rate of approximately 1.3 times, due to the effect of the matches.

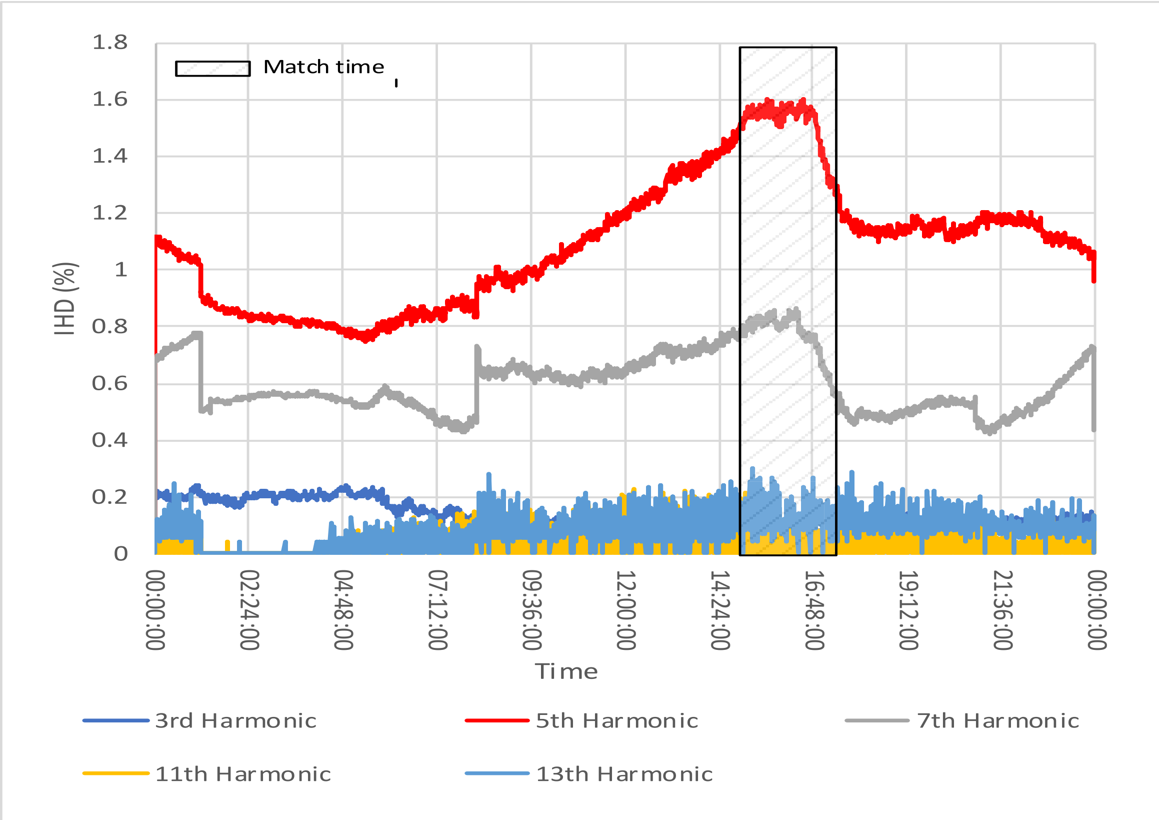

Figure 8.6 – Individual Voltage Harmonic Distortion of: 27th June 2018 (Match day).

These tests revealed that the TV sets, when analysed individually, contain large amounts of 3rd and higher harmonic currents as exemplified in Figure 8.2. Interestingly, it can be assumed that this component will be, for the most part, kept in delta connections of the transformers into the distribution systems. Thus, it can be highlighted that these components adopt a positive or negative component sequence, although some will eventually be relocated to the highest voltage side (primary side).

Generally speaking, and comparing the results from (BROWNE; PERERA; RIBEIRO, 2007; LEITÃO et al., 2007; RIBEIRO et al., 2011; RUBENS et al., 2006), during the Brazil matches in different world cups (2006 and 2010), it is possible to notice that the 5th harmonic level presented lower levels, instead of presenting the same behaviour throughout the years. This phenomenon can be phrased in terms of electrical changes into the grid. Some possible reasons for these results are listed below:

(i) The reduction of the system impedance at harmonic frequencies throughout the years;

(ii) The power supply of modern TV receivers, such as SMART TV and LED TV sets, results in much smaller harmonic injection levels due to the national and international standards that have become stricter regarding the harmonic injection into the systems that is allowed;

(iii) The number of TV receivers produced higher levels of harmonic cancellation;

(iv) The system has become much stronger through the years regarding electrical parameters such as the damping of the system.

At the initial stage of the process of a general analysis of the system regarding a Brazilian match, a preliminary analysis was carried out in order to understand the behaviour of the Brazilian system. As soon as a general analysis considering the load shape, as well as the harmonic profile, has been carried out, we can then conduct an analysis of a local building at the Federal University of Itajuba, which has already been mentioned throughout this thesis. The next section will discuss some PQ indicators as well as their impact on the local hosting capacity due to the FIFA World Cup 2018.

8.2.3 PQ analysis at QMAP during the FIFA World Cup 2018 and Its Impact on the Dynamic Hosting Capacity

Throughout the year of 2016, the QMAP building received 12 kW more on its PV installation, which improved the generation capacity of the building. At this point, a new PQ analysis can be accomplished in order to analyse its impact on the system. Those PQ indicators can be classified according to their voltage profile, THD profile, disequilibrium, among others. As soon as these steps have been carried out, a dynamic hosting capacity analysis regarding the impact of the FIFA World Cup 2018 can be executed following the same procedure described before. The analysis will consider the match day of the 27th of June 2018, compared to a common working day, the 20th of June 2018. Let's start our analysis by comparing three PQ phenomena: the THD and the IHD of voltage and disequilibrium. Moreover, the fundamental current profile will be characterised based on its impact on the calculation of the local hosting capacity.

8.2.3.1 Brazil x Serbia – 27th of June 2018 – PQ Analysis

The power quality monitoring equipment, which is a FLUKE 430 Series II, was installed in a 220 V circuit at the secondary side of the distribution transformer in 3 seconds of resolution during the measured days with 4[3 phases + neutral] dc-coupled inputs (in **APPENDIX E,** the datails of the PQ meter can be found), which supplies the QMAP building from a 13,8 kV feeder. The monitoring results are shown in a way that presents the behaviour of the harmonic profile on a day of a Brazil match, as well as on a common day, with no matches happening. Thus, Figure 8.7 represents the THD profile of voltage throughout the match day, then a common day. It is important to highlight that the match started at 03:00 p.m. (Brasilia time-zone). Moreover, the next analysis pertains to phase A of the 220 V side of the QMAP system.

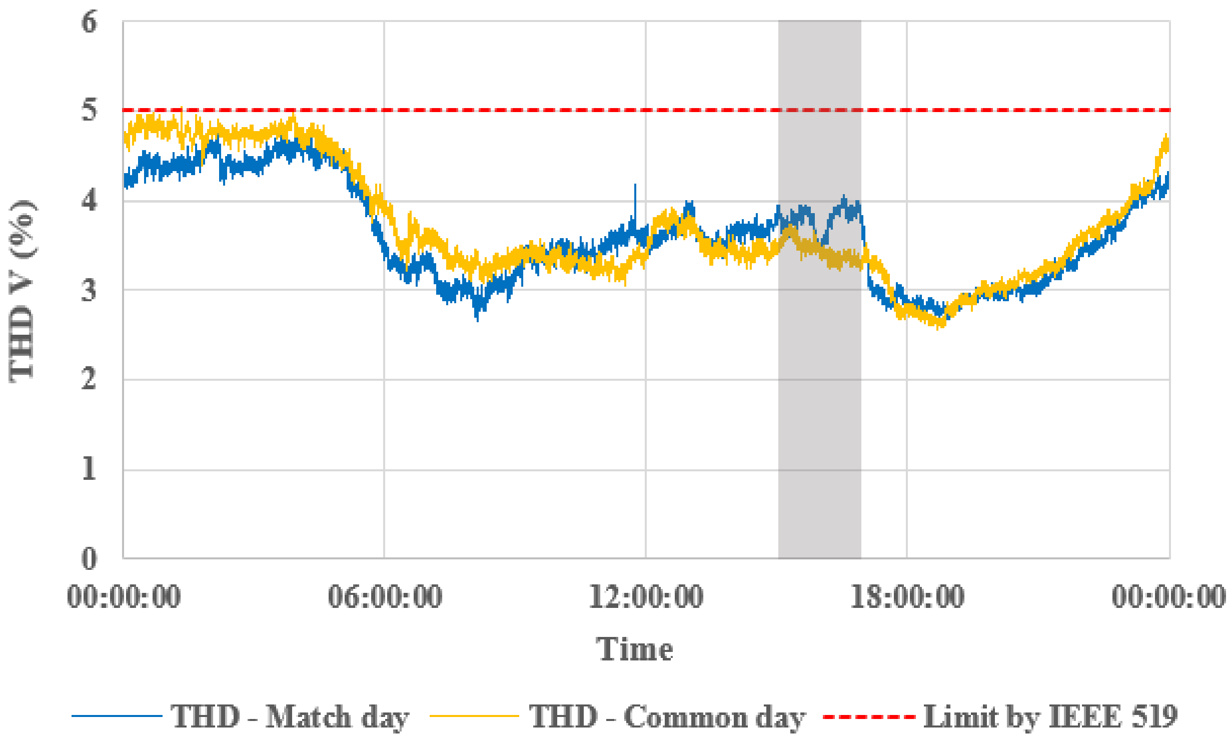

Figure 8.7 – Total voltage harmonic distortion at QMAP: 27th June 2018 x 20th June 2018.

According to Figure 8.7, the THD of voltage has increased noticeably during the match time, although the maximum distortion value registered (4%) is in agreement with the limits adopted by Table 4.2 (limit by IEEE 519) as well as the limit adopted in Table 7.8. Moreover, it is possible to notice that throughout the first-half the distortion reached 3.5%, due to a slight increase of the load during this period. It is also important to highlight that during the period between 12:00 a.m. and 06:00 a.m., the system almost reached its limit at 5%. This can be explained by the unusual characteristics of the QMAP building. Possibly, the PV inverters are not turned off during the night period, which can turn them into pure electronic loads, continuously injecting a considerable harmonic amount. Also, the building's transformer is bigger than necessary and during this period it is working under almost no load.

The behaviour of the system load is shown in Figure 8.8 through the fundamental current registered.

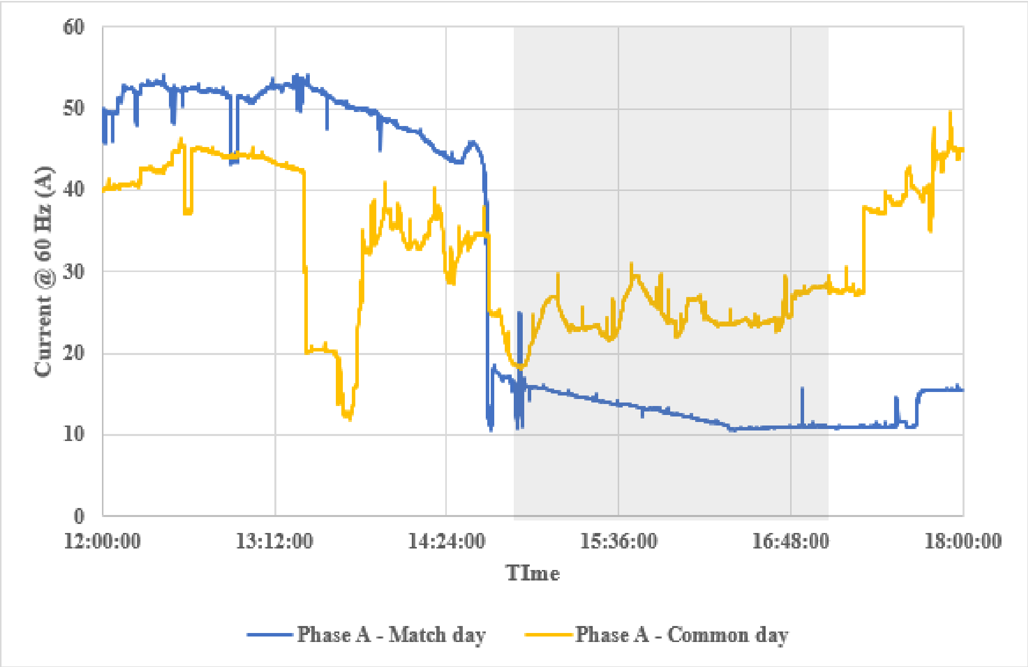

Figure 8.8 – Behaviour of the system load at QMAP: 27th June 2018 x 20th June 2018.

Analysing the previous figure, we can notice that a considerable load reduction happened moments before the match, causing a large drop of 34 A. Then the load observed during the match broadcast kept constant for the rest of the game until 06:00 p.m. when a slight load increase is registered. It is important to notice that the same behaviour has been observed in Figure 8.3 regarding the SIN.

In Figure 8.9 through Figure 8.11, the performance of the IHD of voltage profile regarding the 3rd, 5th and 7th harmonic was registered during the match day.

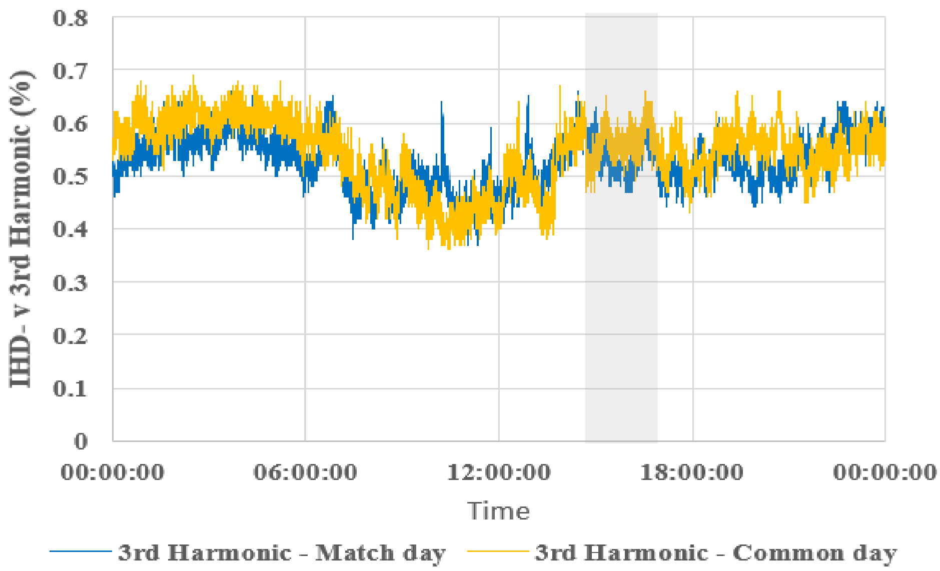

Figure 8.9 – Individual voltage harmonic distortion 3rd harmonic at QMAP: 27th June 2018.

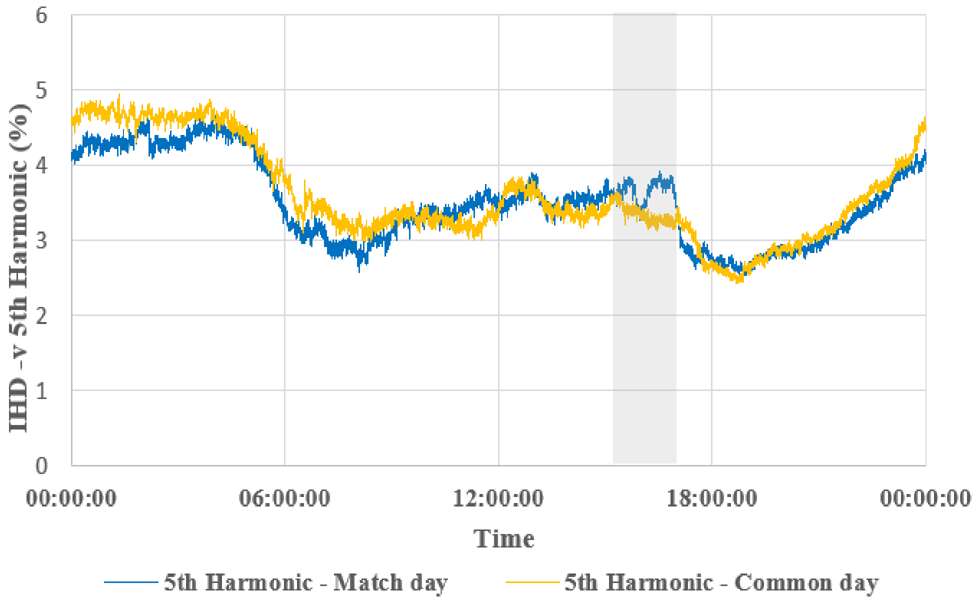

Figure 8.10 – Individual voltage harmonic distortion 5th harmonic at QMAP: 27th June 2018.

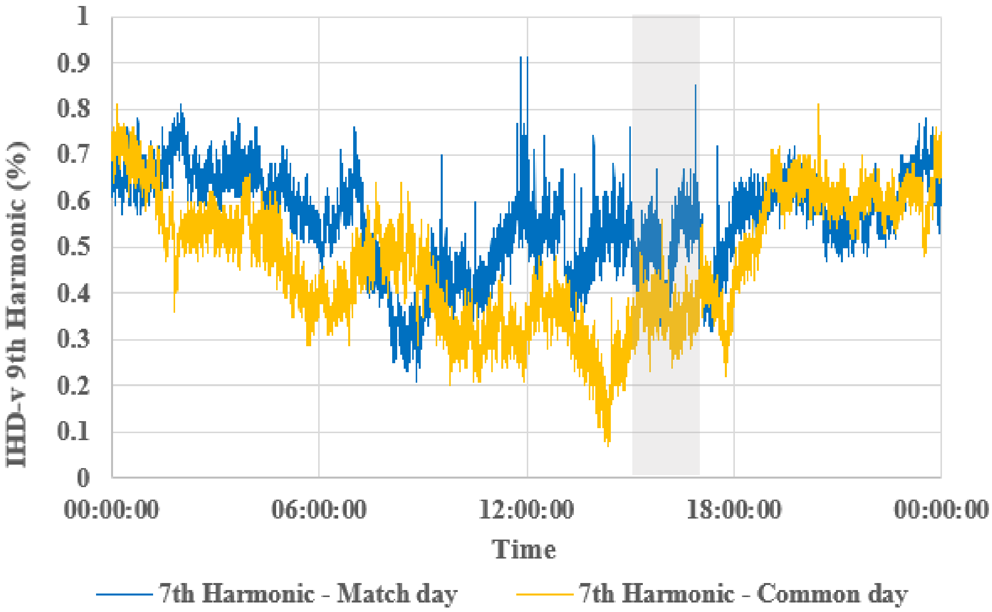

Figure 8.11 – Individual voltage harmonic distortion 7th harmonic at QMAP: 27th June 2018.

As it can be observed in Figure 8.10, the 5th harmonic voltage prevails above the 3rd and 7th orders. The same phenomena can be observed in Figure 8.6 regarding the harmonic profile at 69 kV from the measured data performed by CHESF. Moreover, it can be observed that the 3rd order had basically the same behaviour for both days. We can offer an explanation based on what has been discussed before. We can assume that most of this component will be confined to the delta connection of the transformer at the QMAP building. Consequently, the behaviour of the 3rd harmonic is standard for all distribution transformers that can keep the same 3rd harmonic distortion independent, whether the match is happening or not.

Figure 8.12 presents the index behaviour of voltage unbalance during the match day and compared to a common day.

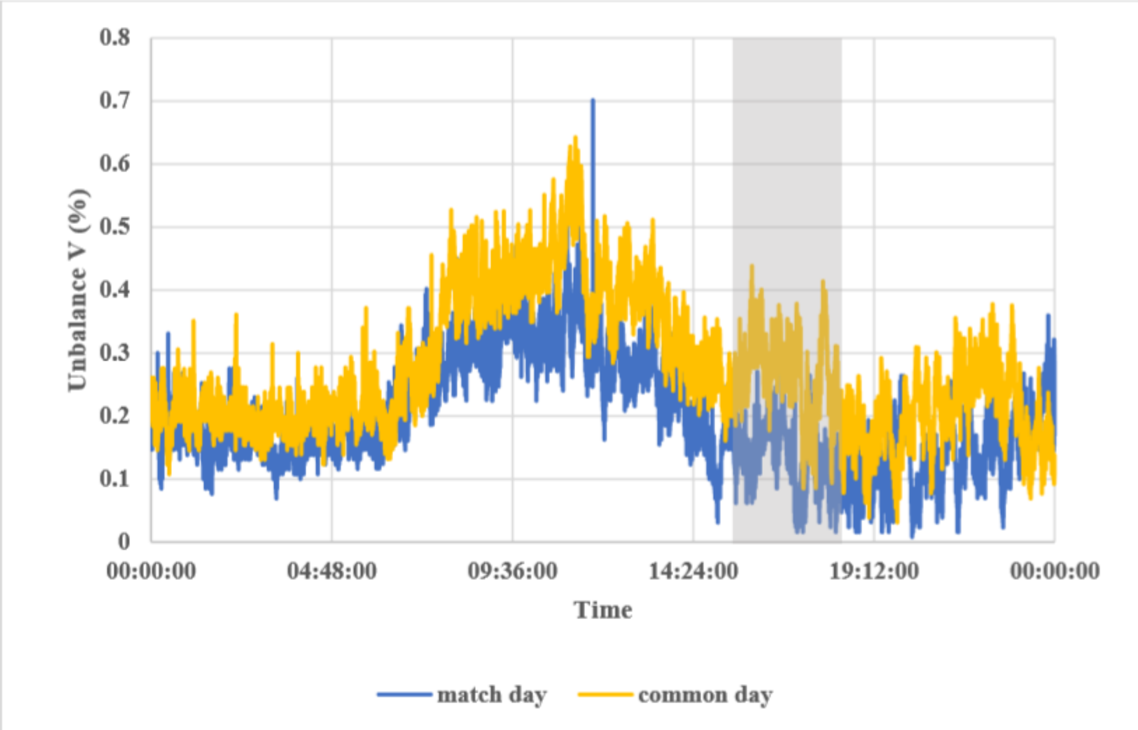

Figure 8.12 – Voltage unbalance behaviour at QMAP: 27th June 2018.

For this specific case of metering made at the QMAP building, the expected result wasn't observed in relation to the behaviour of the voltage unbalance. The voltage unbalance is calculated as the relation between the positive-sequence and the negative-sequence and it is given in percentage. This index presented a decrease of approximately 0.1% in its amplitude on the match day. The mentioned decrease can be explained by the fact that the positive harmonic sequences components, thus during the match are higher than on a common day. Due to this fact, the denominator of the voltage unbalance calculator became higher (the positive voltage sequence), which means the voltage unbalance is lower when compared to a common day, whereas, for example, the 7th harmonic is almost the same, with the unbalance voltage factor reaching higher values. As a conclusion, during the match day the unbalance voltage factor is lower than the unbalance voltage factor during a common day. Another possible explanation is due to the fact that the PV production during the match day was not as high as during the common day. It is well-known that the inverters have a single-phase connection, which means the unbalance will present standard values as shown in Chapter 5. This is corroborated by the fact that, commonly, the voltage unbalance decreases during events for which the background distortion is higher than expected.

8.2.3.2 Brazil x Serbia – 27th of June 2018 – The Dynamic Hosting Capacity Profile and Its Impact

In this section, the daily dynamic hosting capacity (DHC) regarding the match day and a common day will be described and analysed. Strong evidence of the relation between the background harmonic distortion and the impact on the DHC profile was found after running the results. Once the background harmonic profile has been defined, we can then define the dynamic hosting capacity profile. This sets the stage for the next steps. Firstly, the daily background harmonic distortion regarding the match day and the common day are defined. Following this, the power factor profile is identified as well as the electrical parameters, which were already described in section 7.3. Finally, using equation (6.3.1) we can obtain the daily DHC profile regarding both days in order to compare and analyse its impact. The daily DHC for both days is shown in Figure 8.13.

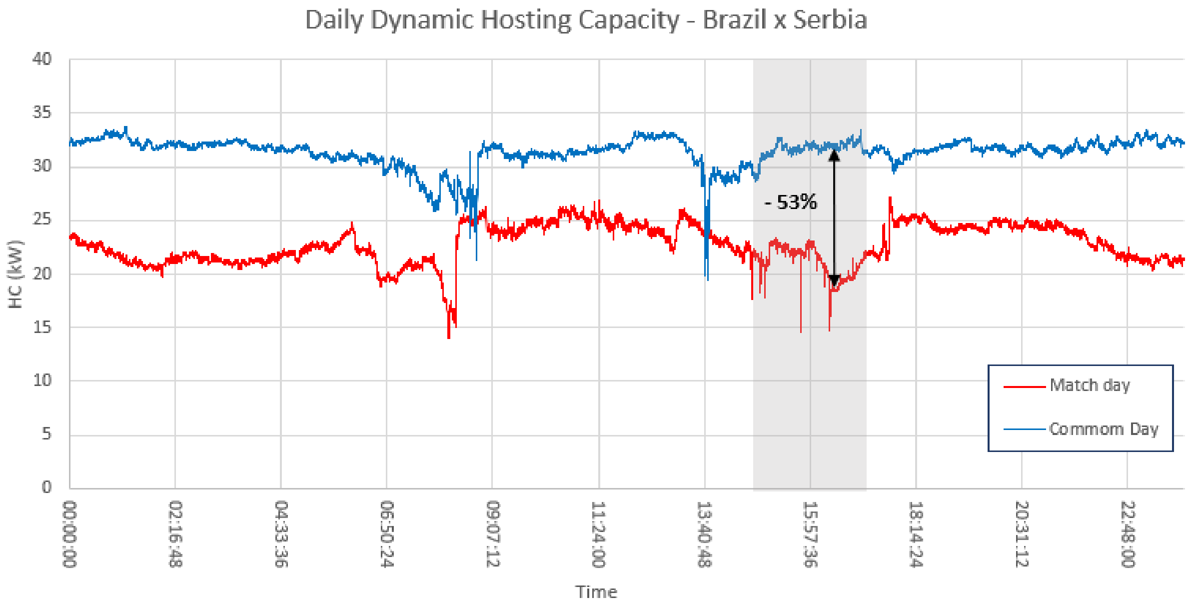

Figure 8.13 – Daily dynamic hosting capacity profile at QMAP: 27th June 2018 x 20th June 2018.

The association between the background harmonic distortion shown in Figure 8.7 and its impact on the DHC profile was tested. These tests highlighted the importance of the background harmonic voltage on the performance of the grid. The most striking result to emerge from the data is that the background distortion will decrease the grid's performance. These results thus need to be interpreted with care. Significantly, the daily dynamic hosting capacity will present an average value lower than expected mainly during the match time. It was found that the daily DHC decreased by 40% on average when compared to a common day. At the peak of the match, the decrease of the local hosting capacity reached 53 %, as shown in Figure 8.13. As expected, our experiment proves that the background harmonic distortion has a significant impact and must be taken into account. Thus, our formula (6.3.1) reproduces the response of the background distortion regarding the local hosting capacity. However, a more careful analysis revealed that there is a significant association between the local hosting capacity and the load conditions registered on the match day. During the match day, there is a significant load reduction, which means the impedance of the system will increase significantly. Due to this fact, the damping of the system will be reduced and, as a consequence, a voltage rise will occur.

In conclusion, our analysis can be summarised in a loss hosting capacity profile, as shown in Figure 8.14. The results of this analysis indicate that the most remarkable loss in the value of the hosting capacity occurred during the match, reaching peaks of more than 50% of loss.

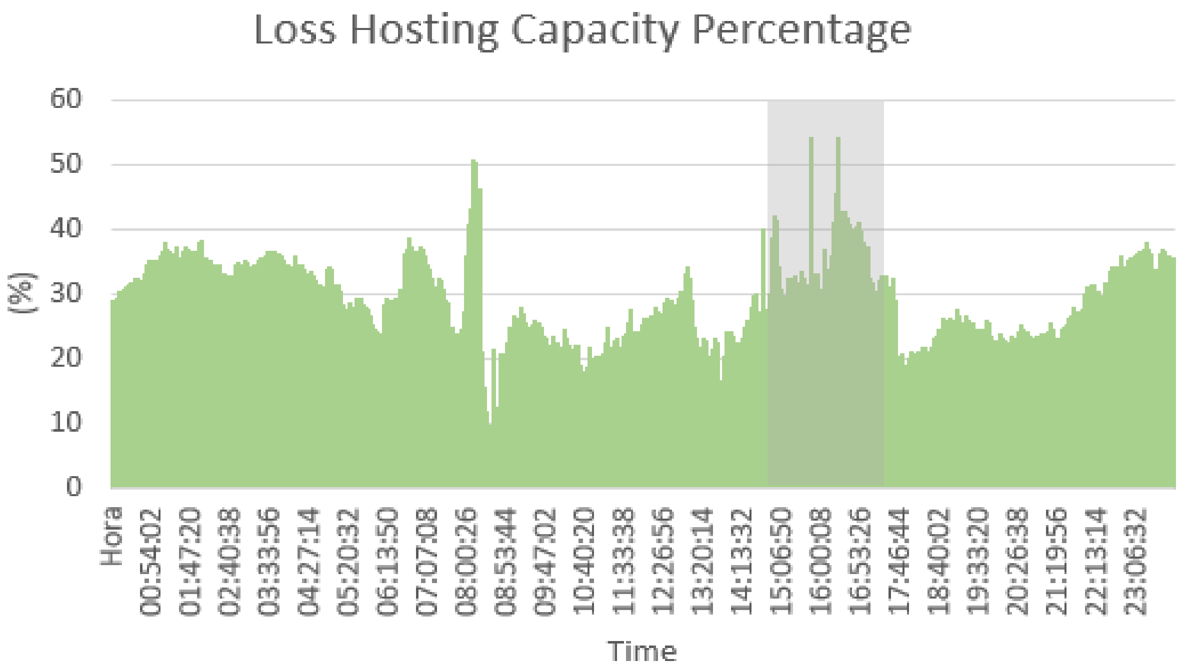

Figure 8.14 – Loss hosting capacity profile at QMAP: 27th June 2018.

8.2.1 A Global Analysis of the Harmonic Distortion During the FIFA World Cup 2018 – The Spanish case

According to a report received from Mr. de Apráiz, Mr. Barros, and Mr. Diego through aPITS-SG2 group, harmonic distortion measurements were taken during Sunday the 1st of July, the day of the Spain versus Russia match. Moreover, according to their report, this televised football match was found to be the one with more viewers in Spain. Figure 8.15 shows the THD of voltage profile during the match day and a normal day. Those values were computed using 10-minute time aggregation intervals.

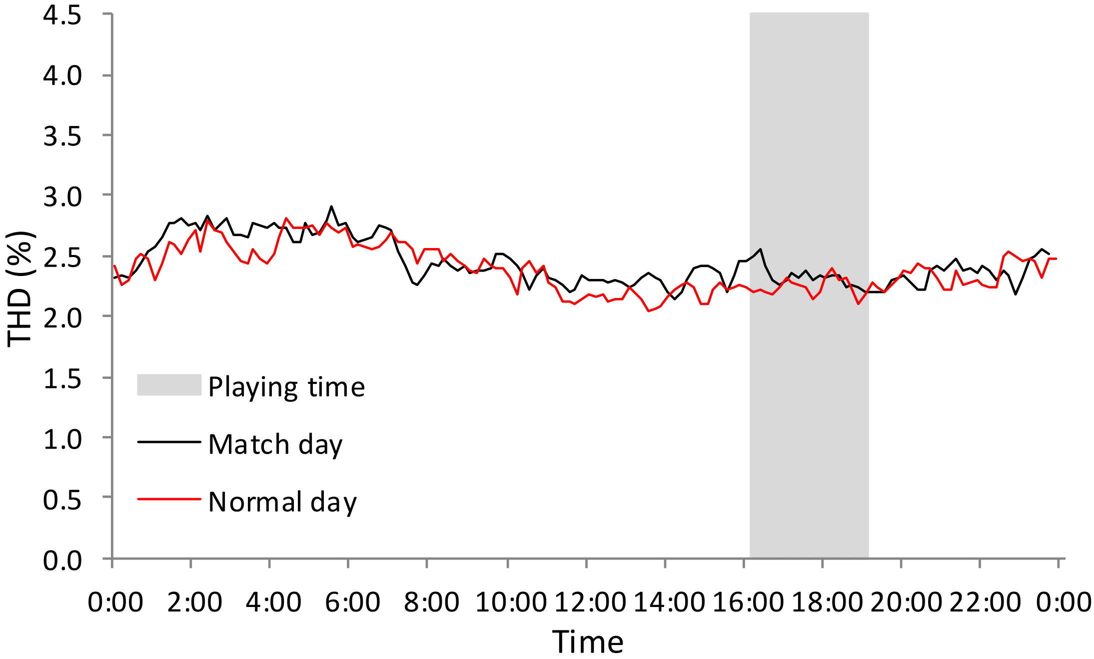

Figure 8.15 – THD of Voltage profile: Spain x Russia and during a normal day using 10-minute aggregation intervals.

On the other hand, in Figure 8.16 through Figure 8.18 the daily time evolution regarding the 3rd, 5th and 7th harmonic voltages will be represented, comparing all the results with those measured during a day with no televised football matches.

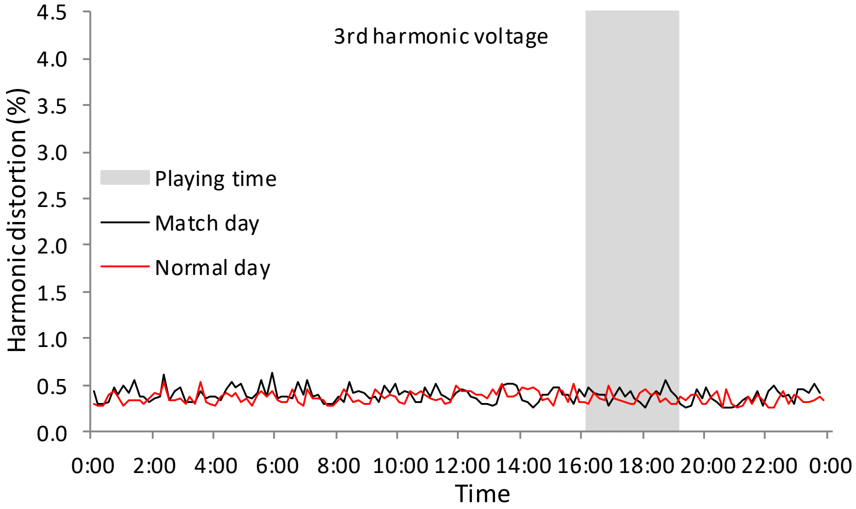

Figure 8.16 – Individual voltage harmonic distortion 3rd harmonic is Spain: 1st of July 2018.

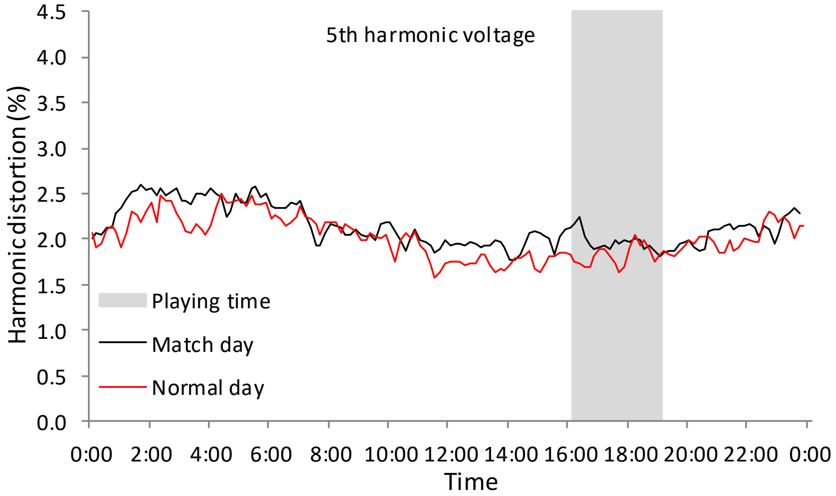

Figure 8.17 – Individual voltage harmonic distortion 5th harmonic is Spain: 1st of July 2018

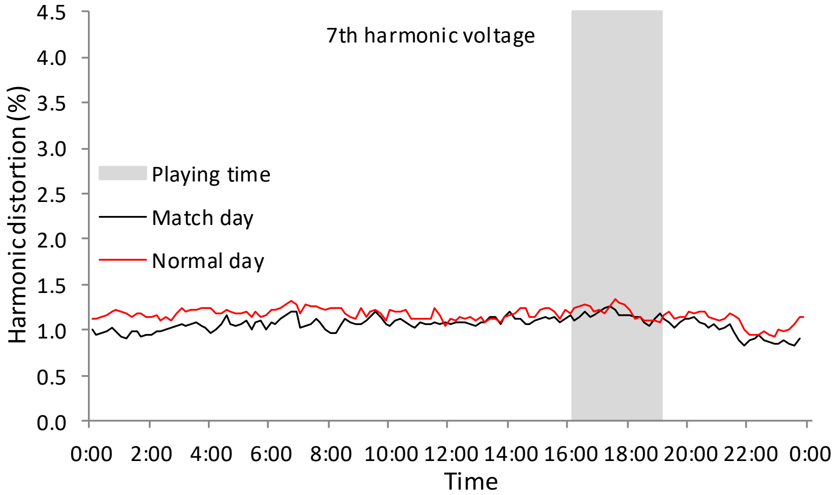

Figure 8.18 – Individual voltage harmonic distortion 7th harmonic is Spain: 1st of July 2018

Unlike the previous results regarding the Brazil match, and contrary to what was expected, there is almost no significant influence of the televised football match on the harmonic distortion when compared to a typical day. Only a small increase in THD can be observed in the measured harmonic distortion during the match, respecting the international limits. Thus, the difference between the impact of a Brazil match and a Spain match is clear, and it might be explained by the electrical and cultural differences observed in both countries. Normally, Brazilians take the world cup event more seriously, as the country basically stops during the match day and the citizens take the day off because of the matches.

8.3 Final Considerations

The evidence from this chapter points towards the idea that the impact of television viewing on the utility grid during the FIFA World Cup has some significant increase of harmonic pollution, in particular the 5^{th} harmonic. In general, these results suggest that for both transmission and distribution system, significant levels of harmonic background distortion were observed.

This chapter has highlighted the importance of the background distortion on the value of the hosting capacity profile. We have obtained comprehensive results demonstrating that the hosting capacity can be reduced by the nonlinear loads during the matches. Moreover, we have provided further evidence that the higher the background distortion is, the lower the hosting capacity will be, as mentioned before.

Measurements from Spain system has shown a trivial impact when compared to impact in the Brazilian system. Cultural and electrical differences may have been the cause of minor impact of the THD of voltage.

Finally, it can be provided that the background harmonic distortion levels have a strong association to TV sets which depend on the system. Also, those levels have a stable profile which has been decreasing over the last years. When the background distortion levels from the FIFA world cup 2010 (section 5.5.1) are compared to the levels during the FIFA world cup 2018, it is clear the difference between the THD profiles throughout the years. Moreover, it can be explained due to the fact that the technologies are becoming less polluted than before, as well as the changing of the electrical characteristics of the systems, such as the damping, the short-circuit level, among others.

9. CONCLUSION

This final chapter concludes the research described in this thesis by presenting the main findings and understandings. Firstly, a brief summary of the research in relation to the objective and the main topics is provided. Secondly, the scientific contribution of the thesis to the relevant applied field is proposed and discussed. Finally, the chapter presents conclusions with the practical and theoretical recommendations for future research in this field as a planning and improvement tool.

9.1 General Conclusions

The hosting capacity approach has been introduced as an important planning tool to analyse and predict the impact on power quality of the integration of PV systems into distribution networks. Three concepts were introduced as part of the necessary framework to establish the hosting capacity approach: a performance index, which needs to be established for a specific system under analysis; a corresponding power quality limit, to be defined according to local standards; and a method to calculate the performance index based on the new production and consumption quantities. Furthermore, this research allows the conclusion that the local hosting capacity shouldn't be analysed statically as its dynamic nature can help operators to better deal with distributed renewable resources. Thus, the evidence from this study suggests that it is possible to find the dynamic hosting capacity profile from previous evidence. This concept can also be defined as an important tool in order to get further results and information for distribution systems under high penetration of distributed generation.

To conclude, a more thorough methodology to calculate the local hosting capacity to be added to the dynamic hosting capacity concept was necessary to improve the understanding of the use of energy storage systems in order to improve the system's performance. Additionally, this study has emphasised that the energy storage system, when used as a tool to increase hosting capacity, has the potential to be established as a voltage regulator to the PCC.

A number of research questions were formulated to achieve the objective of this thesis. The following sections re-examine the outcomes in relation to the research questions.

9.1.1 The advantages and implications of creating a global hosting capacity analysis with respect to different power quality phenomena

The first outcome proposed a performance index that values voltage rise and harmonic voltage distortion under background harmonic distortion at the PCC for different PV system injection scenarios. Furthermore, the work compared the proposed approach against other simpler approaches to show that there are significant risks in taking simplistic approaches to determine the system's hosting capacity. The results show, among other things, that the information on background distortion is relevant to determine hosting capacity and that, consequently, one cannot easily determine the generation interconnection limits of a given system without gathering specific data on such distortion.

9.1.2 Dynamic hosting capacity as a way to bring better planning and improving into the distribution systems.

As hypothesized, the second outline demonstrates that the hosting capacity must be considered as a time variant function. There is satisfactory agreement among the previous studies in the hosting capacity field, which has been considered as a static planning and improving tool for distribution systems. Thus, the findings appear to be well supported by further analysis. In general, these results would seem to suggest that, for now, all hosting capacity approaches must be considered in a period of time chosen by planners of the system.

Satisfactory results demonstrated that the dynamic hosting capacity has a greater range of reliability because the hosting capacity approach is no longer presented for a single value, since it is calculated for a range of values. Indeed, it was found a way to determine a dynamic hosting capacity, in a way that it is believe has not been done before. The investigation into this area is in progress and is likely to confirm the initial hypothesis. These findings add substantially to the understanding of the dynamics of the hosting capacity concept.

9.1.3 The impact of worldwide events on hosting capacity related to the background distortion.

As hypothesized in Chapter 5, the experiments demonstrate that the background distortion will cause a significant impact on the hosting capacity approach. Those procedures capture the response of the background distortion as a phenomenon that will remarkably decrease the local hosting capacity. The results of the hosting capacity confirmed those findings. They are significant in relation to the number of TV sets connected during the matches and the harmonic background distortion. As a conclusion, it was possible to take into account that the higher the number of TV sets is, the larger the background distortion is, and the lower the hosting capacity will be during a match, as well as during the day of a match. This can be justified by the fact that people usually take match days off.

It is important to notice that there are cultural considerations that must be taken into account. Since those especial occurrences were registered in Brazil, these rules do not apply to all countries.

9.2 Proposal for Planning and Improvement of Networks

The research presented in this thesis permits attention to some interesting questions. In this case, the network could be planned and improved using procedures which will be optimised by applying an integrated hosting capacity methodology, as well as analysing their impact on voltage profile disturbances mitigation. The evidence from this study points towards the idea that the network procedures when the hosting capacity is being analysed, must follow proposed procedures.

Dynamic Hosting Capacity Procedure – Transmission and Distribution level:

STEP 1: **The measurement and recording data must be defined to register the harmonic voltage measurement vector for each instant of time**. The steady state measurement is performed in **intervals of 10 minutes at the PCC and its period is one week, which is equal to 1008 intervals**, following (PRODIST – Modulo 8, 2015);

STEP 2: **The best limits impose by international and local standards must be analysed and chosen**. The limit will give to the analysis the maximum working value to the system regarding power quality disturbances. In this case, the **voltage rise limit** considered is the performance index for the Brazilian standard, where the **limit used is 5%** at the bus voltage under analysis. For international standards, **the limit is 10%** (IEEE 519, 2014);

STEP 3: When the **local hosting capacity is analysed using the methodology presented in Section 7.3**, it is necessary to define a **system's performance index as cited in step 2.** For the present analysis, the four scenarios must be defined previously, as was the limit performance index for the hosting capacity. As a result, it is possible to illustrate the hosting capacity approach taken its acceptable deterioration region.

STEP 4: **Using the methodology proposed previously in step 3**, it will be possible to draw **the daily DHC profile considering the measured week**, where for each instant of measurement, a maximum power generation, is calculated, as well their **hosting capacity value for each instant of time using equation (6.3.1) and applying the ordered pair methodology ($P_g; P_g^{max}$) for each instant of time.**

STEP 5: **Based on step 4**, the most remarkable result which emerges from the set of **data is that the weekly DHC profile can be determined for the system using those values previously found.**

STEP 6: **The considerations proposed in step 5**, shows that the **weekly DHC must be considered and calculated for the systems** in order to minimise issues of planning and improvement and to give a new perspective regarding this prevailing analysis tool.

STEP 7: Finally, these previous steps were the first towards enhancing the **understanding of the use of energy storage systems (APPENDIX X) in order to improve the dynamic hosting capacity profile**. This methodology has highlighted that the storage system, when used as a tool to increase the hosting capacity, has the potential to be set up as a voltage regulator at the PCC. This can prevent reverse power flow and the voltage rise caused by the phenomena.

Based on this proposed procedure regarding the DHC methodology, it is important to notice that will cause a restructuring of the Brazilian electrical system introducing as part of the regulation step, the proposed methodology to analyse the DHC in order either to improve the grid or for planning, which can cause a restructuring of utilities and establish a several and careful access to the GDs and the impact of the background distortion. Thus, Figure 9.1 presents an overview of the Brazilian electrical system regulatory and operation agencies based on Figure 4.1 including the procedure proposed before.

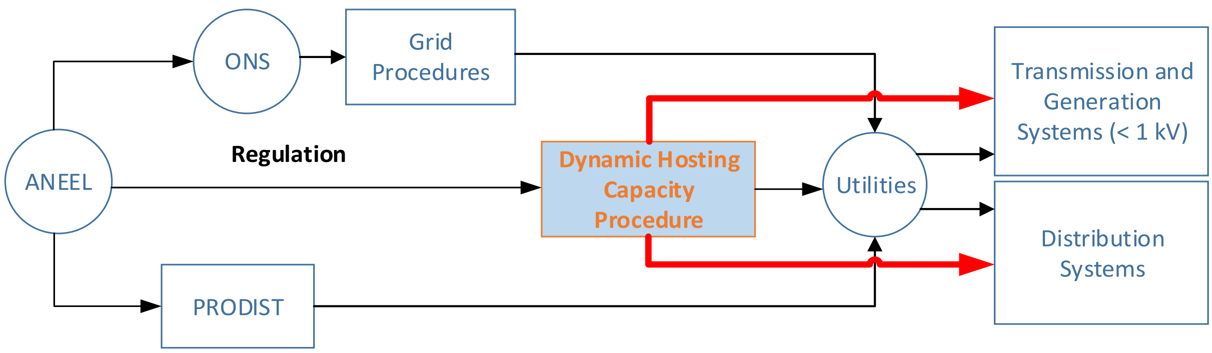

Figure 9.1 – The new proposed structure of the Brazilian electrical system using the DHC methodology.

9.3 Recommendations for Future Research

Several recommendations for future applications research directions are listed in this section in order to propose further discussions in the final thesis.

- This study is the first step towards enhancing the understanding of an integrated platform of power quality indexes in order to calculate the hosting capacity value for distribution systems. These observations have many implications for research into planning and improvement of electrical networks. The procedure and methodology could be applied to distribution grids, such as IEEE 13 busbars or real distribution systems, in order to validate their requirements to improve the comprehension of local and dynamic hosting capacity profile.
- Results so far have been very promising and also worthy to consider an improved methodology to planning and improvement of electrical networks, using the three main implications of this research: Local hosting capacity considering voltage rise due to harmonic distortion, the dynamic hosting capacity profile and its implication, and finally the mitigation of the grid using energy storage systems.
- These early successes may hope to deal with the social and environmental issues into the hosting capacity field in order to bring improvements and their technical solutions, as well as the social and environmental suggestions which are important to build up sustainability atmosphere for the future. This question may have been solved in the next chapter.

10. SOCIAL-ENVIRONMENTAL ASSESSMENT

AN ANALYTICAL ANALYSIS OF THE MAXIMIZATION OF SOCIAL-ENVIRONMENTAL WELL-BEING BASED ON THE HOSTING CAPACITY APPROACH

10.1 Initial Considerations

Hosting Capacity is widely considered to be the most important analytical tool into distribution systems regarding allocation of distributed generation (DG). Thus, DG is increasingly becoming a vital factor for a more sustainable type of power supply. According to major DG's reports (WOLSINK, 2012), when a multi-generation system is considered, it may lead to significant benefits into the systems, such as energy efficiency, reducing carbon emissions and social environmental effects.

The present chapter is an overview of the impact of the hosting capacity approach considering the improvement of social and environmental issues. The hosting capacity approach can be examined as a tool aimed at maximizing socio-environmental well-being. Our knowledge of the maximization of socio-environmental well-being is based on an analytical consequence of hosting capacity into distribution systems. The aim of the research was consequently to establish the variables to define the best scenarios regarding social and environmental issues.

10.2 Environmental and Social Considerations of Distributed Generation Planning

The term Distributed Generation has come to be used to refer to environmental and social benefits. In the literature (ODARNO; MARTIN; ANGER, 2015; RUGTHAICHAROENCHEEP; AUCHARIYAMET, 2012), those benefits are classified as improved air quality, access to electricity, increased economic productivity, small business creation in underprivileged communities, among others. On the other hand, when DG plants are badly designed, negative aspects regarding environmental and social well-being can be noticed. In relation to environmental issues, this may translate into: the quality of the air, quality of the water, noise pollution, disruption of local ecologies, among others. As far as technical issues are concerned, the increasing of the background distortion into the distribution systems, as well as the decreasing of the hosting capacity value for the system can be highlighted. Finally, socially speaking, social conflicts and economic disturbances will become a concern as a consequence of environmental and technical issues (ODARNO; MARTIN; ANGER, 2015). In the field of social and environmental well-being, many analytical points, either positive or negative, regarding social and environmental impacts can be found.

The first analytical point to analyse is the social impact. Positively speaking, the promotion and implementation of DG into distribution systems can create a range of downstream jobs in system installation, project management, operation systems, maintenance, among others (ODARNO; MARTIN; ANGER, 2015; WOOD et al., 2014). Social impacts of DG are responsible for an assessment of the employment potential created from an assumption that, the government and energy policies have been innovating the satisfactory incentive to related economic and environmental benefits into the grids. Based on this assumption, those analytical assessments can include the expected number of jobs, types of jobs, the human knowledge necessary for their implementation, energy market statement, among others (ODARNO; MARTIN; ANGER, 2015; WOOD et al., 2014). On the other hand, negative aspects of the poor implementation of DG into distribution systems can increase the social conflicts between the concessionary and consumers, as well as the economic divisions due to energy taxes and their aggregation.

Secondly, the environmental impacts of the implementation of DG into distribution systems will be addressed. In general, DG can positively affect the environment in four main aspects: The reduction of air pollutant emissions, water being used for steam production or cooling, the reduction of waste generation, and the land required for their operation (EPA) However, DG can cause some negative environmental impacts such as an unpleasant view because the DG is located closer to the end-users. Moreover, DG involves combustion, particularly fossil fuels, causing air pollution, and DG technologies may require water for stream generation or cooling (EPA).

Finally, the introduction of DG into distribution systems can impact, either positively or negatively, the power flow of the grid, voltage conditions such as regulation and maintenance of the voltage profile at the PCC, transmission and distribution capacity, the background distortion at the PCC, which will impact directly the voltage RMS value, among others (RUGTHAICHAROENCHEEP; AUCHARIYAMET, 2012; REPORT, 2010)

Furthermore, based on the previous discussion, social, environmental and technical impacts interrelated forming a triangle of consequences, where all those impacts will be a consequence of the others. As far as we know, these cycles can be defined as positive or negative consequence cycles. The triangle of consequences is shown in Figure 10.1.

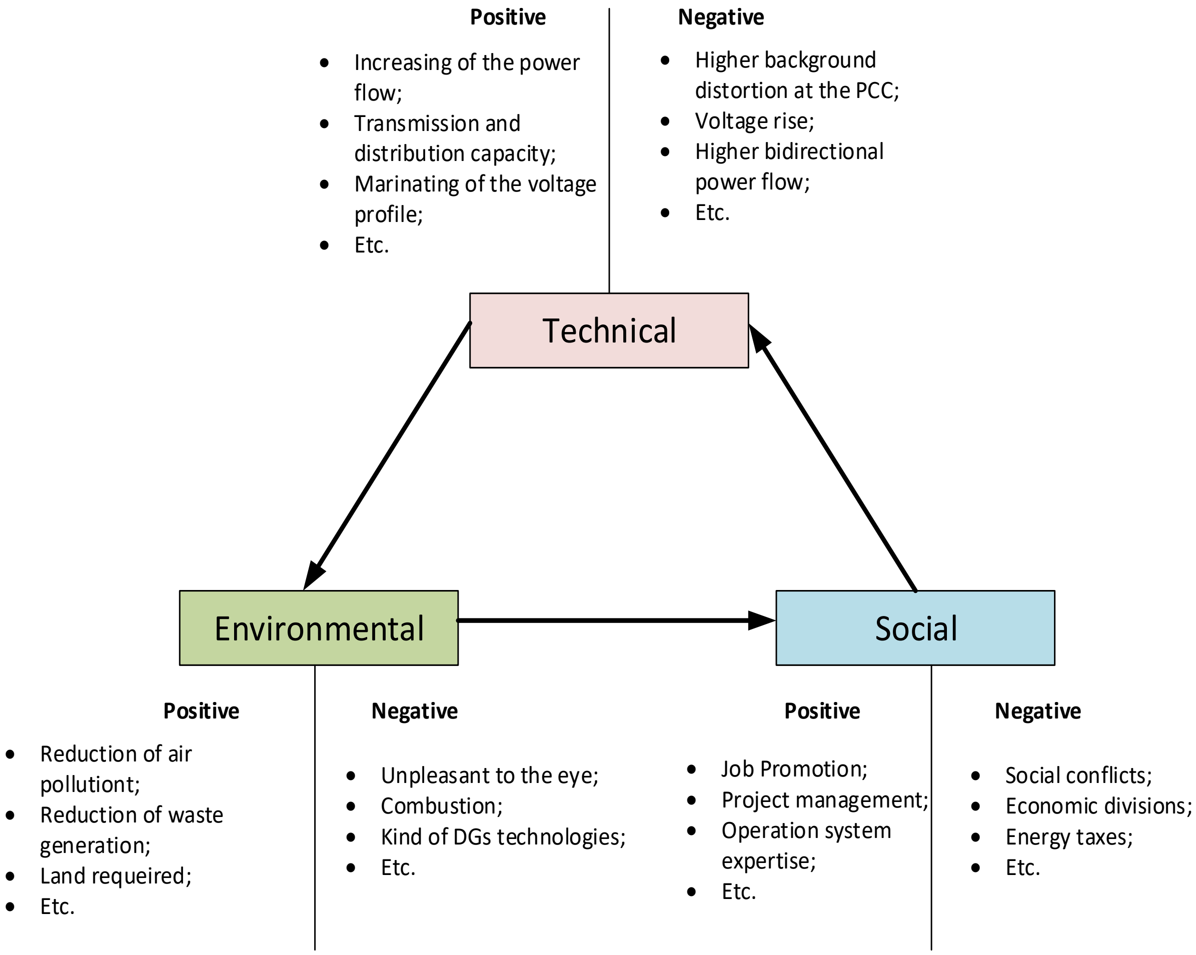

Figure 10.1- Triangle of Consequences of DG Implementation

The next section takes a new look at the technical impact as the principle of maximization of social and environmental well – being issues regarding the hosting capacity approach. Within the framework of these criteria, we tried to create a mathematical concept of hosting capacity related to the social and environmental issues within the scope of societies' well-being considering a feeder into the distribution systems and its connected DG.

10.3 Analytical Social-Environmental Well-Being Based on the Hosting Capacity Approach

It is common knowledge that the hosting capacity is understood as the maximum amount of distributed generation that can be included into the grid without causing any electrical disturbance in the system considering particular phenomena, such as voltage rise, harmonic distortion, capability of the wide, flickers, among others. Although the technical characteristics of hosting capacity have been dealt with in depth for the last decades, the Social and Environmental impact of this tool still requires further analysis.

In order to investigate the analytical consequences of the hosting capacity regarding social and environmental issues, our analytical experiment is based on the connection of DG into a general distribution feeder. The mentioned system is shown in Figure 2.

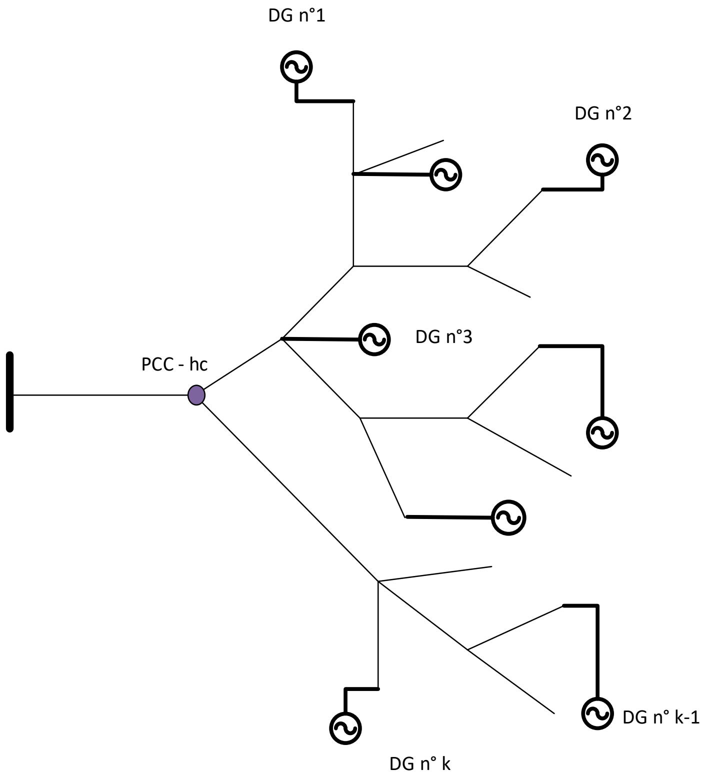

Figure 10.2 – A general feeder and its connected DG

In the system shown in Figure 10.2, it is important to notice that the amount of DG connected is defined as $Amount_{DG} = DG_1 + DG_2 + DG_3 + \cdots + DG_{k-1} + DG_k$. Moreover, the connection point of the system in order to define its hosting capacity is defined as PCC_{hc}. This point has been chosen because it is the main point where the impact of all DG sources can be quantified in order to determine the analytical consequence of their connections into the distribution feeder based on the formulation presented ahead.

This problem can be graphically illustrated in terms of the hosting capacity approach. It is easily verifiable that the system has an initial background distortion due to nonlinear loads, and the increment of DG will directly impact the defined phenomena index in order to reach the hosting capacity point. A graphical analysis of the hosting capacity at the PCC_{hc} has been shown in Figure 3.

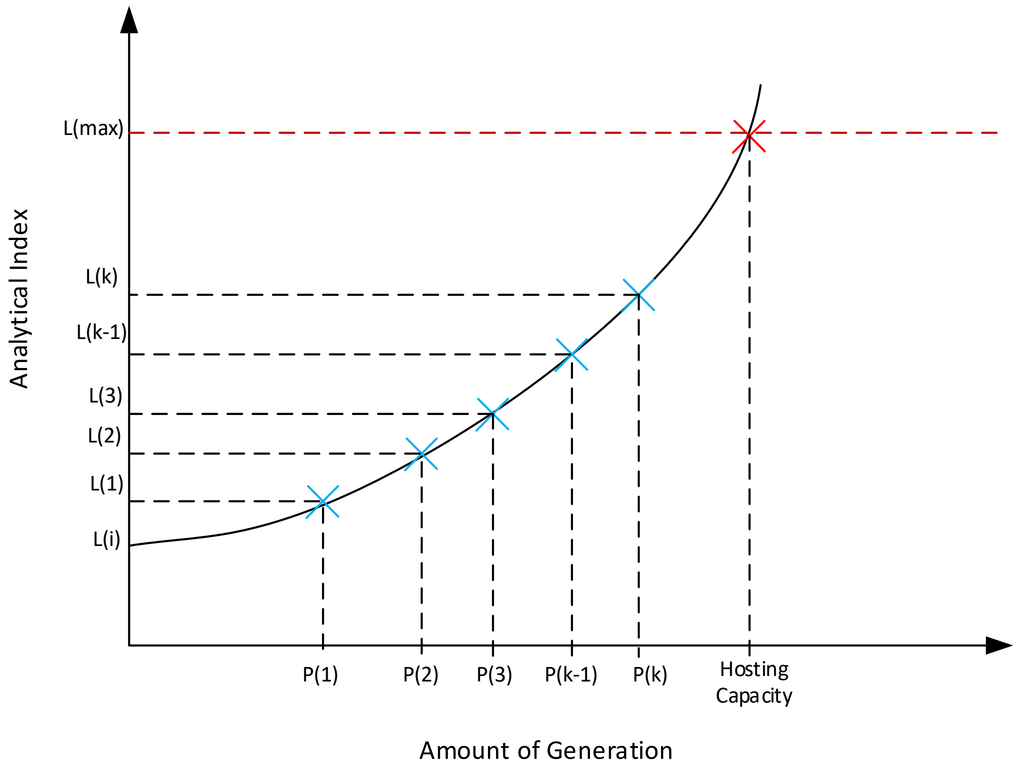

Figure 10.3 – Maximum Amount of Generation Increment.

Based on Figure 10.3, the initial background is defined as L_i since the index is defined for the system. It is important to highlight that to the initial power generation the amount of DG is neglectable. Combining the first DG, defined as P_1 , into the system we have an increment of the limit index L_1. It is observable that the more DG is connected into the system, the higher the limit index will be. This gives the formal solution where the last DG connected P_k gives the maximum index at the PCC point, L_k. It doesn't mean the maximum limit index to the system has been reached. When the maximum limit index is reached, the system will find its hosting capacity value. Before that, the system still has an acceptable region to connect more DGs. By combining these phenomena with limit indexes and amount of DG into the system, we infer calculated areas in order to define the social and environmental well-being indicator as $SEWB$. The measured unity can be defined as $kW.index$. The graphical definition of SEWB is shown in Figure 10.4.

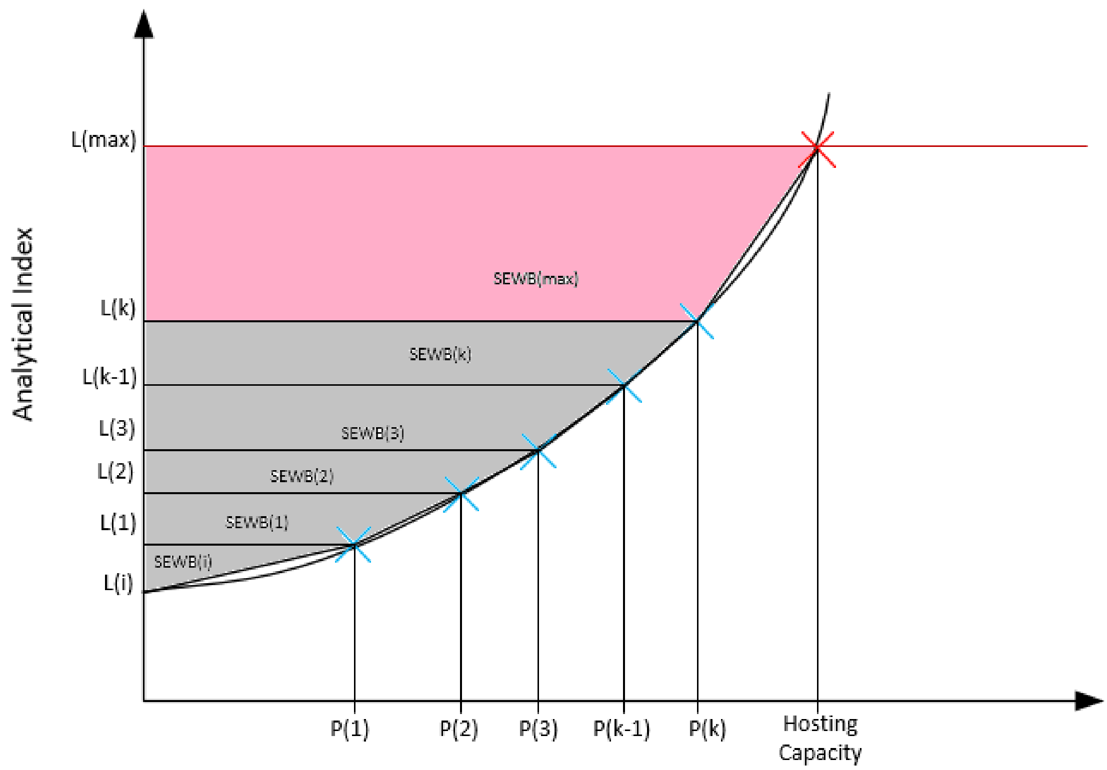

Figure 10.4 – The Social and Environmental Well-Being Factor definition.

At this point, we used reliable techniques based on the recommendations of area calculation bringing the hosting capacity curve closer to the triangles and trapezium for each limit index and its amount of DG. For example, initially, the first SEWB is given by $SEWB_i$ and it can be calculated by the following equation.

$$SEWB_i = \frac{P_1.(L_1 - L_i)}{2} \tag{10.1}$$

The second area will be defined as a trapezium, as the system is evolving from the current DG to one more DG connected into the system. Thus, the $SEWB_1$ is given by equation (10.2).

$$SEWB_1 = \frac{(P_2 + P_1).(L_1 - L_i)}{2} \tag{10.2}$$

The $SEWB_{??}$ was gradually summed to reach the limit index L_k when the last current DG is connected into the system. The described fact is given by (10.3).

$$SEWB_{k-1} = \frac{(P_k + P_{k-1}).(L_k - L_{k-1})}{2} \tag{10.3}$$

Based on (10.1), (10.2) and (10.3), the final solutions contained all reached areas from $DG_1 + DG_2 + DG_3 + \cdots + DG_{k-1} + DG_k$. Furthermore, the total social environmental well-being factor is defined by the following equation.

$$SEWB_{total} = \sum_{k=1}^{k} \frac{(P_k + P_{k-1}).(L_k - L_{k-1})}{2} \tag{10.4}$$

Having an $SEWB_{total}$ meant that we could determine the reminiscent $SEWB_{max}$, which defines the social environmental well-being the system could reach, as well as improves the existent amount of generation into the system. In this case, this value is defined by equation (10.5).

$$SEWB_{max} = \frac{(Hosting\ Capacity + P_k).(L_{max} - L_k)}{2} \tag{10.5}$$

Once these steps have been completed, we are now ready to define the impact of HC on the social environmental well-being and its robustness in order to define important scenarios. At this point, the maximization of the social environmental well-being can be defined using optimization tools. As soon as the social environmental well-being factor is defined, the final adjustments can be made to determine an analytical consequence of these factors. By reducing the amount of background distortion, for example, a maximization of the SEWB can then be done. The social and environmental experiment proceeds following the steps outlined below. In order to maximize the procedure, let's take a look at the following definition:

$$\begin{aligned} Max \quad SEWB_{total} &= \sum_{k=1}^{L_{max}} \frac{(P_k + P_{k-1}).(L_k - L_{k-1})}{2} \\ s.t \quad & L_k < L_{max} \\ & L_i = 0 \end{aligned} \tag{10.6}$$

Where, L_{max} defines the maximum limit index as well as the hosting capacity point to be reached.

This condition cannot be reached unless the background distortion of the networks has been reduced approximately to zero by mitigation procedures, for example. Considerable care must be taken when the system is maximizing the social environmental well-being. For example, based on (10.6), we can define the worst and the best-case scenarios. Thus, to do this entails reducing the background.

Some conclusions can be drawn from the previous analysis:

- If $L_i = 0$, the social environmental well-being factor is at its maximum as far as the system is kept within mitigation procedures. Thus, this defines the best-case scenario where a great amount of DG can be included into the system and create the positive technical, social and environmental aspects.

- On the other hand, if $L_i \simeq L_{max}$, the social environmental well-being is close to its lower value, which means no DG can be included until mitigation procedures have been applied to the system. It defines the worst-case scenario.
- As a conclusion, the lower the background distortion is, the better the social and environmental conditions of the system will be. To mitigate the risk of negative aspects of social and environmental well-being, the risk of background distortion can be reduced by applying technical improvement procedures to all the background distortion originated by local loads.
- A great deal of attention must be paid when DG sources are about to be included into the system. Thus, before any DG installation, extreme caution must be taken regarding the values of background distortion created by technical procedures.

10.4 Final Considerations

The association among technical, social and environmental aspects is worth mentioning because the positive and negative consequences of including DG into the system must be carefully analysed. The most surprising association concerns the fact that those factors impact each other, resulting in a circle of consequences, both positive and negative. Essentially, the technical aspect can be considered the most remarkable factor. Socially and environmentally speaking, the technical is considered the top of the triangle of consequences.

On the other hand, there is strong evidence the background distortion caused by nonlinear loads and the existent DG installed into the system is considered to be the most outstanding factor. These results are significant at a maximization of the social and environmental well-being level. Interestingly, the association between the background distortion and the social environmental well-being factor is related to an analytical factor based on the hosting capacity approach. These results have further strengthened our belief that social and environmental factors must be taken into account as a tool for the planning and improvement of electrical grids, together with technical factors. Furthermore, these results extend our knowledge of hosting capacity not just as a technical tool. This finding confirms that the social and environmental well-being is inversely proportional to the current background distortion into the grid. Finally, our analytical validation of social and environmental well-being captures the importance of a deeper analysis considering collective and environmental factors

11. PUBLISHED PAPERS

MAGAZINES AND JOURNALS:

OLIVEIRA, TIAGO E. C.; CARVALHO, PEDRO M. S.; RIBEIRO, PAULO F.; BONATTO, BENEDITO D. **PV Hosting Capacity Dependence on Harmonic Voltage Distortion in Low-Voltage Grids: Model Validation with Experimental Data**. Energies, v. 11, p. 465, 2018. doi.org/10.3390/en11020465 (Energies Magazine – CAPES QUALIS A2).

OLIVEIRA, TIAGO E. C.; CARVALHO, PEDRO M. S.; RIBEIRO, PAULO F.; BOLLEN, MATH; DE SOUZA, ANTÔNIO C. Z.; BONATTO, BENEDITO D. **The Concept of Dynamic Hosting Capacity for Distributed Energy Resources: Analytics and Practical Considerations.** IEEE Smart Grids (In revision by the authors and co-authors).

CONFERENCES:

MATEUS D. BRAGA, SAMIR D. MACHADO, IBERÊ C. OLIVEIRA**, TIAGO E. C. DE OLIVEIRA**, PAULO F. RIBEIRO, BENEDITO ISAIAS L. LOPES. **Harmonic Hosting Capacity Approach in a radial Distribution System due to PV Integration Using OpenDSS**. 2018 13th International Conference in Industry and Applications (paper accepted)

FRANCINEI L. VIEIRA, PAULO F. RIBEIRO, BENEDITO D. BONATTO, **TIAGO E. C. DE OLIVEIRA**. **Harmonic Studies in Open DSS Considering Renewable DG and Aggregate Linear Load Models**. 2018 13th International Conference in Industry and Applications (paper accepted)

BRAGA, M. D.; MARCONDES, W. A.; **OLIVEIRA, T. E. C**.; RIBEIRO, P. F. ; BONATO, B. D**. Considerações sobre a Qualidade de Energia em um Prédio Universitário com Geração Fotovoltaica**. In: CBQEE 2017 – Conferência Brasileira Sobre Qualidade de Energia Elétrica, 2017, Curitiba. CBQEE2017 – 0138, 2017.

OLIVEIRA, T. E. C.; RIBEIRO, P. F.; NUNES, I. S.; CARVALHO FILHO, J. M.; BONATO, B. D. **STUDY OF HOSTING CAPACITY OF DISTRIBUTEDGENERATION SOURCES IN THE ELECTRIC SYSTEM OF A UNIVERSITY CAMPUS**. In: Cigré SC-C4 IC 2016., 2016, Curitiba. Cigré SC-C4 IC 2016., 2016.

DE OLIVEIRA, TIAGO E. C.; RIBEIRO, PAULO F. ; SANTOS, IVAN. N**. Determining the harmonic hosting capacity of PV sources for a university campus.** In: 2016 17th International Conference on Harmonics and Quality of Power (ICHQP), 2016, Belo Horizonte. 2016 17th International Conference on Harmonics and Quality of Power (ICHQP), 2016. p. 836

CAMPELLO, LAURA D.; DUARTE, PRISCILA M.; RIBEIRO, PAULO F.; **DE OLIVEIRA, TIAGO E. Hosting capacity of a university electrical grid considering the inclusion of wind-turbines for different background distortions**. In: 2016 17th International Conference on Harmonics and Quality of Power (ICHQP), 2016, Belo Horizonte. 2016 17th International Conference on Harmonics and Quality of Power (ICHQP), 2016. p. 1026.

REFERENCES

ABDEL-SALAM, M. et al. Effect of Micro-Grid Renewable Micro-sources on Short Circuit Capacity of Hosting Distribution Networks. **35th International Telecommunications Energy Conference, SMART POWER AND EFFICIENCY**, p. 458–463, 2013.

ABDULGALIL, M. A. et al. Sizing of Energy Storage Systems to Enhance Microgrid Reliability. **2018 IEEE International Conference on Industrial Technology (ICIT)** p. 1302–1307, 2018.

Agência Nacional de Energia Elétrica – **ANEEL Procedimentos de Distribuição de Energia Elétrica no Sistema Elétrico Nacional – PRODIST Módulo 3** – Acesso ao Sistema de Distribuição. 2012. (In Portuguese)

Agência Nacional de Energia Elétrica – **ANEEL Procedimentos de Distribuição de Energia Elétrica no Sistema Elétrico Nacional – PRODIST Módulo 7** – Cálculo de Perdas na Distribuição. 2015. (In Portuguese)

AGÊNCIA NACIONAL DE ENERGIA ELÉTRICA, A. **Procedimentos de Distribuição de Energia Elétrica no Sistema Elétrico Nacional – PRODIST Módulo 8** – Qualidade da Energia Elétrica. 2015. (In Portuguese)

ALTIN, M. Distributed Generation Hosting Capacity Calculation of MV Distribution Feeders in Turkey. **2014 IEEE PES Innovative Smart Grid Technologies, Europe**. p. 1–7, 2014.

ANDRÉN, F. et al. DERri Common Reference Model for Distributed Energy Resources – Modelling Scheme , Reference Implementations and Validation of Results AIT Austrian Institute of Technology, **Center for Renewable Energy Sources, National Technical University of Athens.** 2014.

BACCINO, F. et al. A methodology for evaluating PEVs hosting capacity margins in distribution grids. **IEEE Power and Energy Society General Meeting**, p. 1–6, 2012.

BLANCO, A. M.; STIEGLER, R.; MEYER, J. Power quality disturbances caused by modern lighting equipment (CFL and LED). **2013 IEEE Grenoble Conference PowerTech, POWERTECH 2013**, 2013.

BOLLEN, M. H. J.; RÖNNBERG, S. K. Hosting capacity of the power grid for renewable electricity production and new large consumption equipment. **Energies**, v. 10, n. 9, 2017.

BOLLEN, M. H. J.; YANG, Y.; HASSAN, F. Integration of distributed generation in the power system – a power quality approach. **2008 13th International Conference on Harmonics and Quality of Power**, p. 1–8, 2008.

BOLLEN, M.; HASSAN, F. Integration of Distributed Generation in the Power System. p. 6–83, Aug 2011, **Wiley-IEEE Press.**

BROWNE, N.; PERERA, S.; RIBEIRO, P. F. Harmonie levels and television events. **2007 IEEE Power Engineering Society General Meeting, PES**, p. 7–12, 2007.

CIGRE. **Power quality and EMC issues associated with future electricity networks – Status report**. March, 2018.

C4-115 CIGRE 2014 Guidelines for monitoring power quality in contemporary and future power networks – results from **CIGRE / CIRED JWG C4 . 112 Jovica V** .

CALIFORNIA PUBLIC UTILITIES COMMISSION ENERGY DIVISION STAFF. Impacts of Distributed Generation Final Report. **Itron, Inc**, n. January, 2010.

CAPITANESCU, F. et al. Assessing the Potential of Network Reconfiguration to Improve Distributed Generation Hosting Capacity in Active Distribution Systems. **IEEE Transactions on Power Systems**. v. 30, n. 1, p. 1–11, 2014.

CARVALHO, P. M. S.; CORREIA, P. F.; FERREIRA, L. A F. Distributed Reactive Power Generation Control for Voltage Rise Mitigation in Distribution Networks. **IEEE Transactions on Power Systems**, v. 23, n. 2, p. 766–772, 2008.

CHIDURALA, A.; SAHA, T.; MITHULANANTHAN, N. Harmonic characterization of grid connected PV systems & validation with field measurements. **IEEE Power and Energy Society General Meeting**, v. 2015–Septe, p. 9–13, 2015.

COLNAGO, G. P. et al. The New Brazilian Power Quality Standard and a Low Cost Device Meter. **Energy and Power Engineering**, v. 04, n. 03, p. 144–152, 2012.

ĆUK, V; COBBEN, J. F. G. ; KLING, W. L.; RIBEIRO, P. F. Considerations on Harmonic Impedance Estimation in Low Voltage Networks. **2012 IEEE 15th International Conference on Harmonics and Quality of Power,** December 2012.

ĆUK, V; COBBEN, J. F. G. ; KLING, W. L.; RIBEIRO, P. F. Analysis of harmonic current summation based on field measurements. **IET Generation, Transmission & Distribution**, ISSN 1751-8687. April 2013.

ĆUK, V; COBBEN, J. F. G. ; RIBEIRO, P. F. A Review of International Limits for Harmonic Voltages and Currents in Public Networks. **2014 16th International Conference on Harmonics and Quality of Power (ICHQP).** Bucharest, Romania, June 2014.

DE OLIVEIRA, T. E. C.; RIBEIRO, P. F.; SANTOS, I. N. Determining the harmonic hosting capacity of PV sources for a university campus. **Proceedings of International Conference on Harmonics and Quality of Power, ICHQP**, v. 2016–December, p. 836–841, 2016.

Diverse Authors. Power Quality Requirements for Connection to the Transmission System. n. September, p. 1–32, 2015.

DRINČIĆ, F.; MUJOVIĆ, S.; MEMBER, S. Energy storage systems : an overview of existing technologies and analysis of their applications within the power system of Montenegro. **2018 23rd International Scientific-Professional Conference on Information Technology (IT)**. p. 0–3, 2018.

DUBEY, A.; SANTOSO, S. On Estimation and Sensitivity Analysis of Distribution Circuit's Photovoltaic Hosting Capacity. **IEEE Transactions on Power Systems**, v. 32, n. 4, p. 2779–2789, 2017.

DUDIAK, I. J. Integration of renewable energy sources to the power system. **2014 14th International Conference on Environment and Electrical Engineering**. p. 1–4, 2014.

WORLD ENERGY TRILEMA. **Changing Dynamics – Using Distributed**

Energy Resources to Meet the Trilemma Challenge. 2017.

TECHNOLOGICAL UNIVERSITY OF EINDHOVEN. **PQ-SmartGrid laboratory**. February, p. 1–16, 2015.

ETHERDEN, N. Increasing the hosting capacity of distributed energy resources using storage and communication. **Doctoral Thesis**, Luleå 2014.

ETHERDEN, N.; BOLLEN, M. H. J. Increasing the hosting capacity of distribution networks by curtailment of renewable energy resources. **2011 IEEE PES Trondheim PowerTech: The Power of Technology for a Sustainable Society, POWERTECH 2011**, p. 1–7, 2011.

FAN, S. et al. Evaluation of impact of integrated distributed generation on distribution network based on time-series analysis. **2016 China International Conference on Electricity Distribution (CICED)**. p. 10–13, 2016.

FERREIRA, P. D. F.; CARVALHO, P. M. S.; FERREIRA, L. A. F. M.; LLIC D. Distributed Energy Resources Integration Challenges in Low-Voltage Networks: Voltage Control Limitations and Risk of Cascading. **IEEE Transactions on Sustainable Energy,** V. 4, I. 1, Jan. 2013.

GARCÍA, H.; SEGUNDO, J.; MADRIGAL, M. Harmonic analysis of power systems including thyristor-controlled series capacitor (TCSC) and its interaction with the transmission line. **Electric Power Systems Research**, v. 106, p. 151–159, 2014.

GHIJSELEN, J. A.; RYCKAERT, W. R.; MELKEBEEK, J. A. Required Load Behaviour for Power Quality Improvement. **IEEE Power Engineering Society Summer Meeting**, n. 3, p. 998–1003, 2002.

GONÇALVES, A. F. Q. et al. Análise de conversores CC-CA conectados em redes de distribuição e utilizados em sistemas de geração distribuída. **2010 9th IEEE/IAS International Conference on Industry Applications, INDUSCON 2010**, 2010.

GRADY, W. M.; CHOWDHURY, A. H.; SAMOTYJ, M. J. I. An investigation of harmonics attenuation and diversity among distributed single-phase power electronic loads. **IEEE Transactions on Power Delivery** V. 10, I. 1, Jan 1995

HARRISON, G. P.; DJOKIC, S. Z. Incorporating harmonic limits into assessment of the hosting capacity of active networks. **CIRED 2012 Workshop: Integration of Renewables into the Distribution Grid**, v. 5, p. 325–325, 2012.

IEEE. **IEEE 1547 Standard for Interconnecting Distributed Resources with Electric Power Systems.** n. July, 2003.

IEEE 1159, S. **IEEE Std 1159™ – 2009, IEEE Recommended Practice for Monitoring Electric Power Quality**. v. 2009

J. DEUSE, D. BENINTENDI, P. J. A. . P. B. Power System and Market Integration of DER, **the EU-Deep approach.** n. 6, p. 6–9, 2005.

KEY, T. S.; HALL, W. IEEE and International Harmonic Standards Impact on Power Electronic Equipment Design. **Proceedings of the IECON'97 23rd International Conference on Industrial Electronics, Control, and Instrumentation**. v. 2, 1992.

LARSSON, A.Evolution of the Harmonic Distortion from State of art computers – 2002 to 2008. **CIRED 2009 – The 20th International Conference and Exhibition on Electricity Distribution – Part 2**. n. June, p. 8–11, 2009.

LEITÃO, J. J. A. L. et al. Harmonic distortion on a transmission system during games of the Brazilian National Team in the 2006 world cup. **2007 IEEE Power Engineering Society General Meeting, PES**, p. 1–2, 2007.

HATZIARGYVRIOU, N. D. Microgrids – Large scale integration of microgeneration to low voltage grids. **CIGRE 2006**, Aug 2006, Paris, France.

MEHRIZI-SANI, A. Distributed Energy Resources. n. February, p. 0–5, 2013.

MENNITI, D. et al. Distribution network analysis: A comparison between hosting and loading capacities. **SPEEDAM 2012 – 21st International Symposium on Power Electronics, Electrical Drives, Automation and Motion**, p. 926–933, 2012.

MILANOVIC, J. V. et al, International Industry Practice on Power Quality Monitoring, **IEEE Transactions on Power Delivery**, vol. 29, (2) pp. 934-941, 2014.

MÖLLER, F. et al. Impact of Electric Vehicle Charging on Unbalance and Harmonic Distortion – Field Study in an Urban Residential Area. **CIRED 2015 – The 23rd International Conference and Exhibition on Electricity Distribution.** n. June, p. 15–18, 2015.

NUNES, I. V; ISSA, L. Calculando a Capacidade de Hospedagem de Rede com Vistas 'a Inserção de Geração Distribuida no Tocanta as Distorções Harmônicas. **Anais da XII Conferência de Estudos em Engenharia Elétrica.** p. 1–5. (In Portuguese)

ODARNO, L.; MARTIN, S.; ANGER, C. 10 Questions To Ask About Distributed **Generation. World Resources Institute – WWF.** n. September, p. 1–36, 2015. Acess in 1st of May 2018.

OLIVEIRA, T. E. C. DE et al. Estudo da Capacidade de Hospedagem de Fontes de Geração Distribuída no Sistema Elétrico de um Campus Universitário. **Anais do CBQEE 2015 – XI Conferência Brasileira sobre Qualidade da Energia Elétrica**, 2015. (In Portuguese)

OLIVEIRA, T. E. C. DE et al. Estudo da Capacidade de Hospedagem de Fontes de Geração Distribuída no Sistema Elétrico de um Campus Universitário. **Master's dissertation, 2015** – (In Portuguese)

OLIVEIRA, T. E. C. et al. PV Hosting Capacity Dependence on Harmonic Voltage Distortion in Low-Voltage Grids: Model Validation with Experimental Data. **Energies**, v. 11, n. 2, 2018.

OLIVEIRA, F. et al. Considerations on Power Quality Requirements for Integration of Renewable Sources (Photovoltaic and Wind power) into the Transmission Grid National Electrical System Operator. **CIGRE 2014** – Brazil Federal University of Itajubá , UNIFEI, 2014.

ONS. Resultados da Operação do SIN durante o jogo Camarões x Brasil, pela Copa do Mundo FIFA 2014. v. 2018, p. 2, 2014. **Acess in 15th of June 2018** (In Portuguese)

PALUDO, J. A. Avaliação dos Impactos de Elevados Níveis de Penetração da Geração Fotovoltaica no Desempenho de Sistemas de Distribuição de Energia

Elétrica em Regime Permanente. **Master's Thesis**. São Carlos, Brazil. 2014. (In Portuguese)

PAPIC, I. et al. A Benchmark Test System to Evaluate Methods of Harmonic Contribution Determination. **IEEE Transactions on Power Delivery**, v. 8977, n. c, p. 1–8, 2018.

RENO, M. J.; COOGAN, K.; GRIJALVA, S; BRODERICK, R. J.;QUIROZ, E. PV Interconnection Risk Analysis through Distribution System Impact Sugnatures and Feeder Zones. **2014 IEEE PES General Meeting | Conference & Exposition**. July, 2014.

RIBEIRO, P. F. et al. Energy storage systems for advanced power applications. **Proceedings of the IEEE**, v. 89, n. 12, p. 1744–1756, 2001.

RICHARDSON, R.; FLYNN, D.;KEANE, A. Optimal charging of electric vehicles in low voltage distribution systems, **IEEE Transactions on Power Systems,** vol. 27, no. 1, pp. 268-279, February 2012.

RIBEIRO, P. F. et al. Harmonic distortion during the 2010 FIFA World Cup. **2011 IEEE Power and Energy Society General Meeting**, p. 1–8, 2011.

RÖNNBERG, S.; BOLLEN, M. Solar power in northern Scandinavia, its impact on the grid and methods to mitigate this impact. **2013 4th IEEE/PES Innovative Smart Grid Technologies Europe, ISGT Europe 2013**, p. 1–5, 2013.

RÖNNBERG, S. K.; BOLLEN, M. H. J.; WAHLBERG, M. Harmonic emission before and after changing to LED and CFL – Part I: Laboratory measurements for a domestic customer. **ICHQP 2010 – 14th International Conference on Harmonics and Quality of Power**, p. 1–6, 2010.

RUBENS, J. et al. The impact of FIFA World Cup 2006 on Power. 2**007 9th International Conference on Electrical Power Quality and Utilisation**. 2006.

RUGTHAICHAROENCHEEP, N.; AUCHARIYAMET, S. Technical and Economic Impacts of distributed generation on distribution system. **International Journal of Electrical, Computer, Energetic, Electronic and Communication Engineering**, v. 6, n. 4, p. 385–389, 2012.

RYCKAERT, W. R. A.; GHIJSELEN, J. A. L.; MELKEBEEK, J. A. A. Harmonic mitigation potential of shunt harmonic impedances and the influence of background distortion. **2003 IEEE Bologna PowerTech – Conference Proceedings**, v. 2, p. 663–670, 2003.

RYLANDER, M. et al. Voltage impacts from distributed photovoltaics on two distribution feeders. **IEEE Power and Energy Society General Meeting**, p. 2–6, 2013.

RYLANDER, M.; SMITH, J.; SUNDERMAN, W. Streamlined Method for Determining Distribution System Hosting Capacity. **2015 IEEE Rural Electric Power Conference**, p. 3–9, 2015.

SÁIZ-MARÍN, E. et al. Local Hosting Capacity Increase by Means of Wind Farm Voltage Control Provision. **IEEE Transactions on Power Systems.** v. 29, n. 4, p. 1731–1738, 2014.

SANTOS, I. N. et al. Considerations on hosting capacity for harmonic distortions on transmission and distribution systems. **Electric Power Systems Research**, v. 119, p. 199–206, 2015.

SANTOS, I. N.; BOLLEN, M. H. J.; RIBEIRO, P. F. Methodology for estimation of harmonic hosting. **Proceedings of International Conference on Harmonics and Quality of Power, ICHQP**, p. 708–712, 2014.

SMITH, J. Modeling and Hosting Capacity Analysis of 16 Feeders. **EPRI Project Manager**, April 2015.

SHAYANI, R. A. Método para Determinação do Limite de Penetração da Geração Distribuída Fotovoltaica em Redes Radiais de Distribuição. **Doctoral Thesis.** 2010. (In Portuguese)

SCHWANZ, D. et al. Stochastic Assessment of Voltage Unbalance Due to Single-Phase-Connected Solar Power. **IEEE Transactions on Power Delivery** v. 32, n. 2, p. 852–861, 2017.

SLAUGHTER, A.; MOTYKA, M.; MCCUE, J. Managing variable and distributed energy resources: A new era for the grid. **Deloitte Centre for Energy Solutions**. 2016.

SOCIETY, I. P. AND E. IEEE Recommended Practice and Requirements for Harmonic Control in Electric Power Systems IEEE Power and Energy Society. **ANSI/IEEE Std. 519**, v. 2014, 2014.

SPERTINO, F. et al. Storage sizing procedure and experimental verification of stand-alone photovoltaic systems. **2012 IEEE International Energy Conference and Exhibition (ENERGYCON)**. p. 464–468, 2012.

SYSTEMS, P.; COMMITTEE, E. **IEEE 1100:2005 – IEEE Recommended Practice for Powering and Grounding Electronic Equipment**. v. 1999

TAN, W. S. et al. Optimal distributed renewable generation planning: A review of different approaches. **Renewable and Sustainable Energy Reviews**, v. 18, p. 626–645, 2013.

TESTA, A.; LANGELLA, R. Harmonic pollution in Italian distribution networks in coincidence with important sport events. **2007 IEEE Power Engineering Society General Meeting, PES**, p. 1–7, 2007.

TREVISAN, A. S. Efeitos da geração distribuída em sistemas de distribuição de baixa tensão. **Final Graduation Thesis.** 2011. (In Portuguese)

WALLACE, I.; BENDRE, A.; WOOD, N. Harmonic Filters for Hogh Background Voltage Distortion Applications. **TCI Technical Paper**, p. 1–5, 2013.

WOLSINK, M. The research agenda on social acceptance of distributed generation in smart grids: Renewable as common pool resources. **Renewable and Sustainable Energy Reviews**, v. 16, n. 1, p. 822–835, 2012.

WOOD, D. et al. 10 Questions To Ask About Scaling on-Grid Renewable Energy Frameworks for Designing Good. **eneration. World Resources Institute – WWF.** n. January, p. 1–28, 2014. (Acess in 1st of May 2018)

WORLD ENERGY COUNCIL. **World Energy Resources Solar,** 2016.

YANG, K.; BOLLEN, M. H. J.; LARSSON, E. O. A. Aggregation and Amplification of Wind-Turbine Harmonic Emission in a Wind Park. **IEEE Transactions on Power Delivery**, v. 30, n. 2, p. 791–799, 2015.

YANG, K.; SCHWANZ, D. Harmonic aggregation and amplification in a wind-park. **2015 IEEE Power & Energy Society General Meeting.** n. June, p. 15–18, 2015.

APPENDIX. X (SPECIAL RESULTS) – DYNAMIC HOSTING CAPACITY CONSIDERING STORAGE SYSTEMS

This section begins by examining an applicability of the DHC regarding energy storage systems. Throughout this appendix, the impact of the energy storage-hosting capacity of the measured system is examined. This section looks at the question of voltage rise caused by the bi-directional power flow due to the PV system. It is proposed a new procedure based on the DHC concept to improve the power quality indexes of the electrical system. The results will be significant for planning and improving level in regard to the local and the dynamic hosting capacity. If an energy storage system is considered, it is show how it is possible for the voltage level to drop due to power flow reversal and to increase of hosting capacity value of the systems.

Conventional electrical networks consider the total load flow directly from the substation to the load. In regard to this fact, there is a voltage drop throughout the transmission line, as shown in Figure A.1. This unidirectional load flow allows for an easy planning of the distribution transformers and the conductor section of the feeders (PALUDO, 2014).

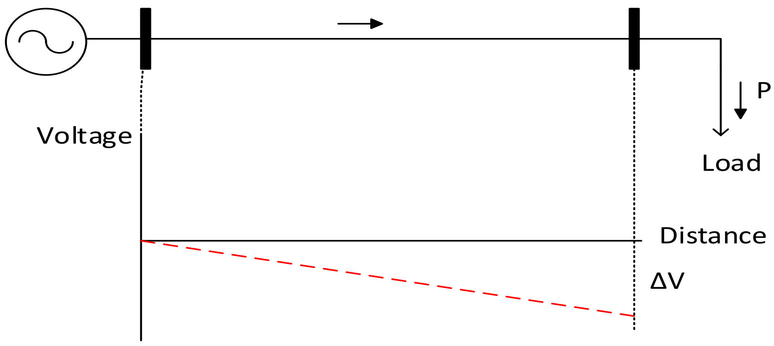

Figure A.1– Conventional power flow.

However, when there is penetration of DERs in the electrical network, there may be a reversal and/or bidirectionality of the power flow. As an example, the DERs absorbs the consumption of the load to which it is connected, and the additional power will be injected into the distribution network, feeding other loads nearby. The phenomenon is shown in Figure A.2. Due to the bidirectional power flow, some negative aspects can be registered, for example, a voltage rise at the connection point where the DERs is installed, which can exceed standard indexes, leading to possible losses (PALUDO, 2014).

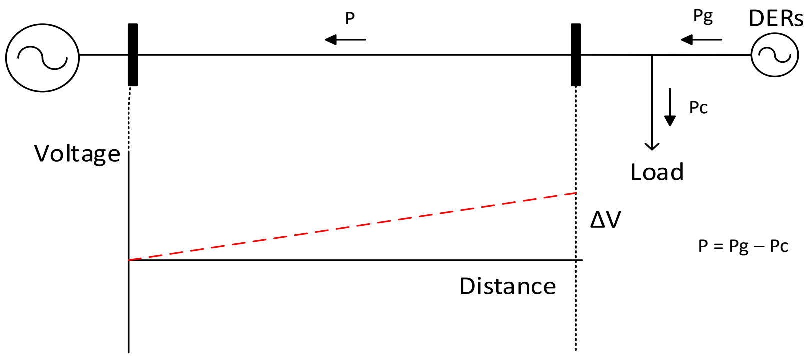

Figure A.2– Bidirectional power flow.

On the other hand, storage systems could help the system at the connection point. Several researchers have called this into question, claiming that storage systems can lead to improvements into the distribution system, such as avoiding the voltage rises due to the bidirectional power flow, as well as improving the hosting capacity of the system (RIBEIRO et al, 2001). Figure A.3 shows the storage system's impact at the connection point. It is possible to understand that the voltage would not rise in the system because there is no bidirectional load flow into the system.

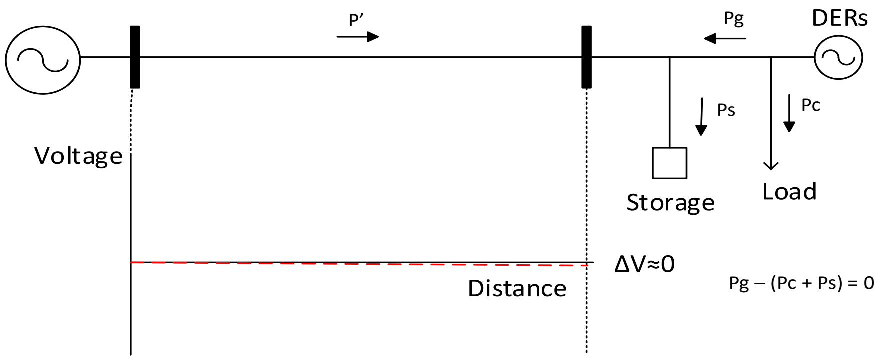

Figure A.3– The storage system and its impact.

This problem can be outlined in terms of the power of the system. In this case, the power´s sum will be zero due to the relation $P_g - (P_s + P_s)$, where P_g is the power generated by DERs, P_c is the power consumed by loads and P_s is the power which will be stored by the storage system. It is important to highlight that the sum will be zero, as long as there is a generation from the DERs. For example, in regard to PVs, only at the moment when there is solar irradiation. This allows for a formal solution to be found, where $\Delta V \approx 0$. In theory, the less the voltage rise, the better the hosting capacity will be.

It is easily verifiable that there are two possible options in order to bring improvement at the connection point: either regulate the voltage through regulators such as LTC or connect some storage systems into the connection point. It is necessary to analyse which option is better economically speaking. In this analysis, the storage systems will be under investigation with the intention of bringing improvement regarding the dynamic hosting capacity profile (DHC) for the system, as shown in Figure A.4.

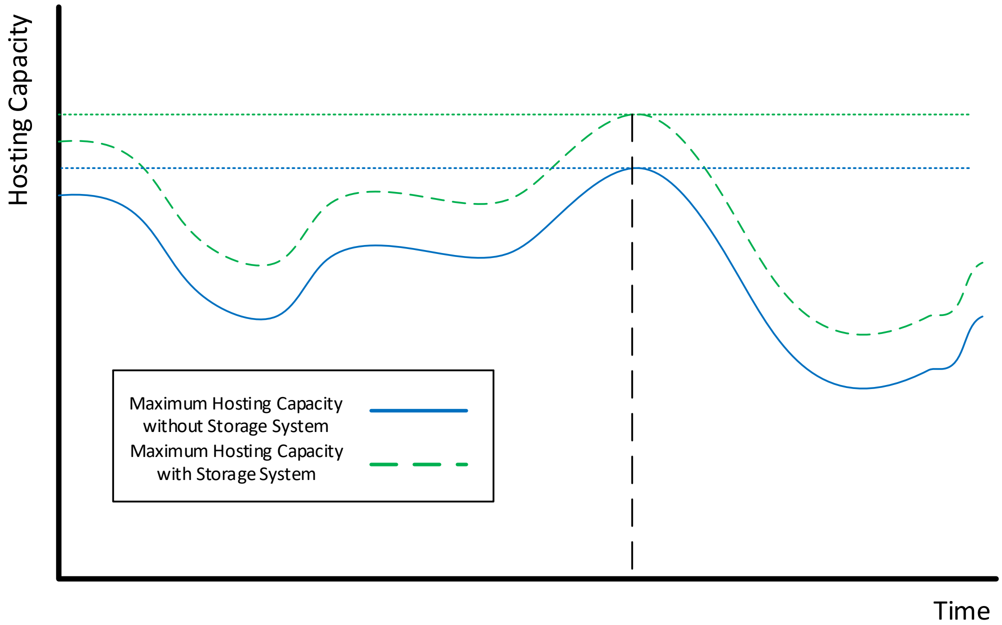

Figure A.4– The DHC with and without the energy storage system.

This proposed hypothesis examines how to solve the voltage rise problem in electrical grids using energy storage systems in order to improve the DHC approach. The energy storage system is examined with the intention of finding the best contribution to decrease the voltage rises, as well as keeping at zero the reverse power flow, thus improving the hosting capacity. This is a feasible solution for distribution systems in relation to voltage rise indexes due to DERs connected at the electrical grid.

i) Formulation of the Dynamic Hosting Capacity with an Energy Storage System

In sections 6.2.1 and 6.3, this study highlights the importance of considering that the maximum amount of energy depends on the harmonic voltage values, which are defined for each instant of time.

The aim of DHC is to calculate the hosting capacity considering energy storage systems, which can be defined as the storage-hosting capacity. Consequently, we need to formulate a hypothesis for it. The hosting capacity concept is applied to the allowed voltage magnitude for the system, in this case, determined by local standards. In theory, the concept of hosting capacity, either static or dynamic, makes it clear that the maximum voltage magnitude allowed is the determining factor to find its global value.

The storage-hosting capacity was prepared using the same procedure as for dynamic hosting capacity, but taking into account one specific consideration, which has already been mentioned before. In this way, this assessment considers the voltage rise caused by the bidirectional load flow into the system, thus determining the outline conditions. Instead of basing the maximum voltage magnitude allowed for the system on local standards, the allowed voltage magnitude in (6.3.1) will be equal to the voltage rise for systems without an energy storage-system. Moreover, the voltage reference will be the nominal, which means, equal to1.0 (p.u). Those considerations are shown below.

$$\begin{cases} V_g^{max,1} = V_o(t) \\ V_o^1(t) = 1.0\ (p.u) \end{cases}$$

This method represents an alternative to analyse the storage system behaviour because, in this case, the maximum voltage rises already existent at the system, considering the DERs, are the determinant factor to find a hosting capacity value. In addition, the maximum storage power is calculated only for the fundamental frequency, where the voltage rise is an important impact factor. Thus, the equation (6.3.1) can be given by (A.1).

$$\Delta P_{storage}^{max}(t) = \frac{1}{R_f} \frac{V_o(t)(V_o(t) - 1{,}0)}{(1 + tan(\varphi)\frac{X_f}{R_f})} \qquad (A.1)$$

Taking advantage of storage-hosting capacity use, we can hypothetically propose that the maximum power stored found by (A.1) is a complement of the maximum power generated given by (6.3.1). Combining (6.3.1) and (A.1), we have a total maximum power generation for the system considering an energy storage system, given by (A.2).

$$P_g^{max\,\prime}(t) = P_g^{max}(t) + \Delta P_{storage}^{max}(t) \qquad (A.2)$$

It is easily verifiable that the maximum dynamic hosting capacity can be extended by (A.1) in (A.3), where it can be defined by linear regression.

$$HC_{total}^{max\,\prime}(t) = HC_{total}^{max}(t) + \Delta HC_{storage}^{max}(t) \qquad (A.3)$$

The new voltage profile for the system after the energy storage system can be verified. There will not be a voltage rise as defined in **Error! Reference source not found.**. The voltage drop can be determined by (A.1). Thus, the new voltage value is given by (A.4).

$$V_o'(t) = V_o(t) - \Delta V^{storage}(t) \qquad (A.4)$$

It is important to highlight that the local DER system, considering an energy storage system, will be dimensioned by (A.3) and (A.4), in order to ensure future improvement in the current installation. The results will be discussed further in this appendix.

ii) An Applicability of Dynamic Hosting Capacity into Energy Storage Systems

During the first phase of analysis, the impact of the energy storage-hosting capacity into the measured system has been examined. Remarkably, the possible values of storage generation, for which the voltage rise due to the reverse power flow is avoided, are shown in Figure A.2. These values respect the relation between the generated power by the PVs and the absorbed power by the local load. Thus, Figure A.5 illustrates the residual power that was injected in the feeder in direction to other loads. These data were collected by the PQ analyser installed in the LV side of the distribution transformer.

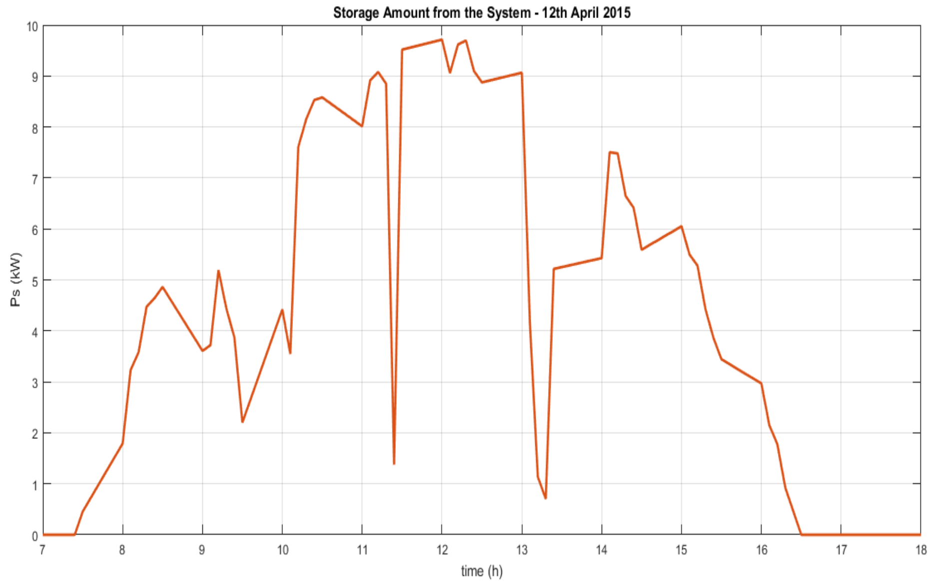

Figure A.5 – Possible amount of energy storage in order to avoid the reversed power flow –April 12th, 2015.

The possible values of energy storage for the other days are shown in Figure A.6.

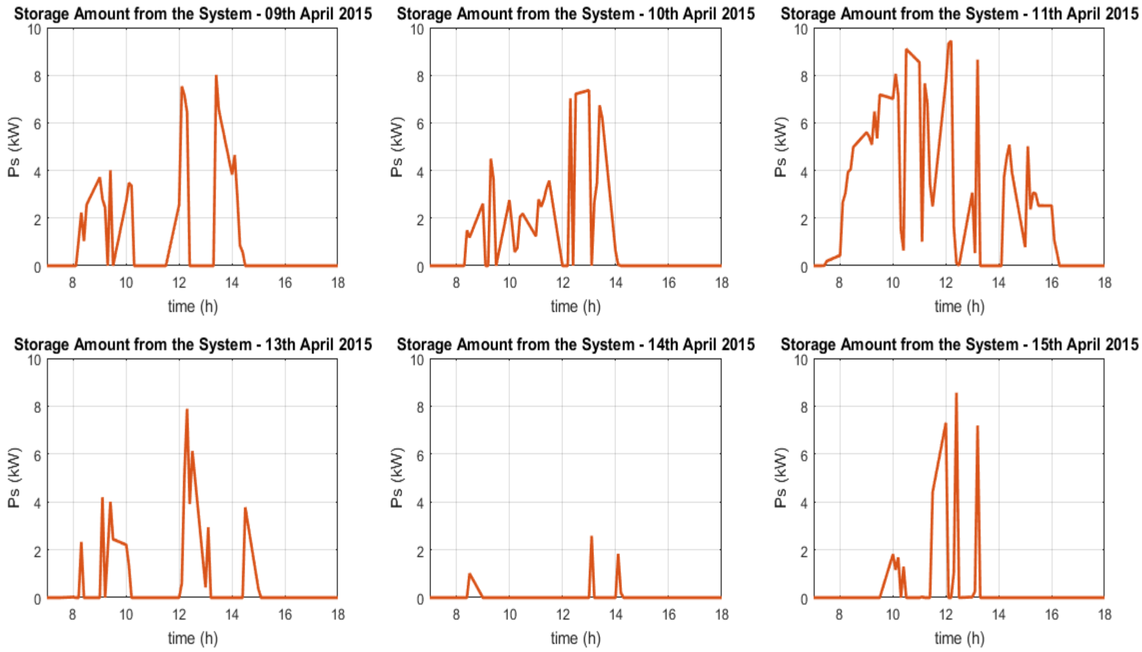

Figure A.6 – Possible amount of energy storage in order to avoid the reversed power flow – Other days.

In this context, the voltage rise caused by power flow reversal is the key to this methodology proposal regarding energy storage-hosting capacity systems. Thus, the maximum increment of energy storage is possible to be found using (A.1), as expected. Due to this fact, a linear dependency is created through linear regression using $y = ax + b$ formulation, shown in Figure A.7 through Figure A.13. Strong evidence was found regarding the 12th of April 2015. The reason why this day was highlighted is because the system could feed itself 100%, and most of the power generated could be stored in order to avoid a power flow reversal and then, there will not be a voltage rise. The possible energy storage-hosting capacity is shown in Figure A.7 regarding the preferred day.

After having calculated the linear extrapolation, one can find the daily and weekly energy storage-hosting capacities. A daily analysis was used to predict the hypothesis proposed in (A.1), where for each increment of maximum power stored calculated, a voltage drop will be achieved in order to minimise the voltage rise for the system. For example, to avoid 1.5% of voltage rise due to the reversed power flow, the system should absorb 4.0 kW from the source based on Figure A.6 example.

Weekly, the maximum power stored is observed when the line crosses the maximum voltage rise measured for the system in relation to the instant of time measured. This value is approximately 0.03 p.u. Therefore, the final solution determined is given by the calculated energy storage-hosting capacity in relation to the chosen day. The calculated energy storage-hosting capacity computed is 8.3 kW for the 9th of April 2015 and is given in Figure A.7.

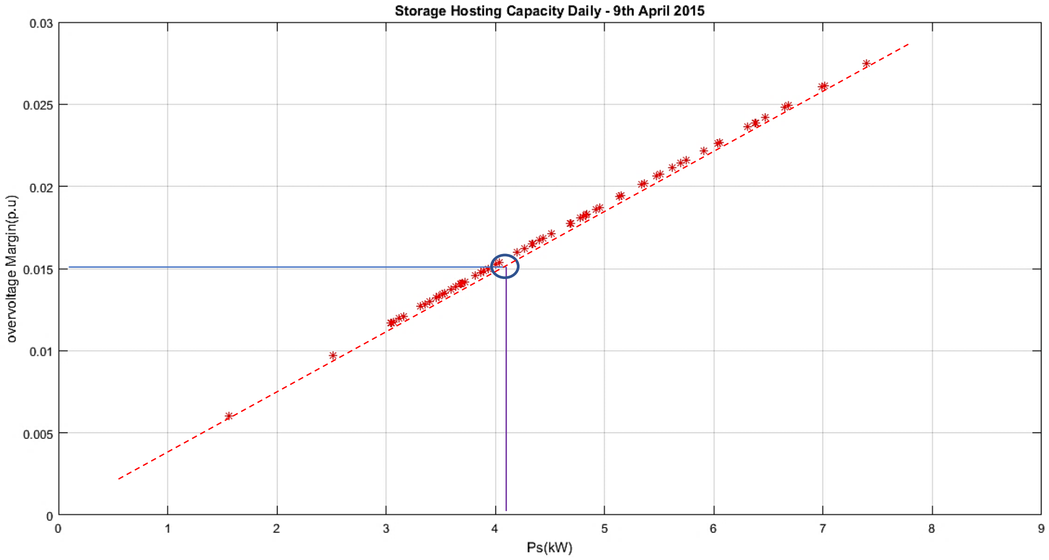

Figure A.7 – Maximum amount of energy storage found by (A.1) regarding 9th April 2015.

The calculated energy storage-hosting capacity calculated is 8.1 kW for the 10th of April 2015. The possible energy storage-hosting capacity is shown in Figure A.8 for the mentioned day.

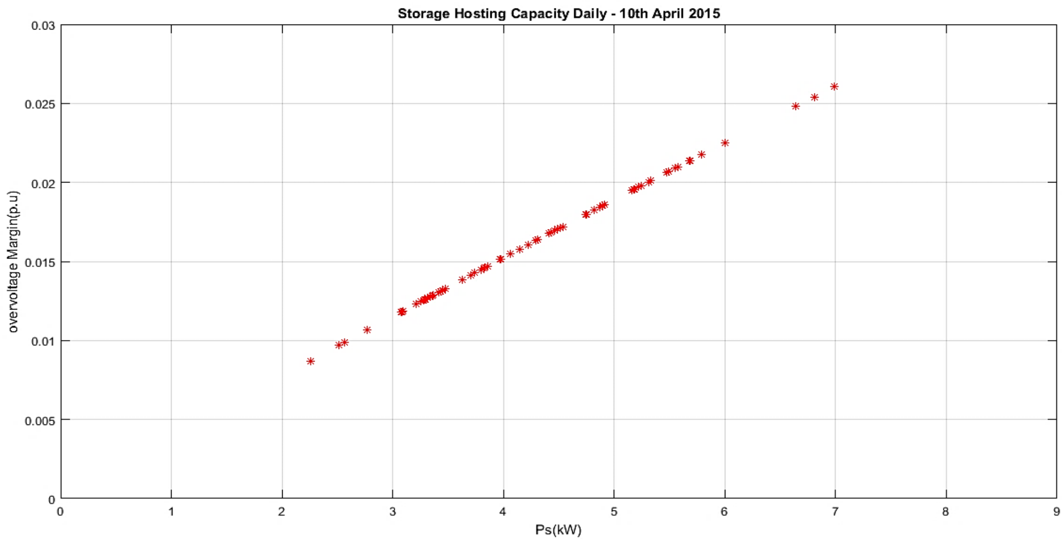

Figure A.8 – Maximum amount of energy storage found by (A.1) regarding 10th April 2015.

Furthermore, the calculated energy storage-hosting capacity computed is 8.0 kW for the 11th of April 2015. The possible energy storage-hosting capacity is shown in Figure A.9 for the mentioned day.

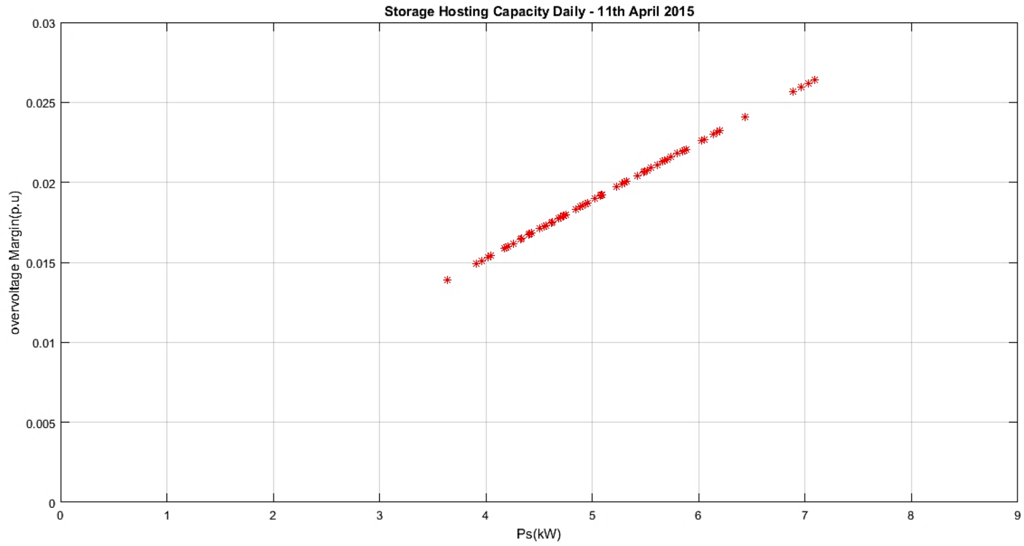

Figure A.9 – Maximum amount of energy storage found by (A.1) regarding 11th April 2015.

The calculated energy storage-hosting capacity computed is 8.0 kW for the 12th of April 2015. The possible energy storage-hosting capacity is shown in Figure A.10 for the mentioned day.

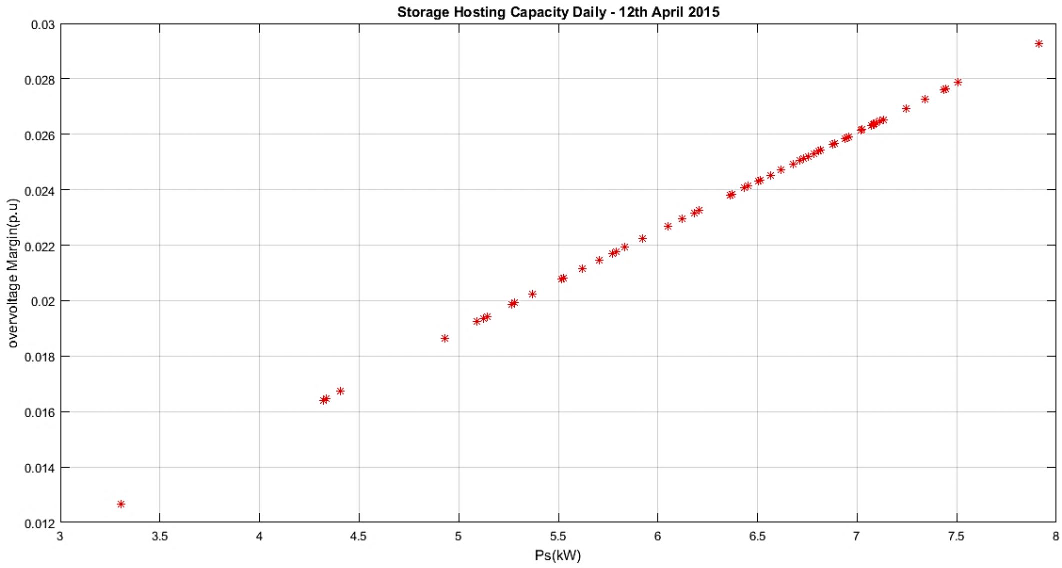

Figure A.10 – Maximum amount of energy storage found by (A.1) regarding 12th April 2015.

Thus, the calculated energy storage-hosting capacity computed is 8.1 kW for the 13th of April 2015. The possible energy storage-hosting capacity is shown in Figure A.11 for the mentioned day.

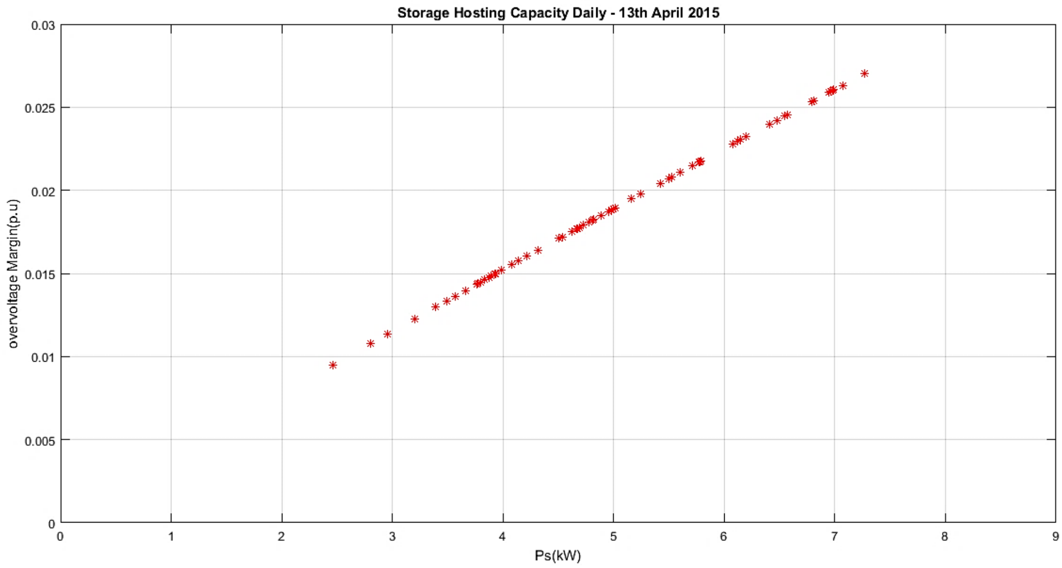

Figure A.11 – Maximum amount of energy storage found by (A.1) regarding 13th April 2015.

Moreover, the calculated energy storage-hosting capacity computed is 8.1 kW for the 14th of April 2015. The possible energy storage-hosting capacity is shown in Figure A.12 for the mentioned day.

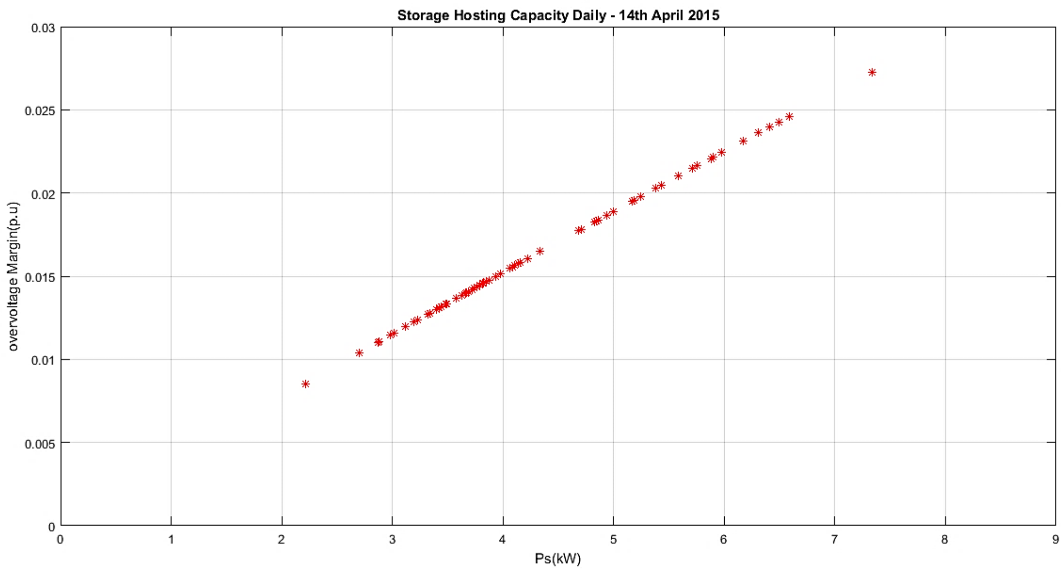

Figure A.12 – Maximum amount of energy storage found by (A.1) regarding 14th April 2015.

Moreover, the calculated energy storage-hosting capacity computed is 8.0 kW for the 15th of April 2015. The possible energy storage-hosting capacity is shown in Figure A.13 the mentioned day.

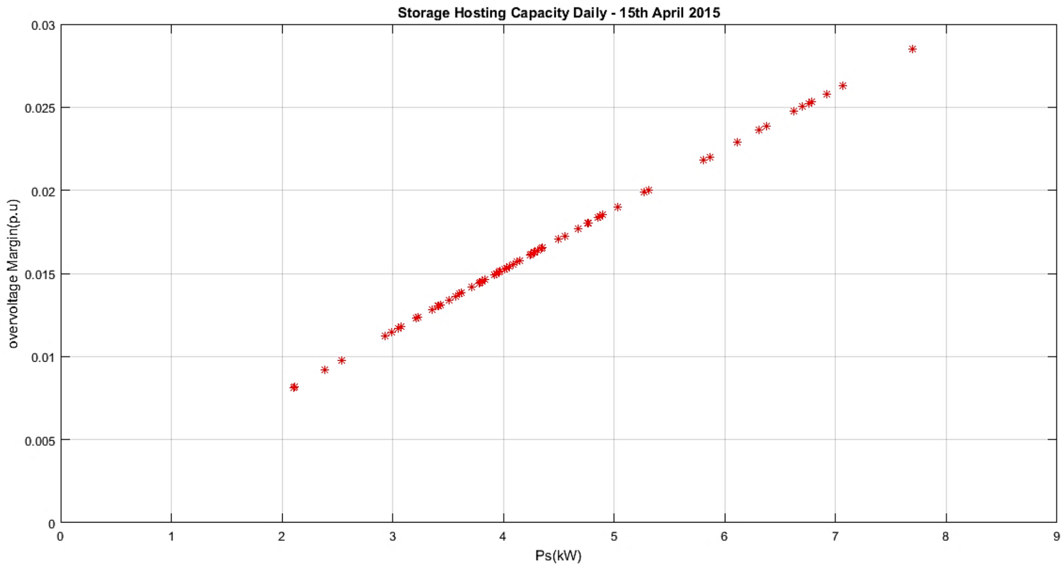

Figure A.13 – Maximum amount of energy storage found by (A.1) regarding 15th April 2015.

The results on energy storage-hosting capacity for all days can be seen in Table A.1.

Table A.1 – Energy Storage-Hosting Capacity values for the measured week.

	9th April	10th April	11th April	12th April	13th April	14th April	15th April
HC	8.1 kW	8.1 kW	8.0 kW	8.0 kW	8.1 kW	8.1 kW	8.0 KW

At this point of the analysis, the energy storage-hosting capacity profile can be drawn considering the days mentioned, where for each instant of measurement, a storage maximum generation, using (A.2), has been computed. As soon as these steps have been carried out, the improved DHC will be calculated using (A.3), where for each measured hosting capacity calculated by (A.1), the global hosting capacity value will be increased by the maximum storage generation, followed by (A.2). The paradox between the system without storage system and with storage system is shown in Figure A.14 through Figure A.20, as follows.

The first DHC profile with and without energy storage system analysed refers to the 9th of April 2015.

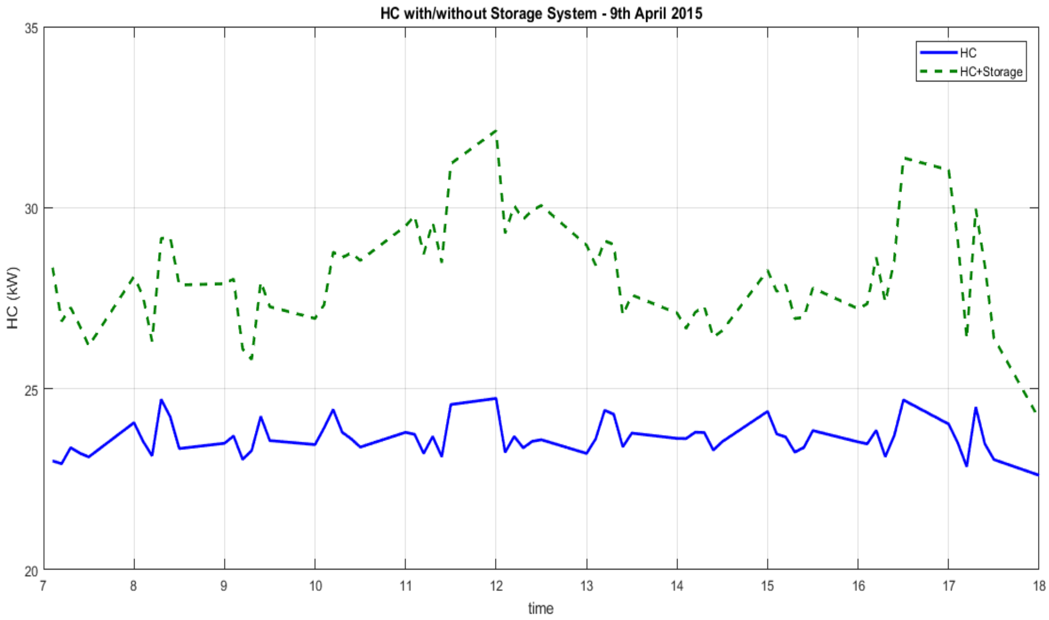

Figure A.14 – The dynamic daily hosting capacity with storage system in relation to April 9th, 2015.

The average mark of daily DHC, in regard to April 9th, 2015, was 24 kW, as calculated before using (6.3.1). In this case, the maximum daily hosting capacity is approximately 25 kW, whereas the minimum value is 22.6 kW. The resulting possible maximum and minimum values are a consequence of external and internal conditions affecting the system. For example, the minimum values were registered at around 12:00 p.m. and 01:00 p.m., when the building was empty because of lunch time, all electronic equipment was turned off and the sun was at its peak. According to Figure C.1 in **APPENDIX C,** the 9th of April of 2015 had the highest solar production. Due to these particular conditions, the level of harmonic distortion (Figure C.2) probably was higher than in usual occasions, which impacts on the voltage profile (Figure C.3) and consequently in the level of the hosting capacity at the moment. It is important to highlight that these values don't reflect the global number of hosting capacity. They reflect special conditions, which may or may not impact the final value of the hosting capacity throughout the DHC weekly profile. An improvement is likely to be registered, in relation to the DHC profile, when the energy storage system is considered. The average improvement registered is approximately 19% every 10 minutes, but it can reach a maximum value of 26%. For the global value in relation to the day mentioned, the global hosting capacity is 32.1 kW as given by (A.3), which grants the system almost 50% of improvement regarding the total installed capacity of the system, in this case, 15 $\mathrm{kW_p}$.

$$HC_{total}^{max}\,' = 24 + 8.1 = 32.1\ kW$$

The next DHC profile with and without energy storage system analysed is regarding 10th April 2015.

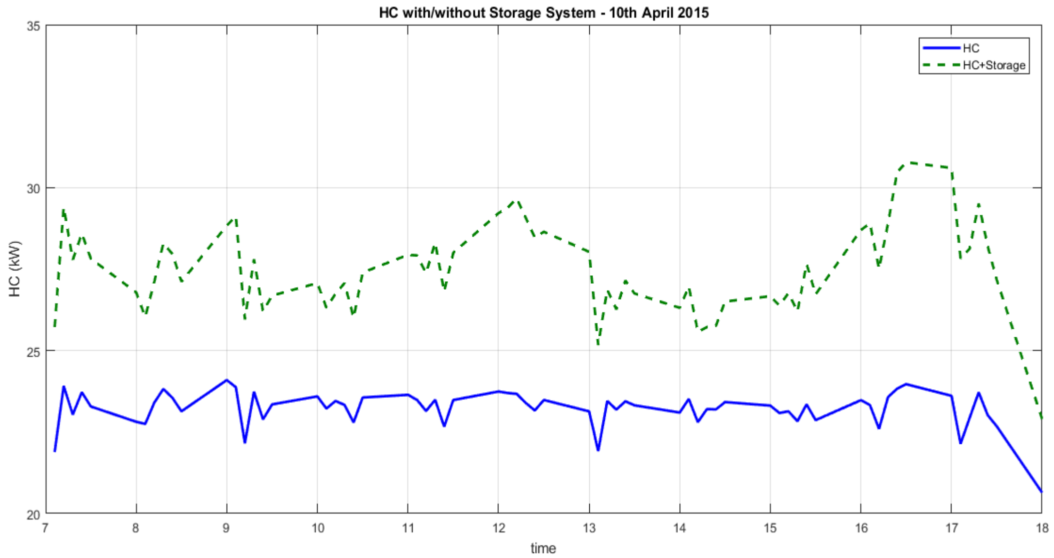

Figure A.15 – The dynamic daily hosting capacity with storage system in relation to April 10th, 2015.

The average mark of daily DHC, in regard to April 10th, 2015, was 23.5 kW, as calculated before using (6.3.1). In this case, the maximum daily hosting capacity is approximately 24.1 kW, whereas the minimum value is 20.6 kW. The resulting possible maximum and minimum values are a consequence of external and internal conditions affecting the system. It is important to notice that those values are similar when compared to the day before. For example, one of the minimum values was registered at around 01:00 p.m., when the building wasn't completely empty because of the beginning of the morning, with some electronic equipment turned on and the sun was almost at its peak. According to Figure C.1 in **APPENDIX C,** the 10th of April of 2015 had one of the highest solar production. Due to these particular conditions, the level of harmonic distortion (Figure C.2) probably was higher than in usual occasions, which impacts on the voltage profile (Figure C.3) and consequently in the level of the hosting capacity at the moment. They reflect special conditions, which may or may not impact the final value of the hosting capacity throughout the DHC weekly profile. An improvement is likely to be registered, in relation to the DHC profile, when the energy storage system is considered. The average improvement registered is approximately 14% every 10 minutes, but it can reach a maximum value of 23%. For the global value in relation to the day mentioned, the global hosting capacity is 31.6 kW as given by (A.3), which grants the system almost 50% of improvement regarding the total installed capacity of the system, in this case, 15 kW_p.

$$HC_{total}^{max}{}' = 23.5 + 8.1 = 31.6\ kW$$

The next DHC profile with and without energy storage system analysed is regarding 11th April 2015.

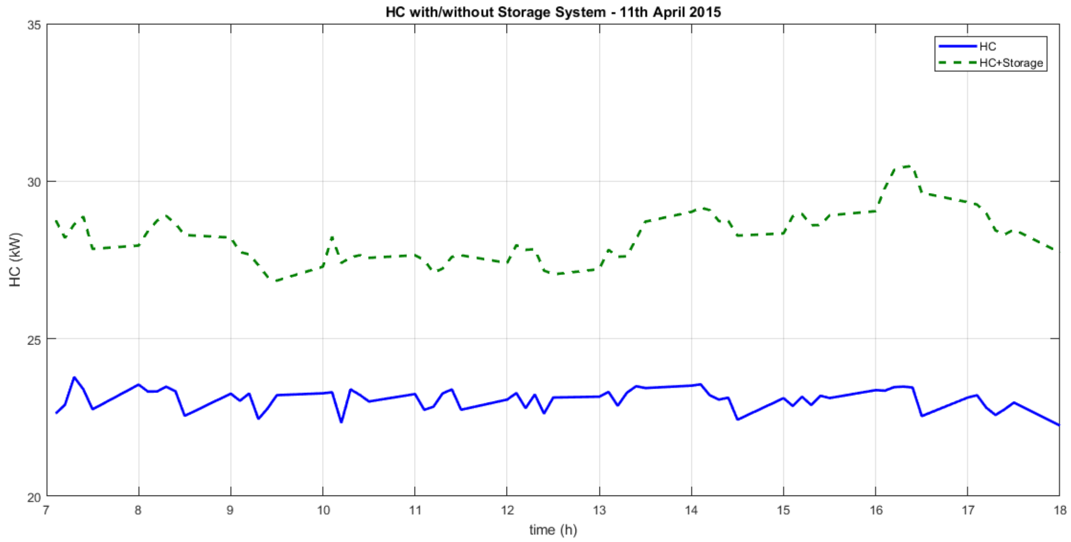

Figure A.16 – The dynamic daily hosting capacity with storage system in relation to April 11th, 2015.

The average mark of daily DHC, in regard to April 11th, 2015, was 23.4 kW, as calculated before using (6.3.1). In this case, the maximum daily hosting capacity is approximately 23.78 kW, whereas the minimum value is 22.24 kW. The resulting possible maximum and minimum values are a consequence of external and internal conditions affecting the system. It is important to notice that those values are similar when compared to the day before. For example, the minimum value was registered at around 02:30 p.m., when the building wasn't completely empty because of the beginning of the morning, with some electronic equipment turned on and the sun was almost at its peak. According to Figure C.1 in **APPENDIX C,** the 11th of April of 2015 had one of the highest solar production. Due to these particular conditions, the level of distortion probably was higher than in usual occasions (Figure C.2), which impacts in the voltage profile (Figure C.3) and consequently in the level of the hosting capacity. It is important to highlight that these values don't reflect the global number of hosting capacity. They reflect special conditions, which may or may not impact the final value of the hosting capacity throughout the DHC weekly profile. An improvement is likely to be registered, in relation to the DHC profile, when the energy storage system is considered. The average improvement registered is approximately 22% every 10 minutes, but it can reach a maximum value of 31%. For the global value in relation to the day mentioned, the global hosting capacity is 31.4 kW as given by (A.3), which grants the system almost 50% of improvement regarding the total installed capacity of the system, in this case, 15 kW_p.

$$HC_{total}^{max}{}' = 23.4 + 8.0 = 31.4\ kW$$

The next DHC profile with and without energy storage system analysed is regarding 12th April 2015.

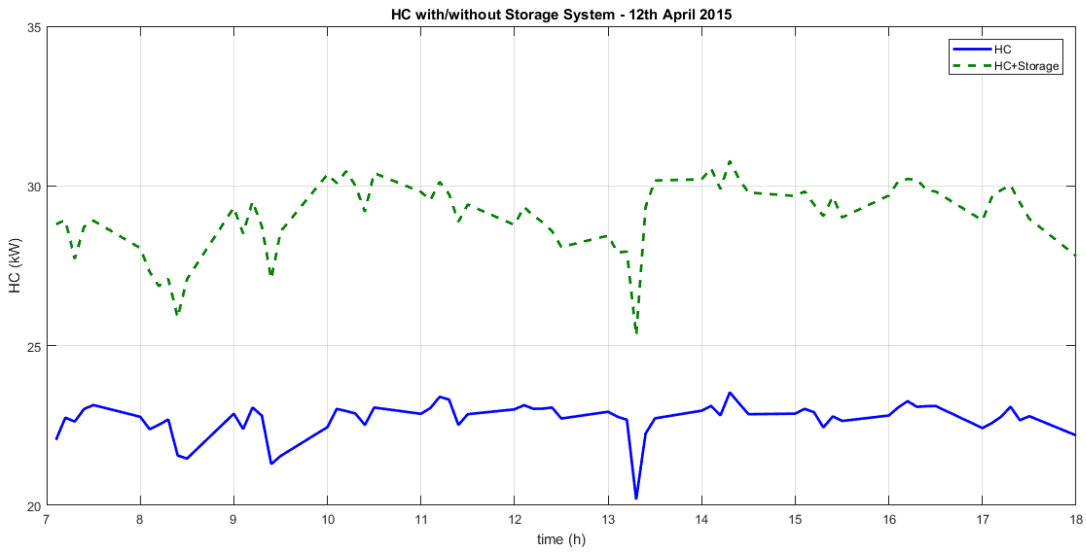

Figure A.17 – The dynamic daily hosting capacity with storage system in relation to April 12th, 2015.

The average mark of daily DHC, in regard to April 12th, 2015, was 20.1 kW, as calculated before using (6.3.1). In this case, the maximum daily hosting capacity is approximately 23.58 kW, whereas the minimum value is 20 kW. The resulting possible maximum and minimum values are a consequence of external and internal conditions affecting the system. It is important to notice that the 12th of April had some particular values of harmonic distortion and voltage rise registered. For example, the minimum value was registered at around 01:30 p.m., when the building wasn't completely empty because of the beginning of the afternoon, with some electronic equipment turned on and the sun was almost at its peak. Even though, according to Figure C.1 in **APPENDIX C**, the 12th of April of 2015 had the lowest solar production. Probably due to these particular conditions, the level of harmonic distortion was registered times higher than in the other days (Figure C.2), which impacts in the voltage profile (Figure C.3) and consequently in the level of the hosting capacity. One possible explanation is the amount of electronic equipment being used at that time and even during the whole day. It is important to highlight that these values don't reflect the global number of hosting capacity. They reflect special conditions, which may or may not impact the final value of the hosting capacity throughout the DHC weekly profile. An improvement is likely to be registered, in relation to the DHC profile, when the energy storage system is considered. The average improvement registered is approximately 28% every 10 minutes, but it can reach a maximum value of 32%. It is important to notice that the improvement average due to ESS was higher than the other days, which can be explained by the voltage and harmonic distortion profiles shown in **APPENDIX C**, as well as the reversed power flow shown in **Error! Reference source not found.**. Thus, for the global value in relation to the day mentioned, the global hosting capacity is 28 kW as given by (A.3), which grants the system almost 50% of improvement regarding the total installed capacity of the system, in this case, 15 $\mathrm{kW_p}$.

$$HC_{total}^{max}{}' = 20 + 8.0 = 28\ kW$$

The next DHC profile with and without energy storage system analysed is regarding 13th April 2015.

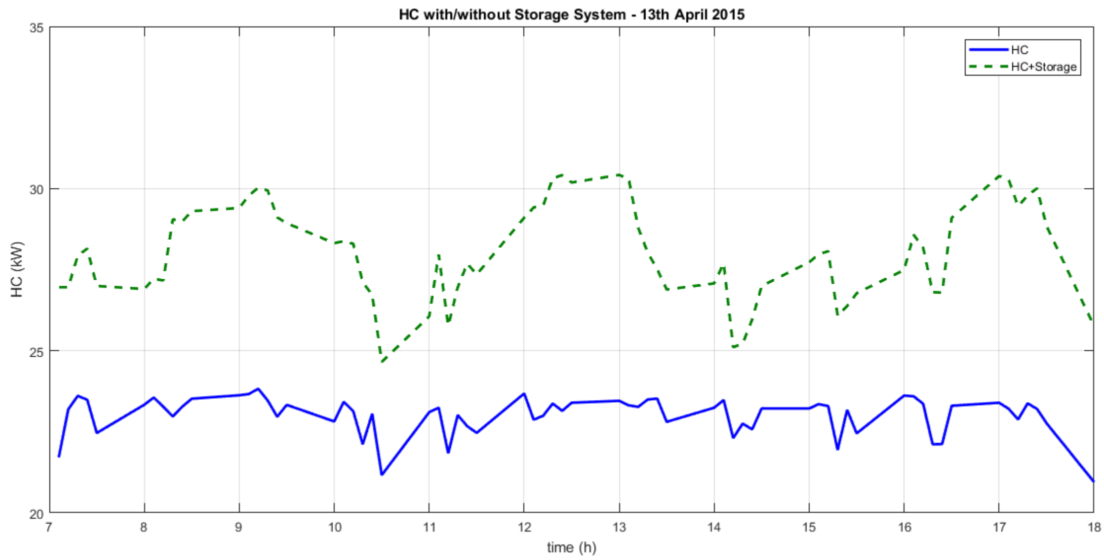

Figure A.18 – The dynamic daily hosting capacity with storage system in relation to April 13th, 2015.

The average mark of daily DHC, in regard to April 13th, 2015, was 23.3 kW, as calculated before using (6.3.1). In this case, the maximum daily hosting capacity is approximately 23.82 kW, whereas the minimum value is 20.94 kW. The resulting possible maximum and minimum values are a consequence of external and internal conditions affecting the system. It is important to notice that those values are similar when compared to the 9th, 10th and 11th of April. For example, the minimum value was registered at around 10:30 a.m., when the building wasn't completely empty because of the beginning of the morning, with some electronic equipment turned on and the sun wasn't at its peak. According to Figure C.1 in **APPENDIX C,** the 13th of April of 2015 had one of the highest solar production. Due to these particular conditions, the level of distortion probably was higher than in usual occasions (Figure C.2), which impacts in the voltage profile (Figure C.3) and consequently in the level of the hosting capacity. It is important to highlight that these values don't reflect the global number of hosting capacity. They reflect special conditions, which may or may not impact the final value of the hosting capacity throughout the DHC weekly profile. An improvement is likely to be registered, in relation to the DHC profile, when the energy storage system is considered. The average improvement registered is approximately 19% every 10 minutes, but it can reach a maximum value of 30%. For the global value in relation to the day mentioned, the global hosting capacity is 31.4 kW as given by (A.3), which grants the system almost 50% of improvement regarding the total installed capacity of the system, in this case, 15 kW_p.

$$HC_{total}^{max}{}' = 23.3 + 8.1 = 31.4\ kW$$

The next DHC profile with and without energy storage system analysed is regarding 14th April 2015.

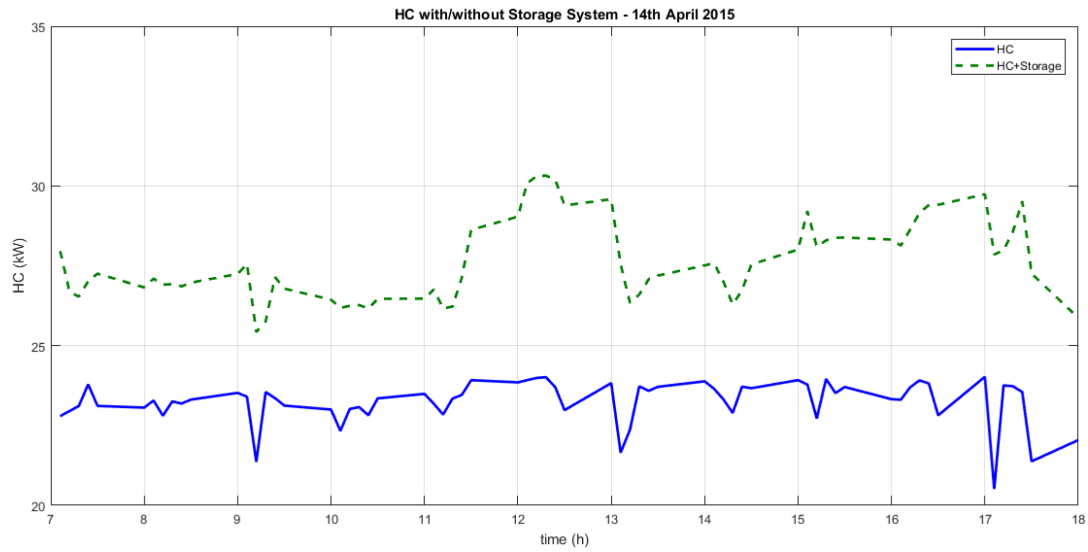

Figure A.19 – The dynamic daily hosting capacity with storage system in relation to April 14th, 2015.

The average mark of daily DHC, in regard to April 14th, 2015, was 23.6 kW, as calculated before using (6.3.1). In this case, the maximum daily hosting capacity is approximately 24 kW, whereas the minimum value is 20.54 kW. The resulting possible maximum and minimum values are a consequence of external and internal conditions affecting the system. It is important to notice that those values are similar when compared to the 9th, 10th, 11th and 13th of April. For example, the minimum value was registered at around 01:30 p.m., when the building wasn't completely empty because of the beginning of the morning, with some electronic equipment turned on and the sun wasn't at its peak. According to Figure C.1 in **APPENDIX C,** the 14th of April of 2015 had one of the highest solar production. Due to these particular conditions, the level of distortion probably was higher than in usual occasions (Figure C.2), which impacts in the voltage profile (Figure C.3) and consequently in the level of the hosting capacity. It is important to highlight that these values don't reflect the global number of hosting capacity. They reflect special conditions, which may or may not impact the final value of the hosting capacity throughout the DHC weekly profile. An improvement is likely to be registered, in relation to the DHC profile, when the energy storage system is considered. The average improvement registered is approximately 18% every 10 minutes, but it can reach a maximum value of 35%. For the global value in relation to the day mentioned, the global hosting capacity is 31.7 kW as given by (A.3), which grants the system almost 50% of improvement regarding the total installed capacity of the system, in this case, 15 $\mathrm{kW_p}$.

$$HC_{total}^{max}\,' = 23.6 + 8.1 = 31.7\ kW$$

Finally, the next DHC profile with and without energy storage system analysed is regarding 15th April 2015.

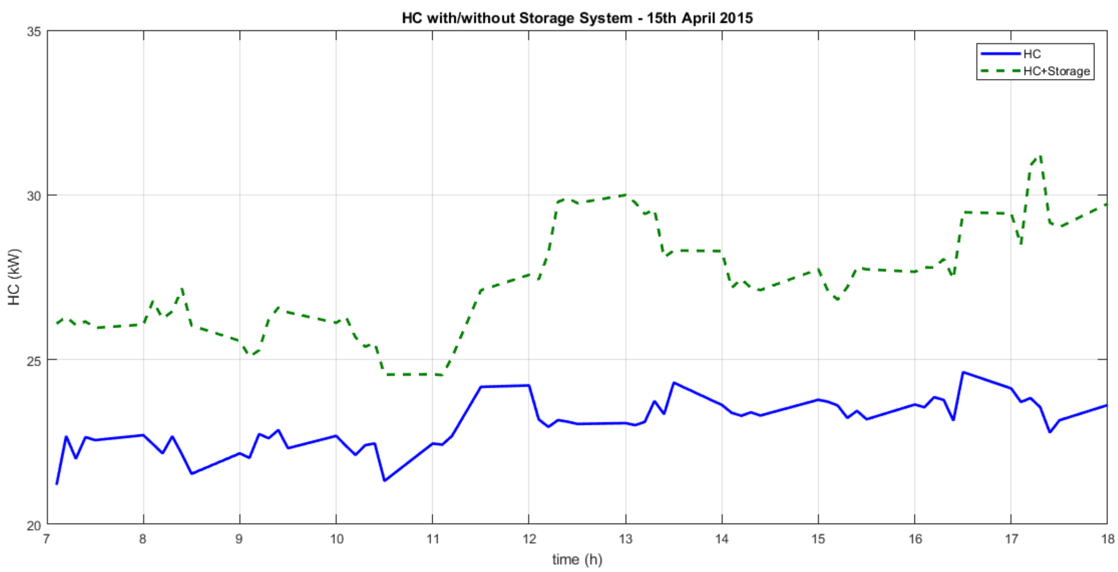

Figure A.20 – The dynamic daily hosting capacity with storage system in relation to April 15th, 2015.

The average mark of daily DHC, in regard to April 15th, 2015, was 23.6 kW, as calculated before using (6.3.1). In this case, the maximum daily hosting capacity is approximately 24.64 kW, whereas the minimum value is 21.19 kW. The resulting possible maximum and minimum values are a consequence of external and internal conditions affecting the system. It is important to notice that those values are similar when compared to the 13th of April. For example, the minimum value was registered at around 10:30 p.m., when the building wasn't completely empty because of the beginning of the morning, with some electronic equipment turned on and the sun wasn't at its peak. According to Figure C.1 in **APPENDIX C,** the 15th of April of 2015 had one of the highest solar production. Due to these particular conditions, the level of distortion probably was higher than in usual occasions (Figure C.2), which impacts in the voltage profile (Figure C.3) and consequently in the level of the hosting capacity. It is important to highlight that these values don't reflect the global number of hosting capacity. They reflect special conditions, which may or may not impact the final value of the hosting capacity throughout the DHC weekly profile. An improvement is likely to be registered, in relation to the DHC profile, when the energy storage system is considered. The average improvement registered is approximately 17% every 10 minutes, but it can reach a maximum value of 32%. For the global value in relation to the day mentioned, the global hosting capacity is 31.7 kW as given by (A.3), which grants the system almost 50% of improvement regarding the total installed capacity of the system, in this case, 15 $\mathrm{kW_p}$.

$$HC_{total}^{max}{}' = 23.6 + 8.0 = 31.6\ kW$$

Figure A.21 shows the increase of DHC during the week. It is noteworthy that using the technique described before, there is a 6 kW average in relation to the global hosting capacity value, which means the system increased its hosting capacity by 40%, thus enabling a huge improvement in the current system. Such an improvement is possible whenever an energy storage system is considered, as described by the proposed hypothesis in this study.

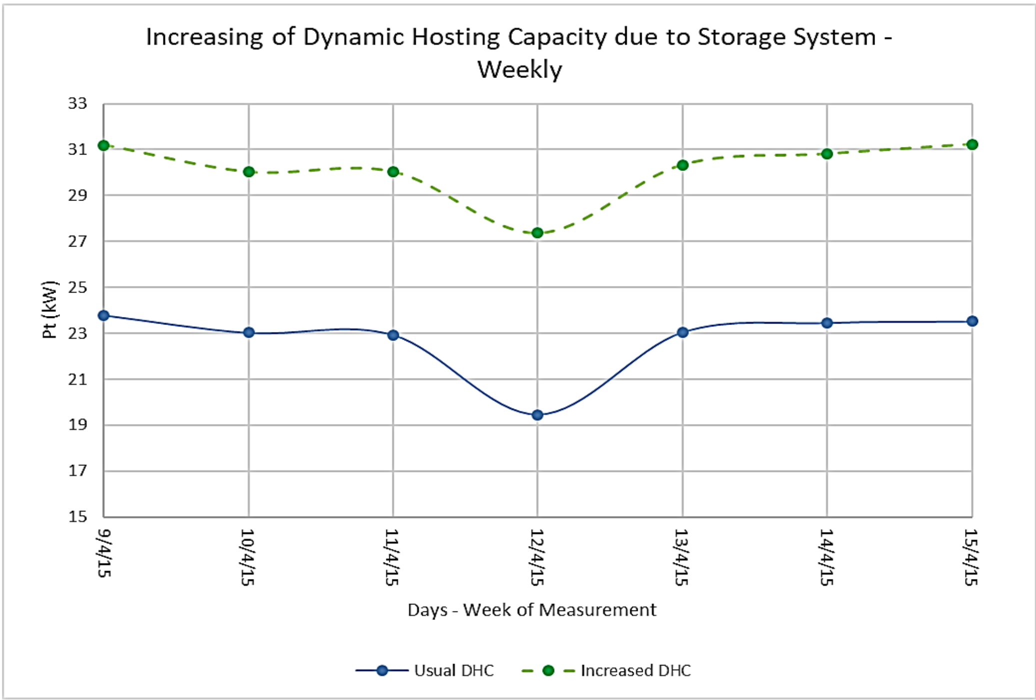

Figure A.21 – The DHC with energy storage system.

These tests showed that the energy storage system would be dimensioned in relation to the $HC_{total}^{max}\,'$ in order to be prepared to receive a higher amount of energy. These results are significant regarding the planning and improving levels of the local hosting capacity as cited before.

In order to power conditioning the system considering an energy storage system, it is possible to decrease the voltage level caused by the reverse power flow as demonstrated in Figure A.3, as well as keep these values around 1.00 p.u regarding the formulation proposed in Chapter 6. This technique clearly is an advantage over the avoiding of reverse power flow and allowing for better conditions in the system. The voltage drop analysis was used to confirm the theory presented in (A.4). These results will be shown in Figure A.22 in relation to the 12th of April 2015. These findings thus need to be interpreted with attention. This formula reproduces the response of the dropped voltage to the system as proposed in Section 6.3.1. As expected, the experiments demonstrate that there will be a voltage regulation preventing the voltage rise. The number of 0.997 p.u average of voltage that confirmed the findings was significant in relation to the system.

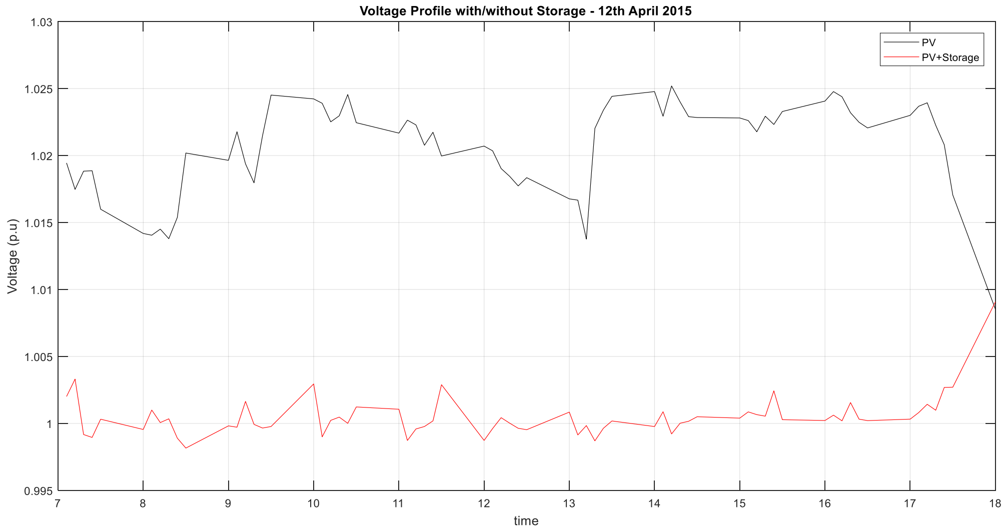

Figure A.22 – Voltage drop due to Energy Storage System in April 12th 2015.

The 12th of April was the day when no power was required from the utility, which means that all generated power was enough to feed the local load and 100% of reminiscent power was injected into the feeder. The performance of the voltage profile had almost no significant variation. There are several possible explanations for this result. This apparent lack of association can be attributed to the load variation during the whole day, considering the 12th of April a day with special external and internal conditions, as mentioned before. Nonetheless, the result of the voltage profile is around 1.00 p.u, which confirms the proposed theory.

This work has led to the conclusion that the association between the energy storage system and the voltage regulation was tested and confirmed along the other days. The load variation occurred without significant voltage variation. Due to this fact, the voltage kept itself regulated at 1.00 p.u. These results are shown in Figure A.23.

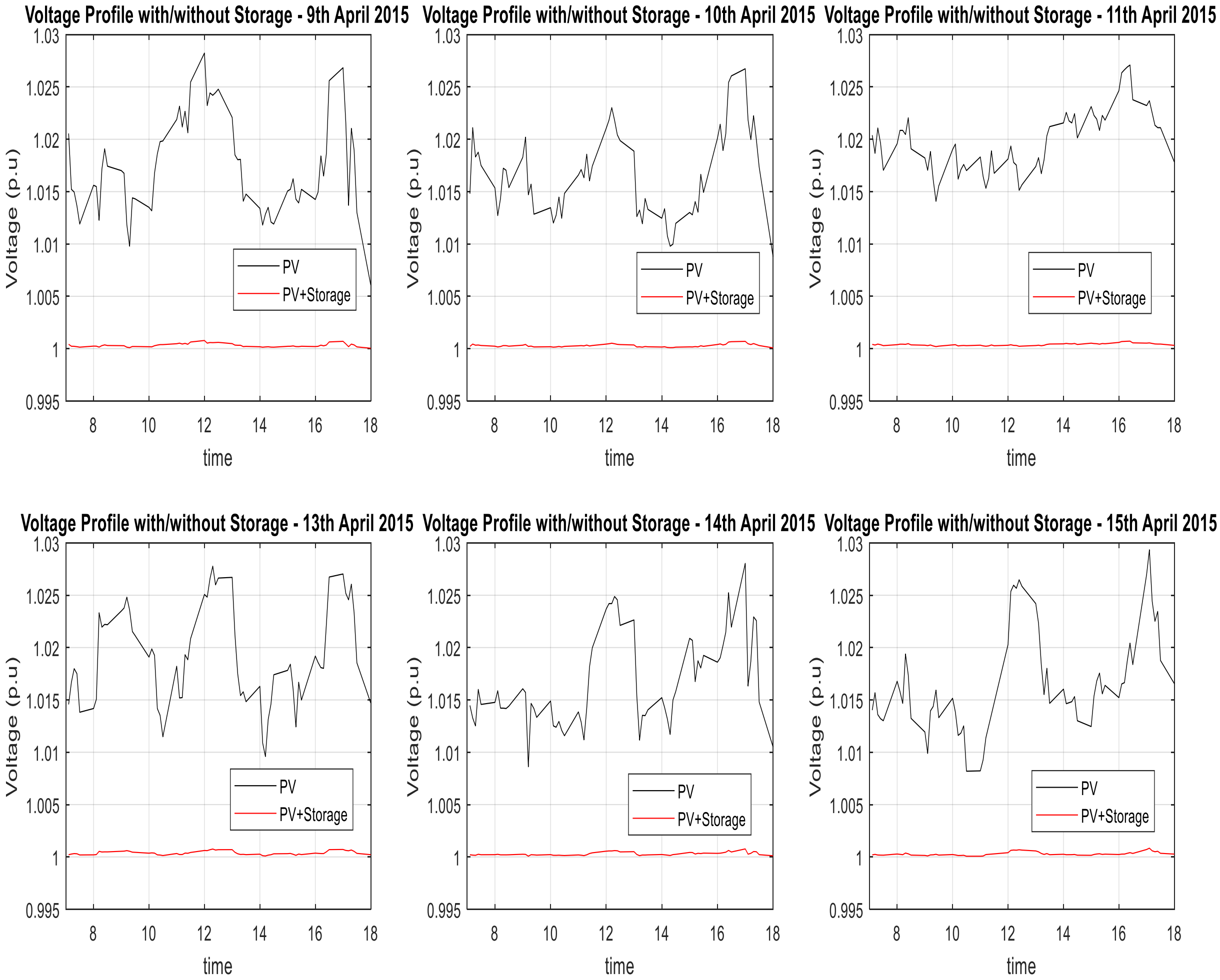

Figure A.23 – Voltage regulation due to Energy Storage System to the other days.

The evidence from these results suggests that the energy storage system can work as a voltage regulator whether a better integrated DER planning is applied to any electrical system. However, the results of this study support the idea that the energy storage system will increase the hosting capacity value, which can be improved resorting to a wide range of possibilities. The energy storage-hosting capacity methodology provides a powerful tool to improve and correct power quality issues.

iii) Conclusion: Voltage rise problems mitigated by incorporating a storage system at the PCC regarding the reverse power flow.

The outline considering the energy storage system showed that the energy storage system would be dimensioned in relation to the dynamic hosting capacity profile, in order to be prepared to receive a higher amount of energy. These results are significant at the planning and improving levels in regard to the local hosting capacity. Considering an energy storage system, it is possible to decrease the voltage level caused by reversed power flow. This hypothesis has led to the conclusion that the association between the energy storage system and the voltage regulation was experienced and confirmed. In general, these results would seem to suggest that an energy storage system incorporation was successful increasing the energy storage without significant voltage change.

APPENDIX. A – The Harmonic Power Flow Algorithm Considering Single-Phase Generation

The software application used to analyse the data was develop in Matlab®. The data were obtained as describe in section 7.3.

CODE IN MATLAB®:

```
clc; clear; close all;

% random number generation
% Set random generation to MATLAB default (simulations will always produce
% the same results every time this script is run)
rng('default');

% bases
Vb = 400  ; % V
Sb = 100e3; % VA
Zb = Vb^2/Sb;
Ib = Sb/(sqrt(3)*Vb);

% topology
t = [
    1 2;
    2 3;
    3 4;
    4 5;
    5 6;
    6 7;
    ];
num_nodes = size(t,1)+1;

% impedance per km
zl_km = [
    0.641 + 1i*0.15;
    0.641 + 1i*0.15;
    0.641 + 1i*0.15;
    0.641 + 1i*0.15;
    0.641 + 1i*0.15;
    0.641 + 1i*0.15;
    ];

% length
lengths = [
    50;
```

```
    10;
    10;
    10;
    10;
    10;
    ];

zl = zl_km*1e-3 .* lengths / Zb; % pu



orders_harmonics = 1:2:15;
%orders_harmonics = 1:2:15;

num_harmonics    = length(orders_harmonics);

%zl_harmonics = repmat(real(zl),[1 num_harmonics]) + 1i*( (1:num_harmonics)
.* repmat(imag(zl),[1 num_harmonics]))
zl_harmonics = repmat(real(zl),[1 num_harmonics]) + 1i*( repmat((1:num_harmonics),[size(t,1)
1]) .* repmat(imag(zl),[1 num_harmonics]));

vref                     = zeros(1, num_harmonics);
vref(orders_harmonics == 1) = 1.0;
vref(orders_harmonics == 3) = rand*(0.03-0.01)+0.01;
vref(orders_harmonics == 5) = rand*(0.05-0.03)+0.03;
vref(orders_harmonics == 7) = rand*(0.05-0.03)+0.03;
vref(orders_harmonics >  7) = rand(sum(orders_harmonics > 7),1)*(0.01-0.005)+0.005;

els     = ones(1, num_harmonics);
els(1)  = 0;



node_loads       = zeros(3, num_nodes, num_harmonics);
consumer_phases = randi(3, 1, num_nodes-1);

base_load = (2e3)*exp(j*pi*-36.87/180)/Sb;

%node_loads(consumer_phases, 2:num_nodes) = base_load*3
node_harmonic_voltages = zeros(3, num_nodes, num_harmonics);
for i=2:num_nodes
    node_loads(consumer_phases(i-1), i, 1) = -base_load*3;


    node_harmonic_voltages(consumer_phases(i-1), i, orders_harmonics == 3) = rand*(0.03-
0.01)+0.01;
    node_harmonic_voltages(consumer_phases(i-1), i, orders_harmonics == 5) = rand*(0.05-
0.03)+0.03;
```

```
    node_harmonic_voltages(consumer_phases(i-1), i, orders_harmonics == 7) = rand*(0.05-
0.03)+0.03;
    node_harmonic_voltages(consumer_phases(i-1), i, orders_harmonics >  7) =
rand(sum(orders_harmonics > 7),1)*(0.01-0.005)+0.005;
end
%node_loads

node_harmonic_currents = zeros(3, num_nodes, num_harmonics);
node_pflow_voltages    = zeros(3, num_nodes, num_harmonics);

for i=1:num_harmonics
    fprintf('\n\n\n**************************************************\n*** Power flow para a
harmonica #%d (%d Hz) ***\n**************************************************\n',
orders_harmonics(i), orders_harmonics(i)*50);
    [node_pflow_voltages(:,:,i), mvn, ~, ~] = pf3ph(t, zl_harmonics(:,i), node_loads(:,:,i), vref(i),
els(i), 50);
    fprintf('Tensoes fase-neutro\n\n');
    Vh= abs(node_pflow_voltages(:,:,i)) * Vb/sqrt(3)



    %fprintf('Tensoes neutro\n\n');
    %abs(mvn) * Vb/sqrt(3)

    if( orders_harmonics(i) == 1 )
        iphase = conj(node_loads(:,:,i) ./ node_pflow_voltages(:,:,1));

        node_harmonic_currents(:, :, orders_harmonics == 3) = iphase*0.4 /100;
        node_harmonic_currents(:, :, orders_harmonics == 5) = iphase*2.4 /100;
        node_harmonic_currents(:, :, orders_harmonics == 7) = iphase*1.4 /100;
        node_harmonic_currents(:, :, orders_harmonics >  7) = repmat(iphase*0.03/100, [1 1
sum(orders_harmonics >  7)]);
        %node_harmonic_currents(:, :, orders_harmonics >  7) = repmat(iphase*0.03/100, [1 1 4]);

        node_loads(:,:,2:end) = node_harmonic_voltages(:,:,2:end) .*
conj(node_harmonic_voltages(:,:,2:end));
    end
end



%node_pflow_voltages(:,:,i)



%for n=2:1:8
Vef_1a_harm = abs(node_pflow_voltages(:,:,1))
```

```
Vef_total =
sqrt(sum(abs(node_pflow_voltages(:,:,2)).^2+abs(node_pflow_voltages(:,:,3)).^2+abs(node_pflo
w_voltages(:,:,4)).^2+abs(node_pflow_voltages(:,:,5)).^2+abs(node_pflow_voltages(:,:,6)).^2+ab
s(node_pflow_voltages(:,:,7)).^2+abs(node_pflow_voltages(:,:,8)).^2,3))

%Vef_total = sqrt(sum(abs(node_pflow_voltages(:,:,n)).^2,3))

THD= ((Vef_total ./ Vef_1a_harm))*100

%end



for i=1:num_harmonics
 filename= 'tensoes';
 xlswrite(filename, abs(node_pflow_voltages(:,:,1)) * Vb/sqrt(3),'Sheet1');
 xlswrite(filename, abs(node_pflow_voltages(:,:,2)) * Vb/sqrt(3),'Sheet2' );
 xlswrite(filename, abs(node_pflow_voltages(:,:,3)) * Vb/sqrt(3),'Sheet3' );
 xlswrite(filename, abs(node_pflow_voltages(:,:,4)) * Vb/sqrt(3),'Sheet4' );
 xlswrite(filename, abs(node_pflow_voltages(:,:,5)) * Vb/sqrt(3),'Sheet5' );
 xlswrite(filename, abs(node_pflow_voltages(:,:,6)) * Vb/sqrt(3),'Sheet6' );
 xlswrite(filename, abs(node_pflow_voltages(:,:,7)) * Vb/sqrt(3),'Sheet7' );
 xlswrite(filename, abs(node_pflow_voltages(:,:,8)) * Vb/sqrt(3),'Sheet8' );

end
%fprintf('\n\n\nPotencias em cada no/harmonica\n');
%node_loads * Sb/3
```

APPENDIX. B – Simulation of Sensitivity Analysis of the Local Hosting Capacity (Table and Figures)

In this appendix, the results got from the HPF, as well as the hosting capacity calculation based on the HPF are shown. The voltage value for all six busbars regarding from fundamental order to 15th harmonic order is provided via simulation.

Table B.1 – Voltage values phases A, B and C – TU/e system, six bars at PQ Lab

	BAR #1			BAR #2			BAR #3		
Order	**VA**	**VB**	**VC**	**VA**	**VB**	**VC**	**VA**	**VB**	**VC**
1	230.2881	231.4225	232.2002	230.1385	231.4461	232.5094	230.0448	231.4499	232.7461
3	6.078623	6.070222	6.057965	6.079825	6.070497	6.054744	6.080579	6.070725	6.052511
5	11.12616	11.09994	11.05798	11.12924	11.10148	11.04504	11.13135	11.10311	11.03385
7	7.535749	7.507257	7.456277	7.540281	7.507772	7.443311	7.542144	7.508893	7.434438
9	2.210759	2.208567	2.207112	2.21106	2.208498	2.206589	2.21123	2.208474	2.206238
11	1.885457	1.88406	1.883256	1.885632	1.884065	1.882784	1.885696	1.884116	1.882443
13	1.268553	1.265958	1.266045	1.268865	1.265832	1.265646	1.269041	1.265772	1.26539
15	1.477292	1.474853	1.475087	1.477593	1.474744	1.47466	1.477746	1.474715	1.474373
	BAR #4			**BAR#5**			**BAR#6**		
Order	**VA**	**VB**	**VC**	**VA**	**VB**	**VC**	**VA**	**VB**	**VC**
1	230.0069	231.4337	232.9103	229.8955	231.474	233.0553	229.8399	231.4941	233.1278
3	6.081066	6.070924	6.070924	6.081817	6.071004	6.04921	6.082307	6.071056	6.048129
5	11.13156	11.10493	11.02608	11.13575	11.10454	11.01855	11.13784	11.10434	11.0148
7	7.542656	7.510318	7.427635	7.546735	7.509416	7.421397	7.548263	7.509079	7.419062
9	2.211298	2.208485	2.206022	2.211446	2.208435	2.205827	2.211544	2.208402	2.205697
11	1.885717	1.884185	1.882151	1.885914	1.884103	1.881922	1.886022	1.884057	1.881796
13	1.269144	1.265747	1.265209	1.269297	1.265673	1.26505	1.269357	1.265645	1.264988
15	1.477844	1.474714	1.474137	1.478039	1.474611	1.473955	1.4781	1.474578	1.473897

B.1) Busbar 1 – Hosting Capacity Phases A, B and C (PF= 1.0) – [axis X (HC in kW) – axis Y (Overvoltage margin in p.u)]

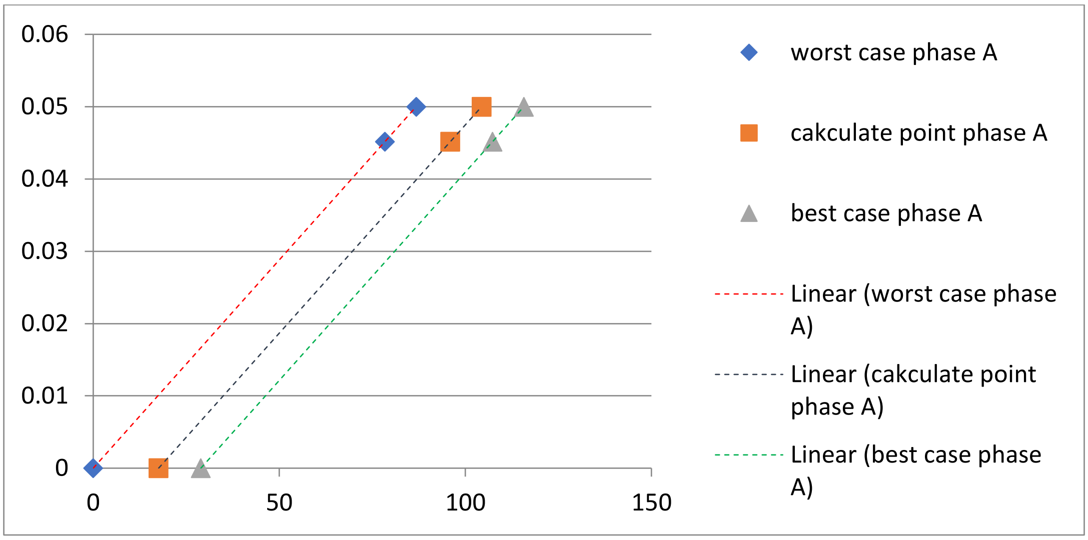

Figure B.1 – Hosting capacity profile #1 PHASE A.

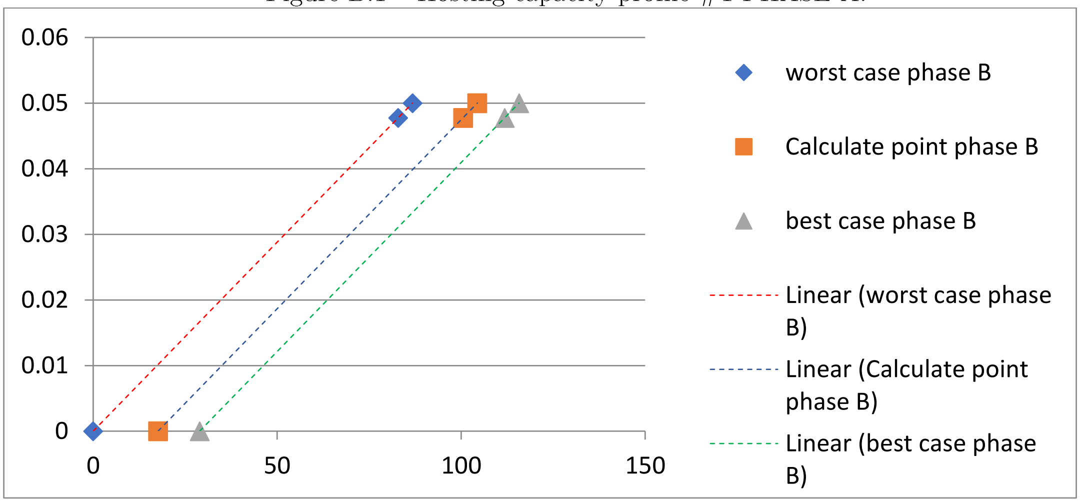

Figure B.2 – Hosting capacity profile #1 PHASE B.

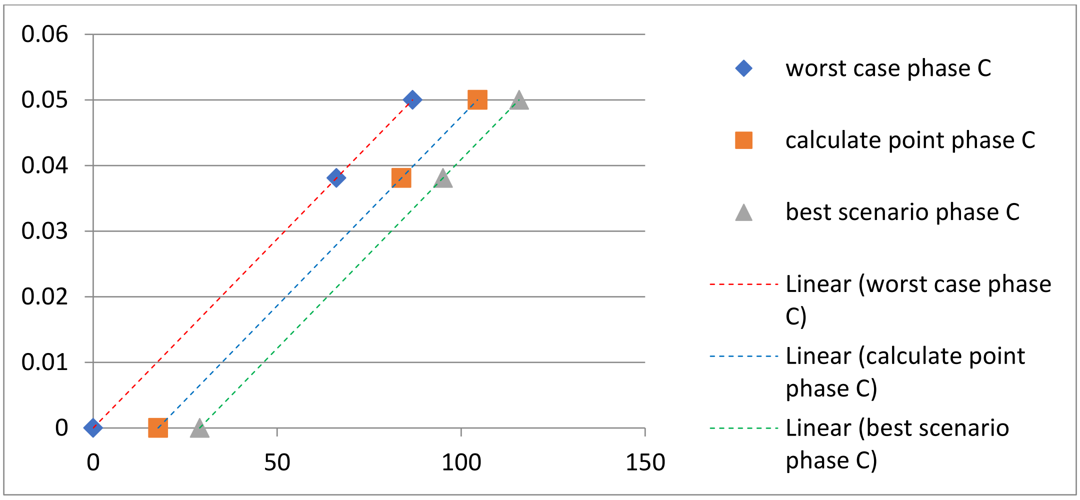

Figure B.3 – Hosting capacity profile #1 PHASE C.

B.2) Busbar 2 – Hosting Capacity Phases A, B and C (PF= 1.0) – [axis X (HC in kW) – axis Y (Overvoltage margin in p.u)]

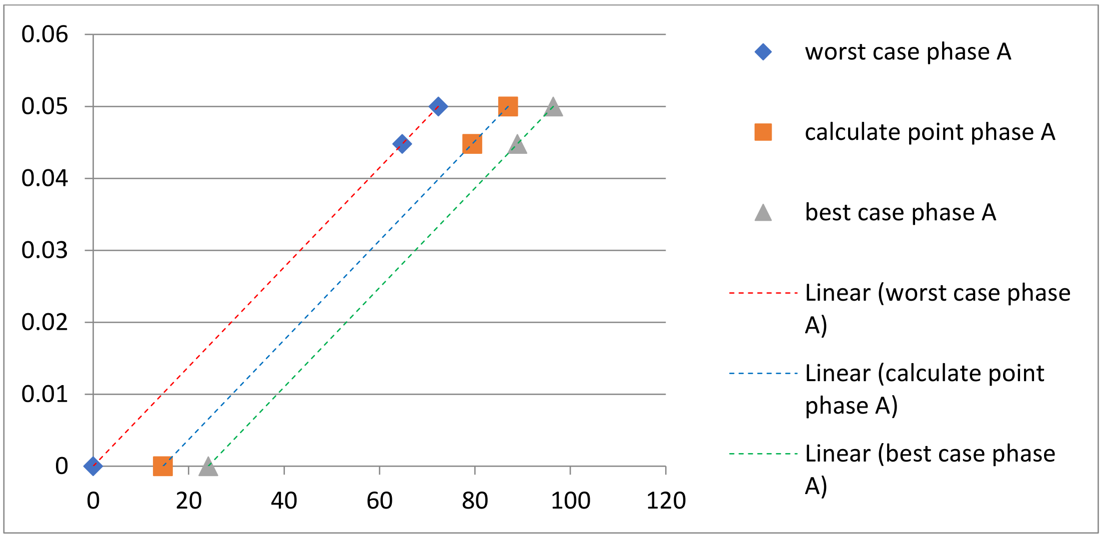

Figure B.4 – Hosting capacity profile #2 PHASE A.

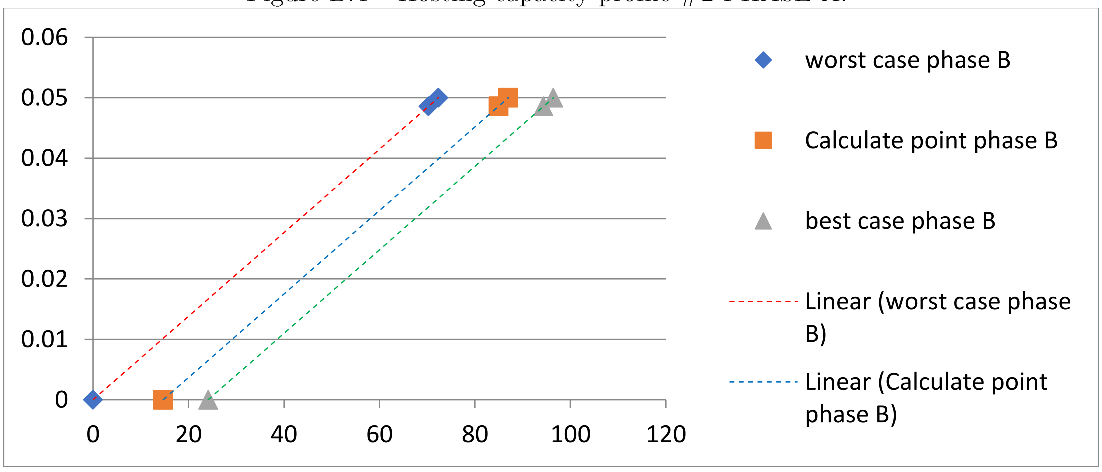

Figure B.5 – Hosting capacity profile #2 PHASE B.

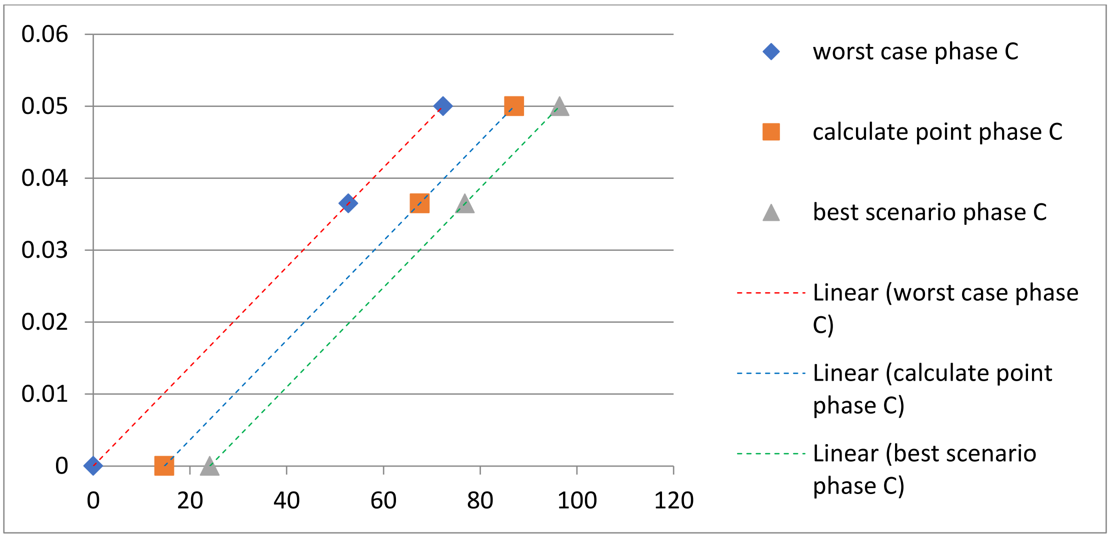

Figure B.6 – Hosting capacity profile #2 PHASE B.

B.3) Busbar 3 – Hosting Capacity Phases A, B and C (PF= 1.0) [axis X (HC in kW) – axis Y (Overvoltage margin in p.u)]

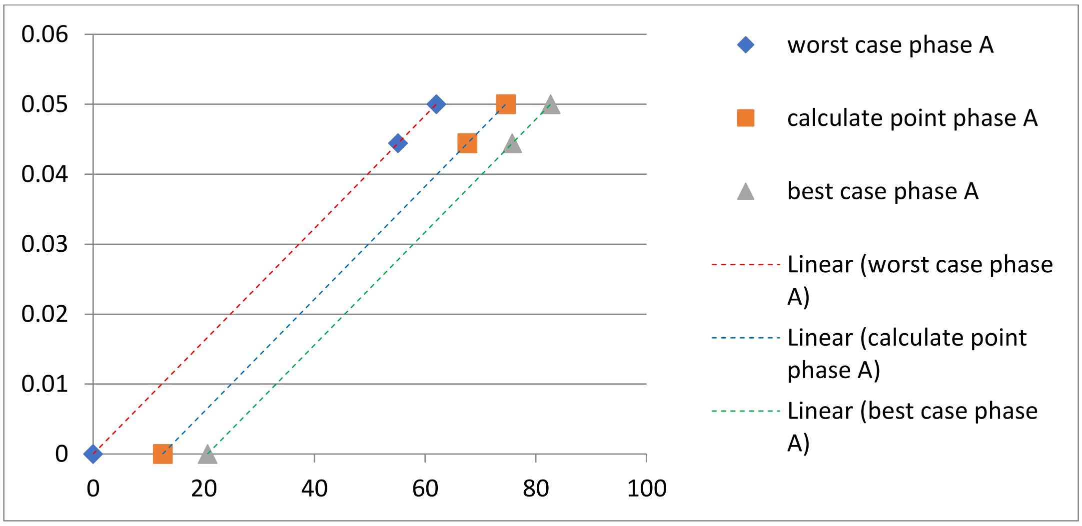

Figure B.7 – Hosting capacity profile #3 PHASE A.

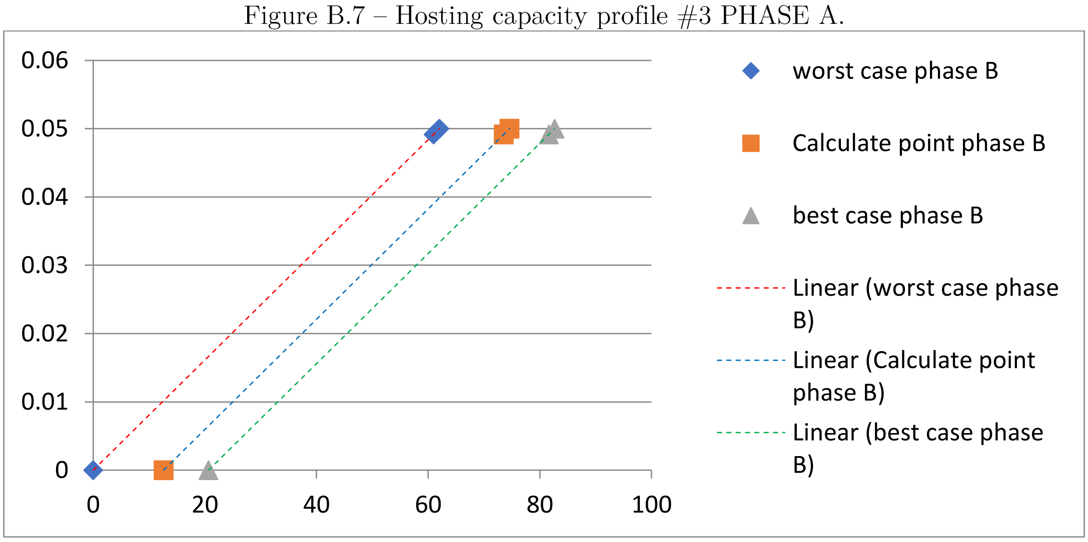

Figure B.8 – Hosting capacity profile #3 PHASE B.

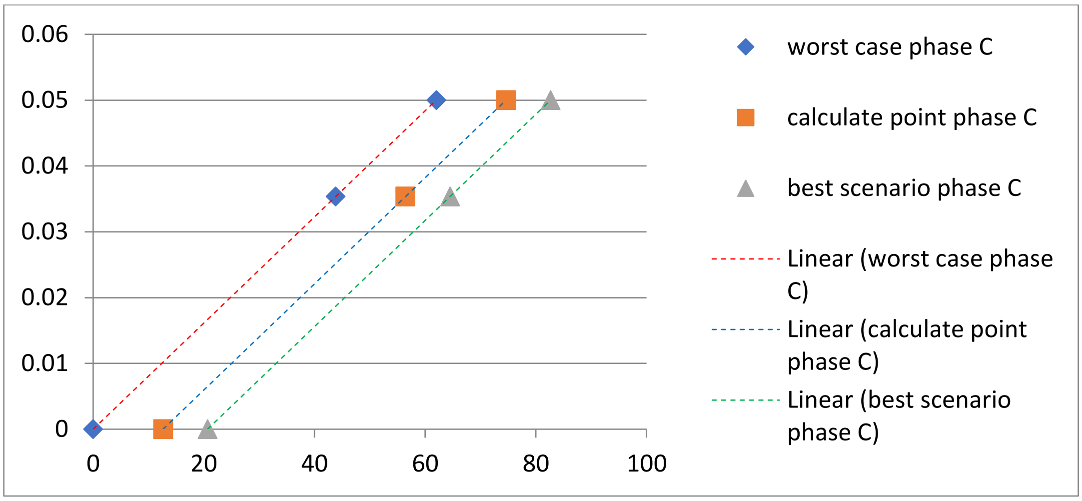

Figure B.9 – Hosting capacity profile #3 PHASE C.

B.4) Busbar 4 – Hosting Capacity Phases A, B and C (PF= 1.0) – [axis X (HC in kW) – axis Y (Overvoltage margin in p.u)]

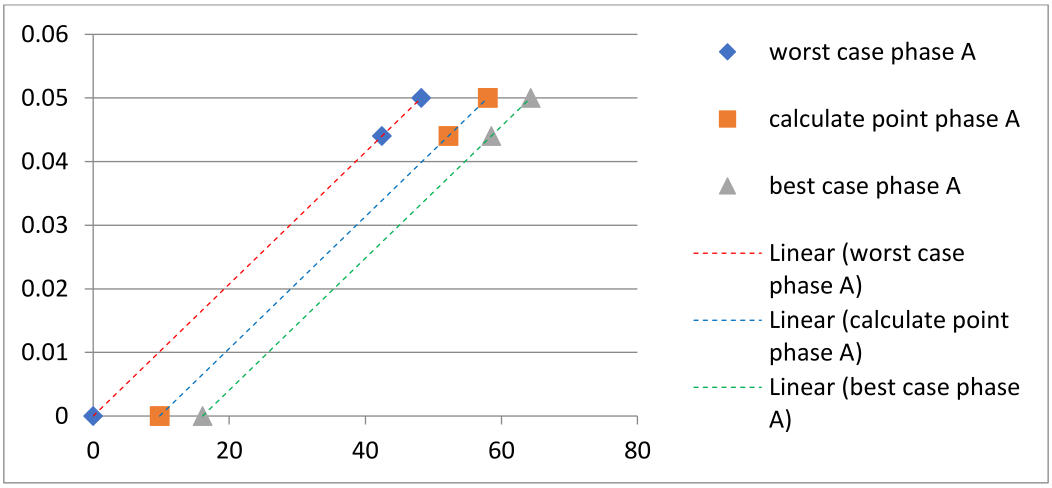

Figure B.10 – Hosting capacity profile #4 PHASE A.

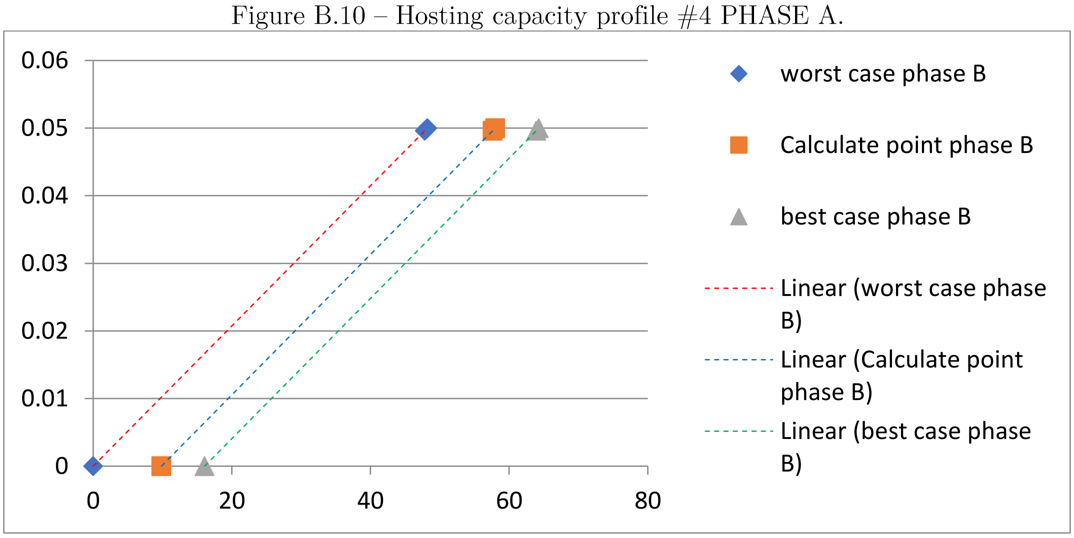

Figure B.11 – Hosting capacity profile #4 PHASE B.

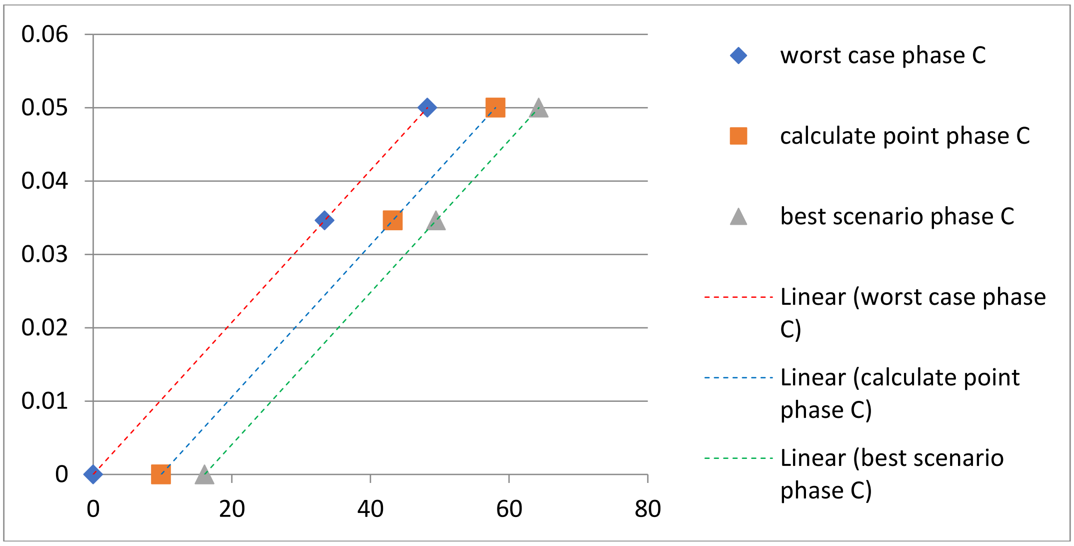

Figure B.12 – Hosting capacity profile #4 PHASE C.

B.5) Busbar 5 – Hosting Capacity Phases A, B and C (PF= 1.0) – [axis X (HC in kW) – axis Y (Overvoltage margin in p.u)]

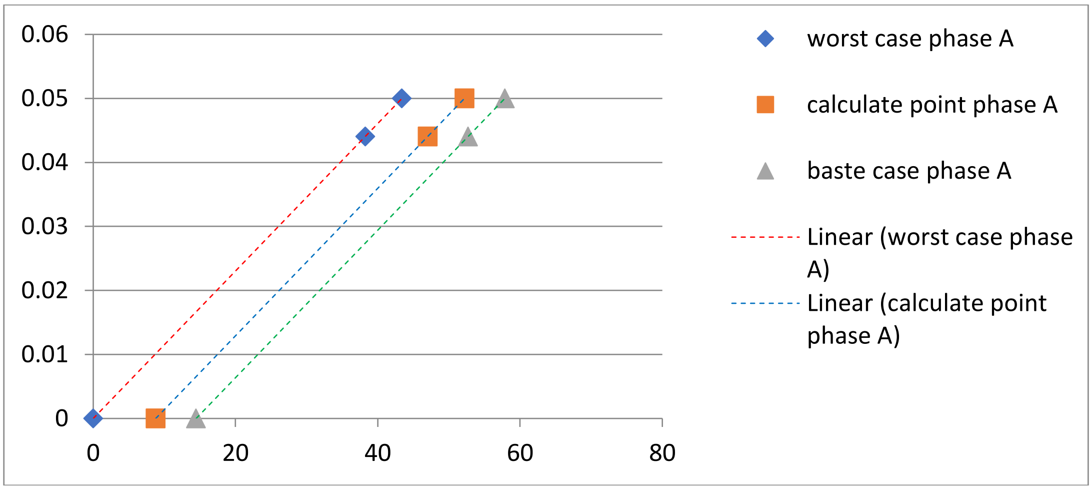

Figure B.13 – Hosting capacity profile #5 PHASE A.

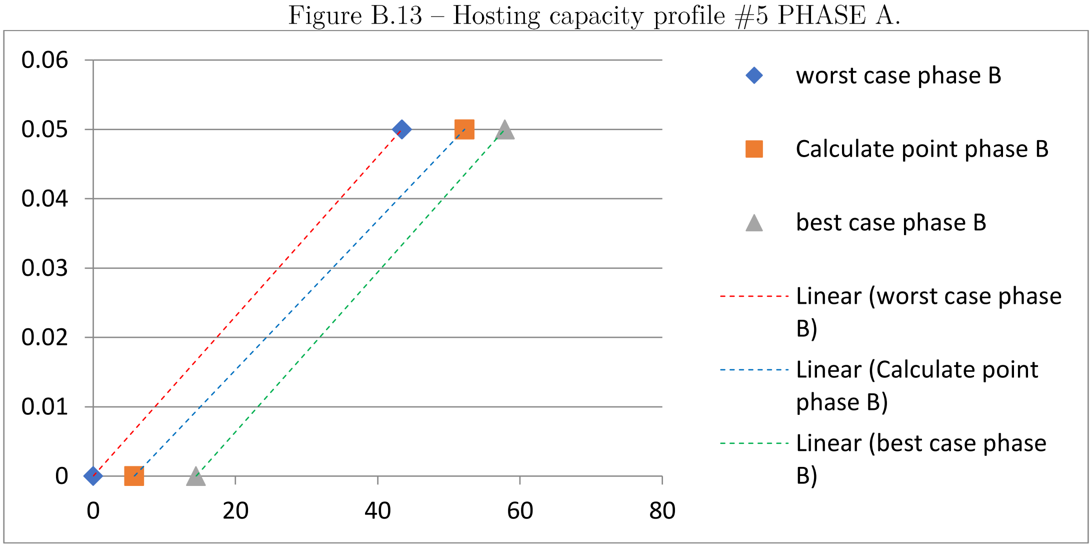

Figure B.14 – Hosting capacity profile #5 PHASE B.

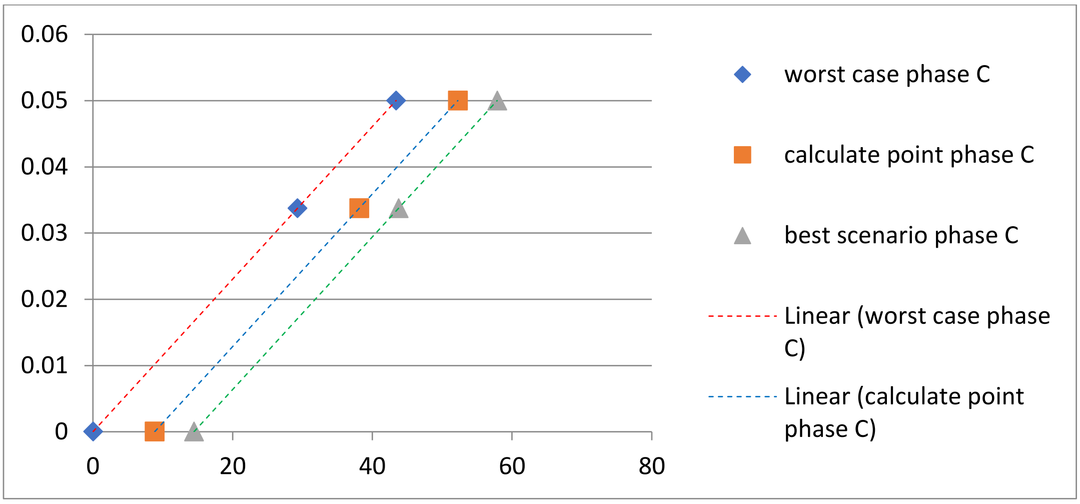

Figure B.15 – Hosting capacity profile #5 PHASE C.

B.6) Busbar 6 – Hosting Capacity Phases A, B and C (PF= 1.0) – [axis X (HC in kW) – axis Y (Overvoltage margin in p.u)]

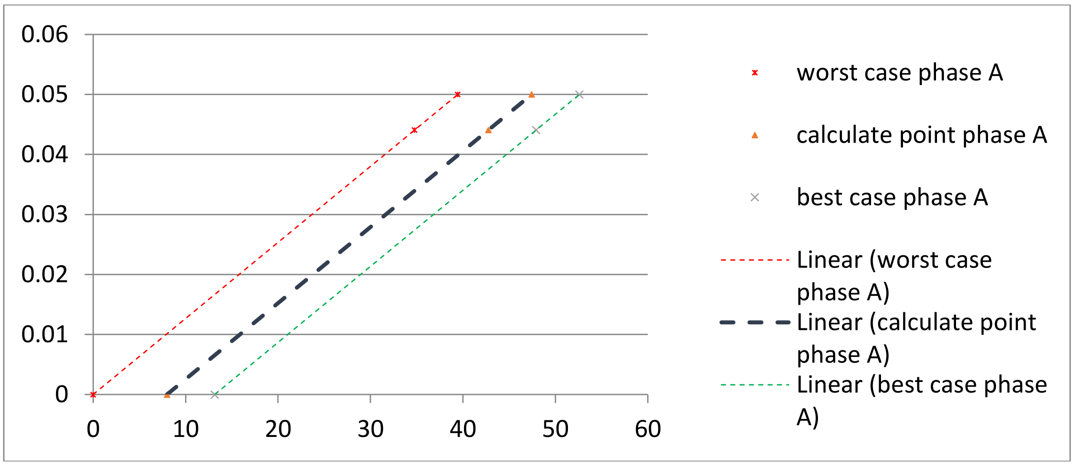

Figure B.16 – Hosting capacity profile #6 PHASE A.

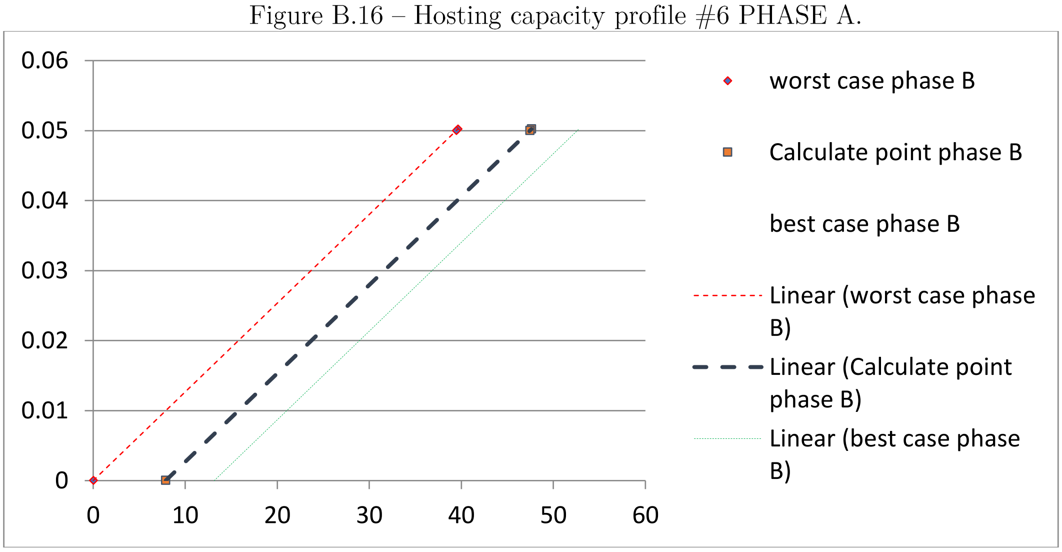

Figure B.17 – Hosting capacity profile #6 PHASE B.

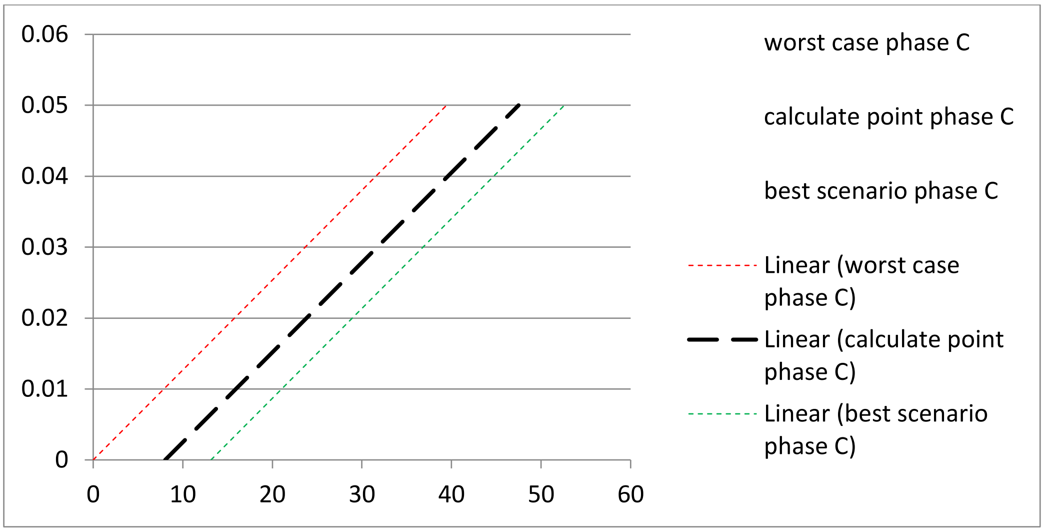

Figure B.18 – Hosting capacity profile #6 PHASE C.

APPENDIX. C – Power Quality Measurements at QMAP

The main measurements were recorded following the PRODIST (Module 8) measurement protocol, which suggests that the set of generating measures regarding the individual indicators should include the recording of 1008 valid analysis obtained in a consecutive integration interval of 10 minutes for 1068 hours (one week of measurement). The values recorded have their maximum, average and minimum values for each measurement interval. It is worth mentioning that the following graphs have been obtained from (OLIVEIRA, 2015) master's dissertation.

The quantities measured through the DRANETZ QEE meters were:

- Active power;
- Reactive and apparent power;
- Power factor;
- Frequency;
- RMS voltage;
- RMS current;
- Total voltage harmonic distortion (THD-V);
- Individual Voltage Harmonic Distortion (IHD-V);
- Total current harmonic distortion (THD-I);
- Individual Voltage Harmonic Distortion (IHD-I).

During the measurement period, several situations were observed, among them, periods of high generation or low energy generation, in addition to the variation in consumption at QMAP building in the observed period of two weeks of measurement between the 8^{th} of April 2015 and the 22^{nd} of April 2015 for reasons of reliability of the measurements. For this reason, this study chose the perspective of observation of the phenomena for seven days of measurement following the protocol proposed in PRODIST and the analysis for the day that had the highest generation within the analysed period.

During the measurement period, no disturbance was registered in the operation of the equipment, only some variations in the electrical network of UNIFEI due to unknown causes.

Group one: Weekly Measurement

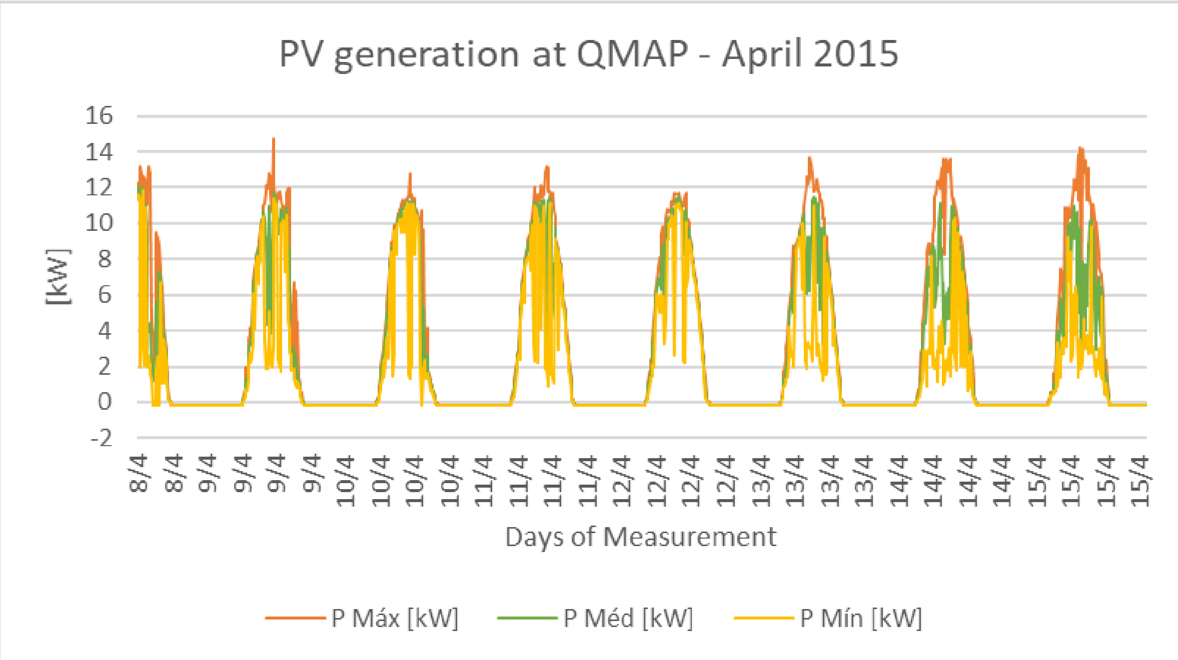

Figure C.1 – PV generation for one week of measurement.

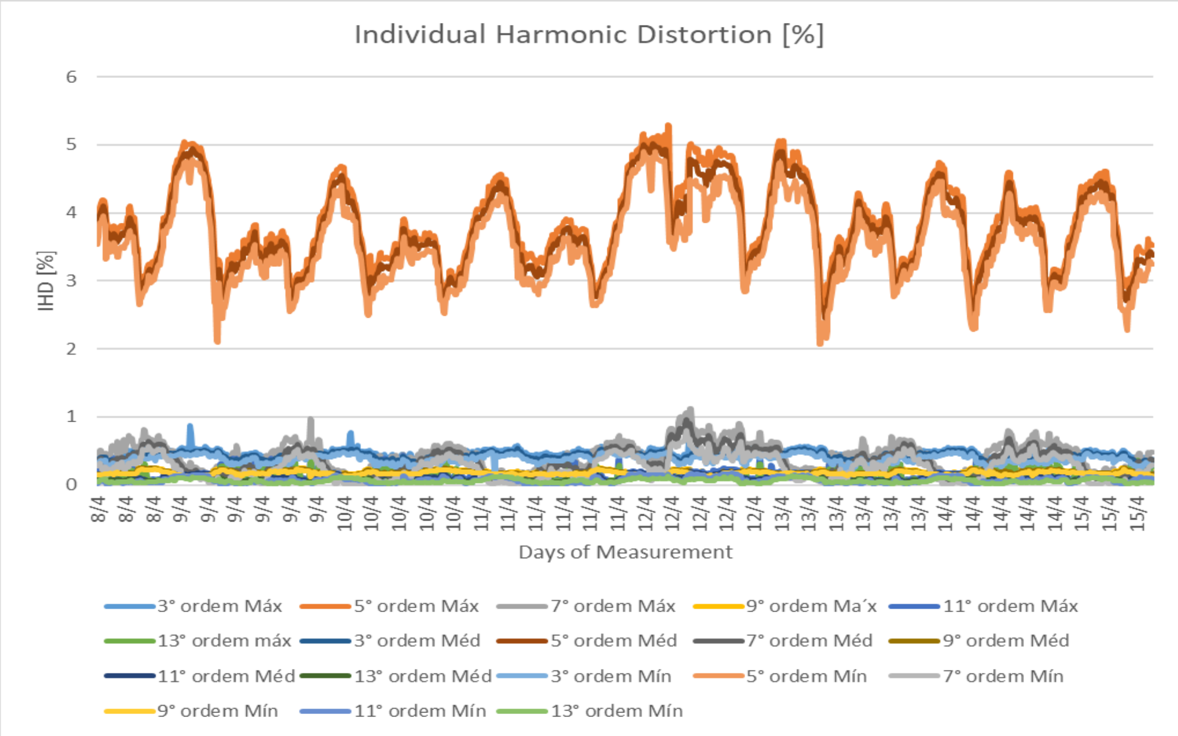

Figure C.2 – THD and IHD for one week of measurement.

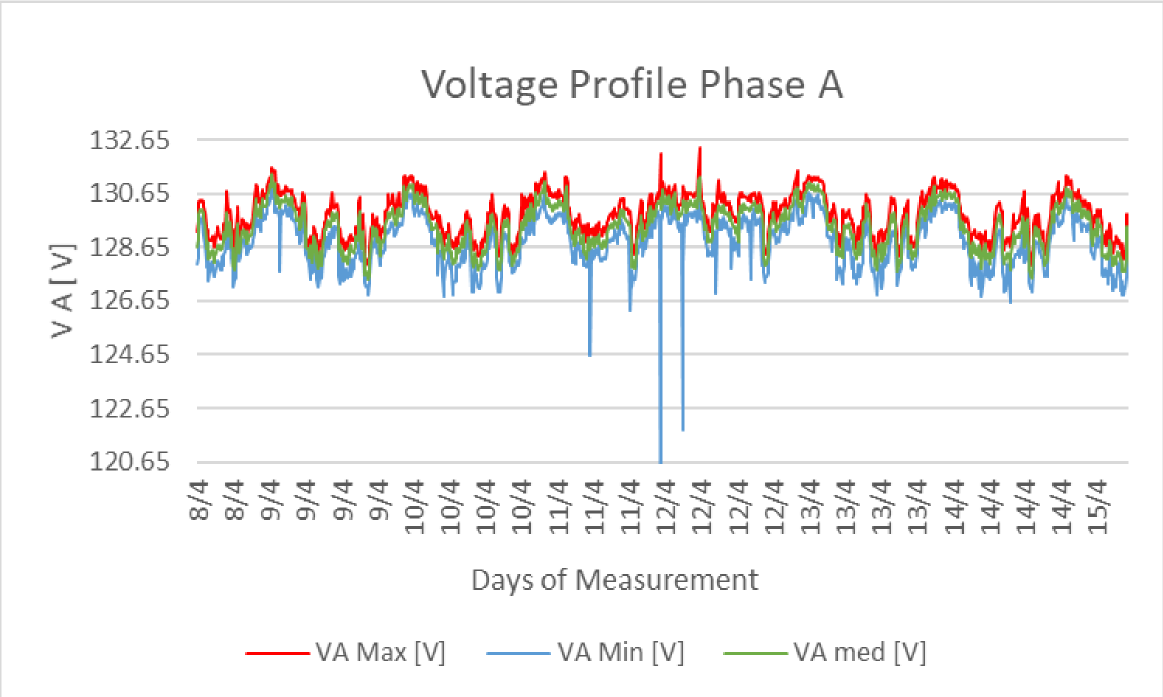

Figure C.3 – Voltage profile of phase A for one week of measurement.

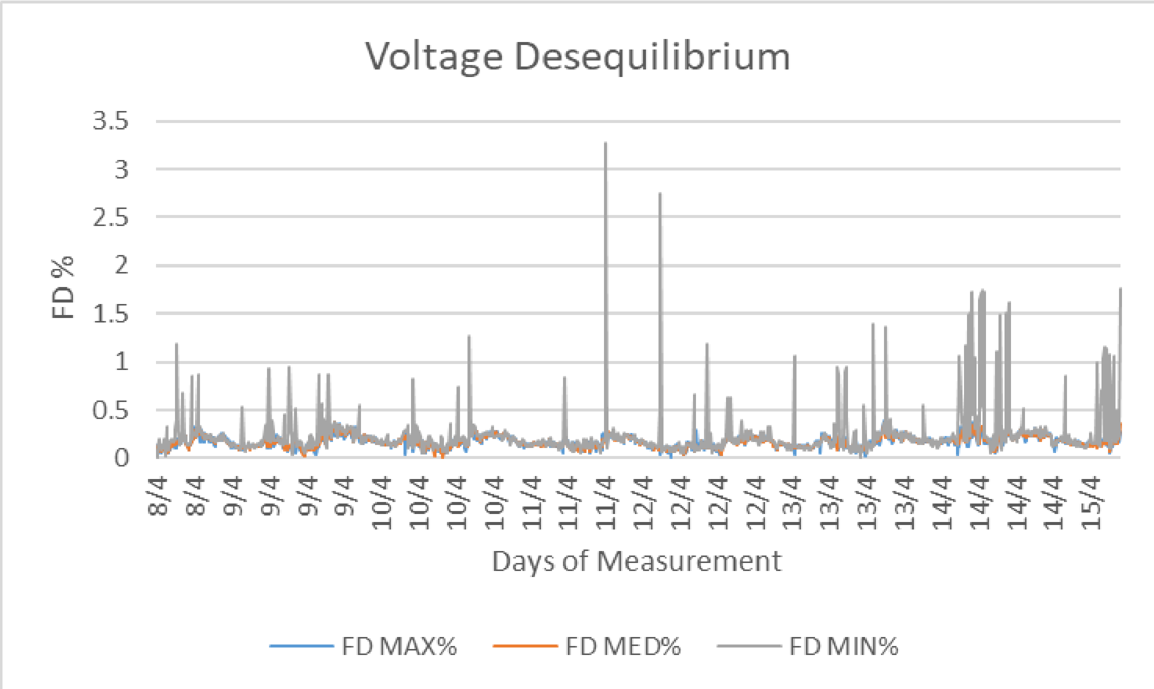

Figure C.4 – Disequilibrium profile of the system for one week of measurement.

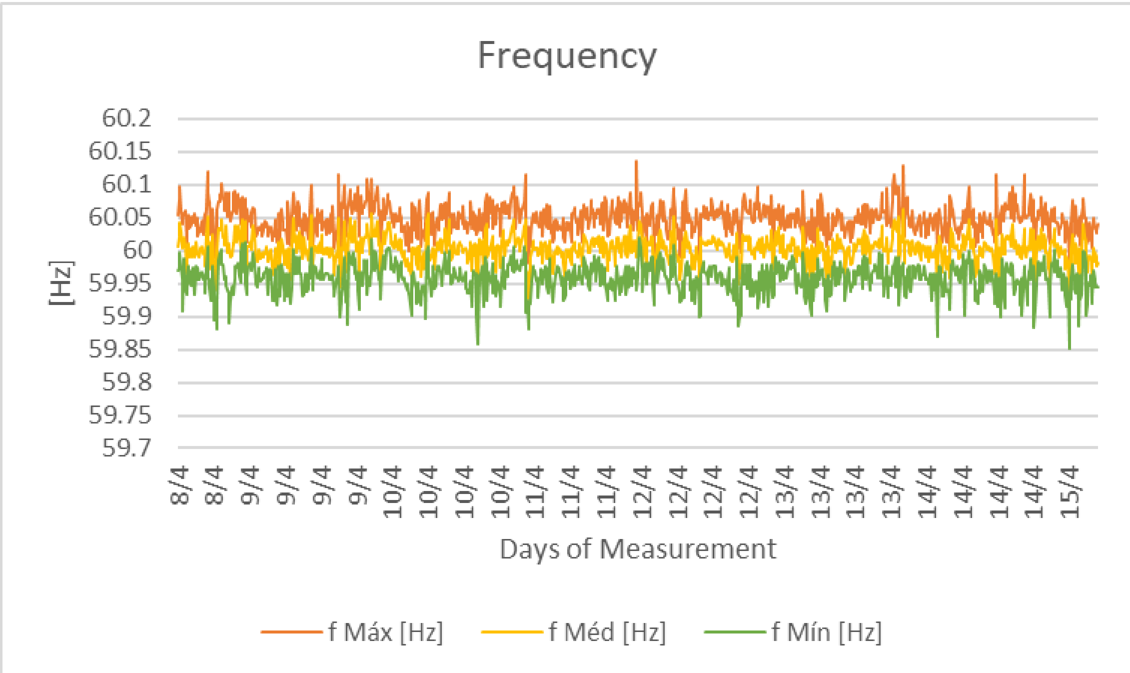

Figure C.5 – Voltage profile of phase A for one week of measurement.

Group Two: Daily Measurement – 9th of April 2015

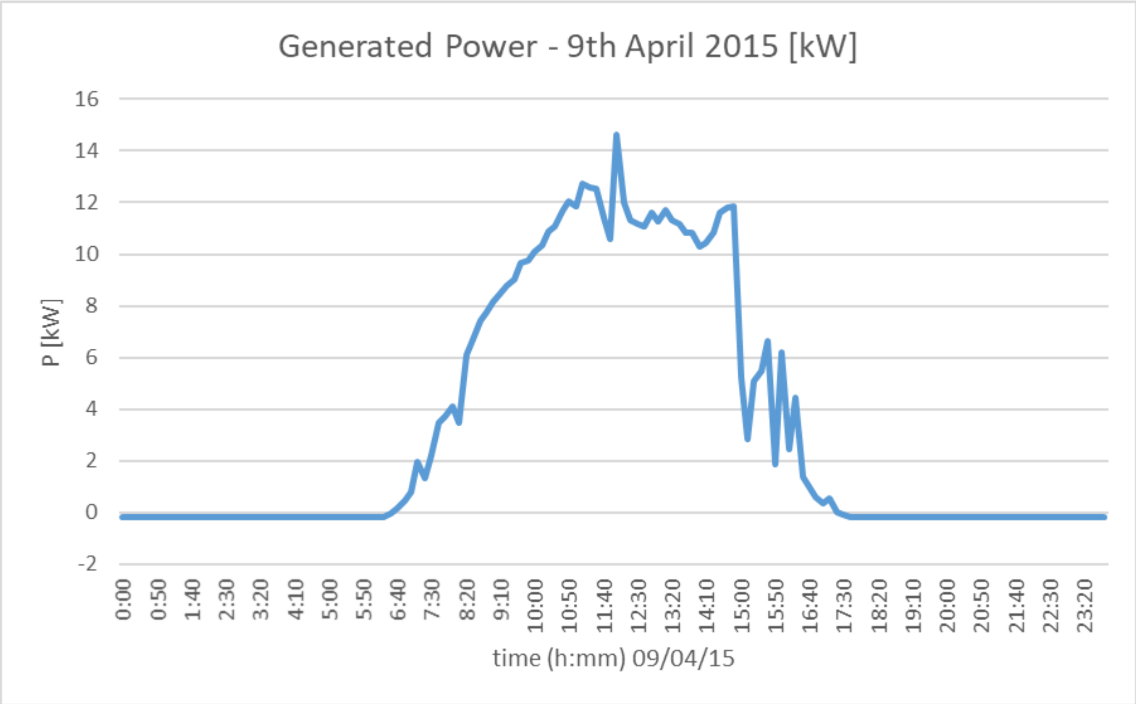

Figure C.6 – Voltage profile of phase A for one day of measurement.

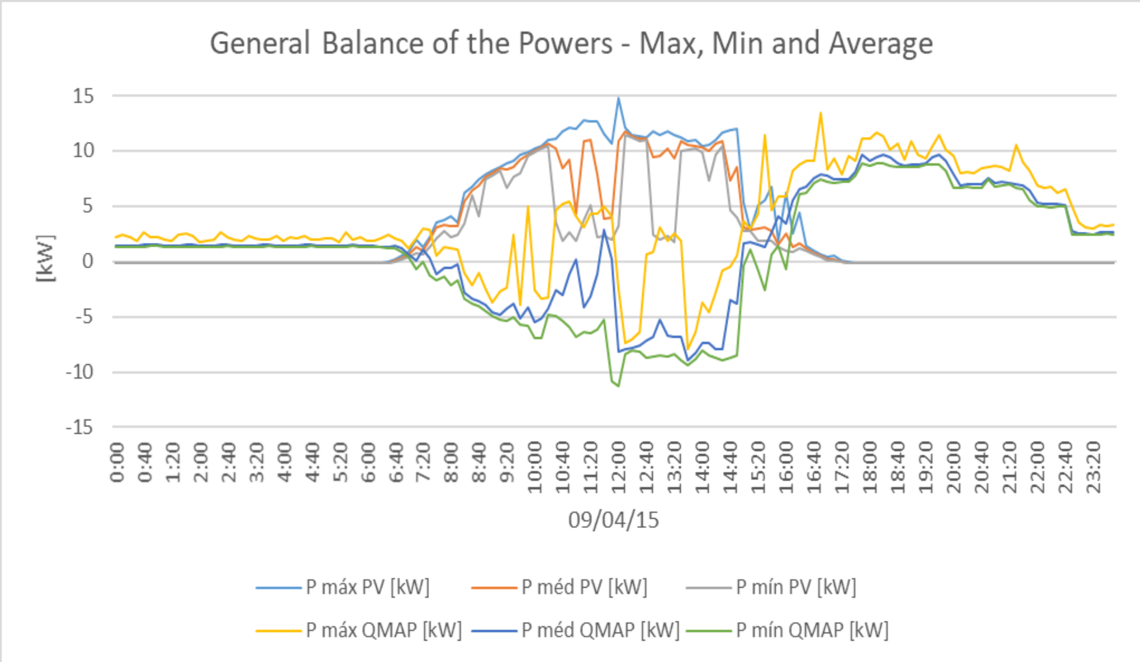

Figure C.7 – General balance regarding one day of measurement.

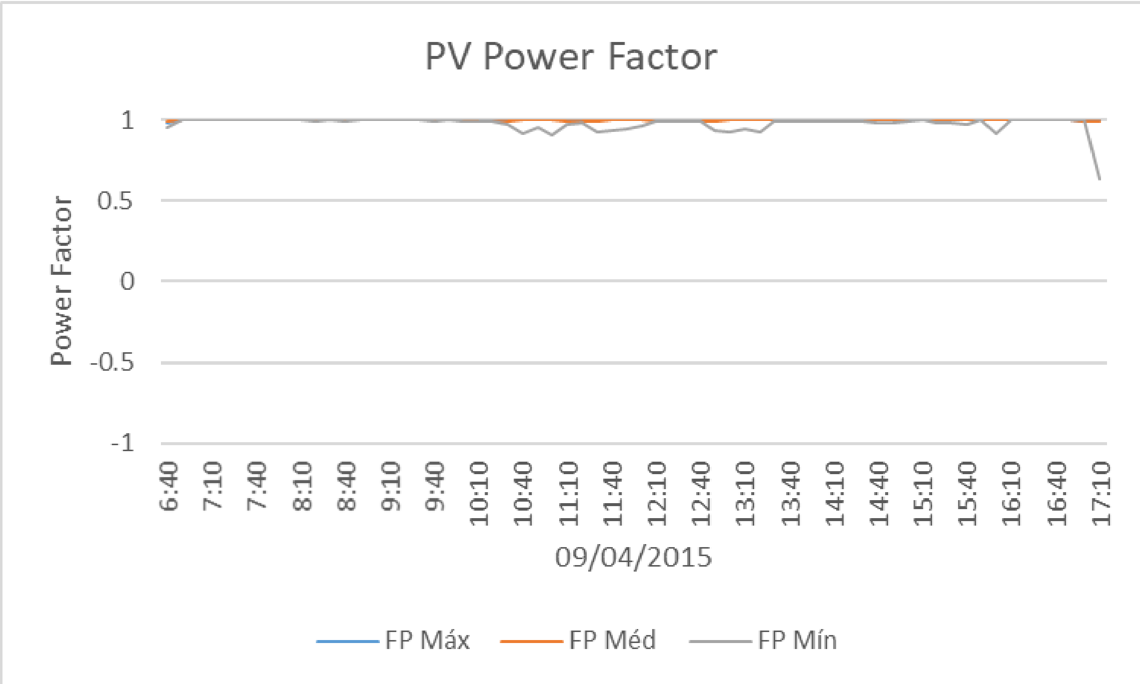

Figure C.8 – PV Power factor for one day of measurement.

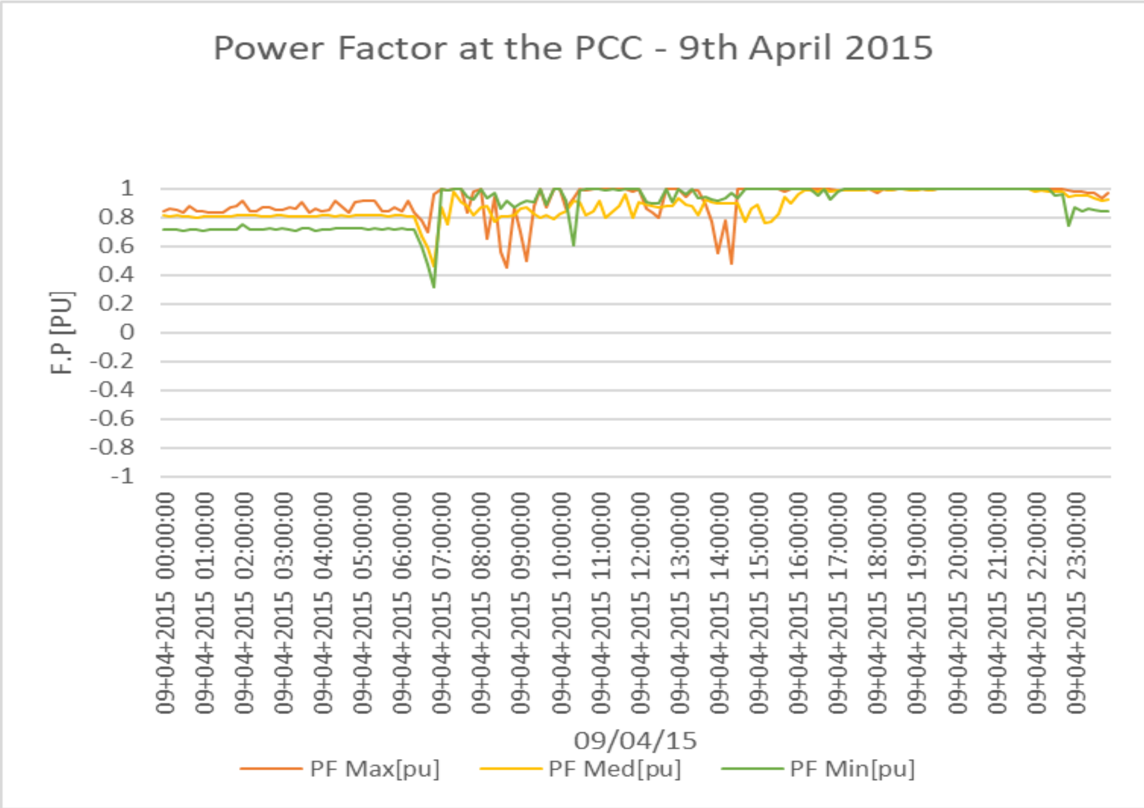

Figure C.9 – Installation Power factor for one day of measurement.

APPENDIX. D – DHC and DH + EES Tables from Section 7.4

Table D.1 – DHC + EES values day 9th of April 2015.

Time	Vo	deltaVmax	deltaV	Pliquido	MaxP	a	b	HC	min	max	storage	HC+Storage
7:10	1.020555	0.02804329	0.020554545	1.969	16.73311	0.0035	-0.03052	23.00645	22.60848	24.73155	5.341964366	28.34841529
7:20	1.015218	0.033125541	0.015218182	1.3391	18.10654	0.0035	-0.03025	22.92781	22.60848	24.73155	3.934404823	26.86221938
7:30	1.014959	0.033372294	0.014959091	2.2263	18.62142	0.0035	-0.0318	23.37219	22.60848	24.73155	3.866434235	27.23862237
7:40	1.013627	0.034640693	0.013627273	3.5037	18.83239	0.0035	-0.03127	23.22076	22.60848	24.73155	3.517581132	26.73834122
7:50	1.0119	0.036285714	0.0119	3.7416	19.19739	0.0035	-0.03091	23.11576	22.60848	24.73155	3.066489243	26.18225134
8:00	1.015609	0.032753247	0.015609091	4.1368	19.13428	0.0035	-0.03422	24.06192	22.60848	24.73155	4.037021644	28.09894457
8:10	1.015482	0.032874459	0.015481818	3.517	18.65379	0.0035	-0.03241	23.5468	22.60848	24.73155	4.003602972	27.55040773
8:20	1.012259	0.035943723	0.012259091	6.1731	19.12938	0.0035	-0.03101	23.14546	22.60848	24.73155	3.160143758	26.30560645
8:30	1.017141	0.031294372	0.017140909	6.7731	19.36353	0.0035	-0.03648	24.70799	22.60848	24.73155	4.439886434	29.14787737
8:40	1.019091	0.029437229	0.019090909	7.4551	18.34828	0.0035	-0.03478	24.22336	22.60848	24.73155	4.954461126	29.17782339
8:50	1.017432	0.031017316	0.017431818	7.8272	17.92377	0.0035	-0.03172	23.34739	22.60848	24.73155	4.516529913	27.86391939
9:00	1.017009	0.031419913	0.017009091	8.2247	18.18476	0.0035	-0.03223	23.49335	22.60848	24.73155	4.405171548	27.89852525
9:10	1.01675	0.031666667	0.01675	8.5378	18.45572	0.0035	-0.03293	23.69382	22.60848	24.73155	4.336964634	28.03078211
9:20	1.011836	0.03634632	0.011836364	8.8638	19.14615	0.0035	-0.03067	23.0472	22.60848	24.73155	3.04989909	26.09710158
9:30	1.009786	0.038298701	0.009786364	9.0833	19.94801	0.0035	-0.03152	23.29124	22.60848	24.73155	2.516562604	25.80779772
9:40	1.014405	0.033900433	0.014404545	9.7049	19.63462	0.0035	-0.03482	24.2345	22.60848	24.73155	3.721068228	27.95556434
9:50	1.014309	0.033991342	0.014309091	9.8386	18.99409	0.0035	-0.03249	23.568	22.60848	24.73155	3.696062011	27.26405855
10:00	1.013495	0.034766234	0.013495455	10.1794	19.10374	0.0035	-0.0321	23.45624	22.60848	24.73155	3.483102141	26.93934369
10:10	1.013168	0.035077922	0.013168182	10.4109	19.65439	0.0035	-0.03371	23.91784	22.60848	24.73155	3.397537392	27.31537594
10:20	1.016782	0.031636364	0.016781818	10.9786	19.17848	0.0035	-0.03549	24.42523	22.60848	24.73155	4.34533908	28.77056778
10:30	1.018605	0.029900433	0.018604545	11.1459	18.05446	0.0035	-0.03329	23.7972	22.60848	24.73155	4.825936041	28.6231315
10:40	1.019777	0.02878355	0.019777273	11.7523	17.55233	0.0035	-0.03265	23.61417	22.60848	24.73155	5.136042627	28.75021127
10:50	1.019841	0.028722944	0.019840909	12.1554	17.30842	0.0035	-0.03186	23.38758	22.60848	24.73155	5.152890152	28.54046738
11:00	1.021891	0.026770563	0.021890909	11.9598	17.1586	0.0035	-0.03328	23.79558	22.60848	24.73155	5.696724556	29.49230764
11:10	1.023159	0.025562771	0.023159091	12.8019	16.758	0.0035	-0.03309	23.74007	22.60848	24.73155	6.034225879	29.77429372
11:20	1.021173	0.027454545	0.021172727	12.658	16.77169	0.0035	-0.03125	23.21325	22.60848	24.73155	5.505958061	28.71920487
11:30	1.022673	0.026025974	0.022672727	12.6105	16.83132	0.0035	-0.03288	23.68104	22.60848	24.73155	5.904693055	29.58573772
11:40	1.020623	0.027978355	0.020622727	11.5098	16.82776	0.0035	-0.03092	23.11966	22.60848	24.73155	5.360042357	28.47970122
11:50	1.025468	0.023363636	0.025468182	10.6442	16.95264	0.0035	-0.03597	24.56303	22.60848	24.73155	6.650847954	31.21387682
12:00	1.028236	0.020727273	0.028236364	14.7561	16.36792	0.0035	-0.03656	24.73155	22.60848	24.73155	7.393645317	32.12520026
12:10	1.023223	0.025502165	0.023222727	12.0848	16.24283	0.0035	-0.03135	23.24222	22.60848	24.73155	6.051183012	29.2933982
12:20	1.024427	0.024354978	0.024427273	11.4323	16.35361	0.0035	-0.03288	23.68076	22.60848	24.73155	6.372546327	30.05330167
12:30	1.0242	0.024571429	0.0242	11.3046	16.10214	0.0035	-0.03179	23.36744	22.60848	24.73155	6.311855178	29.67929678
12:40	1.024459	0.024324675	0.024459091	11.1828	16.21032	0.0035	-0.03241	23.54613	22.60848	24.73155	6.381045187	29.92717046
12:50	1.024786	0.024012987	0.024786364	11.7233	16.1664	0.0035	-0.03257	23.59126	22.60848	24.73155	6.468491963	30.05975458
13:00	1.022086	0.026584416	0.022086364	11.3848	16.52188	0.0035	-0.03124	23.21204	22.60848	24.73155	5.748687495	28.9607305
13:10	1.018505	0.029995671	0.018504545	11.821	17.89691	0.0035	-0.03264	23.61243	22.60848	24.73155	4.799525255	28.41195334
13:20	1.01805	0.030428571	0.01805	11.4194	18.81091	0.0035	-0.03541	24.40275	22.60848	24.73155	4.679540418	29.08228703
13:30	1.018082	0.030398268	0.018081818	11.2649	18.69358	0.0035	-0.03503	24.29408	22.60848	24.73155	4.687935931	28.9820119
13:40	1.014082	0.034207792	0.014081818	10.92	18.88376	0.0035	-0.03189	23.39582	22.60848	24.73155	3.636542077	27.03235842
13:50	1.014764	0.033558442	0.014763636	10.938	19.07587	0.0035	-0.03321	23.77346	22.60848	24.73155	3.815180802	27.58863693
14:00	1.0134	0.034857143	0.0134	10.4049	19.30122	0.0035	-0.0327	23.62775	22.60848	24.73155	3.458140121	27.08588833
14:10	1.011805	0.036376623	0.011804545	10.5142	19.73076	0.0035	-0.03268	23.62315	22.60848	24.73155	3.041604788	26.66475963
14:20	1.012845	0.035385281	0.012845455	10.9361	19.62245	0.0035	-0.03329	23.79809	22.60848	24.73155	3.313214461	27.11129952
14:30	1.013495	0.034766234	0.013495455	11.6965	19.43757	0.0035	-0.03327	23.79008	22.60848	24.73155	3.483102141	27.27318171
14:40	1.012095	0.036099567	0.012095455	11.9169	19.33187	0.0035	-0.03156	23.30343	22.60848	24.73155	3.117457606	26.42088273
14:50	1.0119	0.036285714	0.0119	11.9391	19.62102	0.0035	-0.03239	23.53939	22.60848	24.73155	3.066489243	26.60587875
15:00	1.015059	0.033277056	0.015059091	5.2679	19.59588	0.0035	-0.03531	24.37386	22.60848	24.73155	3.892664445	28.26652903
15:10	1.015218	0.033125541	0.015218182	2.8848	18.93026	0.0035	-0.03313	23.75153	22.60848	24.73155	3.934404823	27.68593783
15:20	1.016227	0.032164502	0.016227273	5.0922	18.56914	0.0035	-0.03283	23.665	22.60848	24.73155	4.199458265	27.8644539
15:30	1.014277	0.034021645	0.014277273	5.5248	18.68407	0.0035	-0.03137	23.24931	22.60848	24.73155	3.687727636	26.93704104
15:40	1.013918	0.034363636	0.013918182	6.7126	18.90724	0.0035	-0.03181	23.37477	22.60848	24.73155	3.593704014	26.96847638
15:50	1.015218	0.033125541	0.015218182	1.8948	19.02194	0.0035	-0.03345	23.84321	22.60848	24.73155	3.934404823	27.77761412
16:00	1.014245	0.034051948	0.014245455	6.246	18.97384	0.0035	-0.03236	23.53043	22.60848	24.73155	3.679393777	27.20982149
16:10	1.014959	0.033372294	0.014959091	2.473	18.72686	0.0035	-0.03217	23.47764	22.60848	24.73155	3.866434235	27.34407196
16:20	1.018409	0.03008658	0.018409091	4.472	18.1606	0.0035	-0.03348	23.85015	22.60848	24.73155	4.774319711	28.62446985
16:30	1.016491	0.03191342	0.016490909	1.3995	17.95529	0.0035	-0.03093	23.12288	22.60848	24.73155	4.268791908	27.39167254
16:40	1.018636	0.02987013	0.018636364	1.0099	17.96024	0.0035	-0.03299	23.71163	22.60848	24.73155	4.834340542	28.54597035
16:50	1.0256	0.023238095	0.0256	0.6317	17.04315	0.0035	-0.03641	24.68941	22.60848	24.73155	6.686130758	31.37553944
17:00	1.026836	0.022060606	0.026836364	0.3786	16.04023	0.0035	-0.03408	24.02291	22.60848	24.73155	7.0174899	31.04040386
17:10	1.021595	0.027051948	0.021595455	0.5584	16.95257	0.0035	-0.03228	23.50916	22.60848	24.73155	5.618212863	29.12736843
17:20	1.013691	0.034580087	0.013690909	0.0281	18.44199	0.0035	-0.02997	22.84768	22.60848	24.73155	3.534229329	26.38191361
17:30	1.021045	0.027575758	0.021045455	-0.0586	18.08622	0.0035	-0.03573	24.49315	22.60848	24.73155	5.472178742	29.96532977
17:40	1.018964	0.029558442	0.018963636	-0.1342	17.63638	0.0035	-0.03217	23.47683	22.60848	24.73155	4.920816755	28.39764229
17:50	1.013009	0.035229437	0.013009091	-0.1596	18.82366	0.0035	-0.03065	23.04382	22.60848	24.73155	3.35596312	26.39978138
18:00	1.006077	0.041831169	0.006077273	-0.1577	20.27453	0.0035	-0.02913	22.60848	22.60848	24.73155	1.557029902	24.16551214

Table D.2 – DHC + EES values day 10th of April 2015.

Time	Vo	deltaVmax	deltaV	Pliquido	MaxP	a	b	HC	min	max	storage	HC+Storage
7:10	1.014795	0.033528139	0.014795	1.5033	16.57315	0.0031	-0.01785	21.88665	24.0943	20.64356	3.823523	25.71017658
7:20	1.021109	0.027515152	0.021109	2.0723	16.664	0.0031	-0.02414	23.91717	24.0943	20.64356	5.489067	29.40624113
7:30	1.018309	0.030181818	0.018309	2.5417	16.64283	0.0031	-0.02141	23.0358	24.0943	20.64356	4.747919	27.78371504
7:40	1.018768	0.029744589	0.018768	3.0241	17.18739	0.0031	-0.02354	23.72139	24.0943	20.64356	4.869165	28.5905571
7:50	1.0175	0.030952381	0.0175	3.1348	17.13922	0.0031	-0.02218	23.28361	24.0943	20.64356	4.534499	27.81811379
8:00	1.01535	0.033	0.01535	4.1594	17.33105	0.0031	-0.02073	22.81492	24.0943	20.64356	3.968999	26.78392226
8:10	1.012714	0.035510823	0.012714	4.8783	18.07653	0.0031	-0.02053	22.75045	24.0943	20.64356	3.278788	26.02924294
8:20	1.014341	0.033961039	0.014341	5.4685	18.22911	0.0031	-0.02255	23.40296	24.0943	20.64356	3.704397	27.10736102
8:30	1.017236	0.031203463	0.017236	6.4074	17.75913	0.0031	-0.02385	23.82253	24.0943	20.64356	4.46503	28.28755914
8:40	1.017041	0.03138961	0.017041	7.42	17.5456	0.0031	-0.023	23.54895	24.0943	20.64356	4.41355	27.96249821
8:50	1.015382	0.032969697	0.015382	7.8032	17.64411	0.0031	-0.02173	23.13775	24.0943	20.64356	3.977351	27.11510539
9:00	1.018277	0.030212121	0.018277	8.53	17.71111	0.0031	-0.02469	24.0943	24.0943	20.64356	4.73952	28.83382117
9:10	1.0202	0.028380952	0.0202	8.8956	16.9037	0.0031	-0.02402	23.87759	24.0943	20.64356	5.247997	29.12558777
9:20	1.0147	0.033619048	0.0147	8.9201	16.87278	0.0031	-0.01869	22.15696	24.0943	20.64356	3.798498	25.95546016
9:30	1.015709	0.032658009	0.015709	9.8935	18.14364	0.0031	-0.02359	23.73783	24.0943	20.64356	4.063285	27.80111931
9:40	1.012845	0.035385281	0.012845	9.7483	18.17568	0.0031	-0.02096	22.89011	24.0943	20.64356	3.313214	26.20332098
9:50	1.012941	0.035294372	0.012941	9.906	18.60427	0.0031	-0.02238	23.34802	24.0943	20.64356	3.33815	26.68617104
10:00	1.013464	0.034796537	0.013464	9.9894	18.69072	0.0031	-0.02314	23.59506	24.0943	20.64356	3.474781	27.06984341
10:10	1.012	0.036190476	0.012	10.1748	18.76611	0.0031	-0.02198	23.22079	24.0943	20.64356	3.092564	26.31335753
10:20	1.012745	0.035480519	0.012745	10.5806	18.77081	0.0031	-0.02271	23.45451	24.0943	20.64356	3.287097	26.74160601
10:30	1.014473	0.033835498	0.014473	10.6249	18.1178	0.0031	-0.02233	23.33215	24.0943	20.64356	3.738933	27.07108531
10:40	1.012455	0.035757576	0.012455	10.8042	18.20141	0.0031	-0.02067	22.79574	24.0943	20.64356	3.211148	26.00689009
10:50	1.014832	0.033493506	0.014832	10.7747	18.23533	0.0031	-0.02304	23.56	24.0943	20.64356	3.833058	27.39306197
11:00	1.016586	0.031822511	0.016586	11.0583	17.77865	0.0031	-0.02329	23.64235	24.0943	20.64356	4.293904	27.93625663
11:10	1.017109	0.031324675	0.017109	11.2751	17.46309	0.0031	-0.02281	23.48739	24.0943	20.64356	4.431506	27.91889359
11:20	1.016327	0.032069264	0.016327	10.9624	17.36246	0.0031	-0.02175	23.14657	24.0943	20.64356	4.225753	27.37232537
11:30	1.018573	0.029930736	0.018573	11.2903	17.01737	0.0031	-0.02282	23.49132	24.0943	20.64356	4.817532	28.30885351
11:40	1.016032	0.032350649	0.016032	11.2326	16.97393	0.0031	-0.02027	22.66727	24.0943	20.64356	4.148079	26.81534913
11:50	1.017432	0.031017316	0.017432	11.2266	17.35944	0.0031	-0.0228	23.48289	24.0943	20.64356	4.51653	27.99941793
12:00	1.021045	0.027575758	0.021045	11.4194	16.51066	0.0031	-0.02361	23.74428	24.0943	20.64356	5.472179	29.21646343
12:10	1.021827	0.026831169	0.021827	11.5393	16.22428	0.0031	-0.02346	23.6981	24.0943	20.64356	5.679811	29.37790646
12:20	1.023027	0.025688312	0.023027	12.8069	15.82963	0.0031	-0.02338	23.67211	24.0943	20.64356	5.999107	29.67121932
12:30	1.021827	0.026831169	0.021827	11.4904	15.92048	0.0031	-0.02252	23.39429	24.0943	20.64356	5.679811	29.07410455
12:40	1.020427	0.028164502	0.020427	11.5951	16.11861	0.0031	-0.0218	23.16232	24.0943	20.64356	5.308225	28.47054029
12:50	1.019873	0.028692641	0.019873	11.3548	16.61059	0.0031	-0.0228	23.48393	24.0943	20.64356	5.161315	28.64524165
13:00	1.018864	0.02965368	0.018864	11.4088	16.57164	0.0031	-0.02172	23.13497	24.0943	20.64356	4.894388	28.02935786
13:10	1.012618	0.035601732	0.012618	11.4185	17.27218	0.0031	-0.01794	21.91678	24.0943	20.64356	3.253864	25.1706417
13:20	1.013236	0.035012987	0.013236	10.7176	18.6192	0.0031	-0.02271	23.45372	24.0943	20.64356	3.415359	26.86907612
13:30	1.011932	0.036255411	0.011932	10.8125	18.75534	0.0031	-0.02189	23.18908	24.0943	20.64356	3.074785	26.26386155
13:40	1.014341	0.033961039	0.014341	10.57	18.27012	0.0031	-0.02268	23.44398	24.0943	20.64356	3.704397	27.14837343
13:50	1.0133	0.034952381	0.0133	10.3537	18.46697	0.0031	-0.0223	23.32104	24.0943	20.64356	3.431994	26.75303873
14:00	1.012455	0.035757576	0.012455	10.2126	18.50466	0.0031	-0.02161	23.09899	24.0943	20.64356	3.211148	26.31014206
14:10	1.013364	0.034891775	0.013364	10.3302	18.64262	0.0031	-0.0229	23.51624	24.0943	20.64356	3.448632	26.96487694
14:20	1.010764	0.037367965	0.010764	10.3242	18.72938	0.0031	-0.02069	22.80423	24.0943	20.64356	2.770547	25.57477446
14:30	1.009786	0.038298701	0.009786	10.7669	19.42996	0.0031	-0.02193	23.20458	24.0943	20.64356	2.516563	25.72113997
14:40	1.009982	0.038112554	0.009982	4.4121	19.36069	0.0031	-0.02191	23.19535	24.0943	20.64356	2.567321	25.7626748
14:50	1.011968	0.036220779	0.011968	9.6879	18.97549	0.0031	-0.0226	23.4204	24.0943	20.64356	3.084267	26.50466516
15:00	1.013009	0.035229437	0.013009	2.5413	18.54691	0.0031	-0.02227	23.31161	24.0943	20.64356	3.355963	26.66757395
15:10	1.012782	0.035445887	0.012782	2.5528	18.39019	0.0031	-0.02156	23.08507	24.0943	20.64356	3.296594	26.38166015
15:20	1.01405	0.034238095	0.01405	2.4859	18.05196	0.0031	-0.02172	23.13645	24.0943	20.64356	3.628211	26.76465714
15:30	1.013041	0.035199134	0.013041	4.1806	18.05917	0.0031	-0.02078	22.83365	24.0943	20.64356	3.364277	26.19792255
15:40	1.01665	0.031761905	0.01665	1.7574	17.46692	0.0031	-0.02239	23.35017	24.0943	20.64356	4.310648	27.6608221
15:50	1.014927	0.033402597	0.014927	1.5817	17.51235	0.0031	-0.02089	22.86635	24.0943	20.64356	3.858089	26.72443539
16:00	1.0201	0.02847619	0.0201	1.2059	16.53542	0.0031	-0.02278	23.47859	24.0943	20.64356	5.221505	28.70009356
16:10	1.021436	0.027203463	0.021436	0.8844	15.97249	0.0031	-0.02231	23.32621	24.0943	20.64356	5.575956	28.90216592
16:20	1.018927	0.029593074	0.018927	0.9804	16.01506	0.0031	-0.02005	22.59794	24.0943	20.64356	4.911206	27.50914498
16:30	1.020523	0.028073593	0.020523	0.7503	16.50422	0.0031	-0.02309	23.57725	24.0943	20.64356	5.333529	28.91078051
16:40	1.025436	0.023393939	0.025436	0.5773	15.24784	0.0031	-0.02387	23.83044	24.0943	20.64356	6.642333	30.47277574
16:50	1.026055	0.022805195	0.026055	0.3624	15.19667	0.0031	-0.0243	23.96919	24.0943	20.64356	6.807863	30.7770557
17:00	1.026736	0.022155844	0.026736	0.0816	14.62964	0.0031	-0.0232	23.61163	24.0943	20.64356	6.99066	30.60228921
17:10	1.021859	0.026800866	0.021859	-0.0959	14.65736	0.0031	-0.01864	22.14095	24.0943	20.64356	5.688267	27.82921689
17:20	1.019973	0.028597403	0.019973	-0.137	16.03079	0.0031	-0.0211	22.93485	24.0943	20.64356	5.187795	28.12264413
17:30	1.02225	0.026428571	0.02225	-0.1199	16.1155	0.0031	-0.02353	23.71918	24.0943	20.64356	5.792206	29.51138998
17:40	1.019936	0.028632035	0.019936	-0.1688	16.12387	0.0031	-0.02135	23.01676	24.0943	20.64356	5.178165	28.19492613
17:50	1.017336	0.031108225	0.017336	-0.166	16.58049	0.0031	-0.02029	22.67462	24.0943	20.64356	4.491377	27.16599244
18:00	1.008777	0.03925974	0.008777	-0.1619	17.17896	0.0031	-0.014	20.64356	24.0943	20.64356	2.254819	22.89838214

Table D.3 – DHC + EES values day 11^{th} of April 2015.

Time	Vo	deltaVmax	deltaV	Pliquido	MaxP	a	b	HC	min	max	storage	HC+Storage
7:10	1.020395455	0.028194805	0.020395455	1.2865	16.01704975	0.0033	-0.024661459	22.62468454	23.78308517	22.243509	6.138423704	28.76310824
7:20	1.018668182	0.029839827	0.018668182	1.874	16.79174051	0.0033	-0.025572917	22.90088389	23.78308517	22.243509	5.299791597	28.20067549
7:30	1.021077273	0.027545455	0.021077273	2.3412	16.97867745	0.0033	-0.028484181	23.78308517	23.78308517	22.243509	4.842745557	28.62583072
7:40	1.019613636	0.028939394	0.019613636	2.6985	17.01190018	0.0033	-0.027199877	23.39390201	23.78308517	22.243509	5.480622799	28.87452481
7:50	1.017040909	0.03138961	0.017040909	2.9457	17.11850941	0.0033	-0.025101471	22.75802141	23.78308517	22.243509	5.09272989	27.8507513
8:00	1.019581818	0.028969697	0.019581818	4.5822	17.16908711	0.0033	-0.027688291	23.54190621	23.78308517	22.243509	4.413550193	27.95545641
8:10	1.02085	0.027761905	0.02085	5.231	16.58538962	0.0033	-0.026969881	23.32420636	23.78308517	22.243509	5.084309553	28.40851591
8:20	1.02085	0.027761905	0.02085	6.0044	16.58605315	0.0033	-0.026972071	23.32486988	23.78308517	22.243509	5.420319424	28.74518931
8:30	1.020459091	0.028134199	0.020459091	6.6043	16.85023175	0.0033	-0.027471566	23.47623202	23.78308517	22.243509	5.420319424	28.89655144
8:40	1.022054545	0.026614719	0.022054545	7.1111	16.24585427	0.0033	-0.0269966	23.33230317	23.78308517	22.243509	5.316659158	28.64896233
8:50	1.019090909	0.029437229	0.019090909	7.5823	16.31853303	0.0033	-0.02441393	22.54967563	23.78308517	22.243509	5.740227086	28.28990271
9:00	1.018213636	0.030272727	0.018213636	7.9623	17.27791807	0.0033	-0.026744402	23.25587951	23.78308517	22.243509	4.954461126	28.21034063
9:10	1.017040909	0.03138961	0.017040909	8.4156	17.38981383	0.0033	-0.025996775	23.02932583	23.78308517	22.243509	4.722722837	27.75204867
9:20	1.018831818	0.029683983	0.018831818	8.6858	17.10578011	0.0033	-0.026765092	23.262149	23.78308517	22.243509	4.413550193	27.67569919
9:30	1.016131818	0.032255411	0.016131818	9.0492	17.07158883	0.0033	-0.024080832	22.44873693	23.78308517	22.243509	4.885979497	27.33471643
9:40	1.014081818	0.034207792	0.014081818	9.3572	18.00323662	0.0033	-0.025202889	22.78875413	23.78308517	22.243509	4.174363433	26.96311757
9:50	1.015545455	0.032813853	0.015545455	9.4951	17.99970437	0.0033	-0.026585172	23.20762776	23.78308517	22.243509	3.636542077	26.84416983
10:00	1.019027273	0.029497835	0.019027273	9.9475	17.05426126	0.0033	-0.026781227	23.26703839	23.78308517	22.243509	4.020311277	27.28734966
10:10	1.019545455	0.029004329	0.019545455	10.3643	16.93819315	0.0033	-0.026891708	23.30051769	23.78308517	22.243509	4.93763791	28.2381556
10:20	1.016195455	0.032194805	0.016195455	10.3934	16.93178741	0.0033	-0.023680093	22.32730099	23.78308517	22.243509	5.074686942	27.40198793
10:30	1.017109091	0.031324675	0.017109091	11.1252	17.73183169	0.0033	-0.027190369	23.39102099	23.78308517	22.243509	4.191092805	27.58211379
10:40	1.017595455	0.030861472	0.017595455	12.0009	17.41764972	0.0033	-0.026616772	23.2172037	23.78308517	22.243509	4.431506169	27.64870987
10:50	1.017009091	0.031419913	0.017009091	11.5254	17.3769647	0.0033	-0.02592407	23.00729396	23.78308517	22.243509	4.559660811	27.56695477
11:00	1.018309091	0.030181818	0.018309091	11.2792	17.23820022	0.0033	-0.026704243	23.24370986	23.78308517	22.243509	4.405171548	27.64888141
11:10	1.016454545	0.031948052	0.016454545	10.9878	17.27235658	0.0033	-0.025050725	22.74264387	23.78308517	22.243509	4.747918879	27.49056275
11:20	1.015318182	0.033030303	0.015318182	11.62	17.69955211	0.0033	-0.025378219	22.84188452	23.78308517	22.243509	4.259226542	27.10111106
11:30	1.016263636	0.03212987	0.016263636	11.2492	17.85004802	0.0033	-0.026775288	23.26523889	23.78308517	22.243509	3.960648229	27.22588712
11:40	1.018895455	0.029623377	0.018895455	11.9312	17.21610895	0.0033	-0.027189783	23.39084331	23.78308517	22.243509	4.209019421	27.59986273
11:50	1.01675	0.031666667	0.01675	12.159	17.18939266	0.0033	-0.025058329	22.74494821	23.78308517	22.243509	4.902796379	27.64774459
12:00	1.018118182	0.030363636	0.018118182	11.9382	17.11703427	0.0033	-0.026122577	23.06744749	23.78308517	22.243509	4.336964634	27.40441213
12:10	1.019354545	0.029186147	0.019354545	11.5015	16.96718158	0.0033	-0.026805552	23.27440971	23.78308517	22.243509	4.697531435	27.97194114
12:20	1.017790909	0.030675325	0.017790909	11.6453	16.93903988	0.0033	-0.025223507	22.7950021	23.78308517	22.243509	5.024179282	27.81918139
12:30	1.017531818	0.030922078	0.017531818	12.6806	17.44839799	0.0033	-0.026657635	23.2295865	23.78308517	22.243509	4.611196146	27.84078264
12:40	1.015122727	0.03321645	0.015122727	12.8646	17.53595296	0.0033	-0.024652195	22.62187714	23.78308517	22.243509	4.542886063	27.1647632
12:50	1.015645455	0.032718615	0.015645455	13.1786	17.89575885	0.0033	-0.026337389	23.13254227	23.78308517	22.243509	3.909359049	27.04190132
13:00	1.0174	0.031047619	0.0174	13.0753	17.41707518	0.0033	-0.026428729	23.16022092	23.78308517	22.243509	4.046571352	27.20679227
13:10	1.018245455	0.030242424	0.018245455	11.816	17.32559123	0.0033	-0.026932027	23.3127354	23.78308517	22.243509	4.508144933	27.82088033
13:20	1.016718182	0.03169697	0.016718182	11.7846	17.32431792	0.0033	-0.025473279	22.87069074	23.78308517	22.243509	4.731121002	27.60181174
13:30	1.01805	0.030428571	0.01805	11.2557	17.35592305	0.0033	-0.026845975	23.28665898	23.78308517	22.243509	4.328590703	27.61524968
13:40	1.020327273	0.02825974	0.020327273	11.6592	16.90335271	0.0033	-0.027521324	23.49131021	23.78308517	22.243509	4.679540418	28.17085063
13:50	1.021209091	0.027419913	0.021209091	11.6315	16.59059472	0.0033	-0.027329049	23.4330452	23.78308517	22.243509	5.281721499	28.7147667
14:00	1.021563636	0.027082251	0.021563636	11.7311	16.56477033	0.0033	-0.027581491	23.50954272	23.78308517	22.243509	5.51561081	29.02515353
14:10	1.022572727	0.026121212	0.022572727	10.7475	16.31523545	0.0033	-0.027719065	23.55123177	23.78308517	22.243509	5.609760409	29.16099218
14:20	1.021759091	0.026896104	0.021759091	10.4247	16.19941022	0.0033	-0.02656195	23.20059085	23.78308517	22.243509	5.87807507	29.07866592
14:30	1.021563636	0.027082251	0.021563636	9.1548	16.12204424	0.0033	-0.026120495	23.06681664	23.78308517	22.243509	5.661690769	28.72850741
14:40	1.022445455	0.026242424	0.022445455	8.8048	15.93051222	0.0033	-0.026328266	23.1297776	23.78308517	22.243509	5.609760409	28.73953801
14:50	1.020131818	0.028445887	0.020131818	8.5166	15.89640796	0.0033	-0.024012259	22.42795722	23.78308517	22.243509	5.844205	28.27216222
15:00	1.023127273	0.025593074	0.023127273	8.3118	15.71629489	0.0033	-0.0262707	23.1123332	23.78308517	22.243509	5.229933674	28.34226687
15:10	1.022281818	0.026398268	0.022281818	7.8433	15.71200485	0.0033	-0.025451348	22.86404473	23.78308517	22.243509	6.025748086	28.88979282
15:20	1.021922727	0.02674026	0.021922727	7.6916	16.10909596	0.0033	-0.026419757	23.1575021	23.78308517	22.243509	5.800669891	28.95817199
15:30	1.02085	0.027761905	0.02085	7.1586	16.15606491	0.0033	-0.025553109	22.89488165	23.78308517	22.243509	5.705182313	28.60006397
15:40	1.022281818	0.026398268	0.022281818	6.4443	16.03703863	0.0033	-0.026523959	23.18907851	23.78308517	22.243509	5.420319424	28.60939793
15:50	1.021827273	0.026831169	0.021827273	5.8554	16.09507005	0.0033	-0.026282562	23.11592798	23.78308517	22.243509	5.800669891	28.91659787
16:00	1.024654545	0.024138528	0.024654545	5.3966	15.53079255	0.0033	-0.027113087	23.36760221	23.78308517	22.243509	5.679810588	29.0474128
16:10	1.02635	0.02252381	0.02635	5.1591	15.02373351	0.0033	-0.027054511	23.34985184	23.78308517	22.243509	6.433263784	29.78311562
16:20	1.026640909	0.022246753	0.026640909	4.2336	15.05341362	0.0033	-0.027429512	23.4634884	23.78308517	22.243509	6.887046169	30.35053457
16:30	1.0269	0.022	0.0269	3.5696	14.99417402	0.0033	-0.027480774	23.47902251	23.78308517	22.243509	6.965054108	30.44407662
16:40	1.027095455	0.021813853	0.027095455	2.9978	14.91035814	0.0033	-0.027390329	23.45161486	23.78308517	22.243509	7.034566217	30.48618108
16:50	1.023777273	0.024974026	0.023777273	2.4361	14.95958656	0.0033	-0.02439261	22.54321505	23.78308517	22.243509	7.087027801	29.63024286
17:00	1.023222727	0.025502165	0.023222727	1.8122	15.70957295	0.0033	-0.026339426	23.13315946	23.78308517	22.243509	6.199039614	29.33219908
17:10	1.023681818	0.025064935	0.023681818	1.3188	15.64990678	0.0033	-0.026579757	23.20598706	23.78308517	22.243509	6.051183012	29.25717007
17:20	1.022509091	0.026181818	0.022509091	0.2153	15.59282989	0.0033	-0.02527452	22.81046074	23.78308517	22.243509	6.173577728	28.98403847
17:30	1.021336364	0.027298701	0.021336364	0.1282	15.69851694	0.0033	-0.024506405	22.57769837	23.78308517	22.243509	5.861139004	28.43883737
17:40	1.021109091	0.027515152	0.021109091	0.03	15.94640457	0.0033	-0.025107984	22.75999502	23.78308517	22.243509	5.549400736	28.30939576
17:50	1.021109091	0.027515152	0.021109091	-0.0641	16.1600587	0.0033	-0.025813042	22.97364915	23.78308517	22.243509	5.48906737	28.46271652
18:00	1.017822727	0.030645022	0.017822727	-0.1614	16.37836445	0.0033	-0.023403581	22.2435094	23.78308517	22.243509	5.48906737	27.73257677

Table D.4 – DHC + EES values day 12th of April 2015.

Time	Vo	deltaVmax	deltaV	Pliquido	MaxP	a	b	HC	min	max	storage	HC+Storage
7:10	1.019445	0.029099567	0.019445	1.6282	15.0823	0.003	-0.01615	22.04911	23.53779	20.18463	6.75550551	28.80461405
7:20	1.017473	0.029099567	0.019445	1.8888	15.77814	0.003	-0.01823	22.74495	23.53779	20.18463	6.182064507	28.92701177
7:30	1.018832	0.030978355	0.017473	2.4006	16.28303	0.003	-0.01787	22.62358	23.53779	20.18463	5.09272989	27.71630613
7:40	1.018864	0.029683983	0.018832	2.5081	16.24602	0.003	-0.01905	23.01803	23.53779	20.18463	5.705182313	28.7232103
7:50	1.015991	0.02965368	0.018864	3.4419	16.3585	0.003	-0.01942	23.14061	23.53779	20.18463	5.774071816	28.91467958
8:00	1.014182	0.03238961	0.015991	4.6569	16.90323	0.003	-0.01832	22.77336	23.53779	20.18463	5.281721499	28.05507748
8:10	1.01405	0.034112554	0.014182	5.4671	17.08945	0.003	-0.01716	22.38527	23.53779	20.18463	4.929227075	27.31449624
8:20	1.014505	0.034238095	0.01405	6.0555	17.27045	0.003	-0.01757	22.52442	23.53779	20.18463	4.336964634	26.86138089
8:30	1.013791	0.033805195	0.014505	6.7984	17.28893	0.003	-0.01806	22.6872	23.53779	20.18463	4.405171548	27.09236755
8:40	1.015377	0.034484848	0.013791	7.3412	16.38923	0.003	-0.01468	21.56095	23.53779	20.18463	4.320217288	25.88116302
8:50	1.020186	0.032974026	0.015377	7.5699	15.78925	0.003	-0.01439	21.46457	23.53779	20.18463	5.618212863	27.08278548
9:00	1.019641	0.028393939	0.020186	8.079	15.66756	0.003	-0.01861	22.86958	23.53779	20.18463	6.451484151	29.32106819
9:10	1.021773	0.02891342	0.019641	7.2038	15.35881	0.003	-0.01716	22.38767	23.53779	20.18463	6.121455964	28.50912598
9:20	1.019382	0.026883117	0.021773	9.3817	15.35801	0.003	-0.01919	23.06363	23.53779	20.18463	6.451484151	29.51511689
9:30	1.017959	0.029160173	0.019382	9.8165	15.85936	0.003	-0.01842	22.80597	23.53779	20.18463	5.921634424	28.72760049
9:40	1.021482	0.030515152	0.017959	8.102	14.79438	0.003	-0.01387	21.28933	23.53779	20.18463	5.792206314	27.08153578
9:50	1.024514	0.027160173	0.021482	8.1348	13.93228	0.003	-0.01464	21.54555	23.53779	20.18463	7.026027801	28.57158278
10:00	1.024227	0.024272727	0.024514	10.1614	13.87237	0.003	-0.01734	22.44813	23.53779	20.18463	7.910647956	30.3587767
10:10	1.0239	0.024545455	0.024227	10.3486	14.53531	0.003	-0.01906	23.02016	23.53779	20.18463	7.069945149	30.09010372
10:20	1.022514	0.024857143	0.0239	10.7752	14.57215	0.003	-0.01886	22.9531	23.53779	20.18463	7.507420931	30.46052412
10:30	1.022964	0.026177489	0.022514	10.7461	14.93344	0.003	-0.01862	22.87427	23.53779	20.18463	7.130964091	30.00523604
10:40	1.02455	0.025748918	0.022964	10.6101	14.43003	0.003	-0.01754	22.51372	23.53779	20.18463	6.677613409	29.19133254
10:50	1.02245	0.024238095	0.02455	10.7531	14.47472	0.003	-0.01919	23.06202	23.53779	20.18463	7.341070158	30.40308752
11:00	1.021673	0.026238095	0.02245	10.8061	14.94489	0.003	-0.0186	22.86553	23.53779	20.18463	6.947986188	29.81351513
11:10	1.022641	0.026978355	0.021673	11.193	15.37175	0.003	-0.01914	23.04563	23.53779	20.18463	6.512235808	29.55786927
11:20	1.022286	0.026056277	0.022641	11.2174	15.41752	0.003	-0.0202	23.39876	23.53779	20.18463	6.729942413	30.12870073
11:30	1.020768	0.026393939	0.022286	11.0422	15.44099	0.003	-0.01993	23.30968	23.53779	20.18463	6.433263784	29.74294196
11:40	1.021736	0.027839827	0.020768	11.7228	15.12873	0.003	-0.01755	22.51546	23.53779	20.18463	6.364047983	28.87950339
11:50	1.019964	0.026917749	0.021736	11.6412	15.1598	0.003	-0.01856	22.85389	23.53779	20.18463	6.564503273	29.41839055
12:00	1.020705	0.028606061	0.019964	11.6098	15.87405	0.003	-0.01902	23.00536	23.53779	20.18463	5.774071816	28.77943011
12:10	1.02035	0.027900433	0.020705	11.6237	15.76997	0.003	-0.01941	23.13649	23.53779	20.18463	6.20752794	29.34401764
12:20	1.019027	0.028238095	0.02035	11.5402	15.76923	0.003	-0.01907	23.02319	23.53779	20.18463	6.051183012	29.07437767
12:30	1.018445	0.029497835	0.019027	11.6721	16.19281	0.003	-0.01908	23.02687	23.53779	20.18463	5.834529353	28.86139713
12:40	1.017732	0.030051948	0.018445	11.2331	16.41384	0.003	-0.01919	23.06319	23.53779	20.18463	5.524057518	28.58724781
12:50	1.018345	0.030731602	0.017732	10.991	16.29663	0.003	-0.01816	22.71943	23.53779	20.18463	5.368479562	28.08791018
13:00	1.016764	0.030147186	0.018345	10.9343	16.31241	0.003	-0.01879	22.93001	23.53779	20.18463	5.51561081	28.44562343
13:10	1.016668	0.03165368	0.016764	10.9984	16.65794	0.003	-0.01832	22.77338	23.53779	20.18463	5.144466131	27.91784603
13:20	1.013759	0.031744589	0.016668	11.1252	16.59544	0.003	-0.01804	22.68057	23.53779	20.18463	5.264858211	27.94543211
13:30	1.022027	0.034515152	0.013759	11.4549	15.02301	0.003	-0.01055	20.18463	23.53779	20.18463	5.126416395	25.31104507
13:40	1.023386	0.026640693	0.022027	11.6776	14.45832	0.003	-0.01673	22.24476	23.53779	20.18463	7.095569901	29.3403277
13:50	1.024418	0.02534632	0.023386	10.2656	14.50614	0.003	-0.01817	22.72404	23.53779	20.18463	7.446239934	30.1702757
14:00	1.024773	0.024363636	0.024418	10.2601	14.41928	0.003	-0.01889	22.96473	23.53779	20.18463	7.244529297	30.20926124
14:10	1.022932	0.024025974	0.024773	10.0129	14.45568	0.003	-0.01934	23.11368	23.53779	20.18463	7.436453416	30.55013716
14:20	1.025195	0.025779221	0.022932	9.3448	14.74368	0.003	-0.01845	22.81727	23.53779	20.18463	7.087027801	29.90429664
14:30	1.024	0.023623377	0.025195	9.1087	14.74558	0.003	-0.02061	23.53779	23.53779	20.18463	7.244529297	30.78231876
14:40	1.0229	0.024761905	0.024	8.7047	14.7782	0.003	-0.01957	23.1909	23.53779	20.18463	7.0174899	30.20838851
14:50	1.022836	0.025809524	0.0229	8.2699	14.79042	0.003	-0.01856	22.85391	23.53779	20.18463	6.938234017	29.79214366
15:00	1.022805	0.02587013	0.022836	7.8023	14.82727	0.003	-0.01861	22.87056	23.53779	20.18463	6.816388705	29.68694994
15:10	1.022609	0.025900433	0.022805	7.6082	14.98714	0.003	-0.01906	23.02033	23.53779	20.18463	6.807863474	29.82819508
15:20	1.021773	0.02608658	0.022609	7.0972	14.9448	0.003	-0.01875	22.91594	23.53779	20.18463	6.503728992	29.41967347
15:30	1.022932	0.026883117	0.021773	6.7749	14.73404	0.003	-0.01732	22.43967	23.53779	20.18463	6.616790196	29.05646168
15:40	1.022318	0.025779221	0.022932	6.3816	14.71058	0.003	-0.01835	22.78417	23.53779	20.18463	6.877298207	29.66146854
15:50	1.023286	0.026363636	0.022318	5.9306	14.76389	0.003	-0.01793	22.64267	23.53779	20.18463	6.372546327	29.01522115
16:00	1.024064	0.025441558	0.023286	5.398	14.62695	0.003	-0.01844	22.8131	23.53779	20.18463	6.887046169	29.70014515
16:10	1.024773	0.024701299	0.024064	4.8077	14.6338	0.003	-0.0192	23.06671	23.53779	20.18463	7.078486218	30.14519164
16:20	1.024386	0.024025974	0.024773	4.2226	14.60389	0.003	-0.01979	23.2619	23.53779	20.18463	6.95651989	30.21841922
16:30	1.023191	0.024393939	0.024386	3.5917	14.54845	0.003	-0.01925	23.0838	23.53779	20.18463	7.113876136	30.19767685
16:40	1.022482	0.025532468	0.023191	3.0421	14.94892	0.003	-0.01931	23.10477	23.53779	20.18463	6.782290875	29.88705753
16:50	1.022059	0.026207792	0.022482	2.4947	15.17969	0.003	-0.01933	23.11043	23.53779	20.18463	6.7116859	29.82211534
17:00	1.023	0.02661039	0.022059	1.939	14.62245	0.003	-0.01726	22.41898	23.53779	20.18463	6.503728992	28.92271165
17:10	1.023677	0.025714286	0.023	1.4064	14.48159	0.003	-0.01773	22.57683	23.53779	20.18463	7.069945149	29.64677186
17:20	1.023936	0.025069264	0.023677	0.2135	14.46806	0.003	-0.01833	22.77831	23.53779	20.18463	7.095569901	29.87387684
17:30	1.022255	0.024822511	0.023936	0.1259	14.69618	0.003	-0.01927	23.08868	23.53779	20.18463	6.938234017	30.02691305
17:40	1.0208	0.026424242	0.022255	0.0475	14.80629	0.003	-0.01799	22.66488	23.53779	20.18463	6.807863474	29.47273906
17:50	1.017055	0.027809524	0.0208	-0.0355	15.39552	0.003	-0.01838	22.79234	23.53779	20.18463	6.182064507	28.97440893
18:00	1.008527	0.031376623	0.017055	-0.1471	15.98277	0.003	-0.01657	22.19057	23.53779	20.18463	5.618212863	27.80877846

Table D.5 – DHC + EES values day 13^{th} of April 2015.

Time	Vo	deltaVmax	deltaV	Pliquido	MaxP	a	b	HC	min	max	storage	HC+Storage
7:10	1.01457	0.033744589	0.01457	1.7085	16.7853	0.0033	-0.0216	21.7111	23.8269	20.9467	5.248	26.95913445
7:20	1.01669	0.031727273	0.01669	1.7661	17.6553	0.0033	-0.0265	23.1925	23.8269	20.9467	3.76395	26.9564145
7:30	1.01799	0.030489177	0.01799	2.4218	17.6967	0.0033	-0.0279	23.609	23.8269	20.9467	4.32022	27.92926183
7:40	1.0175	0.030952381	0.0175	3.1283	17.7141	0.0033	-0.0275	23.4861	23.8269	20.9467	4.66275	28.14890006
7:50	1.01382	0.034454545	0.01382	3.5507	17.7515	0.0033	-0.0241	22.4623	23.8269	20.9467	4.5345	26.99678418
8:00	1.01418	0.034116883	0.01418	5.042	18.5207	0.0033	-0.027	23.3337	23.8269	20.9467	3.56872	26.90247116
8:10	1.01506	0.033277056	0.01506	5.0484	18.4887	0.0033	-0.0277	23.5563	23.8269	20.9467	3.66154	27.21781251
8:20	1.02332	0.025406926	0.02332	5.8868	15.8211	0.0033	-0.0268	23.2735	23.8269	20.9467	3.89266	27.16618395
8:30	1.02195	0.026709957	0.02195	6.3299	15.9157	0.0033	-0.0258	22.9733	23.8269	20.9467	6.07783	29.05111284
8:40	1.02221	0.026463203	0.02221	7.088	16.1423	0.0033	-0.0268	23.2747	23.8269	20.9467	5.71364	28.98832869
8:50	1.02218	0.026493506	0.02218	8.7407	16.397	0.0033	-0.0276	23.5202	23.8269	20.9467	5.78253	29.30272536
9:00	1.02349	0.025251082	0.02349	8.1039	16.1268	0.0033	-0.028	23.6265	23.8269	20.9467	5.77407	29.40053075
9:10	1.02378	0.024974026	0.02378	8.2842	16.0796	0.0033	-0.0281	23.6633	23.8269	20.9467	6.12146	29.78471052
9:20	1.02482	0.023982684	0.02482	8.5562	15.9429	0.0033	-0.0286	23.8269	23.8269	20.9467	6.19904	30.02596713
9:30	1.02358	0.025160173	0.02358	8.826	15.935	0.0033	-0.0274	23.4622	23.8269	20.9467	6.477	29.93919128
9:40	1.02153	0.027112554	0.02153	9.0663	16.0283	0.0033	-0.0258	22.9639	23.8269	20.9467	6.14691	29.11080203
9:50	1.02114	0.027484848	0.02114	9.3383	16.5072	0.0033	-0.027	23.33	23.8269	20.9467	5.60131	28.93130462
10:00	1.01909	0.029437229	0.01909	9.5421	16.5879	0.0033	-0.0253	22.819	23.8269	20.9467	5.49751	29.32443997
10:10	1.01987	0.028692641	0.01987	9.8516	16.9678	0.0033	-0.0273	23.4246	23.8269	20.9467	4.95446	28.37904934
10:20	1.01925	0.029281385	0.01925	10.1808	16.8577	0.0033	-0.0263	23.1361	23.8269	20.9467	5.16131	28.29740926
10:30	1.01418	0.034116883	0.01418	10.3297	17.3013	0.0033	-0.023	22.1144	23.8269	20.9467	4.99773	27.11211231
10:40	1.01353	0.034735931	0.01353	10.7383	18.4314	0.0033	-0.0261	23.0569	23.8269	20.9467	3.66154	26.7184382
10:50	1.01148	0.036688312	0.01148	10.9859	17.1286	0.0033	-0.0198	21.1624	23.8269	20.9467	3.49142	24.65384017
11:00	1.01821	0.030272727	0.01821	11.4498	17.126	0.0033	-0.0262	23.1039	23.8269	20.9467	2.95632	26.06023532
11:10	1.01519	0.033155844	0.01519	12.2328	18.1394	0.0033	-0.0267	23.2437	23.8269	20.9467	4.72272	27.96646244
11:20	1.01522	0.033125541	0.01522	12.6022	16.726	0.0033	-0.0221	21.8395	23.8269	20.9467	3.92606	25.76556535
11:30	1.01932	0.029220779	0.01932	12.1618	16.7193	0.0033	-0.026	23.016	23.8269	20.9467	3.9344	26.95045462
11:40	1.01883	0.029683983	0.01883	12.5381	16.5155	0.0033	-0.0248	22.6718	23.8269	20.9467	5.01456	27.68638999
11:50	1.02085	0.027761905	0.02085	13.6711	15.7273	0.0033	-0.0241	22.4661	23.8269	20.9467	4.88598	27.35205785
12:00	1.02508	0.023735931	0.02508	13.3783	15.722	0.0033	-0.0281	23.6808	23.8269	20.9467	5.42032	29.1010978
12:10	1.02482	0.023982684	0.02482	12.6548	14.9875	0.0033	-0.0255	22.8715	23.8269	20.9467	6.54627	29.41780576
12:20	1.02658	0.022307359	0.02658	12.5754	14.6043	0.0033	-0.0259	22.996	23.8269	20.9467	6.477	29.47299965
12:30	1.02778	0.021164502	0.02778	12.0046	14.6341	0.0033	-0.0271	23.3721	23.8269	20.9467	6.94799	30.32012188
12:40	1.02599	0.022865801	0.02599	11.7551	14.9224	0.0033	-0.0264	23.1449	23.8269	20.9467	7.27019	30.41505269
12:50	1.02664	0.022246753	0.02664	11.9525	14.9861	0.0033	-0.0272	23.3962	23.8269	20.9467	6.79081	30.18699102
13:00	1.0267	0.022186147	0.0267	11.9935	15.026	0.0033	-0.0274	23.4545	23.8269	20.9467	6.96505	30.41953685
13:10	1.02124	0.02738961	0.02124	12.4399	16.4647	0.0033	-0.0269	23.3163	23.8269	20.9467	6.98212	30.29840819
13:20	1.0175	0.030952381	0.0175	11.798	17.4951	0.0033	-0.0268	23.2671	23.8269	20.9467	5.52406	28.79119433
13:30	1.01541	0.032939394	0.01541	11.6126	18.324	0.0033	-0.0275	23.4939	23.8269	20.9467	4.5345	28.02837337
13:40	1.01577	0.032597403	0.01577	11.2004	18.2522	0.0033	-0.0276	23.5257	23.8269	20.9467	3.9857	27.5113742
13:50	1.01483	0.033493506	0.01483	11.3322	17.8053	0.0033	-0.0253	22.8072	23.8269	20.9467	4.08	26.88722013
14:00	1.0163	0.032099567	0.0163	10.7309	17.8177	0.0033	-0.0267	23.2421	23.8269	20.9467	3.83306	27.07511471
14:10	1.01089	0.037246753	0.01089	10.2587	19.6146	0.0033	-0.0275	23.4792	23.8269	20.9467	4.21739	27.69659869
14:20	1.00959	0.038484848	0.00959	10.3012	18.8137	0.0033	-0.0236	22.3032	23.8269	20.9467	2.80366	25.10684075
14:30	1.01314	0.035108225	0.01314	9.4863	18.2403	0.0033	-0.0251	22.753	23.8269	20.9467	2.46582	25.21881581
14:40	1.0146	0.033714286	0.0146	9.0999	17.6395	0.0033	-0.0245	22.5746	23.8269	20.9467	3.38922	25.96382469
14:50	1.0174	0.031047619	0.0174	9.2678	17.4776	0.0033	-0.0266	23.2208	23.8269	20.9467	3.77229	26.99304149
15:00	1.01782	0.030645022	0.01782	8.5562	17.3547	0.0033	-0.0266	23.2198	23.8269	20.9467	4.50814	27.72798375
15:10	1.01841	0.03008658	0.01841	7.8134	17.3177	0.0033	-0.0271	23.3521	23.8269	20.9467	4.61959	27.97168175
15:20	1.016	0.032380952	0.016	7.1364	17.9561	0.0033	-0.0269	23.2952	23.8269	20.9467	4.77432	28.06955618
15:30	1.01242	0.035787879	0.01242	6.7648	17.6355	0.0033	-0.0224	21.9422	23.8269	20.9467	4.13972	26.08193869
15:40	1.01669	0.031727273	0.01669	6.2003	17.6375	0.0033	-0.0265	23.1747	23.8269	20.9467	3.20284	26.37753459
15:50	1.01499	0.033341991	0.01499	5.6451	17.4024	0.0033	-0.0241	22.4503	23.8269	20.9467	4.32022	26.77049417
16:00	1.01919	0.029341991	0.01919	5.1527	17.3566	0.0033	-0.0279	23.6166	23.8269	20.9467	3.87478	27.49138478
16:10	1.01857	0.029930736	0.01857	4.6519	17.5127	0.0033	-0.0279	23.5942	23.8269	20.9467	4.9809	28.57514997
16:20	1.01808	0.030398268	0.01808	4.0971	17.423	0.0033	-0.0271	23.3629	23.8269	20.9467	4.81753	28.1804577
16:30	1.01802	0.030458874	0.01802	3.47	16.1939	0.0033	-0.023	22.1155	23.8269	20.9467	4.68794	26.80343797
16:40	1.02225	0.026428571	0.02225	2.8461	14.978	0.0033	-0.023	22.1208	23.8269	20.9467	4.67115	26.79196581
16:50	1.02674	0.022155844	0.02674	2.3633	14.8648	0.0033	-0.0269	23.3024	23.8269	20.9467	5.79221	29.09461714
17:00	1.02703	0.021874459	0.02703	1.7878	14.8728	0.0033	-0.0272	23.3957	23.8269	20.9467	6.99066	30.38639791
17:10	1.02518	0.023640693	0.02518	1.234	15.2224	0.0033	-0.0266	23.21	23.8269	20.9467	7.06995	30.27999326
17:20	1.02456	0.024229437	0.02456	0.2149	15.0709	0.0033	-0.0255	22.8801	23.8269	20.9467	6.57301	29.453158
17:30	1.02605	0.022805195	0.02605	0.136	15.1378	0.0033	-0.0271	23.3786	23.8269	20.9467	6.40776	29.78639807
17:40	1.02332	0.025406926	0.02332	0.0184	15.7496	0.0033	-0.0266	23.2021	23.8269	20.9467	6.80786	30.00991423
17:50	1.01854	0.029961039	0.01854	-0.0978	16.6895	0.0033	-0.0251	22.7619	23.8269	20.9467	6.07783	28.83978212
18:00	1.0147	0.033619048	0.0147	-0.1614	15.9828	0.0033	-0.0191	20.9467	23.8269	20.9467	4.80913	25.75582694

Table D.6 – DHC + EES values day 14th of April 2015.

Time	Vo	deltaVmax	deltaV	Pliquido	MaxP	a	b	HC	min	max	storage	HC+Storage
7:10	1.01447273	0.033835498	0.01447273	0.7397	17.4047727	0.003	-0.018379	22.7929	24.025171	20.51395	5.16973974	27.96267986
7:20	1.01326818	0.034982684	0.01326818	0.7397	17.9463563	0.003	-0.018856	22.9521	24.025171	20.51395	3.73893265	26.69106098
7:30	1.01251818	0.03569697	0.01251818	1.3013	18.3414206	0.003	-0.019327	23.1091	24.025171	20.51395	3.42367639	26.53277371
7:40	1.016	0.032380952	0.016	2.7442	17.9145504	0.003	-0.021363	23.7876	24.025171	20.51395	3.22775806	27.01532428
7:50	1.01456818	0.033744589	0.01456818	2.996	17.6950968	0.003	-0.019341	23.1136	24.025171	20.51395	4.13971629	27.25328347
8:00	1.01476364	0.033558442	0.01476364	4.4213	17.5787122	0.003	-0.019178	23.0592	24.025171	20.51395	3.76394683	26.82317851
8:10	1.01587273	0.032502165	0.01587273	5.0964	17.4504974	0.003	-0.019849	23.2831	24.025171	20.51395	3.8151808	27.09829005
8:20	1.01421364	0.034082251	0.01421364	5.4893	17.4993042	0.003	-0.018416	22.8052	24.025171	20.51395	4.10627228	26.91149279
8:30	1.01421364	0.034082251	0.01421364	6.6038	17.9475509	0.003	-0.01976	23.2535	24.025171	20.51395	3.67106043	26.92452766
8:40	1.01417727	0.034116883	0.01417727	7.7174	17.892543	0.003	-0.019561	23.1869	24.025171	20.51395	3.67106043	26.85797576
8:50	1.01440455	0.033900433	0.01440455	8.4737	17.9449739	0.003	-0.019934	23.3115	24.025171	20.51395	3.66153724	26.97303353
9:00	1.01606818	0.032316017	0.01606818	8.8804	17.6268702	0.003	-0.020565	23.5215	24.025171	20.51395	3.72106823	27.24259934
9:10	1.01570909	0.032658009	0.01570909	8.8283	17.6192134	0.003	-0.0202	23.3999	24.025171	20.51395	4.15763612	27.55751331
9:20	1.00861364	0.039415584	0.00861364	8.2662	17.8338367	0.003	-0.014086	21.362	24.025171	20.51395	4.06328496	25.42526017
9:30	1.01466818	0.033649351	0.01466818	8.6074	18.096992	0.003	-0.020642	23.5472	24.025171	20.51395	2.21242347	25.75963195
9:40	1.01417727	0.034116883	0.01417727	9.0238	18.0630741	0.003	-0.020072	23.3574	24.025171	20.51395	3.79015713	27.14760352
9:50	1.01333182	0.034922078	0.01333182	9.455	18.0971082	0.003	-0.019369	23.1231	24.025171	20.51395	3.66153724	26.78461946
10:00	1.01489545	0.0334329	0.01489545	9.9	17.4767418	0.003	-0.018997	22.9991	24.025171	20.51395	3.44031295	26.43942128
10:10	1.01251818	0.03569697	0.01251818	11.471	17.5639727	0.003	-0.016995	22.3316	24.025171	20.51395	3.84974493	26.18139441
10:20	1.01239091	0.035818182	0.01239091	11.721	18.2893919	0.003	-0.01905	23.0167	24.025171	20.51395	3.22775806	26.24442266
10:30	1.01294091	0.035294372	0.01294091	12.337	18.174769	0.003	-0.01923	23.0766	24.025171	20.51395	3.19453974	26.27118467
10:40	1.01209545	0.036099567	0.01209545	12.2407	18.1879792	0.003	-0.018464	22.8215	24.025171	20.51395	3.33814952	26.15960631
10:50	1.01157727	0.036593074	0.01157727	12.3587	18.8804906	0.003	-0.020048	23.3495	24.025171	20.51395	3.11745761	26.46692365
11:00	1.01385455	0.034424242	0.01385455	11.9644	18.2988822	0.003	-0.020472	23.4908	24.025171	20.51395	2.98237476	26.4731762
11:10	1.01287727	0.035354978	0.01287727	12.4611	18.2991253	0.003	-0.019542	23.1808	24.025171	20.51395	3.57704845	26.75784762
11:20	1.01118636	0.036965368	0.01118636	13.0656	18.4983915	0.003	-0.01853	22.8433	24.025171	20.51395	3.32152563	26.16479452
11:30	1.01421364	0.034082251	0.01421364	10.2804	18.0359885	0.003	-0.020026	23.3419	24.025171	20.51395	2.88056066	26.22246546
11:40	1.01815	0.030333333	0.01815	13.5761	16.9020455	0.003	-0.020373	23.4576	24.025171	20.51395	3.67106043	27.12866152
11:50	1.01997273	0.028597403	0.01997273	13.0038	16.7852261	0.003	-0.021758	23.9194	24.025171	20.51395	4.70592805	28.62535334
12:00	1.02368182	0.025064935	0.02368182	8.3035	15.538297	0.003	-0.02155	23.85	24.025171	20.51395	5.18779516	29.03778047
12:10	1.0242	0.024571429	0.0242	13.6245	15.4441937	0.003	-0.021761	23.9204	24.025171	20.51395	6.17357773	30.09396186
12:20	1.0242	0.024571429	0.0242	13.4673	15.5114692	0.003	-0.021963	23.9877	24.025171	20.51395	6.31185518	30.29951485
12:30	1.02488182	0.023922078	0.02488182	12.8507	15.3202057	0.003	-0.022039	24.0128	24.025171	20.51395	6.31185518	30.32470158
12:40	1.02455909	0.024229437	0.02455909	13.3026	15.111343	0.003	-0.021105	23.7015	24.025171	20.51395	6.49400755	30.19553815
12:50	1.02211818	0.026554113	0.02211818	13.613	15.1664338	0.003	-0.018945	22.9817	24.025171	20.51395	6.40775925	29.38948891
13:00	1.02264091	0.026056277	0.02264091	12.9545	15.8463708	0.003	-0.021483	23.8276	24.025171	20.51395	5.75714842	29.58476022
13:10	1.01538182	0.032969697	0.01538182	11.5794	15.9723716	0.003	-0.014947	21.6491	24.025171	20.51395	5.89622314	27.54536239
13:20	1.01115455	0.036995671	0.01115455	11.0869	18.029903	0.003	-0.017094	22.3647	24.025171	20.51395	3.97735123	26.3420306
13:30	1.01352727	0.034735931	0.01352727	11.3438	18.6373619	0.003	-0.021176	23.7254	24.025171	20.51395	2.87227689	26.59766185
13:40	1.01349545	0.034766234	0.01349545	10.896	18.5068564	0.003	-0.020754	23.5848	24.025171	20.51395	3.49142385	27.07620236
13:50	1.01405	0.034238095	0.01405	10.9693	18.4574928	0.003	-0.021134	23.7115	24.025171	20.51395	3.48310214	27.19456318
14:00	1.01521818	0.033125541	0.01521818	10.593	18.2581489	0.003	-0.021649	23.883	24.025171	20.51395	3.62821139	27.51117992
14:10	1.01427727	0.034021645	0.01427727	9.9489	18.3254399	0.003	-0.020955	23.6516	24.025171	20.51395	3.93440482	27.58596309
14:20	1.01316818	0.035077922	0.01316818	9.5301	18.346629	0.003	-0.019962	23.3207	24.025171	20.51395	3.68772764	27.00838261
14:30	1.01170455	0.036471861	0.01170455	8.9906	18.3833545	0.003	-0.018678	22.8927	24.025171	20.51395	3.39753739	26.29027144
14:40	1.01499091	0.033341991	0.01499091	9.2853	18.1626717	0.003	-0.021146	23.7153	24.025171	20.51395	3.01554034	26.73088154
14:50	1.01580455	0.0325671	0.01580455	9.1331	17.8567429	0.003	-0.021003	23.6677	24.025171	20.51395	3.87477966	27.54248933
15:00	1.02088182	0.027731602	0.02088182	8.6356	16.4971758	0.003	-0.02176	23.92	24.025171	20.51395	4.08835924	28.00833449
15:10	1.02068636	0.027917749	0.02068636	7.9877	16.422271	0.003	-0.021349	23.783	24.025171	20.51395	5.42876031	29.21178172
15:20	1.01675	0.031666667	0.01675	7.58	16.6080174	0.003	-0.018157	22.7191	24.025171	20.51395	5.37691728	28.09604577
15:30	1.01873636	0.029774892	0.01873636	7.0737	17.2162755	0.003	-0.021874	23.958	24.025171	20.51395	4.33696463	28.29494283
15:40	1.01805	0.030428571	0.01805	6.7113	16.9926658	0.003	-0.020549	23.5165	24.025171	20.51395	4.86075804	28.3772334
15:50	1.01925455	0.029281385	0.01925455	6.2635	16.7982965	0.003	-0.021114	23.7045	24.025171	20.51395	4.67954042	28.38404183
16:00	1.01860455	0.029900433	0.01860455	5.5169	16.6244726	0.003	-0.019973	23.3243	24.025171	20.51395	4.9977303	28.32205863
16:10	1.01902727	0.029497835	0.01902727	4.3369	16.4723703	0.003	-0.019919	23.3064	24.025171	20.51395	4.82593604	28.13236113
16:20	1.0202	0.028380952	0.0202	3.8495	16.4892796	0.003	-0.021087	23.6956	24.025171	20.51395	4.93763791	28.63326671
16:30	1.02146818	0.02717316	0.02146818	3.5267	16.3023919	0.003	-0.021734	23.9113	24.025171	20.51395	5.24799698	29.15933546
16:40	1.02524091	0.023580087	0.02524091	2.853	15.0106815	0.003	-0.021452	23.8173	24.025171	20.51395	5.58440614	29.40172547
16:50	1.02195455	0.026709957	0.02195455	2.3047	15.056566	0.003	-0.01846	22.8199	24.025171	20.51395	6.59003632	29.40995012
17:00	1.02804091	0.02091342	0.02804091	1.1039	14.3296446	0.003	-0.022076	24.0252	24.025171	20.51395	5.71364059	29.73881184
17:10	1.01632727	0.032069264	0.01632727	0.3463	14.537042	0.003	-0.011542	20.514	24.025171	20.51395	7.34107016	27.85502415
17:20	1.01866818	0.029839827	0.01866818	0.1923	17.0349718	0.003	-0.021265	23.755	24.025171	20.51395	4.22575307	27.9807826
17:30	1.02293182	0.025779221	0.02293182	0.041	15.6565347	0.003	-0.02119	23.7301	24.025171	20.51395	4.84274556	28.57287328
17:40	1.02257273	0.026121212	0.02257273	-0.0775	15.5875733	0.003	-0.020642	23.5472	24.025171	20.51395	5.97368153	29.52085074
17:50	1.01479545	0.033528139	0.01479545	-0.1374	15.887574	0.003	-0.014135	21.3782	24.025171	20.51395	5.87807507	27.25626959
18:00	1.01050455	0.037614719	0.01050455	-0.1619	17.9161402	0.003	-0.016134	22.0446	24.025171	20.51395	3.82352306	25.86809038

Table D.7 – DHC + EES values day 15th of April 2015.

Time	Vo	deltaVmax	deltaV	Pliquido	MaxP	a	b	HC	min	max	storage	HC+Storage
7:10	1.014018	0.034268398	0.014018	0.6424	16.94446	0.0037	-0.02843	21.19624	24.62046	21.19624	4.894388	26.09063205
7:20	1.015677	0.032688312	0.015677	1.6725	17.99935	0.0037	-0.03391	22.67819	24.62046	21.19624	3.619881	26.29807031
7:30	1.013595	0.034670996	0.013595	1.4272	17.84903	0.0037	-0.03137	21.992	24.62046	21.19624	4.054928	26.04692785
7:40	1.013205	0.03504329	0.013205	2.8	18.60447	0.0037	-0.03379	22.64683	24.62046	21.19624	3.509258	26.15608383
7:50	1.013009	0.035229437	0.013009	3.4732	18.56408	0.0037	-0.03346	22.55612	24.62046	21.19624	3.407042	25.96316514
8:00	1.016782	0.031636364	0.016782	4.7492	17.74346	0.0037	-0.03401	22.7066	24.62046	21.19624	3.355963	26.06256598
8:10	1.015805	0.0325671	0.015805	4.7095	17.72111	0.0037	-0.033	22.43271	24.62046	21.19624	4.345339	26.77804875
8:20	1.014668	0.033649351	0.014668	5.6202	17.73368	0.0037	-0.03197	22.15277	24.62046	21.19624	4.088359	26.24112871
8:30	1.019386	0.029155844	0.019386	7.0271	17.03952	0.0037	-0.03389	22.67308	24.62046	21.19624	3.790157	26.46323688
8:40	1.017368	0.031077922	0.017368	7.4108	17.01231	0.0037	-0.03187	22.12638	24.62046	21.19624	5.032596	27.15898038
8:50	1.013236	0.035012987	0.013236	7.0788	17.48244	0.0037	-0.02967	21.53299	24.62046	21.19624	4.49976	26.0327485
9:00	1.011932	0.036255411	0.011932	5.5603	18.43889	0.0037	-0.03197	22.15365	24.62046	21.19624	3.415359	25.56900665
9:10	1.009886	0.038203463	0.009886	4.3577	18.82602	0.0037	-0.03145	22.01427	24.62046	21.19624	3.074785	25.08905876
9:20	1.01395	0.034333333	0.01395	10.908	18.5057	0.0037	-0.03414	22.73994	24.62046	21.19624	2.542529	25.28246788
9:30	1.014373	0.033930736	0.014373	9.7727	18.26983	0.0037	-0.03367	22.61287	24.62046	21.19624	3.602033	26.21490718
9:40	1.015936	0.032441558	0.015936	10.7697	18.11834	0.0037	-0.0346	22.86386	24.62046	21.19624	3.712732	26.57659607
9:50	1.0133	0.034952381	0.0133	10.1384	18.24333	0.0037	-0.03255	22.31025	24.62046	21.19624	4.122993	26.43324256
10:00	1.015155	0.033186147	0.015155	10.8836	18.14077	0.0037	-0.03393	22.68506	24.62046	21.19624	3.431994	26.11705297
10:10	1.013823	0.034454545	0.013823	10.3173	18.18394	0.0037	-0.03283	22.38541	24.62046	21.19624	3.917707	26.30312017
10:20	1.011609	0.036562771	0.011609	10.2965	18.47382	0.0037	-0.03179	22.10551	24.62046	21.19624	3.568721	25.67422797
10:30	1.011836	0.03634632	0.011836	10.6373	18.71097	0.0037	-0.03288	22.40116	24.62046	21.19624	2.990665	25.3918226
10:40	1.012518	0.03569697	0.012518	11.4088	18.59032	0.0037	-0.03309	22.456	24.62046	21.19624	3.049899	25.50589846
10:50	1.008191	0.039818182	0.008191	12.2102	18.56471	0.0037	-0.02887	21.31655	24.62046	21.19624	3.227758	24.54430734
11:00	1.008223	0.039787879	0.008223	12.4569	19.69061	0.0037	-0.03307	22.45065	24.62046	21.19624	2.102964	24.55361118
11:10	1.009268	0.038792208	0.009268	11.8704	19.38996	0.0037	-0.03295	22.41909	24.62046	21.19624	2.111199	24.53029311
11:20	1.011382	0.036779221	0.011382	12.4883	19.10658	0.0037	-0.03392	22.67976	24.62046	21.19624	2.382089	25.06184826
11:50	1.020295	0.028290043	0.020295	11.6744	18.30424	0.0037	-0.03944	24.17179	24.62046	21.19624	2.931458	27.10325123
12:00	1.025373	0.023454545	0.025373	12.2946	17.04057	0.0037	-0.0396	24.21501	24.62046	21.19624	3.355963	27.57097725
12:10	1.025959	0.022896104	0.025959	11.851	15.85917	0.0037	-0.03578	23.18455	24.62046	21.19624	4.250857	27.43540826
12:20	1.025664	0.023177489	0.025664	13.2076	15.70766	0.0037	-0.03494	22.95699	24.62046	21.19624	5.27329	28.23027856
12:30	1.026477	0.022402597	0.026477	12.6783	15.70433	0.0037	-0.0357	23.16309	24.62046	21.19624	6.625304	29.78838944
12:40	1.025859	0.022991342	0.025859	12.6123	15.81572	0.0037	-0.03553	23.11536	24.62046	21.19624	6.782291	29.89764739
12:50	1.0242	0.024571429	0.0242	11.892	16.17442	0.0037	-0.03527	23.04701	24.62046	21.19624	6.703167	29.75017215
13:00	1.022314	0.026367965	0.022314	12.5459	16.68506	0.0037	-0.03537	23.0721	24.62046	21.19624	6.921169	29.99326505
13:10	1.018345	0.030147186	0.018345	11.9926	17.64528	0.0037	-0.03514	23.01091	24.62046	21.19624	6.755506	29.76641382
13:20	1.015514	0.032844156	0.015514	11.1289	18.47335	0.0037	-0.03551	23.11007	24.62046	21.19624	6.311855	29.42192133
13:30	1.018018	0.030458874	0.018018	11.0625	18.46217	0.0037	-0.03785	23.74356	24.62046	21.19624	5.809134	29.55269341
13:40	1.014668	0.033649351	0.014668	12.1378	18.9241	0.0037	-0.03637	23.3432	24.62046	21.19624	4.757519	28.10071485
13:50	1.016032	0.032350649	0.016032	13.1717	19.53055	0.0037	-0.03991	24.30065	24.62046	21.19624	4.011957	28.31260573
14:00	1.014636	0.033679654	0.014636	12.7843	19.21041	0.0037	-0.0374	23.62131	24.62046	21.19624	4.671145	28.29245775
14:10	1.014732	0.033588745	0.014732	11.7247	18.95071	0.0037	-0.03653	23.38618	24.62046	21.19624	3.790157	27.1763401
14:20	1.014832	0.033493506	0.014832	4.2322	18.8345	0.0037	-0.03619	23.29572	24.62046	21.19624	4.148079	27.44379538
14:30	1.015318	0.033030303	0.015318	3.6	18.81155	0.0037	-0.03657	23.39795	24.62046	21.19624	3.781817	27.17976959
14:40	1.013009	0.035229437	0.013009	3.5539	19.31012	0.0037	-0.03622	23.30216	24.62046	21.19624	3.806839	27.10900341
14:50	1.012455	0.035757576	0.012455	2.2047	19.53519	0.0037	-0.03652	23.3845	24.62046	21.19624	3.833058	27.21755386
15:00	1.01535	0.033	0.01535	5.7521	19.18638	0.0037	-0.03799	23.78097	24.62046	21.19624	3.960648	27.74162292
15:10	1.016814	0.031606061	0.016814	9.484	18.74722	0.0037	-0.03776	23.71855	24.62046	21.19624	3.355963	27.07451345
15:20	1.017564	0.030891775	0.017564	4.1423	18.44385	0.0037	-0.03735	23.60824	24.62046	21.19624	3.211148	26.81938502
15:30	1.015577	0.03278355	0.015577	9.2535	18.57613	0.0037	-0.03595	23.22923	24.62046	21.19624	3.968999	27.19822531
15:40	1.016391	0.032008658	0.016391	8.7379	18.58225	0.0037	-0.03675	23.44478	24.62046	21.19624	4.353714	27.79849244
15:50	1.015218	0.033125541	0.015218	7.4076	18.62812	0.0037	-0.0358	23.18879	24.62046	21.19624	4.551273	27.7400624
16:00	1.016523	0.031883117	0.016523	7.0885	18.73999	0.0037	-0.03745	23.63644	24.62046	21.19624	4.028666	27.66510735
16:10	1.01665	0.031761905	0.01665	6.3945	18.62512	0.0037	-0.03715	23.55433	24.62046	21.19624	4.242489	27.79682038
16:20	1.0187	0.029809524	0.0187	4.5675	18.40285	0.0037	-0.03828	23.85974	24.62046	21.19624	3.934405	27.79414384
16:30	1.020427	0.028164502	0.020427	4.2488	17.87278	0.0037	-0.03796	23.77426	24.62046	21.19624	4.277162	28.05142342
16:40	1.018377	0.030116883	0.018377	3.5239	17.77319	0.0037	-0.03564	23.14701	24.62046	21.19624	4.310648	27.4576573
16:50	1.027	0.021904762	0.027	2.8489	17.02715	0.0037	-0.0411	24.62046	24.62046	21.19624	4.851151	29.47160631
17:00	1.029341	0.019675325	0.029341	2.2397	15.92852	0.0037	-0.03926	24.12438	24.62046	21.19624	5.308225	29.43260166
17:10	1.024427	0.024354978	0.024427	1.5416	16.78288	0.0037	-0.03774	23.71396	24.62046	21.19624	4.765919	28.47988208
17:20	1.022509	0.026181818	0.022509	0.8582	17.39412	0.0037	-0.03818	23.83147	24.62046	21.19624	7.061405	30.89287167
17:30	1.02345	0.025285714	0.02345	0.1563	16.87473	0.0037	-0.03715	23.55426	24.62046	21.19624	7.691122	31.24538379
17:40	1.018768	0.029744589	0.018768	0.0756	17.30959	0.0037	-0.0343	22.78403	24.62046	21.19624	6.372546	29.15657288
17:50	1.016555	0.031852814	0.016555	-0.0267	18.25533	0.0037	-0.03569	23.15997	24.62046	21.19624	5.861139	29.02111064
18:00	1.016814	0.031606061	0.016814	-0.1609	18.64939	0.0037	-0.0374	23.62072	24.62046	21.19624	6.111761	29.7324858

APPENDIX. E – FLUKE 430 SERIES II DATASHEET

FLUKE

Fluke 430 Series II

Three-Phase Power Quality and Energy Analyzers

Technical Data

More detailed power quality analysis capability, and a new Fluke-patented energy monetization function

The new 430 Series II Power Quality and Energy Analyzers offer the best in power quality analysis and introduce, for the first time ever, the ability to monetarily quantify energy losses.

The new Fluke 434, 435 and 437 Series II models help locate, predict, prevent, and trouble-shoot power quality problems in three-phase and single-phase power distribution systems. Additionally, the Fluke-patented energy loss algorithm, Unified Power Measurement, measures and quantifies energy losses due to harmonics and unbalance issues, allowing the user to pinpoint the origin of energy waste within a system.

- **Energy loss calculator:** Classic active and reactive power measurements, unbalance and harmonic power, are quantified to pinpoint true system energy losses in dollars (other local currencies available).
- **Power inverter efficiency:** Simultaneously measure AC output power and DC input power for power electronics systems using optional DC clamp.
- **PowerWave data capture:** 435 and 437 Series II analyzers capture fast RMS data, show half-cycle and waveforms to characterize electrical system dynamics (generator start-ups, UPS switching etc.).
- **Waveform capture:** 435 and 437 Series II models capture 100/120 cycles (50/60Hz) of each event that is detected in all modes, without set-up.
- **Automatic Transient Mode:** 435 and 437 Series II analyzers capture 200 kHz waveform data on all phases simultaneously up to 6 kV.
- **Fully Class-A compliant:** 435 and 437 Series II analyzers conduct tests according to the stringent international IEC 61000-4-30 Class-A standard.
- **Mains signaling:** 435 and 437 Series II analyzers measure interference from ripple
- **400 Hz measurement:** 437 Series II analyzer captures power quality measurements for avionic and military power systems.
- **Troubleshoot real-time:** Analyze the trends using the cursors and zoom tools.
- **Highest safety rating in the industry:** 600 V CAT IV/1000 V CAT III rated for use at the service entrance.
- **Measure all three phases and neutral:** With included four flexible current probes with enhanced thin flex designed to fit into the tightest places.
- **Automatic Trending:** Every measurement is always automatically recorded, without any set-up.
- **System-Monitor:** Ten power quality parameters on one screen according to EN50160 power quality standard.
- **Logger function:** Configure for any test condition with memory for up to 600 parameters at user defined intervals.
- **View graphs and generate reports:** With included analysis software.
- **Battery life:** Seven hours operating time per charge on Li-ion battery pack.

437 Series II Three-Phase Power Quality and Energy Analyzer will be available in early 2012

Unified Power Measurement

Fluke's patented Unified Power Measurement system (UPM) provides the most comprehensive view of power available, measuring:

- Parameters of Classical Power (Steinmetz 1897) and IEEE 1459-2000 Power
- Detailed Loss Analysis
- Unbalance Analysis

These UPM calculations are used to quantify the fiscal cost of energy loss caused by power quality issues. The calculations are computed, along with other facility-specific information, by an Energy Loss Calculator that ultimately determines how much money a facility loses due to wasted energy.

Energy savings

Traditionally energy savings are achieved by monitoring and targeting, or in other words, by finding the major loads in a facility and optimizing their operation. The cost of power quality could only be quantified in terms of downtime caused by lost production and damage to electrical equipment. The Unified Power Measurement (UPM) method now goes beyond this to achieve energy savings by discovering the energy waste caused by power quality issues. Using the Unified Power Measurement, Fluke's Energy Loss Calculator (see screen shot below) will determine how much money a facility is losing due to waste energy.

Unbalance

UPM gives a more comprehensive breakdown of the energy consumed in the plant. In addition to measuring reactive power (caused by poor power factor), UPM also measures the energy waste caused by unbalance; the effect of unevenly loading each phase in three-phase systems. Unbalance can often be corrected by reconnecting loads on different phases to ensure the current drawn on each phase is as equal as possible. Unbalance can also be corrected by installing an unbalance reactance device (or filter), that will minimize the effects. Correcting unbalance should be basic good housekeeping in the facility as unbalance problems can cause motor failure or shorten equipment life expectancy. Unbalance also wastes energy. Using UPM can minimize or eliminate that energy waste, thus saving money.

Harmonics

UPM also provides details of the energy wasted in your facility due to the presence of harmonics. Harmonics may be present in your facility due to the loads you operate or may be caused by loads in adjacent facilities. The presence of harmonics in your facility can lead to:

- overheating transformers and conductors
- nuisance tripping of circuit breakers
- early failures of electrical equipment

Quantifying the cost of wasted energy due to the presence of harmonics simplifies the return-on-investment calculation needed to justify purchasing harmonic filters. By installing a harmonic filter the ill effects of harmonics can be reduced and energy waste eliminated, resulting in lower operational costs and more reliable operation.

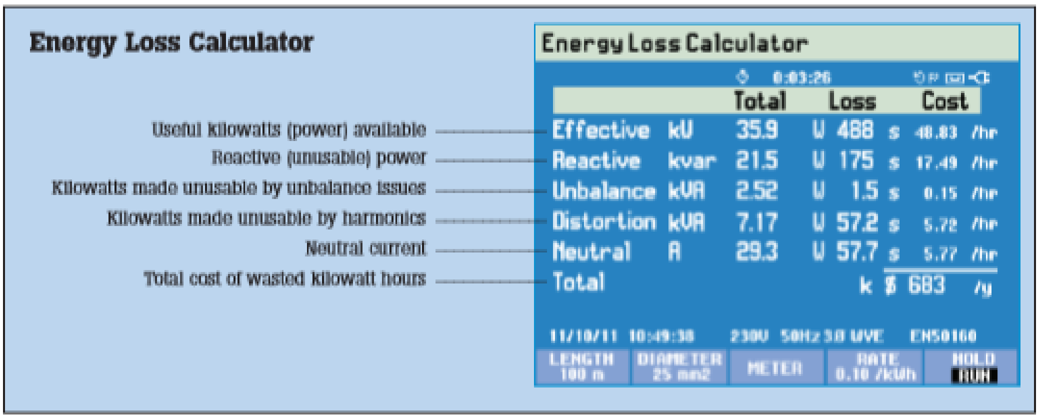

FLUKE

430 Series II Power Quality and Energy Analyzer selection table

Model	Fluke 434-II	Fluke 435-II	Fluke 437-II
Standard compliance	IEC 61000-4-30 Class S	IEC 61000-4-30 Class A	IEC 61000-4-30 Class A
Volt Amp Hz	•	•	•
Dips and swells	•	•	•
Harmonics	•	•	•
Power and energy	•	•	•
Energy loss calculator	•	•	•
Unbalance	•	•	•
Monitor	•	•	•
Inrush	•	•	•
Event waveform capture		•	•
Flicker		•	•
Transients		•	•
Mains signaling		•	•
Power wave		•	•
Power inverter efficiency	•	•	•
400Hz			•
C1740 Soft Case	•	•	
C437-II Hard Case with rollers			•
SD card (Max 32 GB)	8 GB	8 GB	8 GB

All models include the following accessories TL430 test lead set, 4 x i430 thin flexi current probes, BP290 battery, BC430 power adapter with international power adapter set, USB cable A-B mini and PowerLog CD.

Technical specifications

Specifications are valid for models Fluke 434-II, Fluke 435-II, Fluke 437-II unless otherwise specified.
Specificatons for Amp and Watt readings are based upon i430-Flexi-TF unless otherwise specified.

Input characteristics

Voltage inputs	
Number of inputs	4 (3 phase + neutral) dc-coupled
Maximum input voltage	1000 Vrms
Nominal voltage range	Selectable 1 V to 1000 V
Max. peak measurement voltage	6 kV (transient mode only)
Input impedance	4 MΩ//5 pF
Bandwidth	> 10 kHz, up to 100 kHz for transient mode
Scaling	1:1, 10:1, 100:1, 1,000:1 10,000:1 and variable
Current inputs	
Number of inputs	4 (3 phase + neutral) dc- or ac-coupled
Type	Clamp or current transformer with mV output or i430flex-TF
Range	0.5 Arms to 600 Arms with included i430flex-TF (with sensitivity 10x) 5 Arms to 6000 Arms with included i430flex-TF (with sensitivity 1x) 0.1 mV/A to 1 V/A and custom for use with optional ac or dc clamps
Input impedance	1 MΩ
Bandwidth	> 10 kHz
Scaling	1:1, 10:1, 100:1, 1,000:1 10,000:1 and variable

Input characteristics cont.

Sampling system	
Resolution	16 bit analog to digital converter on 8 channels
Maximum sampling speed	200 kS/s on each channel simultaneously
RMS sampling	5000 samples on 10/12 cycles according to IEC61000-4-30
PLL synchronization	4096 samples on 10/12 cycles according to IEC61000-4-7
Nominal frequency	434-II and 435-II: 50 Hz and 60 Hz 437-II: 50 Hz, 60 Hz and 400 Hz

Display modes

Waveform display	Available in all modes via SCOPE key 435-II and 437-II: Default display mode for Transients function Update rate 5x per second Displays 4 cycles of waveform data on screen, up to 4 waveforms simultaneously
Phasor diagram	Available in all modes via Scope waveform display Default view for Unbalance mode
Meter readings	Available in all modes except Monitor and Transients, provides tabulated view of all available readings Fully customizable up to 150 readings for Logger mode
Trend graph	Available in all modes except Transients Single vertical cursor with min max and avg reading at cursor position
Bar graph	Available in Monitor and Harmonics mode
Event list	Available in all modes Provides 50/60** cycles of waveform information and associated 1/2 cycle rms values for Volts and Amps

Measurement modes

Scope	4 voltage waveforms, 4 current waveforms, Vrms, Vfund. Arms, A fund, V @ cursor, A @ cursor, phase angles
Volts/amps/hertz	Vrms phase to phase, Vrms phase to neutral, Vpeak, V Crest Factor, Arms Apeak, A Crest Factor, Hz
Dips and swells	Vrms½, Arms½, Pinst with programmable threshold levels for event detection
Harmonics dc, 1 to 50, up to 9th harmonic for 400 Hz	Harmonics Volts, THD, Harmonic Amps, K factor Amps, Harmonic Watts, THd Watts, K factor Watts, Interharmonic Volts, Interharmonic Amps, Vrms, Arms (relative to fundamental or to total rms)
Power and energy	Vrms, Arms, Wfull, Wfund., VAfull, VAfund., VAharmonics, VAunbalance, var, PF, DPF, CosQ, Efficiency factor, Wforward, Wreverse
Energy loss calculator	Wfund, VAharmonics, VAunbalance, var, A, Loss Active, Loss Reactive, Loss Harmonics, Loss Unbalance, Loss Neutral, Loss Cost (based upon user defined cost / kWh)
Inverter efficiency (requires optional dc current clamp)	Wfull, Wfund, Wdc, Efficiency, Vdc, Adc, Vrms, Arms, Hz
Unbalance	Vneg%, Vzero%, Aneg%, Azero%, Vfund, Afund, V phase angles, A phase angles
Inrush	Inrush current, Inrush duration, Arms½, Vrms½
Monitor	Vrms, Arms, harmonic Volts, THD Volts, PLT, Vrms½, Arms½, Hz, dips, swells, interruptions, rapid voltage changes, unbalance and mains signalling. All parameters are measured simultaneously in accordance with EN50160 Flagging is applied according to IEC61000-4-30 to indicate unreliable readings due to dips or swells
Flicker (435-II and 437-II only)	Pst(1min), Pst, Plt, Pinst, Vrms ½, Arms ½, Hz
Transients (435-II and 437-II only)	Transient waveforms 4x Voltage 4x Amps, triggers: Vrms ½, Arms ½, Pinst
Mains Signaling (435-II and 437-II only)	Relative signaling voltage and absolute signaling voltage averaged over three seconds for up to two selectable signaling frequencies
Power Wave (435-II and 437-II only)	Vrms½, Arms½ W, Hz and scope waveforms for voltage amps and watts
Logger	Custom selection of up to 150 PQ parameters measured simultaneously on 4 phases